Design and Synthesis of Potential Inhibitors of Enzymes Involved in the Biosynthesis and Utilisation of Mycothiol

Nicholas Daniel Watermeyer

Thesis presented for the degree of

DOCTOR OF PHILOSOPHY

in the Department of Chemistry

UNIVERSITY OF CAPE TOWN

Supervisors: A/Prof David Gammon

A/Prof Daniel Steenkamp

June 2012

Abstract

This thesis describes the synthesis of several naphthoquinone- and carbazole-1,4-quinone-derived conjugates of a mycothiol-like scaffold designed to act as redox cycling subversive substrates of the enzyme, Mtr, or potentially inhibit other mycothiol-dependent or biosynthetic enzymes, in order to develop novel antitubercular lead compounds. The expression and purification of Mtr, as well as the attempts made towards the cloning and expression of active *Mycobacterial* glyoxalase I, in order to generate enzymes on which to assay the synthesised molecules, are also described.

Linking of the quinone functionalities to the mycothiol-like scaffold, phenyl-1-thio-D-glucosamine, was envisaged to facilitate delivery of this class of redox active molecules to the active-site of the mycothiol enzymes. Successful completion of the synthesis of naphthoquinone conjugates of this scaffold was not achieved due to a persistent side reaction that took place during an *N-tert*-butoxycarbonyl deprotection step. However, this unexpected result led to the discovery of a new synthetic route to benzo[*g*]indoles and benzo[*h*]quinolines. This route differs from traditional quinoline and indole syntheses in that the aromatic C-N bond is generated by a condensation reaction between a quinone carbonyl and an aliphatic amine, rather than *via* the traditional condensation of an aromatic amine with a distal carbonyl group.

Successful synthesis of the carbazole-1,4-quinone conjugates of phenyl-1-thio-D-glucosamine was achieved, affording three derivatives, **3.35**, **3.36** and **3.37**, which were tested for activity against *M. tuberculosis* strain H37Rv. Assays were carried out *in vitro* to determine minimum inhibitory concentration (MIC) using the microplate alamar blue assay (MABA), and all three conjugates were found to be inactive, with MIC values >128 μm. The addition of the linker and phenyl-1-thio-D-glucosamine unit to the carbazole quinone therefore significantly reduces the anti-TB activity of the parent carbazole quinone, a result which is consistent with the earlier findings of Knölker *et al.* that further substitution of the carbazole-quinone nucleus tends to dampen the anti-TB activity. Attempts have been initiated to have the conjugates tested for activity against Mtr, MshB and related mycothiol-processing enzymes, with results not available to date.

Acknowledgements

The completion of this project would not have been possible without the assistance of the following people:

I would like to thank my supervisor, A/Prof David Gammon, for his guidance, support, insight and positivity during the course of this project. It has truly been a pleasure to be a member of his research group.

I would like to thank A/Prof Daan Steenkamp for his supervision of the biochemical segment of this project, for training a chemist to be a biochemist, and for graciously agreeing to review drafts of the thesis under difficult circumstances.

Over the course of this project I have had the opportunity to spend time in the laboratories of Prof Stefan Oscarson (University College Dublin) and Prof Hans-Joachim Knölker (Technische Universität Dresden), and to them I am most grateful for the opportunity and for hosting me.

I am grateful to my fellow postgraduate students and postdocs for contributing to an enjoyable research environment. Dr Jackson Marakalala, Dr Vuyo Mavumengwana and Gabriel Mashabela at Chemical Pathology, my fellow Gammonites, Taigh Anderson, Ngumbsi Muhunga, Dr Muganza wa Muganza, Millie Hilgart, Nicola Wheat, Dr Denise Saravanakumar, Dr Pieter Levecque, my labmates in the Chibale, Hunter and Jardine groups, as well as my Irish and German colleagues in the Oscarson and Knölker groups, in particular, Dr Martin Hollinger and Ronny Forke.

I am indebted to Dr Jenny Miller, Dr Marlene Espinoza-Moraga and Taigh Anderson for reviewing drafts of my thesis and for providing valuable feedback.

To my cell group who have provided me with spiritual support, great fellowship and numerous prayers for my PhD project, thank you all!

My postgraduate studies have been financially supported by the University of Cape Town, the National Research Foundation and the Stella and Paul Loewenstein Trust, and I would like to extend my gratitude to each of these organisations for their support.

To my family who have encouraged and supported me on this journey, who have lived through my frustrations and triumphs, provided laughs, long cycle rides and a loving home: I am truly blessed to have you all in my life.

Finally, I thank God for His love, grace sufficient for each day, and for strength and endurance. All praise, honour and glory be unto Him!

TABLE OF CONTENTS

List of Abbreviations

[O]	oxidation
µl	microliter
µM	micromolar
ADP	adenosine diphosphate
Bn	benzyl
BSA	bovine serum albumin
CoA	coenzyme A
DCM	dichloromethane
DMAP	4-dimethylaminopyridine
DMF	*N*,*N*'-dimethylformamide
DMSO-d_6	deuterodimethylsulfoxide
DTDP	4,4'-dithiodipyridine
EDC.HCl	1-ethyl-3-(3-dimethylaminopropyl)carbodiimide hydrochloride salt
EI	electron impact
eq	equivalents
ESI	electrospray ionisation
GlxI	glyoxalase I
GlxII	glyoxalase II
GR	glutathione reductase
GSH	glutathione
h	hour(s)
HOBt	1-hydroxybenzotriazole
HRMS	high resolution mass spectrometry
IR	infrared spectroscopy
LipDH	lipoamide dehydrogenase
m.p.	melting point
MG	methyl glyoxal
min	minutes
MS	mass spectroscopy
MSH	mycothiol
NAD	nicotinamide adenine dinucleotide
NADH	reduced form of NAD
NADP	nicotinamide adenine dinucleotide phosphate

NADPH	reduced form of NADP
r.t.	room temperature
R_f	retention factor
SDS	sodium dodecyl sulfate
TBS	*tert*-butyldimethylsilyl
TEA	triethylamine
TEMED	tetramethylethylenediamine
TFA	trifluoroacetic acid
TFAA	trifluoroacetic acid anhydride
TLC	thin layer chromatography
Tris	2-amino-2-hydroxymethyl-propane-1,3-diol
Tris-Cl	hydrochloride salt of Tris
TrxR	thioredoxin reductase
TryR	trypanothione reductase

In NMR Assignments:

bs	broad singlet
d	doublet
dd	doublet of doublets
dt	doublet of triplets
Hz	Hertz
J	coupling constant
m	multiplet
q	quartet
s	singlet
t	triplet

Chapter 1
Introduction

This project forms part of a wider body of research currently being undertaken in our research group with the goal of identifying potential novel antitubercular chemotherapeutic compounds that target the mycothiol biosynthetic pathway and related enzymes.

1.1. Tuberculosis

Tuberculosis (TB) is an infectious pulmonary disease caused by the bacterium, *Mycobacterium tuberculosis* (*Mtb*). Approximately one-third of the world's population is currently infected with the TB bacillus, of which five to ten percent (of non-HIV infected people[i]) develop active tuberculosis and become infectious.[1] Transmission of the disease takes place when infected individuals propel droplets containing the bacterium into the air by coughing, talking, sneezing or spitting, and these are subsequently inhaled, causing infection. Infection does not necessarily lead to disease, and in healthy individuals, the bacilli can lie dormant in the macrophages of the lungs for many years without generating any symptoms. However, once a person's immune system becomes suppressed, the latent bacilli become active and the symptoms of the disease develop. These symptoms include chest pain, breathing difficulty, fatigue, fever, weight loss (giving rise to the historical colloquial term for the disease, consumption) and in advanced cases, haemoptysis (coughing up of blood or blood stained sputum).

Mycobacterium tuberculosis is an aerobic, non-motile, bacillus with a slow replication rate, (generation time of 17-18 h).[2] Although a member of the Gram-positive bacteria (due to it lacking an outer cell membrane), *Mtb* is poorly coloured by Gram stain due to its lipid-rich cell wall. However, it can be visualised under microscope by the Ziehl-Neelsen stain, which stains the organism bright red and is a commonly used technique for the identification of tuberculosis infection in sputum samples.[3]

[i] People co-infected with HIV and TB have a considerably higher probability of developing active tuberculosis.

1.1.1 Pathogenesis and Macrophage Interaction

TB infection occurs when aerosol droplets containing *Mtb* are inhaled, allowing the bacteria to reach the pulmonary alveoli, where they enter the endosomes of alveolar macrophages.[4,5] Here they replicate and generate what is termed the Ghon focus, the primary site of infection in the lungs consisting of a small area of granulomatous inflammation. From here the bacteria can spread to the lymph nodes by dendritic cell transport, and can further spread *via* the bloodstream to other areas of the body where secondary lesions may occur.[6] The formation of a granuloma by macrophages, T cells, B cells and fibroblasts aids in the containment of the infection. Bacteria within the granuloma can become dormant, giving rise to a latent infection with asymptomatic results. The latent bacteria are generally not completely eliminated from the host and can lie dormant for many years until the immune system is compromised. Once this occurs, the latent bacteria become virulent and develop into active tuberculosis. This ability to withstand the host's immune response, and to remain uncompromised within a granuloma consisting of macrophages and lymphocytes is a remarkable adaptation that has allowed *Mtb* to persist as a human parasite for centuries. The means by which *Mtb* is able to evade the immune response is by inhibition of phagolysosome biogenesis.[7] This results in immature phagolysosomes lacking the means to kill the *Mtb* bacilli, and permitting their persistence.

1.1.2 Global Incidence of TB

Tuberculosis is a world-wide problem, with most of the disease burden falling on developing countries where immunisation schemes and appropriate health care facilities are poorly supported. The World Health Organisation (WHO) has been monitoring the epidemiology of TB globally, and since 1997 has published sixteen global reports on tuberculosis, providing comprehensive information on the progress of the disease as well as measures that have been taken at a global, regional and country level to stop TB, using data provided by 198 countries accounting for 99 % of the world's TB cases.

The region with the highest total number of new TB cases is South East Asia, which accounted for 40 % of global incidence in 2010. The region with the highest rate of new cases of TB (per 100,000 population) in 2010 was Africa, with a rate of 276 – considerably greater than the second highest incidence region of SE Asia (rate of 193). The values for the incidence (the number of new cases arising during a defined period), prevalence (the

number of cases - new and previously occurring - that exists at a given point in time) and mortality for each WHO region are given below in Table 1.

Table 1. Estimates of the burden of the disease caused by TB, per WHO region

	YEAR	POPULATION	MORTALITY (EXCLUDING HIV)	PREVALENCE (INCLUDING HIV)	INCIDENCE (INCLUDING HIV)
Global	2010	6.87 billion	1.1 million	12 million	8.8 million
Africa		837 million	250,000	2.8 million	2.3 million
Americas		933 million	20,000	330,000	270,000
E. Mediterranean		597 million	95,000	1 million	650,000
Europe		896 million	61,000	650,000	420,000
SE Asia		1.808 billion	500,000	5 million	3.5 million
W. Pacific		1.798 billion	130,000	2.5 million	1.7 million

[Data taken from WHO Global Tuberculosis Report 2011][8]

Globally it was estimated that there were 1.45 million deaths from TB in 2010 (including HIV-associated), with the greatest number of these deaths occurring in Africa. In all six WHO regions, the estimated per capita incident rate was stable or decreased between 2006 and 2010, suggesting that the programs that have been instigated around the world are beginning to have an effect on the spread of TB. However, despite this global decrease in incident rate, high population growth in Africa meant that this region had an increase in the absolute number of TB cases between 2006 and 2010, the only region globally that this was so.[8] These results and figures indicate that TB is still a global problem, particularly in Africa, and that urgent attention and advanced treatment strategies are required to successfully combat the disease.

1.1.3 Incidence of TB in South Africa

South Africa has one of the highest rates of incidence of TB in the world, with a rate of 981 new cases per 100,000 population in 2010. This gave a total of 490,000 new cases of TB in 2010, with a WHO estimate of prevalence at 400,000, suggesting a considerable number of these new cases were either cured or died during the year (Table 2). 60% of TB patients that were tested were HIV-positive, although the HIV status of only 54% of patients was known, suggesting the co-infection rate could be even higher.

Table 2. Estimates of the mortality, prevalence and incidence of TB in South Africa compared to global and African figures for 2010

	YEAR	POPULATION	MORTALITY (EXCLUDING HIV)	PREVALENCE (INCLUDING HIV)	INCIDENCE (INCLUDING HIV)
Global	2010	6.87 billion	1.1 million	12 million	8.8 million
Africa	2010	837 million	250,000	2.8 million	2.3 million
South Africa	2010	50 million	25,000	400,000	490,000

[Data taken from WHO Global Tuberculosis Report 2011][8]

1.1.4 HIV and Tuberculosis

The Human Immune deficiency Virus (HIV) weakens the immune system and thereby greatly increases the chances that people suffering from the Auto Immune Deficiency Syndrome (AIDS) will develop active tuberculosis when also infected with the TB bacillus. From the 1980's till about 2004, the number of TB cases and TB mortality increased greatly as a result of the HIV epidemic, particularly in Southern and Eastern Africa.[8] Globally, 13% of TB cases occur among people with HIV. In the Africa region, which accounts for 82% of new HIV-positive TB cases globally, approximately 900,000 (39%) of the 2.3 million people who developed TB in 2010 were HIV-positive. As mentioned above, this value is considerably higher (>60%) in South Africa. There were approximately 350,000 deaths worldwide from TB among HIV-positive people in 2010.

1.1.5 Current TB Drugs and Their Biological Targets

The current first line TB drugs in clinical use are isoniazid, rifampicin, ethambutol and pyrazinamide (Figure 1).

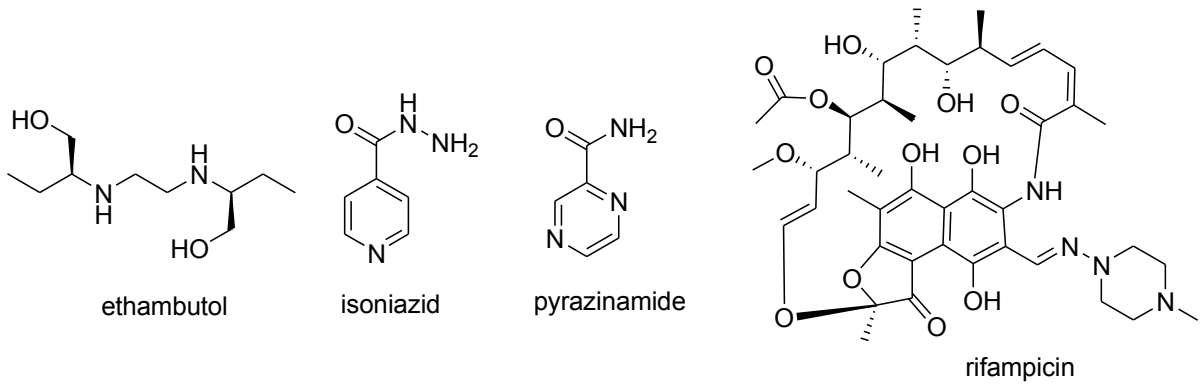

Figure 1. Chemical structures of first line TB drugs

The biological targets of the first-line drugs are varied. Isoniazid is a prodrug that is activated by the catalase peroxidase enzyme, KatG, and then reacts non-enzymatically with nicotinamide adenine dinucleotide (NAD) and nicotinamide adenine dinucleotide phosphate (NADP) to generate several isonicotinoyl adducts, one of which – the 4-*S* isomer of isoniazid-NAD – targets the enoyl-acyl carrier protein reductase, known as InhA,[9,10] thus inhibiting the biosynthesis of mycolic acid, an essential component of the mycobacterial cell wall.

Rifampicin is a semi-synthetic compound isolated from the bacterium, *Amycolatopsis rifamycinica*, and derives its activity by inhibiting bacterial RNA polymerase. This blocks transcription to RNA which in turn inhibits the formation of polypeptides and proteins.[11]

Ethambutol acts by obstructing the formation of the mycobacterial cell wall. A critical component of the cell wall is a macromolecular complex between arabinogalactan, mycolic acid and peptidoglycan.[12] Ethambutol disrupts arabinogalactan biosynthesis by inhibiting several arabinosyl transferases which reduce the formation of this complex and resulting in increased cell wall permeability.[13,14] This allows other co-administered TB drugs (such as rifampicin) to enter the bacterial cell more readily and exert their mode of activity.[15]

Pyrazinamide is included in first line drug regimens since it has been shown to reduce the duration of treatment from 9 months to 6 months.[16] It is a prodrug that is converted to its active form, pyrazinoic acid, by nicotinamidase/pyrazinamidase (PZase).[17] Its mode of action is somewhat disputed and has been proposed to proceed by inhibition of the fatty acid biosynthetic enzyme, fatty acid synthase (FAS) I,[18] by depleting cellular ATP reserves,[19] and by binding to the ribosomal protein S1 (RpsA) thus inhibiting trans-translation (this process is essential for liberating scarce ribosomes in non-replicating organisms, and its inhibition could explain the ability of pyrazinamide to eradicate dormant mycobacteria).[20]

The second-line TB drugs consist of those classes of compounds that are either less active than the first-line drugs (e.g. *p*-aminosalicylic acid), have toxic side-effects (e.g. cycloserine) or are not widely available (e.g. fluoroquinolones). These include the aminoglycosides (e.g. kanamycin), polypeptides (e.g. capreomycin), thioamides (e.g. ethionamide) and fluoroquinolones (e.g. ciprofloxacin, moxifloxacin) (Figure 2).

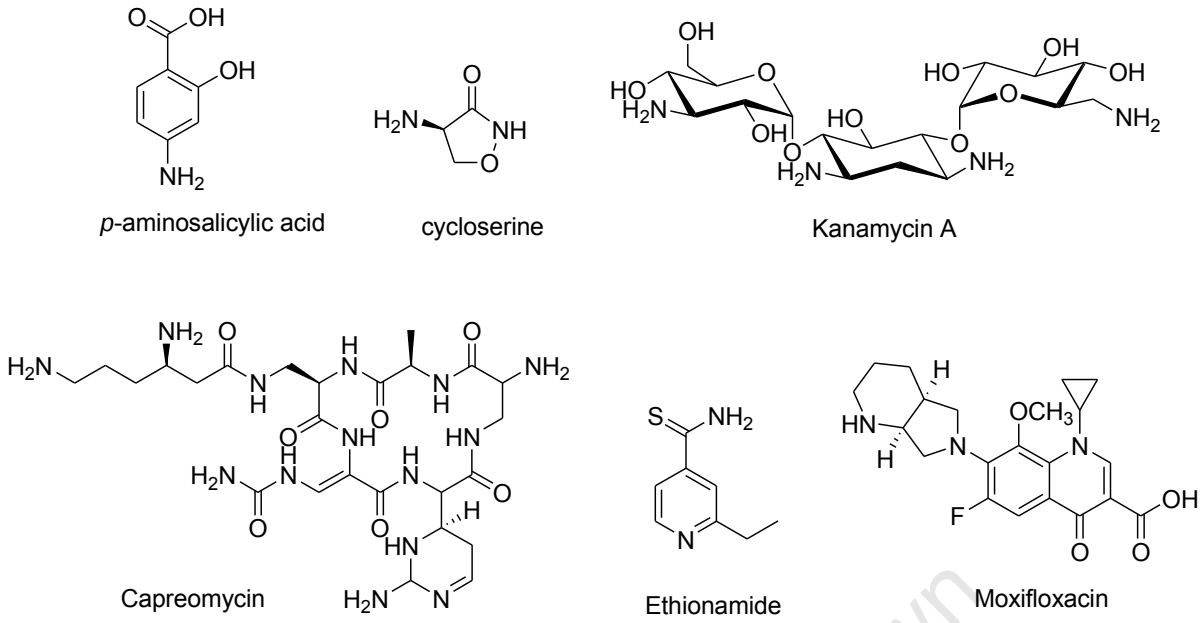

Figure 2. Chemical structures of second-line TB drugs

The mode of action of *p*-aminosalicylic acid has not been confirmed but it has been postulated to interfere with the salicylate-dependent biosynthesis of the iron-chelating mycobactins involved in iron assimilation.[21] Cycloserine is a structural analogue of D-alanine, and a competitive inhibitor of D-alanine racemase and D-alanyl-D-alanine synthetase. It has been implicated in disruption of the cell wall biosynthesis by targeting the mycolylarabinogalactan-peptidoglycan complex.[22] The aminoglycosides inhibit protein synthesis through irreversible binding to the ribosomal subunit, whereas the polypeptides appear to inhibit translocation of peptidyl transfer RNA thus preventing the initiation of protein synthesis.[23,24] The thioamide class of antitubercular agents, which includes ethionamide, appear to inhibit mycolic acid biosynthesis, although the exact mechanism of action has not been elucidated. Like isoniazid, ethionamide is a prodrug requiring activation, but by the monooxygenase, EthA, followed by formation of an adduct with NAD that subsequently inhibits the enoyl-ACP reductase, InhA.[25,26,27] Fluoroquinolones are the primary choice of drug for treatment of patients with multidrug-resistant (MDR-TB) and extensively drug resistant tuberculosis (XDR-TB) and produce the highest level of success in clinical outcomes of any other class of drugs.[28,29] The bactericidal effects of the fluoroquinolones are based upon their interaction with Type II topoisomerase (DNA gyrase), a tetrameric enzyme that catalyses the supercoiling of DNA.[30,31] Inhibition of its activity prevents supercoiling and subsequent processes that rely on DNA topology such as replication and transcription.[21]

The current short course treatment is six months long and consists of isoniazid, rifampicin, pyrazinamide and ethambutol for two months, followed by four months of isoniazid and

rifampicin alone. The rationale for using a multiple drug regimen is based on a statistical argument: in order to reduce the probability of spontaneous mutations leading to drug resistance, combinations of drugs are taken concurrently. This strategy also reduces the possibility of selecting a drug to which the infection strain may already have resistance. With the exception of XDR-TB, it is unlikely that resistance to all four front-line drugs will be present in the particular strain, and therefore the likelihood of successful treatment is enhanced.

1.1.6 Drug Resistant Tuberculosis

Since the development of the first TB drugs 50 years ago, resistant strains of the bacterium have started to develop, and in fact have been reported in every country surveyed by the WHO. Lack of patient compliance with the long duration of drug regimen is the greatest cause of resistance development. Some strains have developed resistance to more than one of the major TB drugs, resulting in MDR-TB and XDR-TB forms of the disease. MDR-TB is defined as resistance to at least isoniazid and rifampicin, the two most effective anti-TB drugs currently commercially available. XDR-TB is defined as resistance to at least isoniazid and rifampicin from among the first line anti-TB drugs, as well as resistance to any member of the fluoroquinolone family and to at least one of three injectable second-line anti-TB drugs (capreomycin, kanamycin and amikacin).[32]

Treatment of drug-resistant TB is generally possible, but requires extensive periods of chemotherapy (up to two years) with second-line TB drugs, which are more costly than first-line drugs and have more side effects. Although more difficult to treat and with higher rates of mortality, XDR-TB has been reported to be treatable, with a study in Russia reporting that 48 % of patients with XRD-TB successfully completed treatment.[33] However, a study from Tugela Ferry, South Africa, reported 52 of 53 patients with XDR-TB died, with a median survival of 16 days from the time of diagnosis. Most patients were co-infected with HIV.[34]

Drug-resistant TB is a concerning problem that threatens to develop into an epidemic because of the limited available treatment possibilities and could reverse the gains made since 2006 against the disease. It is therefore of great importance that new tools are developed for prevention, treatment and diagnostics. In particular, novel chemotherapeutic agents are required that are capable of treating drug-resistant infections. These drugs would have to act on alternate biological targets within the organism circumventing current resistance pathways that the bacterium has developed. One biological pathway not

currently covered by existing TB medicines is the mycothiol biosynthetic pathway and its associated enzymes, and it is these enzymes that form the focus of this project.

1.2. Mycothiol

Low molecular weight thiols play a key role in protecting cells from reactive oxygen and nitrogen species, and maintaining a reducing environment necessary for regular metabolic processes to take place. In eukaryotes and gram-negative bacteria, the dominant thiol performing this role is the tripeptide, glutathione (GSH)(Figure 3).[35] *Mycobacteria*, in common with other *Actinobacteria*, lack glutathione and instead produce the pseudodisaccharide, mycothiol (MSH)(Figure 3), which performs an analogous detoxification and redox stabilising function.[36] The discovery of MSH was first reported in 1994, independently by Spies and Steenkamp,[37] and by Sakuda and co-workers.[38]

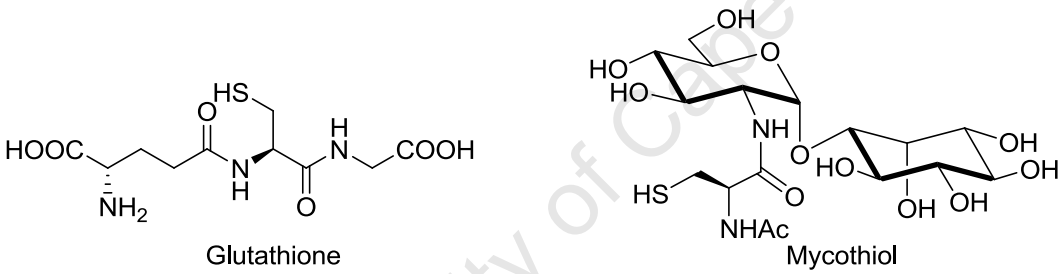

Figure 3. Chemical structures of glutathione and mycothiol

The structure consists of an *N*-acetylated cysteine coupled to D-glucosamine which is α(1-1)-linked to *myo*-inositol. Although initially unconfirmed, the absolute stereochemistry of MSH was finally resolved by total chemical synthesis of the bimane derivative, MSmB, which was shown to have the same optical rotation, circular dichroism and mycothiol-*S*-conjugate amidase (Mca) substrate properties as MSmB obtained from cell extracts.[39,40]

1.2.1 Overview of Mycothiol biosynthesis

The mycothiol biosynthetic pathway begins with L-*myo*-inositol-1-phosphate (L-*myo*-Ins-1-P), which is obtained from glucose-6-phosphate by the action of inositol-1-phosphate synthase. Conversion of L-*myo*-Ins-1-P to mycothiol proceeds *via* five enzymatic stages, as outlined in Scheme 1.

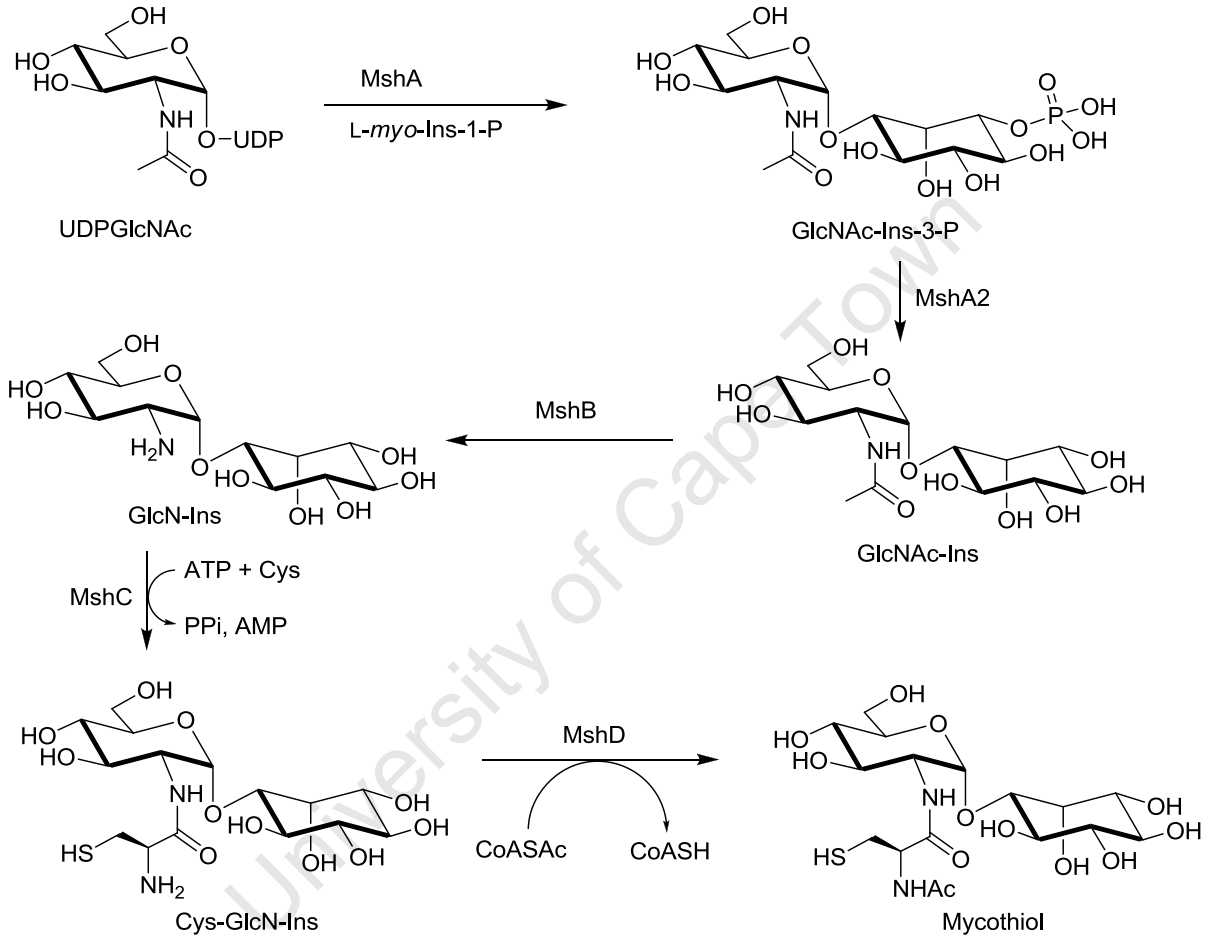

Scheme 1. Mycothiol biosynthetic pathway

The first step involves the formation of a glycosidic linkage between uridine diphospho 2-acetamido-2-deoxy-glucose (UDP-GlcNAc) and L-*myo*-Ins-1-P, catalysed by the glycosyltransferase, MshA.[41] The phosphate on the GlcNAc-Ins-3-P is then removed by an unspecified phosphatase, designated MshA2, followed by deacetylation of the *N*-acetyl of GlcNAc-Ins by the zinc-dependent deacetylase, MshB.[42] The cysteine side-chain is subsequently attached by the ATP-dependent cysteine ligase, MshC.[43] Finally, acetylation of the cysteinyl amine by the acetyl-CoA-dependent acetyltransferase, MshD, completes the biosynthesis of MSH.[44]

The biosynthetic enzymes involved in this process, as well as a few selected mycothiol-dependent proteins are described in greater detail below.

1.2.2 Mycothiol Glycosyltransferase, MshA, and Phosphatase, MshA2

Commencement of the MSH biosynthesis by glycosylation of the L-*myo*-Ins-1-P with UDP-GlcNAc is proposed to proceed as illustrated in Scheme 2.

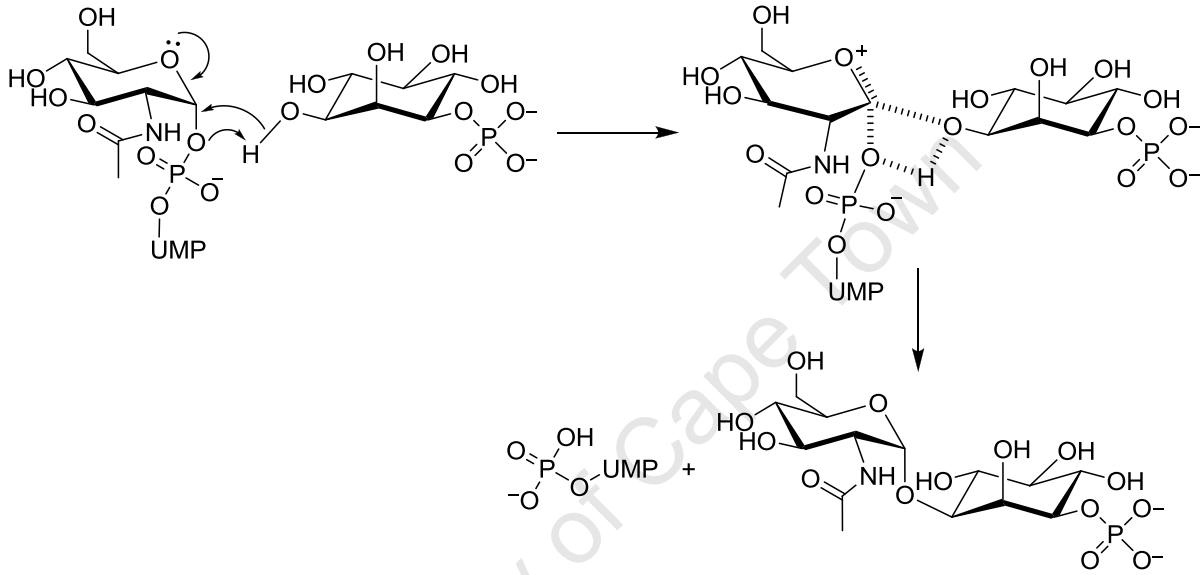

Scheme 2. Proposed catalytic mechanism for MshA-mediated formation of GlcNAc-Ins-P[45]

The exact substrates and biochemistry of MshA were only elucidated several years after the identification of its role in MSH biosynthesis.[46] This was done by proving that *M. smegmatis* extracts synthesised GlcNAc-Ins-P from the racemic 1-D,L-Ins-1-P and UDP-GlcNAc, but not from *myo*-inositol nor 1-D-Ins-1-P and UDP-GlcNAc. This demonstrated that the substrate for MshA was 1-L-Ins-1-P. Protein crystal structure analysis revealed that active-site binding of UDP-GlcNAc, which generates the binding site for 1-L-Ins-1-P,[45] involves a considerable conformational change. The inositol phosphate was shown to be stabilised by electrostatic interactions and multiple hydrogen bonds to amino acid residues within the binding site, which could explain why *myo*-inositol lacking the phosphate group could not serve as a source of inositol for the enzyme reaction.[47] The first step of the proposed mechanism is elimination of the UDP by delocalisation of the glucosamine ring oxygen lone pair to generate an oxocarbenium ion, followed by glycosylation with the inositol-1-P in a semi-concerted process that involves deprotonation of the acceptor hydroxyl by the eliminated UDP phosphate group. The inositol-1-P is presumably held in the correct orientation by the

afore-mentioned electrostatic and H-bond interactions of the phosphate (and inositol hydroxyl groups) with residues in the active site, thus directing the α-glycosylation.

Dephosphorylation of GlcNAc-Ins-P to generate the substrate for MshB is carried out by the as yet unidentified phosphatase, MshA2. Screening of *M. smegmatis* MSH-deficient mutant libraries with mutant phosphatases proved fruitless. It is therefore possible that more than one mycobacterial phosphatase with MshA2 activity exists. Even alkaline phosphatase has been shown to be capable of dephosphorylating GlcNAc-Ins-P.[45,47] Consequently, MshA2 may not be a viable target for tuberculosis drug development, and it continues to remain uncharacterised.

The requirement of MshA for the production of mycothiol was established in *Streptomyces coelicolor*, a member of the actinobacteria that also produces mycothiol.[48] The study was able to identify the homologues of *mshA*, *mshB*, *mshC* and *mshD* in the *Streptomyces* genome, and they were shown to serve the same role as their corresponding genes in the *mycobacteria*. The production of mycothiol was halted when the *mshA* gene was disrupted by PCR mutagenesis, and then fully restored when the mutant was complemented with the *mshA* gene. This finding established that MshA is necessary for the production of mycothiol within this organism. Extension of this finding to include the *mycobacteria* was done by Fahey and co-workers,[49] who demonstrated the requirement of MshA for the production of MSH in *M. smegmatis*. A subsequent study confirmed the requirement of the *mshA* gene for the growth of *M. tuberculosis* Erdman.[50] These results indicate that MshA is a viable drug target.

1.2.3 Mycothiol Deacetylase, MshB

MshB, the deacetylase responsible for converting GlcNAc-Ins to the free amine, GlcN-Ins, is a zinc metalloprotein and a homologue of mycothiol *S*-conjugate amidase, Mca, since both enzymes cleave the glucosamine amide bond (see below for a more detailed description of Mca).[51] The proposed catalytic mechanism based on the crystal structure is illustrated below in Scheme 3.

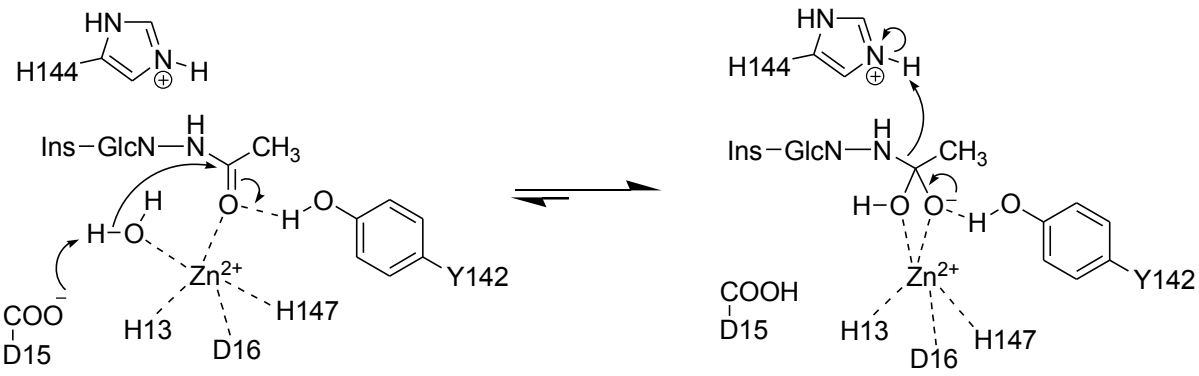

Scheme 3. Catalytic mechanism for deacetylation of GlcNAc-Ins by MshB[52]

The reaction is initiated by deprotonation of a molecule of water, by the conserved Asp_{15} residue. Coordination of the amide carbonyl to the zinc atom results in enhanced electrophilicity at the carbonyl carbon, which is attacked by the generated hydroxide. The resulting negative charge on the amide oxygen is stabilised by coordination to the phenolic proton of Tyr_{142}. This function was initially thought to performed by Asp_{146}, but this has recently been shown to be too far from the active site to perform such a role.[52] Conversion of the tetrahedral intermediate to the reaction products proceeds by protonation of the departing free amine by His_{144}.

A study of the substrate specificity of MshB led to several interesting findings (Figure 4). The des-*myo*-inositol substrate had a 70-fold decrease in activity over the natural substrate, clearly illustrating the importance of that subunit. Mycothiol was shown to be a very poor substrate with a relative activity of just 0.3. This is an interesting result, which indicates a highly necessary adaptation that precludes MshB from undoing the work of the subsequent mycothiol biosynthetic enzymes. As mentioned above, there is some overlap of activity with Mca, and some of the MSR-type substrates of Mca were shown to be reasonable substrates for MshB as well, albeit with lower rates of cleavage than the natural substrate. Surprisingly, the monobimane derivative, CySmB-GlcN-Ins was 60 times more reactive with MshB than Mca, and was almost 5 times more reactive with MshB than the substrate, GlcNAc-Ins. This is presumably due to favourable interactions of the bimane or the cationic amine with residues near to the active site.

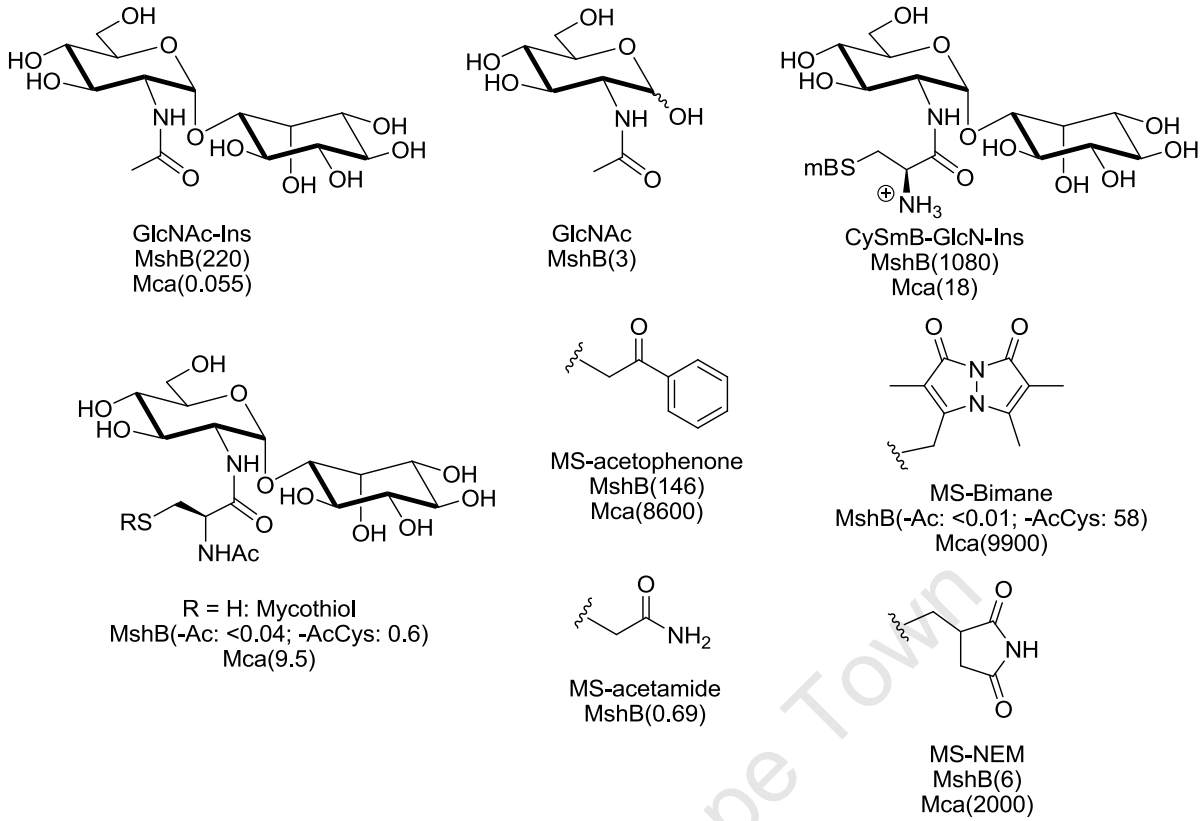

Figure 4. Activities (nmol/min/mg) of *M. tuberculosis* MshB and Mca (where available) with various substrates at 0.1 mM[53]

The overlap in amidase activity between MshB and Mca has been proposed to explain the redundancy of MshB as a crucial enzyme in the production of MSH. Disruption of *mshB* in *M. smegmatis* caused the levels of MSH production to fall to 5-10% of that of the parent strain, but not to completely cease, suggesting that another enzyme is capable of carrying out the GlcNAcIns deacetylation. Epichromosomal expression of Mca in the *mshB* mutants did not restore MSH levels to those of the parent strain, suggesting that perhaps Mca was not the complementary deacetylase responsible for the background production of MSH.[54] However, a recent comprehensive study performed by Jacobs and co-workers[55] on the independent deletion mutants for all four genes involved in MSH biosynthesis in *M. smegmatis*, demonstrated that *mshA* and *mshC* single deletion mutants produced no MSH, the *mshB* deletion mutant generated decreased levels of MSH, and the double *mshB*- and *mca*-mutant completely ceased production of MSH. This study also demonstrated that MSH production was essential for isoniazid (INH) and ethionamide (ETH) susceptibility in *M. smegmatis*, with MSH-deficient mutants being resistant to both INH and ETH, whereas the low levels of MSH produced by the *mshB* mutant were sufficient to convey sensitivity to INH but not to ETH. This appears to implicate MSH in the activation of these two prodrugs.

1.2.4 Mycothiol Cysteine Ligase, MshC

The fourth step in the biosynthesis of MSH involves coupling of L-cysteine to the amine group of GlcN-Ins, carried out by the mycothiol cysteine ligase, MshC. The enzyme activity was first discovered by Steenkamp and co-workers[41] from crude *M. smegmatis* cell extracts. Purified enzyme was then obtained by Fahey and co-workers[56] after purification of ligase activity from *M. smegmatis* cell extracts, followed by *N*-terminal sequencing, and cloning and expression of the identified gene. MshC is a homologue of cysteine tRNA synthetase due to its mode of activating cysteine by forming a cysteine-AMP intermediate, which is subsequently attacked by the GlcN-Ins amine resulting in the formation of the amide product (Scheme 4).[56]

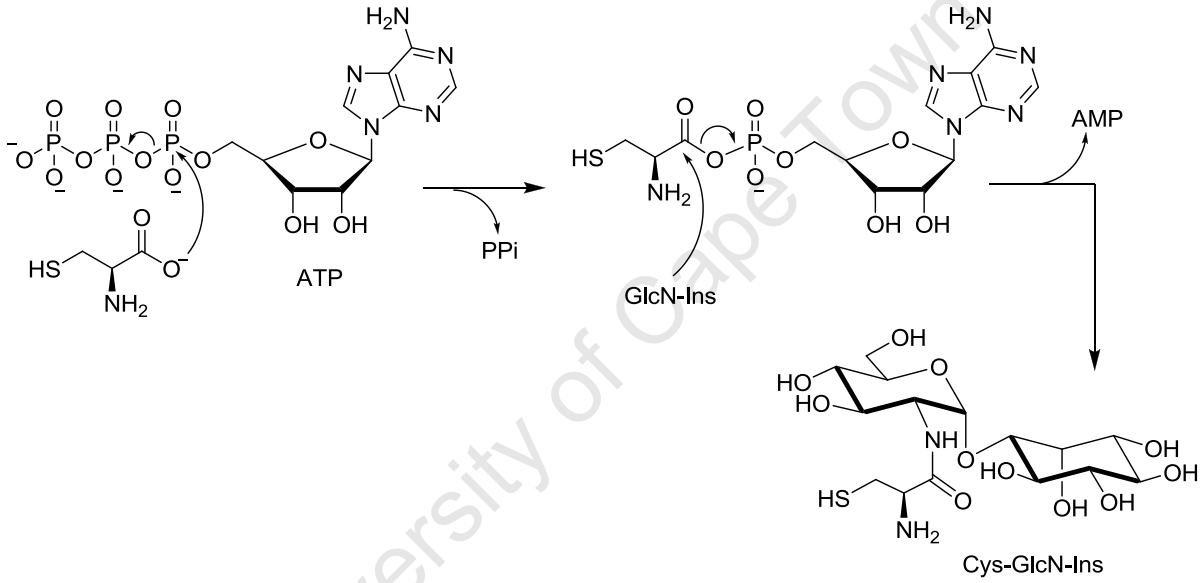

Scheme 4. Mechanism of mycothiol cysteine ligase

As such, MshC has been shown to be inhibited by the cysteine adenylate analogue, 5'-*O*-[*N*-(L-cysteinyl) sulfamoyl]adenosine (Figure 5), which is a known cysteine and proline tRNA synthetase inhibitor, having an ATP competitive inhibition constant of 304±40 nM against His-tagged *M. smegmatis* MshC.[57] The crystal structure of *M. smegmatis* MshC was elucidated by Blanchard and co-workers in 2008.[58]

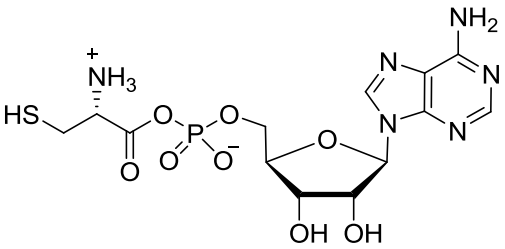

Cysteine adenylate

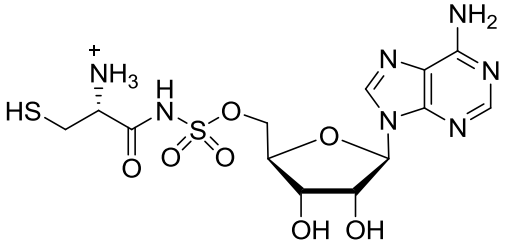

5'-*O*-[*N*-(L-cysteinyl)sulfamoyl]adenosine

Figure 5. Chemical structure of cysteine adenylate and its sulfamoyl derivative, a nanomolar inhibitor of tRNA synthetases

The importance of MshC for the growth of *Mtb* was demonstrated by the combined findings of two studies. Firstly, a study by Av-Gay and co-workers[59] confirmed the importance of MshC for the growth of mycobacteria. *M. smegmatis* MSH-deficient mutants were developed by both chemical and transposon mutagenesis, and consequently lacked MshC activity. They were found to be more sensitive to alkylating agents, oxidative stress and had a 3- to 16-fold enhanced sensitivity to a range of antibiotics including penicillin G, erythromycin, vancomycin and azithromycin over the wild-type strain. This demonstrated the importance of MSH for the protection of *M. smegmatis* against such stresses. Supporting the later findings of Jacobs and co-workers,[55] these mutant strains demonstrated a 16- to 125-fold enhanced resistance to isoniazid, further confirming the involvement of MSH in the activation of the isoniazid prodrug. Secondly, a study by Fahey and co-workers discovered that after targeted disruption of the native *mshC* gene in *M. tuberculosis* Erdman, no viable clones possessing MSH were found.[60] This was found to be reversible, and when the *mshC* gene was inserted into the chromosome, normal levels of MSH were produced and the clones survived. These studies suggest that MshC, and mycothiol, are essential for mycobacterial survival and pose a viable drug target for future drug development.

1.2.5 Mycothiol Synthase, MshD

Mycothiol synthase, also referred to as mycothiol acetyltransferase or MshD, is the fifth and final enzyme involved in the biosynthesis of MSH, and catalyses acetylation of the amino group of Cys-GlcN-Ins with acetyl-CoA.[47] The presence of MshD activity was first demonstrated in *M. smegmatis*,[41] and the purified *Mtb* enzyme was later cloned in *Escherichia coli* (*E. coli)*.[61] A study of the *M*. *smegmatis* transposon mutagenesis mutant, *mshD*::Tn5, lacking the *mshD* gene, showed that it produced only 1% of the normal amount of MSH and accumulated high levels of Cys-GlcN-Ins. This demonstrated the importance of

the enzyme in the biosynthesis of MSH. Another study on *mshD*::Tn5 showed that in the absence of MSH, two novel thiols were formed, *N*-formyl-Cys-GlcN-Is and *N*-Succinyl-Cys-GlcN-Ins, that acted as surrogates for MSH and enabled the mutant to resist oxidative challenge by peroxides.[62] However, under a simulated macrophage environment, *N*-formyl-Cys-GlcN-Ins was found to be incapable of supporting normal cell growth of an *mshD*-deficient mutant of *M. tuberculosis*.[63] These findings seem to suggest that MshD is a potential target for drug development, and since the crystal structure is known, structure-based design of small molecule inhibitors should be possible.[64] A catalytic mechanism, based upon the crystal structure of the mixed disulfide of Cys-GlcN-Ins and CoA and on the pH dependence of enzyme activity was proposed, and is illustrated below in Scheme 5. Glu_{234} is proposed to act as a general base that initiates a proton transfer from the substrate *via* an interstitial water molecule, which promotes nucleophilic attack of the acetate thioester by the substrate amine. Electrophilicity of the acetate carbonyl carbon is enhanced by coordination to the amine of Leu_{238}. Finally, a proton transfer from Tyr_{294} releases CoA in the thiol form (CoASH) and produces MSH.[47]

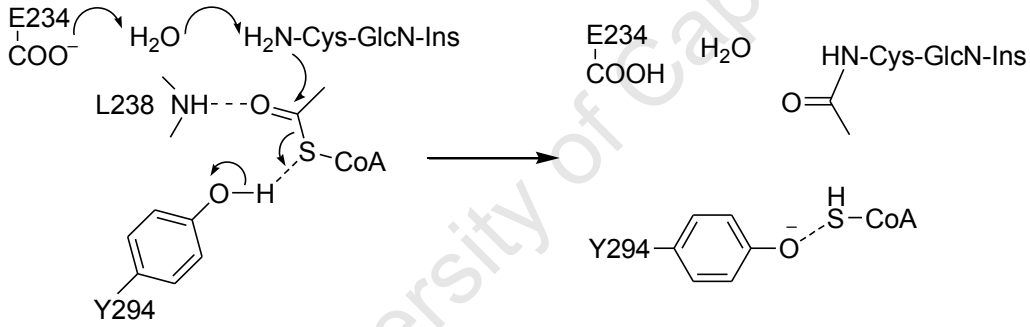

Scheme 5. MshD active-site mechanism of acetyl transfer from acetyl-CoA to Cys-GlcN-Ins[47]

1.2.6 Mycothiol *S*-Conjugate Amidase, Mca

When MSH reacts with an intracellular toxin, it forms a mycothiol *S*-conjugate, which is subsequently cleaved by the enzyme, mycothiol *S*-conjugate amidase, or Mca, at the glucosamine amide bond to cysteine (details of process summarised in Figure 6 below). Upon cleavage, a mercapturic acid conjugate (AcCySR) of the form, Cys-toxin, is formed and subsequently excreted from the cell. The liberated GlcN-Ins is recycled back into the mycothiol biosynthetic pathway as a substrate for MshC. Mca was first isolated from *M. smegmatis* and analysis of its *N*-terminal sequence was used to identify the orthologous

gene in *M. tuberculosis*, which was subsequently cloned and expressed and found to be a zinc-dependent protein.[65]

Substrate specificity of Mca is reserved for the MSH functionality of substrate conjugates, and those lacking the *N*-acetyl or inositol groups have a 900-fold reduction in activity. Replacement of the *N*-acetyl with an *N*-formyl results in a 20-fold drop in activity. A wide range of substituents on the sulfur are tolerated, as would be expected from the range of xenobiotic particles likely to be intercepted by MSH. Aryl CH_2 groups attached to the sulfur are the most reactive, whilst MSH itself is poorly active and has been shown to inhibit Mca at intracellular millimolar concentration levels.[66]

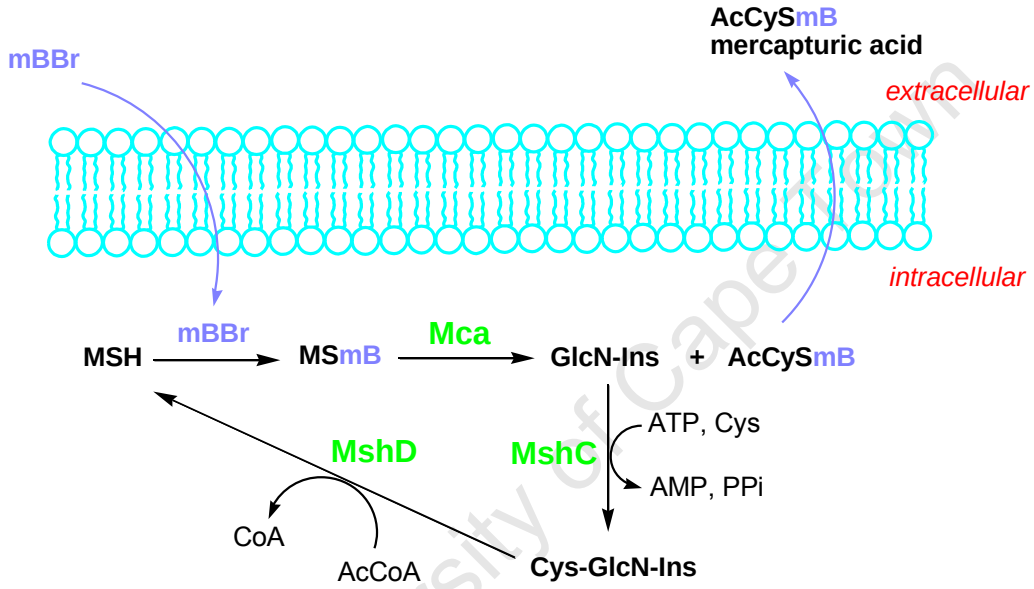

Figure 6. Mycothiol-dependent detoxification pathway of MCA with a simulated toxin, monobromobimane (mBBr). The thiol-reactive reagent mBBr reacts with MSH to form MSmB, which is cleaved by Mca to generate GlcN-Ins and the mercapturic acid, AcCySmB, which is subsequently excreted. The generated GlcN-Ins is recycled back into the MSH biosynthetic cycle as a substrate for MshC.[47]

Mca has potential as a drug target due to its unique role in the MSH detoxification pathway. A mutant of *M. smegmatis* lacking the *mca* gene was reported by Av-Gay and co-workers[67] to lack amidase activity and to accumulate MSH conjugates of mBBr inside the cell, in contrast to the wild-type strain that rapidly cleaved off and excreted the bimane mercapturic acid. The mutant was also shown to have enhanced sensitivity to alkylating agents and several antibiotics.[35] In a separate study, Bewley and co-workers[68] screened 1500 natural product extracts and identified several inhibitors of Mca as lead compounds. Two bromotyrosine-derived compounds were shown to be competitive inhibitors of Mca, and after a library of related bromotyrosine derivatives were prepared and screened, one lead

compound, EXEG1706, was shown to display low inhibitory values against a number of bacterial organisms, including *M. smegmatis* and *M. bovis* BCG.[69,70] This demonstrated the broad spectrum of activity of this class of compounds and a lack of specificity for Mca, which is not necessarily a negative attribute for such inhibitors since in order to inhibit MSH-related amidase activity, inhibition of both Mca and MshB is required.

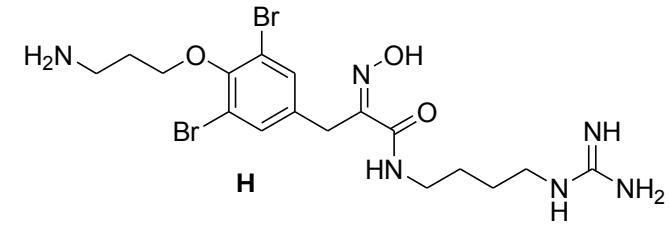

H

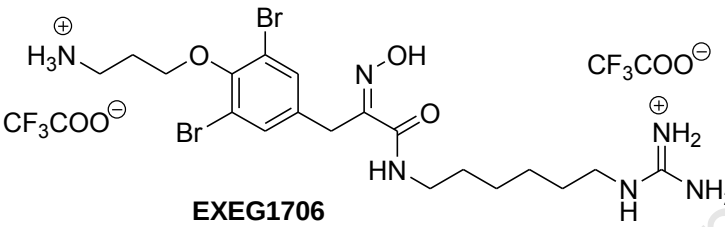

EXEG1706

Figure 7. Chemical structures of hydroxamate inhibitors of Mca. H, a bromotyrosine alkyloid from the marine sponge *Oceanapia* sp., and a related synthetic analogue, EXEG1706.

1.2.7 Mycothiol Disulfide Reductase, Mtr

During the natural process of redox buffering, MSH is oxidised to its symmetrical disulfide MSSM. Regeneration of the active thiol monomer from MSSM is carried out by the flavoprotein, mycothiol disulfide reductase or Mtr (also called mycothione reductase). Mtr maintains a high thiol:disulfide ratio by the reduction of MSSM using NADPH as a co-factor. This process occurs in a similar manner to that of the glutathione- (GR) and trypanothione-reductase (TryR) pathways found in eukaryotes and Gram negative bacteria, and trypanosomes, respectively.[40] Mtr appears to have a considerable degree of specificity towards disulfide substrates, although it is able to tolerate substitutions at some sites better than others (Table 3). Due to the scarcity of the natural substrate, Mtr was first characterised using the truncated substrate des-*myo*-inositol mycothiol disulfide, which first demonstrated the non-essentiality of the inositol substituent.[71,72] It was also found that the inositol could be replaced by a methyl or benzyl without considerable loss of activity.[73] Since the synthesis of the GlcN-Ins with the Ins in the correct stereochemical orientation is non-trivial, this provides a synthetically accessible route for the preparation of potential Mtr

inhibitors. Substitutions at the cysteinyl amine, including removal of the acetate or its replacement by a formyl or succinyl residue, however, were found to result in considerable loss of activity.[62] NADPH and NADH are both tolerated as co-factors, although NADH has a 20-fold lower activity than NADPH.

Table 3. Relative activities of various disulfides with Mtr, using NADPH as a co-factor, MSSM rate normalized to 100 (adapted from Newton *et al*)[47]

Thiol source of disulfide	Relative rate
AcCys-COOH	$<10^{-3}$
AcCys-$COOCH_3$	$<10^{-3}$
AcCys-GlcN (DI-MSH)	6,[a] 25[b]
AcCys-GlcN-1-*O*-CH_3	15[b]
AcCys-GlcN-1-*O*-CH_2Ph	68[b]
AcCys-GlcN-Ins (MSH)	100
HCO-Cys-GlcN-Ins	13[c]
Cys-GlcN-Ins	≤4[c]
$HOOCCH_2CH_2CO$-Cys-GlcN-Ins	0.8[c]

[a] From reference 72

[b] From reference 73

[c] From reference 62

Kinetic studies on *M. tuberculosis* Mtr have provided a detailed mechanism for the reduction of MSSM, which has been proposed to proceed by an analogous route to GR and TryR. The mechanism is described below in Scheme 6. Binding of NADPH to the oxidised enzyme is fast and is followed by transfer of a hydride to the flavin adenine dinucleotide (FAD) and reduction of the active-site disulfide. The thiolate anions are stabilised by the FAD and His_{444}, respectively. NADP is then lost and binding of MSSM leads to cleavage of the substrate disulfide with liberation of one equivalent of MSH and the formation of a mixed disulfide between the active-site Cys_{39} thiolate and the substrate. This is then reduced to liberate a second equivalent of MSH and regenerate the active-site disulfide.

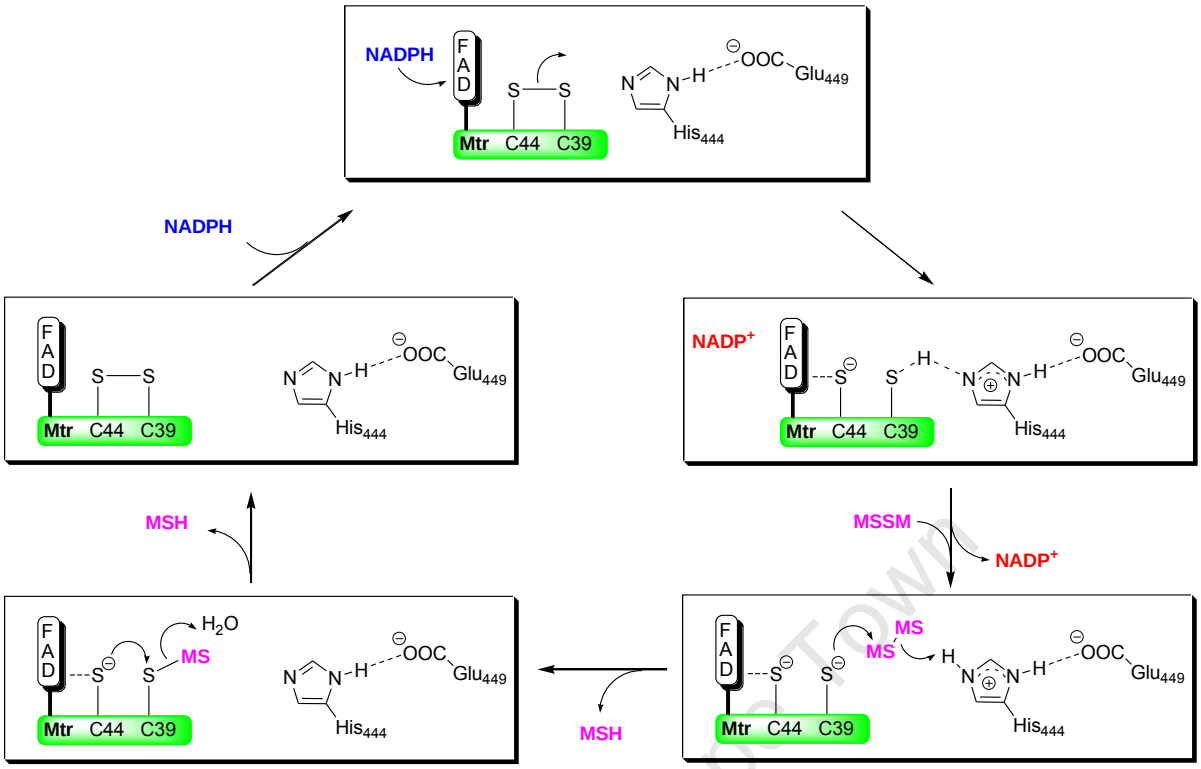

Scheme 6. Mechanism of Mtr[40]

It is currently uncertain whether Mtr is essential for the growth of mycobacteria. A Himar-1 transposon mutagenesis screen indicated that Mtr is essential to the survival of the *Mtb* H37Rv strain.[74] However, it has also been reported that an *Mtb* transposon mutant in *mtr* was viable, suggesting it is non-essential.[75] Full phenotypic characterisation of an actinomycete *mtr* mutant, which would be able to give a clearer picture, has not yet been reported.[35] Further investigation by Hayward and co-workers[76] reported that application of antisense *M. tuberculosis mtr* oligonucleotides produced a 66% drop in the growth index after 7 days' incubation, relative to the control culture.

Transcriptional analysis of the related organism, *M. bovis* BCG, revealed that *mtr* is actively transcribed during growth, but that *mtr* mRNA is absent in the stationary phase, suggesting its necessity for maintaining the redox balance is limited to the growth phase,[76] although Av-Gay and co-workers[35,77] have also reported that MSH levels remain high during the stationary phase, suggesting disulfide reductase activity. It is possible that there is a homologous thiol reductase within *Mtb* capable of performing a substitutionary role for Mtr in a similar manner to that of thioredoxin reductase which is capable of reducing glutathione disulfide.[78,79]

Since the discovery of Mtr over a decade ago,[71,72] neither the crystal structure nor Mtr-specific inhibitors have been reported, and these represent important areas for future study. Several quinones have been shown to function as "subversive substrates" of Mtr, through promotion of redox cycling and the subsequent generation of superoxide, and are toxic to mycobacteria. Similar subversive substrates have been shown to act against the analogous GR and TryR targets.[80,81] Mtr itself recognises a range of quinone and naphthoquinone derivatives as subversive substrates and therefore this pathway provides a potential strategy for the development of antitubercular chemotherapeutic agents.[72]

1.2.8 Glyoxalase

The ubiquitously present glyoxalase (Glx) system is responsible for the detoxification of methylglyoxal (MG), an unavoidable side product of glycolysis.[82,83] MG is formed during glycolysis when the deprotonation of dihydroxyacetone phosphate (DHAP) by triose phosphate isomerase (TIM) results in phosphate elimination rather than protonation and equilibration to the aldehyde (Scheme 7).[84] While protonation takes place considerably more frequently than phosphate elimination, a high cellular concentration of TIM can result in the accumulation of large quantities of MG. Due to the reactive nature of MG and its ability to form adducts with proteins and nucleic acids, inhibit protein biosynthesis and generate advanced glycation endproducts,[85,86] the Glx system is crucial to maintaining the integrity of the cell.

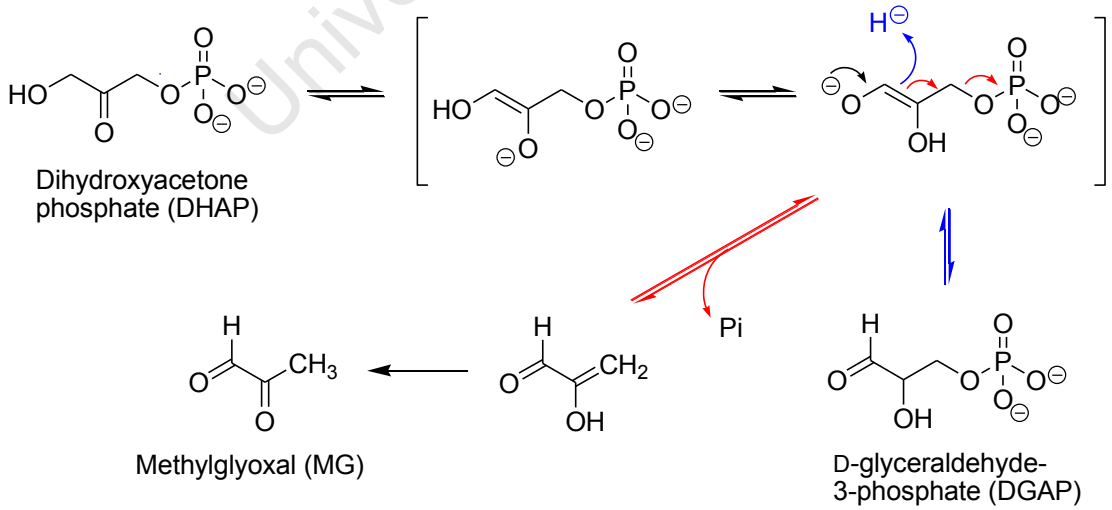

Scheme 7. The triose phosphate isomerase (TIM) pathway leading to the formation of methylglyoxal (MG) (with elimination of inorganic phosphate, Pi) and D-glyceraldehyde-3-phosphate (DGAP) from dihydroxyacetone phosphate (DHAP)[84]

In organisms that produce glutathione, GlxI is a metal-dependant isomerase that converts the methylglyoxal thiohemiacetal of glutathione to *S*-D-lactoylglutathione *via* an enediolate intermediate. GlxII completes the cycle by the hydrolysis of *S*-D-lactoylglutathione to regenerate GSH and form D-lactate (Scheme 8).[83,87] GSH may be substituted with alternate low molecular weight thiols in different organisms, such as trypanothione in the trypanosomatidae, or mycothiol in the actinomycetes. In such cases, the essential function of the Glx system remains the same, with the thiol forming a thiohemiacetal with MG, and ultimately being regenerated by GlxII.

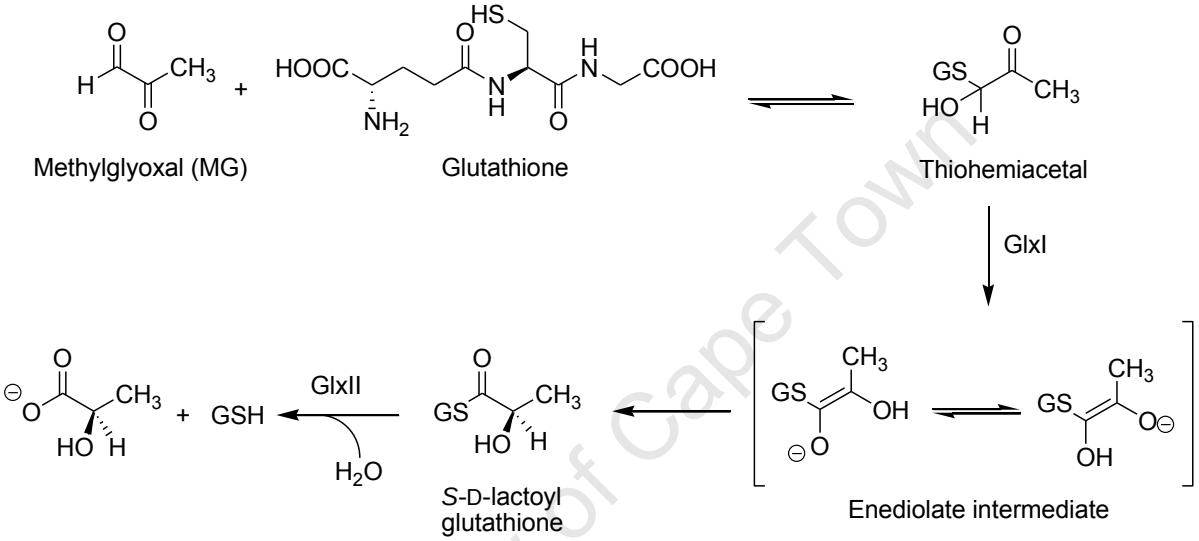

Scheme 8. Glutathione-dependent detoxification of MG by the two enzyme glyoxalase (Glx) system, composed of GlxI and GlxII

The Glx enzyme system has been identified in a wide range of organisms including humans,[88] yeast,[89,90] plants,[91] insects,[83] protozoa (including trypanosomatids)[92,93,] and over forty bacterial species[83,94] (including *E. coli*).[95,96] The presence of a glyoxalase pathway in such a diverse range of organisms supports the possibility of its presence in the *mycobacteria*. The discovery of such a pathway and the enzymes involved would provide a novel target for the development of anti-mycobacterial agents due to its essential role in the removal of cytotoxic MG.

The glyoxalase enzyme system of *Trypanosoma* and *Leishmania* parasitic protozoa is distinct from glutathione-dependent homologues in their dependence on the dithiol, trypanothione (Figure 8), for detoxifying MG.[97,98,99] A second difference between the two enzyme systems is the metal cofactor, with the *Trypanosome* GlxI having a nickel centre and the eukaryote GlxI having a zinc centre. These differences indicate a considerable variation

between the active sites of the Trypanosomatid enzyme and that of the mammalian counterpart, which suggests that the Glx system of the protozoan parasite is a potential chemotherapeutic target.[93]

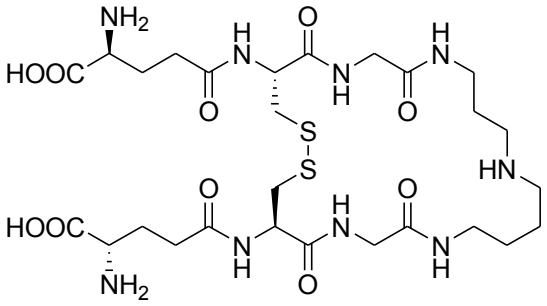

Figure 8. Chemical structure of trypanothione

Similarly, an as yet undescribed mycothiol-dependent glyoxalase system may exist within the *mycobacteria*, and could provide a viable target for chemotherapy with the basis for drug selectivity based on the large structural difference that exists between MSH and GSH and the likely divergent substrate specificity that would exist between the two Glx systems. The search for such a mycobacterial GlxI is described further in Chapter 5.

1.3 Aims and Objectives

The aims of this project were to synthesise several naphthoquinone- and carbazole-1,4-quinone-derived conjugates of a mycothiol-like scaffold that would act as redox cycling subversive substrates of the enzyme, Mtr, or potentially inhibit other mycothiol-dependent or biosynthetic enzymes, in order to develop novel antitubercular lead compounds. The synthesis of these compounds is described in Chapter 2 (naphthoquinone derivatives) and Chapter 3 (carbazole-1,4-quinone derivatives). The cloning, expression and purification of Mtr, in order to generate purified enzyme on which to evaluate the activity of the conjugates, is described in Chapter 4. A further investigation towards the cloning, expression, and purification of a mycobacterial GlxI was also undertaken, and is described in Chapter 5.

References

1. World Health Organisation Factsheet No. 104, November 2010, http://www.who.int/mediacentre/factsheets/fs104/en/index.html
2. L.G. Wayne, *Infect. Immun.*, **1977**, *17*, 528-530
3. B.M. Madison, *Biotech. Histochem.*, **2001**, *76*, 119-125
4. E.N.G. Houben, L. Nguyen and J. Pieters, *Curr. Opin. Microbiol*., **2006**, *9*, 76–85
5. S.H. Kaufmann and A.J. McMichael, *Nat. Med*., **2005**, *11*, S33–S44
6. J.-L. Herrmann and P.-H. Lagrange, *Pathol. Biol.*, **2005**, *53*, 35–40
7. (a) I. Vergne, J. Chua, H.-H. Lee, M. Lucas, J. Belisle and V. Deretic, *PNAS*, **2005**, *102*, 4033-4038; (b) V. Deretic, S. Singh, S. Master, J. Harris, E. Roberts, G. Kyei, A. Davis, S. de Haro, J. Naylor, H.-H. Lee, I. Vergne, *Cell Microbiol*., **2006**, *8*, 719-727
8. Global Tuberculosis Report 2011, World Health Organisation, http://www.who.int/tb/publications/global_report/en/index.html
9. D.A. Rozwarski, G.A. Grant, D.H. Barton, W.R. Jacobs, Jr. and J.C. Sacchettini, *Science*, **1998**, *279*, 98–102
10. F. Wang, P. Jain, G. Gulten, Z. Liu, Y. Feng, K. Ganesula, A.S. Motiwala, T.R. Ioerger, D. Alland, C. Vilchèze, W.R. Jacobs Jr. and J.C. Sacchettini, *Antimicrob. Agents Chemother*., **2010**, *54*, 3776-3782
11. E.A. Campbell, N. Korzheva, A. Mustaev, K. Murakami, S. Nair, A. Goldfarb and S.A. Darst, *Cell*, **2001**,*104*, 901–912
12. P.J. Brennan and H. Nikaido, *Annu. Rev. Biochem.*, **1995**, *64*, 29-63
13. K. Takayama and J.O. Kilburn, *Antimicrob. Agents Chemother*., **1989**, *33*, 1493-1499
14. K. Mikusova, R.A. Slayden, G.S. Besra and P.J. Brennan, *Antimicrob. Agents Chemother*. **1995**, *39*, 2484-2489
15. A.E. Belanger, G.S. Besra, M.E. Ford, K. Mikusova, J.T. Belisle, P.J. Brennan and J.M. Inamine, *PNAS*, **1996**, *93*, 11919-11924
16. Hong Kong Chest Service/British Medical Research Council, *Lancet*, **1981**, *317*, 171-174
17. Y. Zhang and D. Mitchison, *Int. J. Tuberc. Lung Dis*., **2003**, *7*, 6-21
18. (a) O. Zimhony, J.S. Cox, J.T. Welch, C. Vilchèze and W.R. Jacobs, Jr, *Nature Medicine*, **2000**, *6*, 1043-1047; (b) O. Zimhony, C. Vilchèze, M. Arai, J.T. Welch and W.R. Jacobs, Jr., *Antimicrob. Agents Chemother*., **2007**, *51*, 752–754
19. P. Lu, A.C. Haagsma, H. Pham, J.J. Maaskant, S. Mol, H. Lill, D. Bald, *Antimicrob*. *Agents Chemother*., **2011**, *55*, 5354-5357
20. W. Shi, X. Zhang, X. Jiang, H. Yuan, J.S. Lee, C.E. Barry 3rd, H. Wang, W. Zhang, Y. Zhang, *Science*, **2011**, *333*, 1630-1632
21. I. Chopra and P. Brennan, *Tubercle Lung Dis*., **1998**, *78*, 89-98
22. F.C. Neuhaus and J.L. Lynch, *Biochemistry*, 1964, 3, 471-480

23. H.L. David, A. Laszlo and N. Rastogi, *Acta Leprol.*, **1989**, *7***,** 189-194
24. J.A. Caminero, G. Sotgiu, A. Zumla and G.B. Migliori, *Lancet Infect. Dis.*, **2010**, *10*, 621-629
25. A. Banerjee, E. Dubnau, A. Quemard, V. Balasubramanian, K.S. Um, T. Wilson, D. Collins, G. de Lisle and W.R. Jacobs, Jr., *Science*, **1994**, *263*, 227-230
26. P.E.A. Da Silva and J.C. Palomino, *J. Antimicrob. Chemother*., **2011**, *66*, 1417-1430
27. F. Wang, R. Langley, G. Gulten, L.G. Dover, G.S. Besra, W.R. Jacobs, Jr. and J.C. Sacchettini, *J. Exp. Med*., **2007**, *204*, 73-78
28. J.A. Caminero, *Int. J. Tuberc. Lung Dis.,* **2006**, *10*, 829–837
29. E.D. Chan, V. Laurel, M.J. Strand, J.F. Chan, M.-L.N. Huynh, M. Goble and M.D. Iseman, *Am. J. Respir. Crit. Care Med.*, **2004**, *169*, 1103-1109
30. A.S. Ginsburg, J.H. Grosset, W.R. Bishai, *Lancet Infect. Dis.*, **2003**, *3*, 432-442
31. K. Drlica, *Curr. Opin. Microbiol*., **1999**, *2*, 504-508
32. World Health Organisation (2006). Press release, http://www.who.int/mediacentre/news/notes/2006/np29/en/index.html
33. (a) H. Cox and C. McDermid, *Lancet*, **2008**, *372*, 1363-1365; (b) S. Keshavjee, I.Y. Gelmanova, P.E. Farmer, S.P. Mishustin, A.K. Strelis, Y.G. Andreev, A.D. Pasechnikov, S. Atwood, J.S. Mukherjee, M.L. Rich, J.L. Furin, E.A. Nardell, J.Y. Kim and S.S. Shin, *Lancet*, **2008**, *372*, 1403-1409
34. N.R. Gandhi, A. Moll, A.W. Sturm, R. Pawinski, T. Govender, U. Lalloo, K. Zeller, J. Andrews and G. Friedland, *Lancet*, **2006**, *368*, 1575–1580
35. M. Rawat and Y. Av-Gay, FEMS Microbiol. Rev., 2007, 31, 278-292
36. G.L. Newton, K. Arnold, M.S. Price, C. Sherrill, S.B. delCardayré, Y. Aharonowitz, G. Cohen, J. Davies, R.C. Fahey and C. Davis, *J. Bacteriol.*, **1996**, *178*, 1990-1995
37. H.S.C. Spies and D.J. Steenkamp, *Eur. J. Biochem*., **1994**, 224, 203-213
38. S. Sakuda, Z.-Y. Zhou, Y. Yamada, *Biosci. Biotech. Biochem*., **1994**, *58*, 1347-1348
39. G.M. Nicholas, P. Kováč and C.A. Bewley, *J. Am. Chem. Soc*., **2002**, *124*, 3492-3493
40. V.K. Jothivasan and C.J. Hamilton, *Nat. Prod. Rep.*, **2008**, 25, 1091-1117
41. C. Bornemann, M.A. Jardine, H.S.C. Spies and D.J. Steenkamp, *Biochem.J.*, **1997**, *325*, 623-629
42. G.L. Newton, Y. Av-Gay and R.C. Fahey, *J. Bacteriol*., **2000**, *182*, 6958-6963
43. D. Sareen, M. Steffek, G.L. Newton and R.C. Fahey, *Biochemistry*, **2002**, *41*, 6885-6890
44. T. Koledin, G.L. Newton and R.C. Fahey, *Arch. Microbiol*., **2002**, *178*, 331-337
45. M.W. Vetting, P.A. Frantom and J.S. Blanchard, *J. Biol. Chem*., **2008**, *283*, 15834-15844
46. G.L. Newton, P. Ta, K.P. Bzymek and R.C. Fahey, *J. Biol. Chem*., **2006**, *281*, 33910-33920
47. G.L. Newton, N. Buchmeier and R.C. Fahey, *Microbiol. Mol. Biol. Rev.*, **2008**, *72*, 471-494
48. J.H. Park, C.J. Cha and J.H. Roe, *J. Microbiol*., **2006**, *44*, 121-125
49. G.L. Newton, T. Koledin, B. Gorovitz, M. Rawat, R.C. Fahey and Y. Av-Gay, *J. Bacteriol*., **2003**,*185*, 3476-3479
50. N. Buchmeier and R.C. Fahey, *FEMS Microbiol. Lett*., **2006**, *264*, 74-79

51. J.T. Maynes, C. Garen, M.M. Cherney, G.L. Newton, D. Arad, Y. Av-Gay, R.C. Fahey and M.N. James, *J. Biol. Chem.*, **2003**, *278*, 47166-47170
52. X. Huang and M. Hernick, *J. Biol. Chem.*, **2012**, DOI: 10.1074/jbc.M111.320184
53. G.L. Newton, M. Ko, P. Ta, Y. Av-Gay and R.C. Fahey, *Protein Expres. Purif.*, **2006**, *47*, 542–550
54. M. Rawat, S. Kovacevic, H. Billman-Jacobe and Y. Av-Gay, Microbiology, **2003**, *149*, 1341-1349
55. X. Xu, C. Vilchèze, Y. Av-Gay, A. Gómez-Velasco and W.R. Jacobs, Jr, *Antimicrob. Agents Chemother.*, **2011**, *55*, 3133-3139
56. D. Sareen, M. Steffek, G. L. Newton and R. C. Fahey, *Biochemistry*, **2002**, *41*, 6885–6890
57. F. Fan, A. Luxenburger, G.F. Painter and J.S. Blanchard, *Biochemistry*, **2007**, *46*, 11421-11429
58. L.W. Tremblay, F. Fan, M.W. Vetting and J.S. Blanchard, *Biochemistry*, **2008**, *47*, 13326-13335
59. M. Rawat, G.L. Newton, M. Ko, G.J. Martinez, R.C. Fahey, Y. Av-Gay, *Antimicrob. Agents Chemother*., **2002**, *46*, 3348-3355
60. D. Sareen, G.L. Newton, R.C. Fahey and N.A. Buchmeier, *J. Bacteriol*., **2003**, *185*, 6736-6740
61. T. Koledin, G.L. Newton and R.C. Fahey, *Arch. Microbiol*., **2002**, *178*, 331-337
62. G.L. Newton, P. Ta and R.C. Fahey, *J. Bacteriol.*, **2005**, *187*, 7309-7316
63. N.A. Buchmeier, G.L. Newton and R.C. Fahey, *J. Bacteriol.*, **2006**, *188*, 6245-6252
64. M.W. Vetting, S.L. Roderick, M. Yu and J.S. Blanchard, *Protein Sci*., **2003**, *12*, 1954-1959
65. G.L. Newton, Y. Av-Gay and R.C. Fahey, *Biochemistry*, **2000**, *39*, 10739-10746
66. M. Steffek, G.L. Newton, Y. Av-Gay and R.C. Fahey, *Biochemistry*, **2003**, *42*, 12067-12076
67. M. Rawat, M. Uppal, G. Newton, M. Steffek, R.C. Fahey and Y. Av-Gay, *J. Bacteriol*., **2004**, *186*, 6050-6058
68. G.M. Nicholas, L.L. Eckman, G.L. Newton, R.C. Fahey, S. Ray and C.A. Bewley, *Bioorg. Med. Chem.*, **2003**, *11*, 601-608
69. G.M. Nicholas, G.L. Newton, R.C. Fahey and C.A. Bewley, *Org. Lett*., **2001**, *3*, 1543-1545
70. N. Pick, M. Rawat, D. Arad, J. Lan, A.S. Kende and Y. Av-Gay, *J. Med. Microbiol*., **2006**, *55*, 407-415
71. M.P. Patel and J.S. Blanchard, *J. Am. Chem. Soc*., **1998**, *120*, 11538-11539
72. M. P. Patel and J. S. Blanchard, *Biochemistry*, **1999**, *38*, 11827-11833
73. M.J.G. Stewart, V.K. Jothivasan, A.S. Rowan, J. Wagg and C.J. Hamilton, *Org. Biomol. Chem*., **2008**, *6*, 385-390
74. C. Sassetti, D. Boyd, E. Rubin, *Mol. Microbiol*., **2003**, *48*, 77-84
75. R.A. McAdam, S. Quan, D.A. Smith, S. Bardarov, J.C. Betts, F.C. Cook, E.U. Hooker, A.P. Lewis, P. Woollard, M.J. Everett, P.T. Lukey, G.J. Bancroft, W.R. Jacobs Jr., K. Duncan, *Microbiology*, **2002**, *148*, 2975-2986
76. D. Hayward, I. Wiid and P.D. van Helden, *IUBMB Life*, **2004**, *56*, 131-138

77. M. Rawat, S. Kovacevic, H. Billman-Jacobe and Y. Av-Gay, *Microbiology*, **2003**, *149*, 1341-1349
78. S.M. Kanzok, A. Fechner, H. Bauer, J.K. Ulschmid, H.M. Muller, J. Botella-Munoz, S. Schneuwly, R. Schirmer and K. Becker, *Science*, **2001**, *291*, 643-646
79. G. Salinas, M.E. Selkirk, C. Chalar, R.M. Maizels and C. Fernandez, *Trends Parasitol*., **2004**, *20*, 340-346
80. C. Biot, H. Bauer, R.H. Schirmer and E. Davioud-Charvet, *J. Med. Chem.*, **2004**, *47*, 5972-5983
81. L. Salmon-Chemin, E. Buisine, V. Yardley, S. Kohler, M.A. Debreu, V. Landry, C. Sergheraert, S.L. Croft, R.L. Krauth-Siegel and E. Davioud-Charvet, *J. Med. Chem*., **2001**, *44*, 548-565.
82. I.A. Rose and J.S. Nowick, *J. Am. Chem. Soc*., **2002**, *124*, 13047-13052
83. P.J. Thornalley, *Biochem. Soc. Trans*., **2003**, *31*, 1343-1348
84. J.P. Richard, *Biochem. Soc. Trans*., **1993**, *21*, 549-553
85. S.R. Thorpe and J.W. Baynes, *Drug. Aging*, **1996**, *9*, 69–77
86. M. Krautwald and G. Münch, *Exp. Gerontol.*, 2010, 45, 744-751
87. I.R. Booth, G.P. Ferguson, S. Miller, C. Li, B. Gunasekera, S. Kinghorn, *Biochem*. *Soc*. *Trans*., **2003**, *31*, 1406-1408
88. a) A.D. Cameron, M. Ridderstrom, B. Olin, B. Mannervick, *Structure*, **1999**, *7*, 1067-1078; b) A.D. Cameron, B. Olin, M. Ridderstrom, B. Mannervik, T.A. Jones, *EMBO J.*, **1997**, *16*, 3386-3395; c) A.D. Cameron, M. Ridderstrom, B. Olin, M.J. Kavarana, D.J. Creighton, B. Mannervik, *Biochemistry*, **1999**, *38*, 13480-13490
89. Y. Inoue and A. Kimura, *J. Biol. Chem.*, **1996**, *271*, 25958-25965
90. Y. Inoue, K. Maeta, W. Nomura, *Semin. Cell Dev. Biol*., **2011**, *22*, 278-284
91. V.S. Veena Reddy and S.K. Sopory, *Plant J.*, **1999**, *17*, 385-395
92. R. Iozef, S. Rahlfs, T. Chang, H. Schirmer and K.Becker, *FEBS Lett*., **2003**, *554*, 284-288
93. S.C. Chauhan, P.K. Padmanabhan, R. Madhubala, *Curr Drug Targets*, **2008**, *9*, 957-65
94. S.L. Clugston, E. Daub and J.F Honek, *J. Mol. Evol*., **1998**, *47*, 230-234
95. M.M. He, S.L. Clugston, J.F. Honek, B.W. Matthews, *Biochemistry*, **2000**, *39*, 8719-8727
96. C.E. Hand, Investigations into Intracellular Thiols of Biological Importance, PhD Thesis, **2007**, University of Waterloo, Ontario, Canada
97. N. Greig, S. Wyllie, T.J. Vickers, A.H. Fairlamb, *Biochem. J*., **2006**, *400*, 217-223
98. T.J.Vickers, N. Greig, A.H. Fairlamb, *Proc. Natl. Acad. Sci. USA*, **2004**, *101*, 13186-13191
99. R.K. Padmanabhan, A. Mukherjee, R. Madhubala, *Biochem. J*., **2006**, *393*, 227-234

Chapter 2
Naphthoquinone-Derived Target Molecules

2.1 Quinones in Drug Discovery

The quinone scaffold is a common component of many natural products and has been shown to display a range of activities including anticancer, antibacterial, antimalarial, antifungal and antimycobacterial.[1,2,3] The biological activity is derived from the quinone's ability to accept one or two electrons and generate a radical anion or dianion. Additional cytotoxic effects include alkylation of thiols, amines and DNA residues, and oxidation of essential protein thiols by activated oxygen species. The capacity for accepting or donating single electrons is influenced by the substituents on the quinone, which modulate the redox properties that cause oxidative stress.[4] The flavin cofactors in flavoenzymes, such as the disulfide reductases, can exist as stable semiquinone radicals. This allows flavoenzymes to catalyze the one electron reduction of quinone electron acceptors, such as the naphthoquinones, to semiquinones, which in turn can mediate the reduction of molecular oxygen to superoxide anion radicals with associated regeneration of the quinone.[1,2] This redox cycling, with attendant superoxide generation, leads to high levels of hydrogen peroxide and cell damage.

Many naphthoquinone drugs, including menadione, plumbagin and lapachol (Figure 1), display activity against the trypanosomes responsible for several human parasitic diseases, including African sleeping sickness (*Trypanosoma brucei rhodesiense* and *Trypanosoma brucei gambiense*), Chagas' disease (*Trypanosoma cruzi*) and Kala-azar (*Leishmania donovani*).[5,6,7] These parasitic protozoa are particularly sensitive to oxidative stress and utilize the unique antioxidant, trypanothione, $T(SH)_2$ to maintain redox equilibrium.[8] $T(SH)_2$ is maintained in its reduced form by the flavoenzyme, trypanothione reductase (TryR), which is one of the enzymes targeted by naphthoquinones. Selectivity of these naphthoquinones for TryR over human glutathione reductase (hGR) is reportedly based on charge differences at the catalytic sites of the two enzymes.[9] Thus the active site of GR has positively charged residues that are complimentary to the carboxyl groups of the glycine residues present in

glutathione and these glycines are in amide linkage to spermidine in trypanothione. 1,4-Naphthoquinones,[10,11,12] including menadione and plumbagin,[13] have been shown to act as subversive substrates of *Trypanosoma cruzi* TryR by inhibiting the physiological reduction of $T(S)_2$ and generating superoxide, following the single-electron reduction of the quinone by the flavoprotein, as described above. Conversely, against GR, 1,4-naphthoquinones largely display weak, reversible inhibition.[14,15]

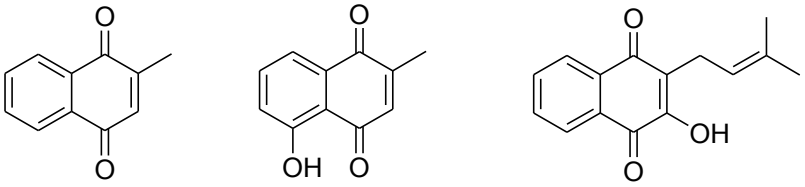

Menadione Plumbagin Lapachol

Figure 1. Chemical structures of the 1,4-naphthoquinones, menadione, plumbagin and lapachol

By analogy, it should be likely that this class of compounds also displays such subversive substrate activity against Mtr, which performs an analogous role to that of GR and TryR. Sufficient structural differences between the natural substrates should impart a considerable degree of selectivity to such inhibitors, if synthesised in such a way as to incorporate a fragment of the substrate through which the selectivity could be derived.

Several 1,4-naphthoquinones were evaluated for their subversive substrate activity against Mtr, which was measured as maximum turnover rate (k_{cat}) over the substrate binding efficiency (K_m). This value (k_{cat}/K_m) was used to compare subversive substrate activity with whole cell antitubercular activity, and the results are summarised in Table 1.[16]

Table 1. Subversive substrate activity (k_{cat}/K_m) of naphthoquinones with Mtr compared with whole cell antitubercular activity, MIC (μM)[17]

	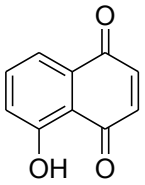 Juglone	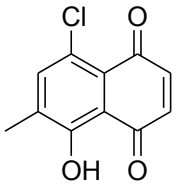	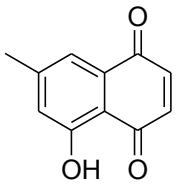 Methyljuglone
K_m (μM)	320	36	250
k_{cat}/K_m ($M^{-1}.s^{-1}$)	3400	16000	9300
MIC (μM)	6	22	3

	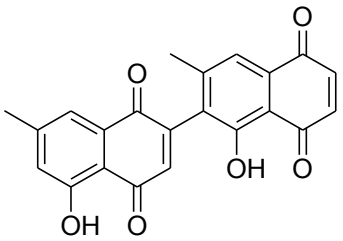 Diospyrin	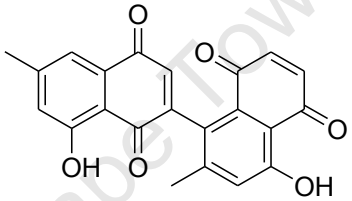 Neodiospyrin
K_m (μM)	33	63
k_{cat}/K_m ($M^{-1}.s^{-1}$)	3600	4900
MIC (μM)	21	27

Although several of these compounds displayed anti-tubercular activity in whole-cell assays, and several of them showed good subversive substrate activity, there was no direct relationship between the two properties, suggesting that the biological activity was derived from interaction with alternate or multiple redox-active proteins and enzymes. This study supported earlier findings that 1,4-naphthoquinones display biological activity against *M. tuberculosis*.[3] Despite the lack of selectivity for Mtr, it is conceivable that by attaching a mycothiol scaffold to the structure, the naphthoquinone might display enhanced activity against Mtr, or against one of the mycothiol biosynthetic enzymes. This strategy has already been explored and reported by Gammon and co-workers,[18] who attached a 1,4-naphthoquinone to a phenylthioglucosamine scaffold to generate a class of inhibitors that displayed strong activity against the mycothiol enzymes, MshB and Mca (Figure 2).

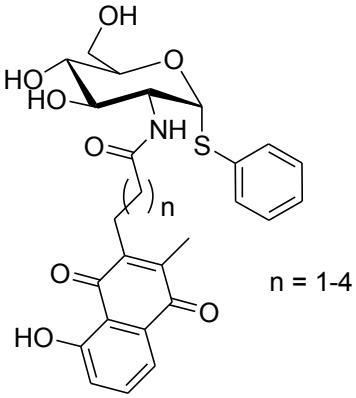

Figure 2. Naphthoquinone-glucosamine conjugates with inhibitory activity against MshB and Mca

Following on from this, similar inhibitors with select structural differences were proposed as target molecules for this project, and their design and synthesis is described below.

2.2 Target Molecule Design

The general structure of the naphthoquinone-derived target molecules for this project is illustrated below in Figure 3. This includes a naphthoquinone coupled to a mycothiol-like scaffold (glucosamine with *N*-acetyl cysteine side chain), and a *myo*-inositol surrogate at the anomeric position of the sugar, which could be either a phenylthio or glyceryl unit. Previously published findings from our research group have demonstrated the inhibitory activity of similar naphthoquinone derivatives, where X=SPh and the NHAc is absent on the linker, against the mycothiol enzymes MshB and Mca.[18] In this study, the utility of this class of inhibitors has been extended to include the enzyme Mtr.

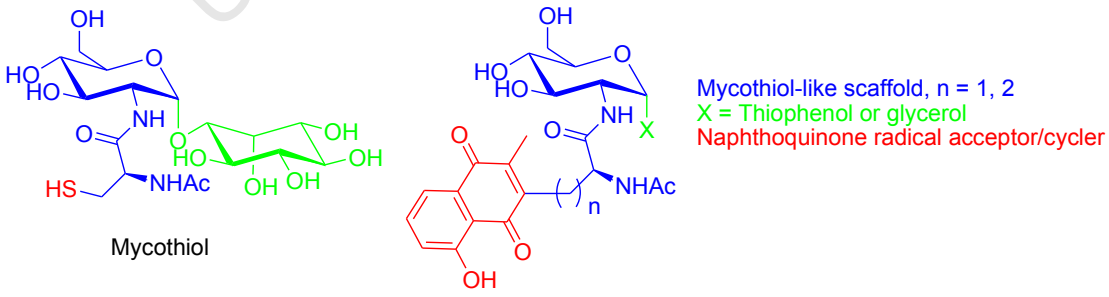

Figure 3. Chemical structure of MSH and target inhibitors

The structure of the target molecule with n = 1 is similar to MSH, except for the glycosyl substituent and the replacement of the sulfhydryl group with a naphthoquinone. The positioning of the electrophilic quinone C=C at the point where the disulfide bond of

mycothiol disulfide (MSSM) would be, invites the possibility of alkylation of the Mtr active-site thiolate, Cys_{39}-S^-. This thiolate has the native function of liberating free MSH from MSSM by nucleophilic attack at one of the sulfurs of the disulfide bond.[19,20] There is potential, therefore, for this compound to irreversibly inhibit Mtr, in addition to the possibility of acting as a subversive substrate. The naphthoquinone used was 5-hydroxy-2-methyl-1,4-naphthoquinone, also known as plumbagin (due to its isolation from the plant genus *Plumbago*). Although several different naphthoquinones with different substitution patterns exist, this particular derivative was selected since (i) it is commercially available, (ii) it has a methyl at the 2-position thereby controlling substitution of the quinone exclusively at the 3-position, and (iii) derivatives of this type were shown to display the highest activity as subversive substrates against the related enzymes, trypanothione reductase and lipoamide dehydrogenase.[2]

The substrate specificity of Mtr with respect to the *N*-acyl substituent on the natural substrate, MSSM, has been demonstrated by comparative assays of the symmetrical disulfides of the *N*-formyl (fCys-GlcN-Ins), *N*-succinyl (succ-Cys-GlcN-Ins) and des-acetyl (Cys-GlcN-Ins) derivatives of MSSM (Figure 4).[21]

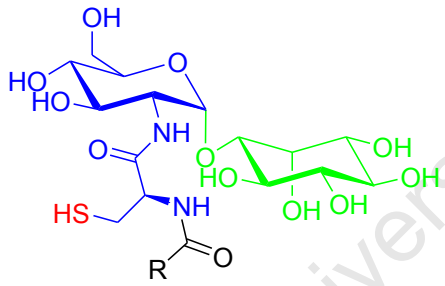

R = CH_3	MSH
R = H	fCys-GlcN-Ins
R = $^-OOCCH_2CH_2$	Succ-Cys-GlcN-Ins

Figure 4. Chemical structure of mycothiol and its acyl derivatives

These results indicated that the relative rates of reaction, relative to MSSM (100 %), were 13 %, 0.8 % and ≤ 4 %, respectively, for fCys-GlcN-Ins, succ-Cys-GlcN-Ins and Cys-GlcN-Ins. This illustrates that an acetate on the cysteinyl amine contributes significantly to binding in the active site of Mtr. Consequently, the design of the target molecules has taken this factor into account, and includes an NHAc group in appropriate configuration on the linker between the naphthoquinone and glucosamine, derived from aspartic (n = 1, Figure 3) and glutamic (n = 2, Figure 3) acids respectively, in order to maximise active-site binding.

The incorporation of the *myo*-inositol substituent on mycothiol is a laborious, multi-step process that requires several selective protecting group manipulations to arrive at the product with the correct stereochemistry,[22] which is clearly an undesirable factor when trying

to develop a new drug. A range of analogues with alternative aglycones has been synthesised as substrate analogues of various mycothiol enzymes in order to simplify the synthetic route. These alternative anomeric substituents have included quinic acid,[23] methoxy and benzyloxy groups,[24] cyclohexylthiol,[25] cyclohexylsulfone,[26] and thiophenol,[18] the latter being one of the target aglycones in this project. Most of these substitutions resulted in a significant reduction in active-site binding/activity relative to the natural substrate, suggesting that the *myo*-inositol fragment is a crucial component of substrate recognition for the mycothiol biosynthetic enzymes. It also appears that the correct 1-D-*myo*-inositol stereoisomer is required, since the 1-L-*myo*-inositol isomer was shown to display no deacetylase activity as a substrate for MshB.[27]

Notwithstanding the foregoing evidence for the requirement of the *myo*-inositol component in alternative substrates and/or inhibitors, the practical need for a simplified derivative led to consideration of two alternatives. Firstly, phenylthio-glycosides were considered, due to the literature reports of moderate activity of these analogues, and secondly, (2*S*)-glyceryl glycosides, which could be considered to be truncated inositol fragments, with the correct stereochemistry in the vicinity of the glycosidic linkage, and with freely rotating hydroxyl groups that would be available to participate in active-site hydrogen-bonding, should this be a factor, thus maintaining a similar binding affinity to that of the natural substrate (Scheme 1).

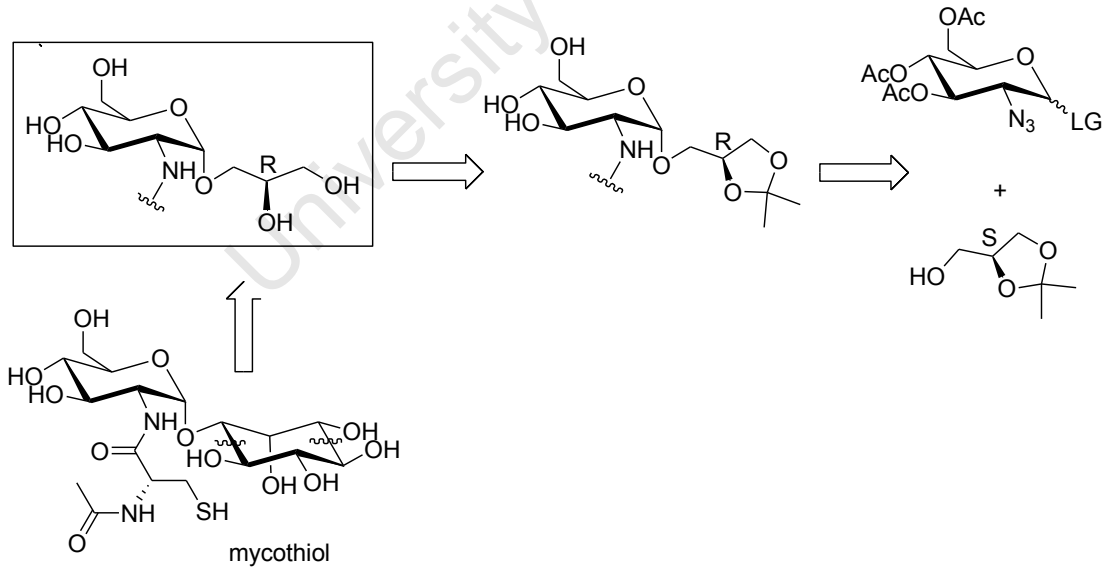

Scheme 1. Retrosynthetic analysis of the general structure of a mycothiol derivative with a glycerol aglycone. The theoretical disconnection positions on the 1-D-*myo*-inositol substituent of mycothiol is indicated, illustrating the rationale behind the selection of the (*S*)-enantiomer of isopropylidene glycerol as glycosyl acceptor. The acetylated 2-azidoglucose with a leaving group (LG) at the anomeric position is given as the donor.

2.3 Retrosynthetic analysis of Target Molecules

A retrosynthetic analysis of the naphthoquinone-derived target molecules is given below in Scheme 2. The final structure **I** was envisaged to have been formed from intermediate **II**, after removal of the acetate protecting groups and conversion of the Boc-protecting group to the desired acetate. The requirement of the Boc protecting group was firstly due to a lack of commercial availability of the *N*-acetate, and secondly due to its resistance to cleavage under the basic conditions that were used for debenzylation in the second step of the synthesis. Performing a disconnection of **II** at the C-N bond affords the two amide coupling partners, **III** and **IV**. Intermediate **III** can be obtained from the azido sugar, **V**, by hydrogenation. This intermediate represents the glycosylated product where X = thiophenol or glycerol, both of which are proposed to be prepared from starting material, tetra-*O*-acetyl 2-azidoglucose **VI**. Disconnection of peptide coupling partner **IV** at the quinone junction, with an oxidative decarboxylation in mind, gives the plumbagin starting material **VII** and selectively-protected aspartic and glutamic amino acids **VIII**.

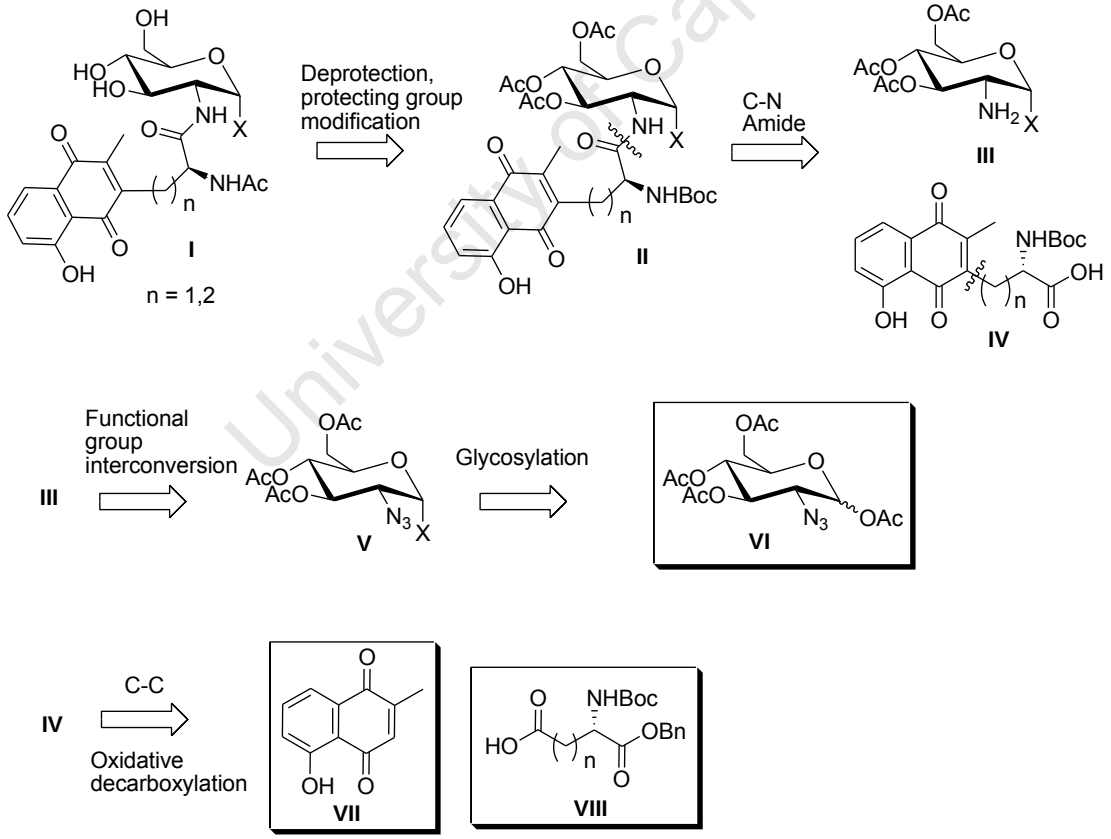

Scheme 2. Retrosynthetic analysis of the naphthoquinone-derived target molecules

2.4 Results

2.4.1 Synthesis of the Glucosamine-Derived Thioglycoside

The synthesis of thioglycoside **2.5**, having a selectively unprotected 2-amino group, is outlined in Scheme 3 and Scheme 4 below. This compound is a key intermediate in the synthesis of a number of target molecules in this project, and its preparation requires the amine to be protected or masked as in a non-participating form to facilitate selective synthesis of an α–thioglycoside. The classic 2-azido-glucose approach was thus chosen, and the introduction of the azide at C-2 achieved by diazotransfer to glucosamine using triflic azide **2.2**. This reagent was prepared by reacting triflic anhydride **2.1** with sodium azide in an emulsion of H_2O/toluene at 0 °C (Scheme 3), to provide a 1 M stock solution after work up.[28] This reagent is shock-sensitive and had to be handled with care.

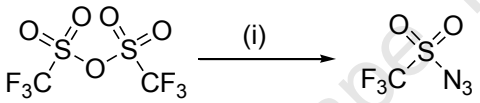

2.1 **2.2**

Scheme 3. (i) NaN_3, H_2O/toluene, 0 °C

The triflic azide **2.2** was then reacted with glucosamine hydrochloride **2.3** in the presence of $CuSO_4$ as catalyst to yield the unprotected 2-azidoglucose **2.4**. After prolonged drying under reduced pressure, this was acetylated with acetic anhydride in pyridine to produce **2.5** in 89 % yield over two steps.

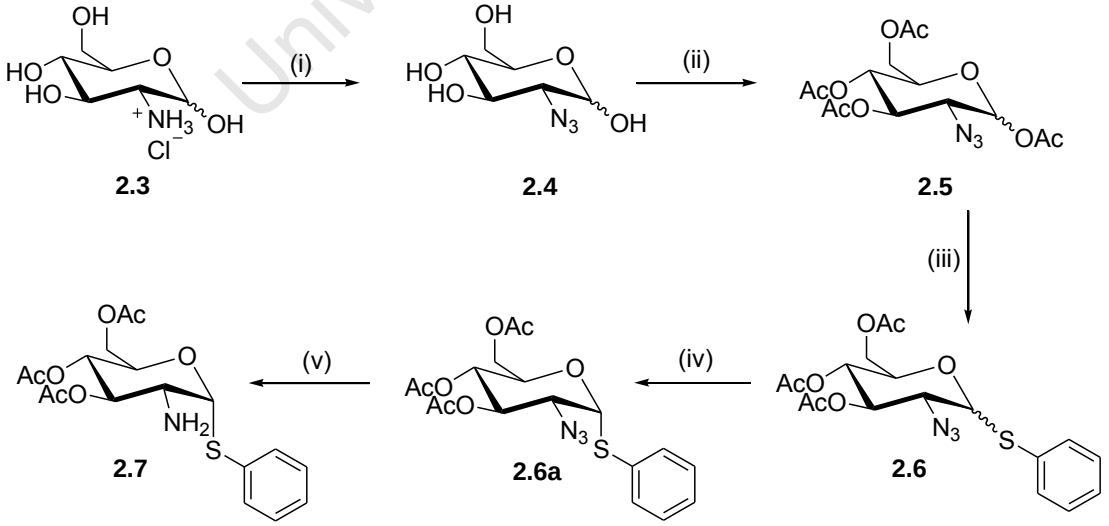

2.3 **2.4** **2.5**

2.6 **2.6a** **2.7**

Scheme 4. Synthesis of acetylated thioglycoside: (i) **2.2**, $NaHCO_3$, $CuSO_4.5H_2O$, H_2O/MeOH/toluene, 15 h, r.t.; (ii) Ac_2O, pyridine, 0 °C – r.t., 18 h, 89 %; (iii) $BF_3.OEt_2$, dry CH_2Cl_2, PhSH, reflux, 80 %; (iv) recrystallisation from EtOH (80 %; α: 46 % isolated); (v) H_2, Pd/C, Et_2O, 24 h, 99 %.

Thioglycosylation of acetylated intermediate **2.5** was attempted in dry CH_2Cl_2 using $BF_3.Et_2O$ as Lewis acid, according to a reported literature procedure.[29] However, several attempts on a small-scale (60 - 84 mg) were unsuccessful in producing any detectable product, even after prolonged stirring at room temperature or refluxing for several days. A trial reaction (51 mg of **2.5**) using $SnCl_4$ as the Lewis acid was also attempted with no detectable product. It was only when the reaction was scaled-up that the desired product was detected. On a scale of 142 mg of **2.5** the thioglycoside product was produced as a mixture of α/β anomers in 48 % yield after refluxing for 14 h. From these results, it appeared that the reaction was highly sensitive to moisture, and that on a small scale the proportion of residual water in the reaction mixture was sufficient to prevent the reaction from proceeding due to hydrolysis of the Lewis acid. It should be noted that a reaction on a 60 mg scale required 92 μl of $BF_3.OEt_2$ which could be easily consumed by a relatively small amount of water (~38 μl). Following this finding, the reaction was scaled up to start with 10 g of **2.5**, and after refluxing for 14 h, the starting material was completely consumed and the desired thioglycoside obtained as an α/β mixture in 80 % yield. The α isomer crystallized selectively from EtOH in 46 % yield.

Reduction of the azide was achieved by mild hydrogenation over Pd/C. Initially, the reaction was performed in ethanol, requiring a subsequent relatively long period of heating under vacuum on the rotary evaporator to remove solvent. It appeared that these conditions promoted an undesired acetyl migration to the free NH_2 group. The solvent was then changed to Et_2O, which resulted in a longer reaction time for complete reduction (24 h vs. 16 h for ethanol), but a far simpler recovery of the product as the Et_2O was removed relatively easily at room temperature on the rotary evaporator. Initially the product was purified by column chromatography, but the problem of removing the solvent was once again encountered, and in subsequent attempts the amine product was used without purification in the next step. The reduction proceeded cleanly in Et_2O, with the only impurity being the NAc side product, which if handled carefully, could be reduced to a trace impurity. Consequently the reaction yields increased to near quantitative after filtration through Celite and removal of solvent.

The metal-catalysed diazo transfer reaction for the synthesis of azido sugars from amino sugars [step (i), Scheme 4] was first reported by Wong and co-workers,[30] who later also proposed the likely mechanism.[31] This is illustrated below in Scheme 5. Amine complexation to the Cu(II) catalyst gives rise to intermediate **2.8**. Due to the electron-withdrawing nature of the triflic group, the terminal nitrogen of the azide is electrophilic and

can be attacked by the glucosamine nitrogen under basic conditions to form the copper-stabilised tetrazene **2.10** after deprotonation of intermediate **2.9**. The tetrazene can then undergo one of two pathways, indicated in blue and red, to either form the 2-azidoglucose product (red pathway) or regenerate the starting triflic azide (blue pathway), possibly *via* a reverse [3 + 2] dipolar cycloaddition. Both pathways would lead to the formation of an imido complex, either **2.11** or **2.13**, in equilibrium with one another, as supported by computational results by Brandt *et al*.[32] From here, coordination of the glucosamine starting material to **2.11** could eventually lead to the formation of **2.8** and thereby continue the catalytic cycle to the stabilised tetrazene **2.10** and subsequent 2-azidoglucose reaction product. Alternatively, interaction of **2.13** with triflic azide could also give rise to the tetrazene intermediate.

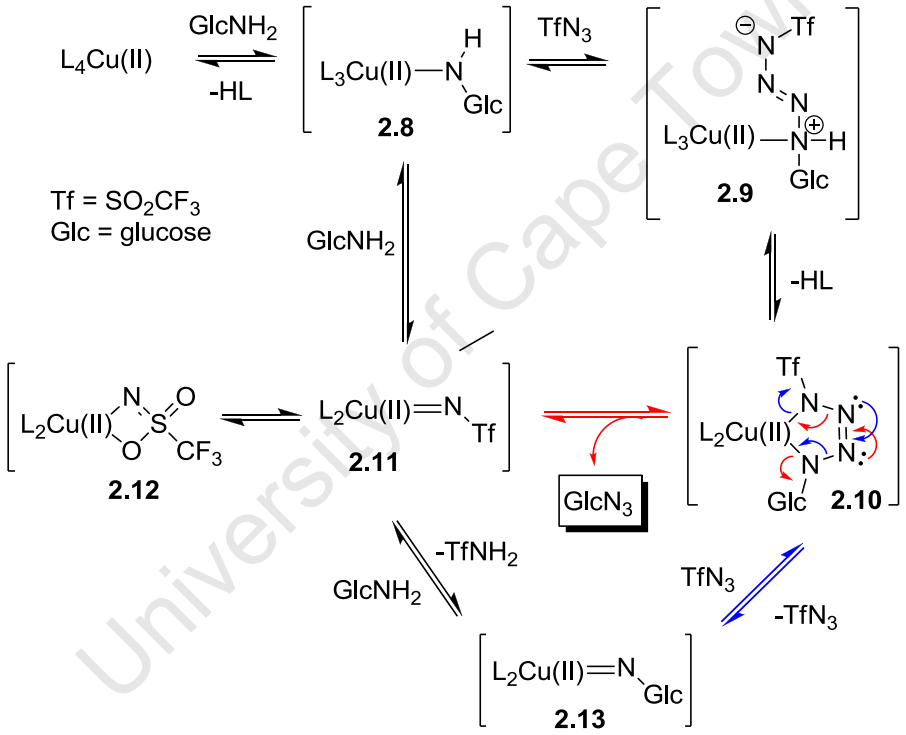

Scheme 5. Proposed mechanism of copper-catalysed diazotransfer reaction[31]

2.4.2 Attempts Toward the Synthesis of a Glycerol Glycoside

The synthesis of a glycerol glycoside required careful consideration of several variables associated with the glycosylation reaction. Firstly, since an α-glycoside was required, the glycosyl donor had to have a non-participating group at C-2. This was to be the site of

further derivatisation, and therefore an azide was selected for its non-participating character and also since it can be considered to be a masked amine.

Secondly, the influence of the protecting groups on the success of the glycosylation could also be a factor, and this was investigated by performing the reaction with both acetate (potentially disarming) and benzyl (potentially arming) protecting groups. There has been extensive literature published on this effect and it seemed prudent to evaluate it as a factor.[33]

Thirdly, an appropriate glycosylation strategy had to be selected. In general, the standard methods for 1,2-cis *O*-glycosylations include (i) the Schmidt trichloroacetimidate approach,[34] (ii) the use of a glycosyl halide donor,[35,36] and (iii) the use of a thioglycoside donor,[37,38] although numerous other approaches do exist.[39] Each of these three glycosylation strategies were investigated, with procedures selected from the literature that utilised substrates with the greatest structural similarity to the target reaction. These are described in detail below.

The first strategy employed a 2-azidoglucosyl trichloroacetimidate as donor, which was treated with an isopropylidene glyceryl acceptor using trimethylsilyl triflate (TMSOTf) or $BF_3.OEt_2$ as activator. Precedent for this reaction was provided by the published synthesis of an isopropylidene glyceryl glucose derivative by Wu *et al* (Table 2).[40]

Table 2. Glycosylation of (*S*)-isopropylidene glycerol with trichloroacetimidate donor[40]

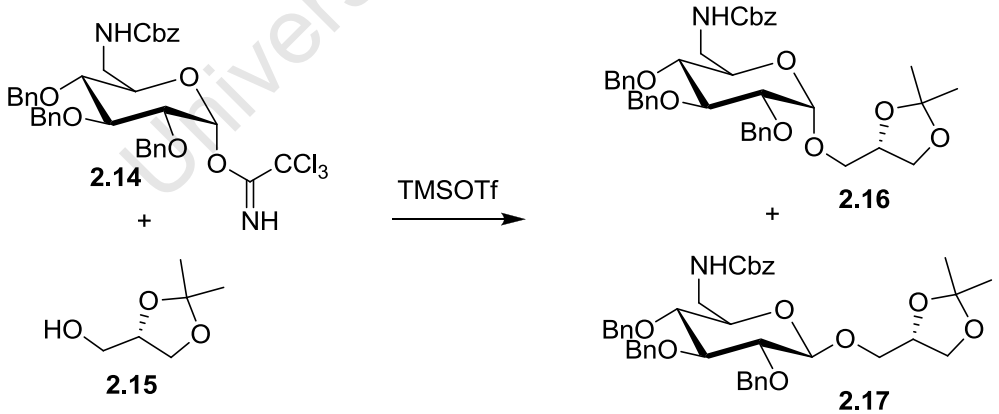

Entry	**2.14** (equiv.)	Solvent	Time/h	α:β[a]	Yield/%
1	1.2	CH_2Cl_2	0.5	5:1	94.0
2	1.2	CH_2Cl_2:Et_2O = 1:1	1.0	5:1	90.1
3	1.2	CH_2Cl_2:Et_2O = 1:5	6.0	8:1	80.2
4	1.2	Et_2O	6.0	Only α[b]	78.2

[a] Determined from the ^{1}H NMR spectrum

[b] Trace β isomer, which could be isolated in later steps

The published reaction gave excellent yields in CH_2Cl_2, Et_2O and mixtures of the two solvents, and increasing α-selectivity as the proportion of Et_2O in the solvent mix increased. The conversion of an α-trichloroacetimidate donor to an α-enriched product suggests that the reaction proceeded *via* an oxocarbenium ion, and the selectivity results suggest that the oxocarbenium ion was stabilised by coordination of Et_2O in a β-orientation, which then facilitated S_N2 attack by the acceptor to generate an α-product.

The reaction conditions utilised for this approach are summarised below in Scheme 6. In the preparation of the glycosyl donor, the tetra-*O*-acetyl-2-azidoglucoside **2.5** was used as starting material. Selective anomeric deprotection of **2.5** was successfully achieved using ethylene diamine and acetic acid: under these conditions the mono-protonated ethylene diamine was generated as the reactive species, which then selectively removed the anomeric acetate by transacetylation, forming alcohol **2.18** in quantitative yield. The trichloroacetimidate was then generated by treatment of the anomeric alcohol with trichloroacetonitrile in the presence of K_2CO_3 in a respectable yield of 74 %. A mixture of anomers was employed for the glycosylation since the literature suggested the reaction outcome was independent of the starting material stereochemistry (Table 2). The reaction was first carried out utilising trimethylsilyl triflate (TMSOTf) as activator in anhydrous diethylether, in accordance with the most successful literature conditions, however, this failed to generate the desired glyceryl glycoside with no reaction product visible by thin layer chromatography (TLC). $BF_3.OEt_2$ was then employed as an alternative activating agent, since it has been successfully used in our laboratory as an activator of glycosyl trichloroacetimidates.[41] However, this approach also failed to generate the desired product, instead forming the anomeric alcohol starting material, **2.18**. An attempt was made, perhaps ambitiously, to convert the acetate protecting groups of the trichloroacetimidate to more activating benzyl groups, in a single step employing the conditions described by Misra and co-workers,[42] although this resulted in decomposition of the substrate due to the harsh reaction conditions and the high reactivity of the imidate. Time constraints precluded the possibility of preparing the benzylated trichloroacetimidate and it could therefore not be evaluated as a glycosyl donor, although it might have displayed superior reactivity to the acetylated analogue by way of the inductive effect of the benzyl groups.

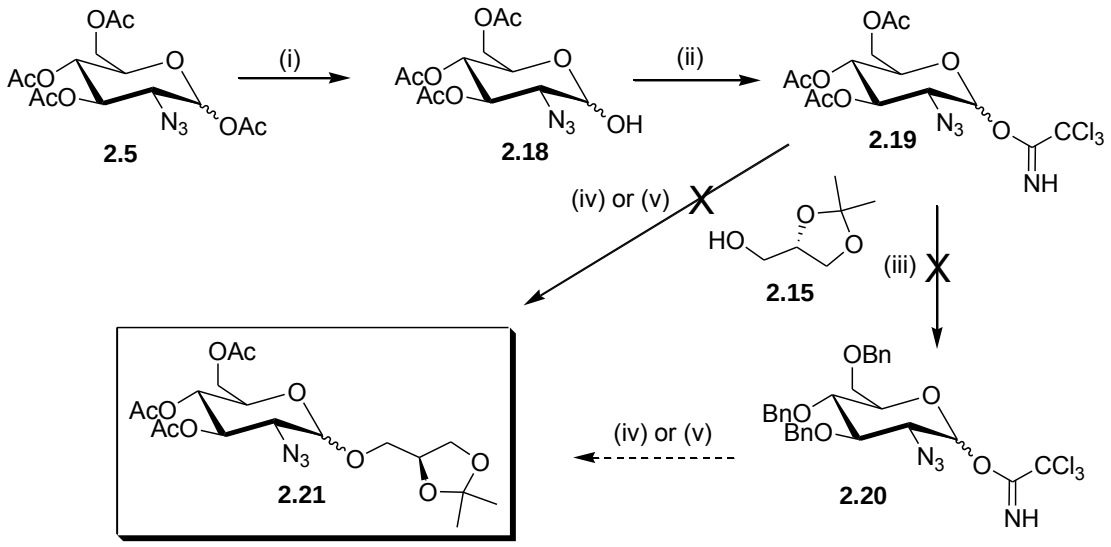

Scheme 6. Attempted synthesis of glycerol glycoside. (i) Ethylene diamine, AcOH, 18 h, r.t., quantitative; (ii) trichloroacetonitrile, K_2CO_3, dry CH_2Cl_2, r.t., 2 h, 74 %; (iii) BnBr, TBAI, NaOH, THF, r.t., 1h; (iv) **2.15**, TMSOTf, dry Et_2O, r.t., 1 h 15 min; (v) **2.15**, $BF_3.OEt_2$, dry CH_2Cl_2, 0 °C, 3 h;

The second procedure that was explored utilised a glycosyl fluoride as donor, with $BF_3.OEt_2$ as activator. The literature precedent for this approach was provided by the reported glycosylation of a *myo*-inositol derivative in high yield and α-selectivity using an acetylated glucosyl fluoride acceptor in previously published work by our group (see Scheme 7).[43] After a reaction time of 2 h, the glycosylated product was obtained in 73 % yield, predominantly as the α anomer (α:β >99:1). Interestingly, isomerisation of the double bond on the substituent at the 2-position of the sugar took place during the glycosylation. Structurally, the fluorinated donor in this published reaction bears a close resemblance to the fluorinated donor that was used in the glycerol glycosylation reaction, with the only difference being the identity of the non-participating group at the 2-position (prenyl vs. azide). There is, however, a great difference structurally between the benzylated *myo*-inositol in the reported reaction and the isopropylidene glycerol acceptor of the proposed glycosylation reaction.

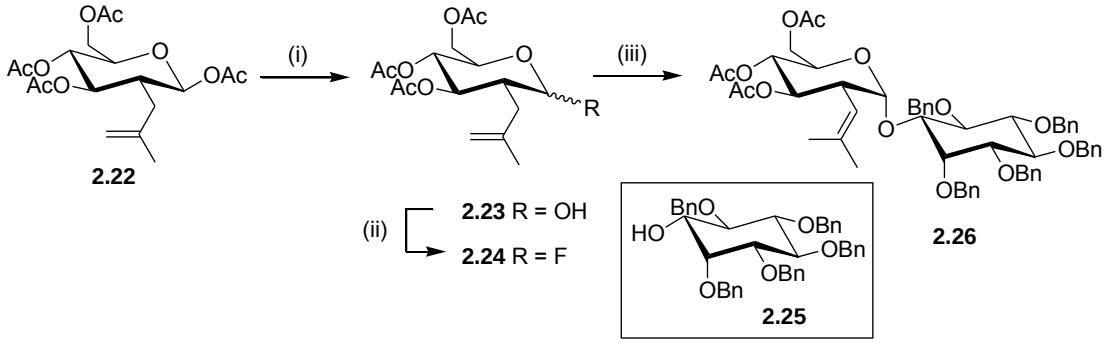

Scheme 7. Reported glycosylation of an inositol derivative utilising a glucosyl fluoride as donor and $BF_3.OEt_2$ as activator. (i) Hydrazine acetate (2 eq), DMF, 60 °C, 30 min, 98 %; (ii) DAST (3 eq), THF, r.t., 30 min, 90 % (α:β=2:1); (iii) **2.24** (1.4 eq), **2.25** (1.0 eq), $BF_3.Et_2O$ (5 eq), anhydrous CH_2Cl_2, 4 Å ms, r.t., 2 h, 73% (α:β >99:1).[43]

Precedent for the use of a 2-azidoglucosyl fluoride as donor in a glycosylation reaction with a *myo*-inositol derivative as acceptor is given by the reported reaction of Cottaz *et al* (Scheme 8).[36] Here they employed a benzyl-protected 2-azidoglucosyl fluoride donor and zirconocene dichloride, tetramethyl urea and silver perchlorate activating agents to selectively effect α-glycosylation of a selectively-protected *myo*-inositol acceptor. They report a 34 % yield for the reaction after removal of a para-methoxybenzyl (PMB) protecting group and subsequent chromatography.

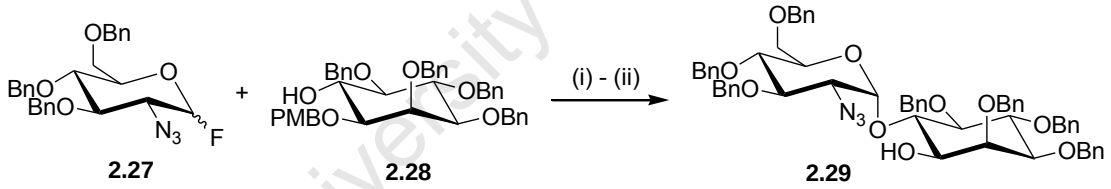

Scheme 8. Reported glycosylation of a *myo*-inositol derivative utilising a 2-azidoglucosyl fluoride as donor. (i) Donor (1.4 eq), acceptor (1.0 eq), zirconocene dichloride (5.5 eq), $AgClO_4$ (1.1 eq), 1,1,3,3-tetramethylurea (1.2 eq), Et_2O, r.t., overnight; (ii) CAN (2.1 eq), CH_3CN-H_2O, 0 °C, 1 h, 34 % over two steps[35]

The combination of these two results seemed to suggest that the acetylated 2-azidoglucosyl fluoride donor would be a suitable candidate for the glycosylation of the "truncated inositol" **2.15**, since acetylation did not lower the yield of glycosylation relative to benzylation. The choice of $BF_3.OEt_2$ was also demonstrated to be a suitable one, since the glycosylation step in which it was used gave a high yield with high selectivity. The details of the synthetic procedure carried out are given below in Scheme 9. Intermediate **2.18** was prepared from the acetylated 2-azidoglucose **2.5** as described above.

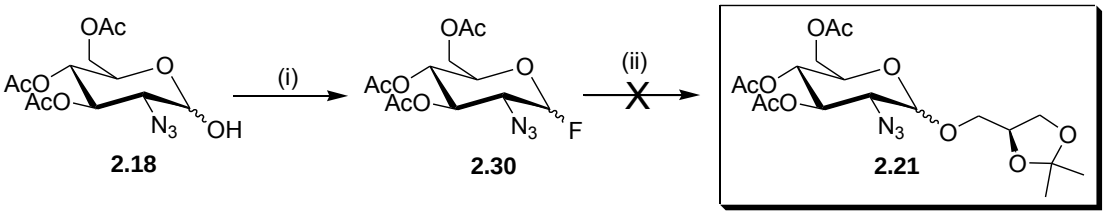

Scheme 9. Attempted synthesis of glyerol glycoside. (i) Ethylene diamine, AcOH, 18 h, r.t., quantitative; (ii) DAST, dry THF, 0 °C – r.t., 45 min, 85 %; (iii) **2.15**, $BF_3.OEt_2$, dry CH_2Cl_2 or dry THF or dry Et_2O, MS (4 Å), r.t. – 50 °C, 24 h.

Fluorination at the anomeric position was then carried out using diethylaminosulfur trifluoride (DAST) in anhydrous THF resulting in formation of the glycosyl fluoride **2.30** within 45 min in 85 % yield. A mixture of anomers (α:β = 1:2.2 by ^{1}H NMR) was obtained, in accordance with literature results,[44] although it was surprising that in the equilibrium mixture the anomeric enrichment was in favour of the β-anomer since the anomeric effect would predict that the α-anomer would predominate. It was also interesting to note that this constituted a reversal of α/β enrichment of the starting material (α:β = 1.6:1), supporting the view that fluorination occurs *via* an S_N2-type mechanism (Scheme 10).[45]

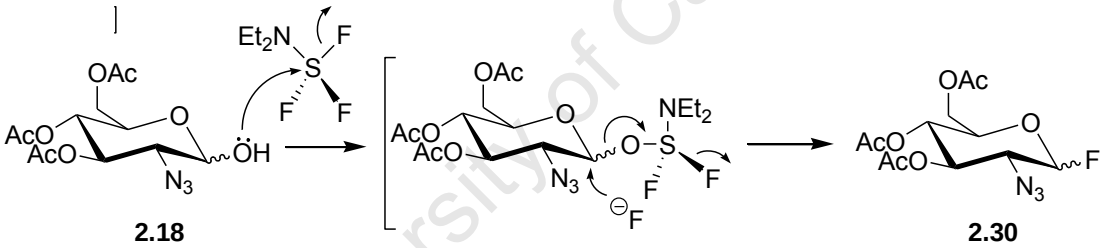

Scheme 10. Mechanism of fluorination by DAST

The mixture of fluoride anomers was, however, not a concern since the mechanism of fluoride substitution has been reported to follow an S_N2-type pathway, rather than generating an oxocarbenium intermediate, and preferentially forms *via* the β-anomer, resulting in an enriched α-glycosyl product. This is due to the lower activation energy of the β-fluoro anomer as a result of the kinetic anomeric effect and the α-anomer has a lower reactivity due to ground-state stabilisation by an endo anomeric effect.[45] In fact, selective α-glycosylation (α:β > 99:1) has been reported from an anomeric mixture (α:β = 2:1),[43] which seems to suggest that either there is anomerisation during the glycosylation reaction, with an α-glycosyl product favoured, or that once the β-fluoride anomer has been substituted by the acceptor, the liberated fluoride then substitutes an α-fluoride, forming a reactive β-anomer which is then substituted by the acceptor in a cyclic process until the starting material is consumed (Scheme 11).

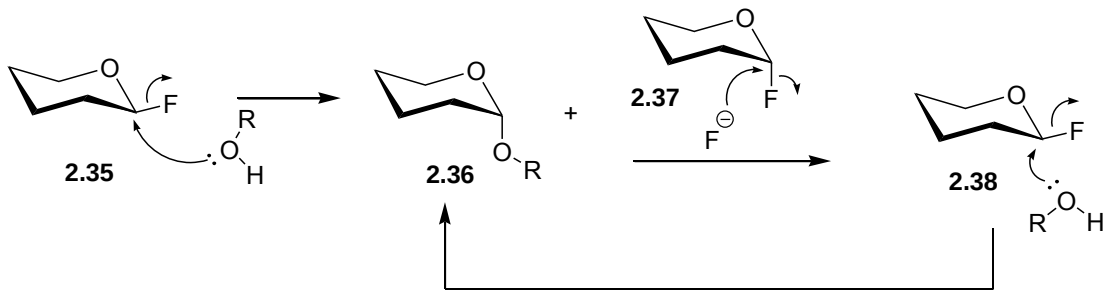

Scheme 11. Possible mechanism of glycosylation of glycosyl fluorides leading to α-anomeric enrichment

Several different reaction conditions were investigated in the attempts to effect glycosylation, with each proving to be unsuccessful. Initially the reaction was carried out in dry THF at r.t. under argon with furnace-dried, powdered, 4 Å molecular sieves and $BF_3.OEt_2$ as activator. The reason for the choice of THF was based on the ability of ethers to coordinate to the oxocarbenium intermediate and block the β face, thereby promoting the formation of a predominantly α product, [46] as evinced in the reported trichloroacetimidate-diethyl ether approach – see Table 2. After 2 h there was no product visible by TLC, and so additional $BF_3.OEt_2$ (4 eq) was added and the reaction left overnight, by which stage there was still no product. The reaction was then repeated in dry THF, and after 2 h there was once again no product detectable by TLC. The temperature was then raised, first to 40 °C for 2.5 h (still no product), and then to 50 °C overnight, after which there was still no product, and only polymerised THF – as determined by ^{1}H NMR spectroscopy. The solvent was then changed to dry CH_2Cl_2, and similar conditions employed. After 5 h there was no discernable product formed, and the reaction was left overnight. After 22 h the starting material was consumed and the product extracted, purified and characterised. It was found to be the hydrolysis product **2.18**, present as a mixture of anomers with α:β = 2:1 (by ^{1}H NMR). It was interesting to note the reversal of α/β enrichment from the starting material (α:β = 1:2.2). The attempted glycosylation reaction was then repeated in dry Et_2O under the same reaction conditions, and after 19 h partial conversion of the starting material to **2.18** had again occurred.

The fact that the glycosyl fluoride gave rise to the hydrolysis product in two cases indicated that the donor was in fact activated by the $BF_3.OEt_2$, but that the glycerol was not sufficiently nucleophilic to effect the glycosylation, even after prolonged reaction times. Traces of H_2O that entered the reaction vessel after these extended periods resulted in the formation of the hydroxylated glycoside. It is possible that the deactivating acetate protecting groups contributed negatively to the outcome of the reaction, although the success of the reported glycosylation with benzylated *myo*-inositol utilising an acetylated glycosyl fluoride would suggest that this is not a considerable dominating factor. Future attempts towards a

successful reaction will have to be aimed at modifying the structure of the acceptor to enhance its reactivity.

The third glycosylation strategy employed a phenylthio donor, activated by *N*-iodosuccinamide (NIS). Precedent for this approach was provided by the publication of a synthetic route to substituted glyceryl-type glycosides utilising a phenylthio-2-azidoglucoside donor (Scheme 12).[47] This reported reaction selectively generated the desired α-glucoside in 66 % yield (over two steps) after 2 h reaction time. Here there were some notable differences between the reactants reported and those to be used in the glycerol glycosylation. Firstly, the protecting groups at the 3- and 4-positions of the sugar were para-methoxybenzyl groups, which are highly activating/arming due to their electron-donating inductive effect, and the substituent at the 6-position was an azide, whereas the donor used for the glycerol glycosylation study incorporated three *O*-acetates or three *O*-benzyl groups at the 3-, 4- and 6-positions. The glycerol-type acceptor also differed in that it had a *tert*-butyldimethylsilyl (TBS)-protected alcohol at the 2-position and an azide at the 3-position of the propyl chain – differences that are likely to make the reactivity of the free hydroxyl group differ from that in isopropylidene glycerol.

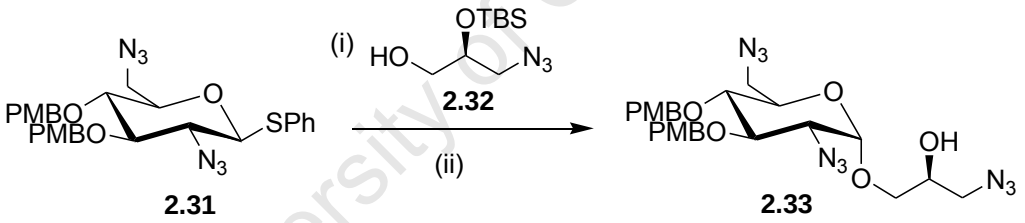

Scheme 12. Reported glycosylation using phenylthioglycoside donor, activated by NIS. (i) **2.31** (1.0 eq), **2.32** (1.5 eq), NIS (2. 0 eq), MS (4 Å), Et_2O/CH_2Cl_2 (4:1, 0.03M), 2 h, -30 – 0 °C; (ii) silyl-ether (1.0 eq), TBAF (1.2 eq), THF (0.1M), 1 h, 0 – 23 °C, 66% over two steps.[47]

The glycosylation reaction utilising the thiophenol donor was expected to proceed with high reactivity, since the related published procedure had been performed at -30 °C and was complete after 2 h.[47] Unfortunately, this reactivity did not materialise. Both the acetylated and benzylated phenylthio-2-azidoglucosides (**2.6** and **2.34**) were treated in turn with *N*-iodosuccinimide (NIS) and isopropylidene glycerol in anhydrous CH_2Cl_2 and anhydrous CH_2Cl_2:Et_2O (1:4), respectively, and in neither case was the isopropylidene glycerol able to displace the thiophenol substituent, despite relatively high temperatures (r.t.) and extended reaction times (~20 h) (Scheme 13).

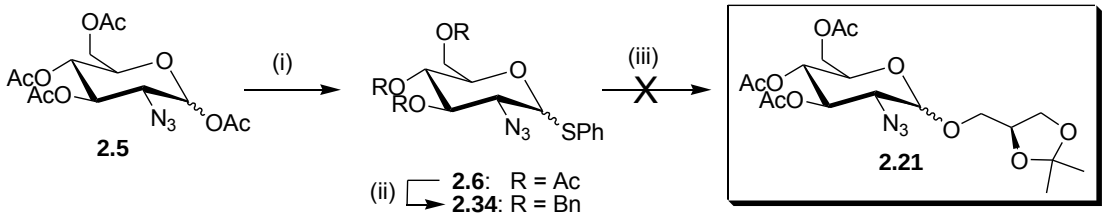

Scheme 13. Attempted synthesis of glycerol glycoside. (i) $BF_3.OEt_2$, dry CH_2Cl_2, PhSH, reflux, 80 %; (ii) conversion of the Ac protecting groups to Bn: 1. NaOMe (cat.), MeOH, 16 h, 0 °C – r.t., 96 %; 2. TBAI, NaOH, BnBr, THF, r.t., 2.5 h, 79 %; (iii) **2.6** or **2.34**, **2.15**, NIS, dry CH_2Cl_2, -40 °C – r.t. – reflux overnight.

In both cases the starting materials remained unchanged, suggesting ineffective activation of the phenylthio group. As was seen with the glycosyl fluoride glycosylations, it appears that the isopropylidene glycerol alcohol is insufficiently nucleophilic to displace the thiophenol.

2.4.3 Oxidative Decarboxylation to Generate the Tethered Naphthoquinone

There are several examples in the literature of radical conjugate additions to quinones. These have been shown to be promoted by organotellurium compounds and by carbon-centred radicals generated by metal ions such as Mn(III) and Ce(IV).[48,49] One of the most common procedures utilizes the Barton decarboxylation,[50] which involves a thiohydroxamic ester (Barton ester) as intermediate (Scheme 14). Homolytic cleavage of the nitrogen-oxygen bond in the *N*-hydroxypyridyl compound, initiated by light or heat, leads to a 2-pyridylthiyl radical and an alkyl radical ($R^{\cdot}$) after decarboxylation of the acyloxy radical intermediate.[51] Double alkylation of the quinone proceeds by trapping of the alkyl and 2-pyridylthiyl radicals, and after rearomatisation affords the alkylated thiylated quinone.[52] A drawback of this reaction is the difficulty in desulfurisation of the product after alkylation, in the case of naphthoquinones.[53]

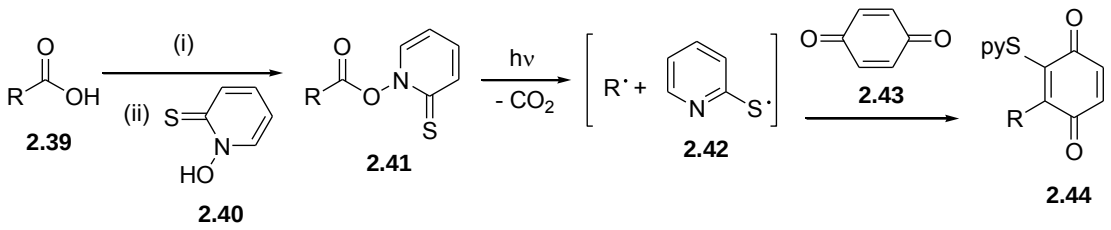

Scheme 14. Barton-type radical decarboxylation and addition to benzoquinone. (i) $SOCl_2$ or $(COCl)_2$ or DCC

It therefore seemed advantageous to employ the procedure reported by Salmon-Chemin *et al*[2] using $Ag(NO_3)$ as catalyst and ammonium persulfate (APS) as radical initiator to achieve

naphthoquinone alkylation by radical decarboxylation. This approach was employed for the synthesis of similar substituted naphthoquinones in earlier work published by our group.[18] The ease of handling and direct access to the desired product in a single step were sufficiently advantageous for the low reported yields to be overlooked, although optimisation of the reaction was investigated in this project.[54] This strategy was first reported by Anderson and Kochi in 1970,[55] and involved generating a carbon-centred radical by reacting a carboxylic acid in a mixture of CH_3CN/H_2O. A related procedure is the Minisci reaction, which involves radical-based C-C bond formation between an alkyl radical, obtained by oxidative decarboxylation in the presence of Ag(I) and APS, and an electron-deficient heteroaromatic compound.[56]

The first step in the synthesis involved coupling of the selectively-protected amino acids, aspartic acid and glutamic acid, to the naphthoquinone, plumbagin, in a logical extension of the earlier work (Scheme 15).[18] The reaction was highly temperamental and generally low yielding, with yields ranging from 18 – 36 % and 24 – 51 % for the aspartic and glutamic alkylations, respectively. Despite these low yields, the ability to recover unreacted plumbagin starting material and recycle it in subsequent reactions diminished the cost associated with loss of expensive reagents, and could be said to give the reaction a higher yield based on recovered starting material.

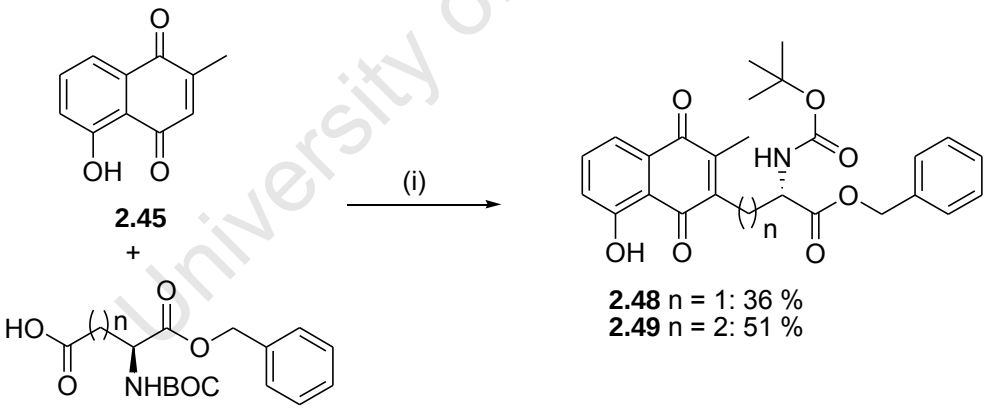

2.48 n = 1: 36 %
2.49 n = 2: 51 %

2.46: n = 1: BOC-Asp-OBn
2.47: n = 2: BOC-Glu-OBn

Scheme 15. Synthesis of the naphthoquinone-amino acid conjugate: (i) $(NH_4)_2S_2O_8$, $AgNO_3$, 30 % (aq) MeCN, 60 °C, 6 h.

Several attempts were made to optimise the reaction, including modifying the rate of addition of APS to the reaction mixture (as well as the amount added), increasing the amount of amino acid added, degassing the solvent to remove oxygen (which may have been poisoning the radical intermediates), and changing the order in which the reagents were

added. These modifications had no positive improvement on the yield or selectivity, with the exception of degassing, which appeared to give a slight improvement in yield. It was not possible to lower the temperature of the reaction, as this resulted in precipitation of the reactants. While elevating the temperature resulted in increased proportions of side products. Possible enhancements to the reaction by changing the catalyst were not investigated, partly since it was reported that the addition of Cu(II) acetate to the reaction mixture resulted in a decrease in radical decarboxylation and an increase in reaction time (from 1 h to 20 h),[55] and partly in maintaining reaction conditions close to the most successful reported procedures. Many of these findings are supported by the results of Desolin and co-workers[54] who performed an extensive study of the parameters required to optimise the yield of radical addition to naphthoquinones using this procedure.

The reaction mechanism is outlined in Scheme 16. The first step involves thermal homolytic cleavage of the persulfate bond to generate two sulfate radicals which oxidise the Ag(I) catalyst to Ag(II). The Ag(II) then coordinates to the carboxylate of the acid and oxidises it to $COO^{\cdot}$ and is itself reduced back to Ag(I). Decarboxylation then occurs to form the alkyl radical, which alkylates the plumbagin at the unsubstituted carbon of the quinone. The resultant intermediate, undergoes keto-enol tautomerism to regenerate the aromaticity of the naphthalene ring. Oxidation to the naphthoquinone product is finally achieved by a second equivalent of sulfate radical.

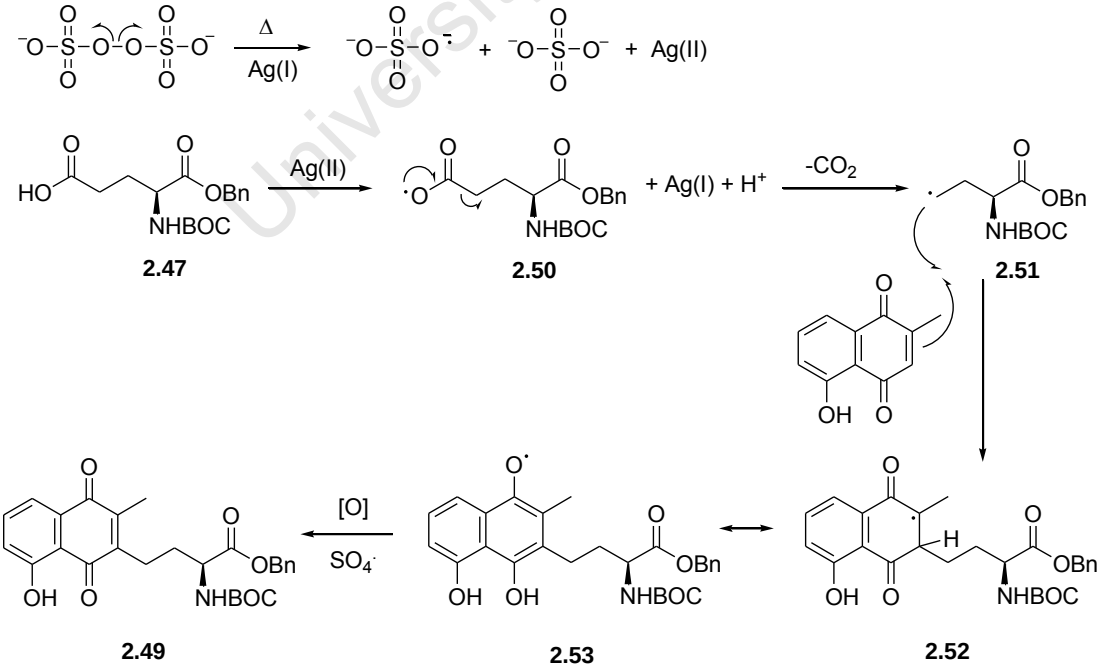

Scheme 16. Mechanism of radical addition to plumbagin[55]

2.4.4 Amide Coupling

Following the success of the oxidative alkylation step the next step involved saponification to deprotect the carboxylic acid in preparation for amide coupling to the phenylthio-2-aminoglucoside **2.7** (Scheme 17). Debenzylation was achieved by treatment with LiOH in aqueous THF in excellent yields of 89 % and 91 % for aspartic and glutamic derivatives, respectively.

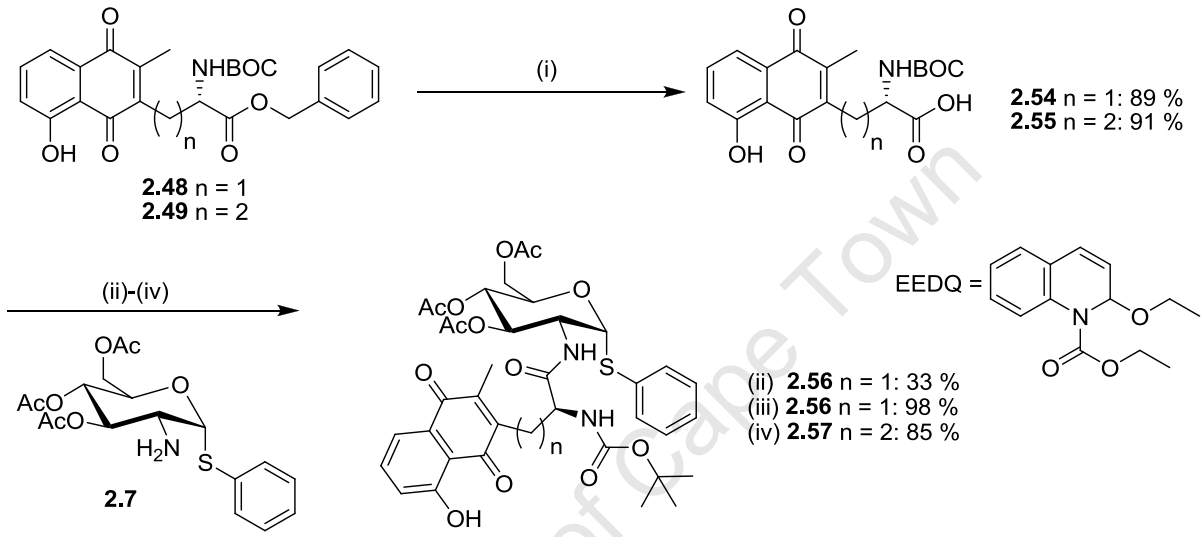

Scheme 17. Debenzylation and amide coupling. (i) LiOH, aqueous THF, r.t., 4 h; (ii) EDC.HCl, HOBt, DIEA, dry THF, r.t., 42 h; (iii) EEDQ, dry THF, 40 °C, 15 h; (iv) EEDQ, dry THF, r.t., 39 h.

The amide coupling between **2.7** and the plumbagin-coupled amino acid **2.54** was then investigated. It was initially attempted using the standard peptide coupling reagents EDC.HCl and HOBt in anhydrous THF, giving coupled product **2.56** in a yield of 33 % after stirring at r.t. under argon for 42 h (Scheme 17). In an attempt to increase the yield, an alternative coupling agent, 2-ethoxy-1-ethoxycarbonyl-1,2-dihydroquinoline (EEDQ) was then used, and this reagent gave more satisfying results with yields of 69 % and 85 % obtained for **2.56** and **2.57** respectively, when the reaction was performed at r.t.. The yield for the aspartate derivative **2.56** increased from 69 % to 98 % when the temperature was raised to 40 °C and the equivalents of amine were increased from 1.2 to 2.1 (in order to account for the transacetylation side reaction that takes place in solution at this temperature).

The use of EDC is preferred over other diimide reagents (such as 1,3-dicyclohexylcarbodiimide) since the urea side product is easily removed during aqueous work up by protonation of the nitrogen in the side chain. The use of EEDQ as a coupling

agent also circumvents this problem since the reaction generates only quinoline, ethanol and CO_2 as by-products, which are removed with relative ease. The mechanism for EEDQ-mediated coupling is illustrated in Scheme 18.

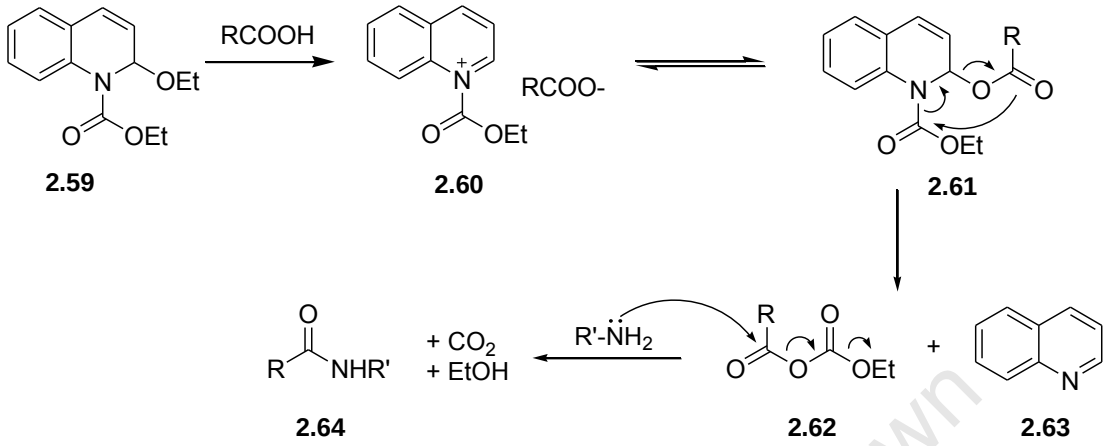

Scheme 18. Reaction mechanism of EEDQ-mediated amide coupling[57]

Protonation of the ethyloxy substituent at the 2-position of the dihydroquinoline facilitates its elimination by delocalisation of the lone-pair on the nitrogen at the 1-position. The driving force for this elimination is conjugation of the quinoline. There is a subsequent equilibrium set up between the conjugated quinoline with a positively-charged nitrogen, and the addition product of the carboxylate to the 2-position to alleviate the cationic quinoline. Eventually there is an intramolecular rearrangement that results in the formation of the active mixed anhydride and conjugated quinoline. The amine then attacks the anhydride at the ester carbonyl, rather than the carbonate (since it is the more electrophilic centre and is also entropically-favoured due to the release of CO_2 and EtOH), to give the amide product.

2.4.5 Attempted Removal of the tert-Butyloxycarbonyl Protecting Group and Serendipitous Discovery of Novel Route to Benzo[*g*]indoles and Benzo[*h*]quinolines

Having now prepared the hybrid sugar-naphthoquinone structures *via* the amino acid tether, the conversion of *N*-Boc to *N*-acetate was necessary in order to mimic the cysteine side chain of mycothiol. In the case of the aspartic acid derivative, the Boc deprotection was attempted using the standard conditions of trifluoroacetic acid and anisole in CH_2Cl_2 at 0 °C, with warming to room temperature, with the intention to immediately acetylate the product using acetic anhydride in pyridine. However, initial attempts to deprotect the aspartic

derivative resulted in decomposition of the starting material without conversion to an obvious product. Reaction times of 3.5 h, 6 h, 32 h and 5 days were recorded for reactions containing 0.07, 0.23, 0.03, 0.03 % TFA, respectively, in all cases resulting in decomposition of the starting material. Eventually, however, it was discovered that staining the TLC with ferric chloride revealed a different product to the starting material that was otherwise not visible by staining with acidic anisaldehyde or acidic ceric ammonium sulfate (CAS) solutions, and allowed the reaction to be monitored and stopped before decomposition set in. The starting material and product had very similar R_f values. The anisaldehyde and CAS stained both spots black, whereas ferric chloride stained the starting material black and the reaction product dark brown. There was also a difference observed when directly applying a sample from the reaction mixture to the TLC plate, and carrying out a mini work-up to neutralise the acid, and then spotting a sample from the reaction on TLC. In the former case, the product (R_f 0.41, EtOAc:hexane, 2:3) moved faster than the starting material (R_f 0.38, EtOAc:hexane, 2:3), whereas in the latter case, the product (R_f 0.36, EtOAc:hexane, 2:3) was fractionally slower than the starting material. The reaction mixture was purified and the product isolated and characterised. The ^{1}H NMR spectrum indicated that the *tert*-butyl group had been successfully removed. The phenolic proton was evident from a singlet at 11.8 ppm, the aromatic region contained the correct number of signals, and signals for the acetylated glucosamine were also accounted for. The signals for the free amine were initially not obvious, but a D_2O wash revealed an exchangeable proton signal within the multiplet at 7.55 ppm (Figure 5) that showed a coupling to the H_9 proton in the COSY spectrum. Another exchangeable proton was indicated by the signal at 6.85 ppm which showed a correlation to the signal for H_2 in the COSY spectrum. The interesting feature of the NH signal at 7.55 ppm was that it integrated for one hydrogen and not two, suggesting that the amine was alkylated or acylated. Evidence for the true nature of this attachment was provided by the ^{13}C spectrum. In addition to the expected naphthoquinone, carbohydrate and acetate signals, there were two quartets at 157.5 (q, 1C, J = 37.9 Hz, C_{12}) and 115.5 (q, 1C, J = 287.7 Hz, C_{13}) ppm. These signals are indicative of the presence of the trifluoroacetyl group, since the three fluorine atoms couple to the methyl carbon and to the carbonyl carbon, giving large geminal and smaller vicinal coupling constants. This result suggested that after deprotection of the Boc carbamate, the liberated amine was acylated by TFA, or by trifluoroacetic anhydride present as an impurity in the reagent bottle.

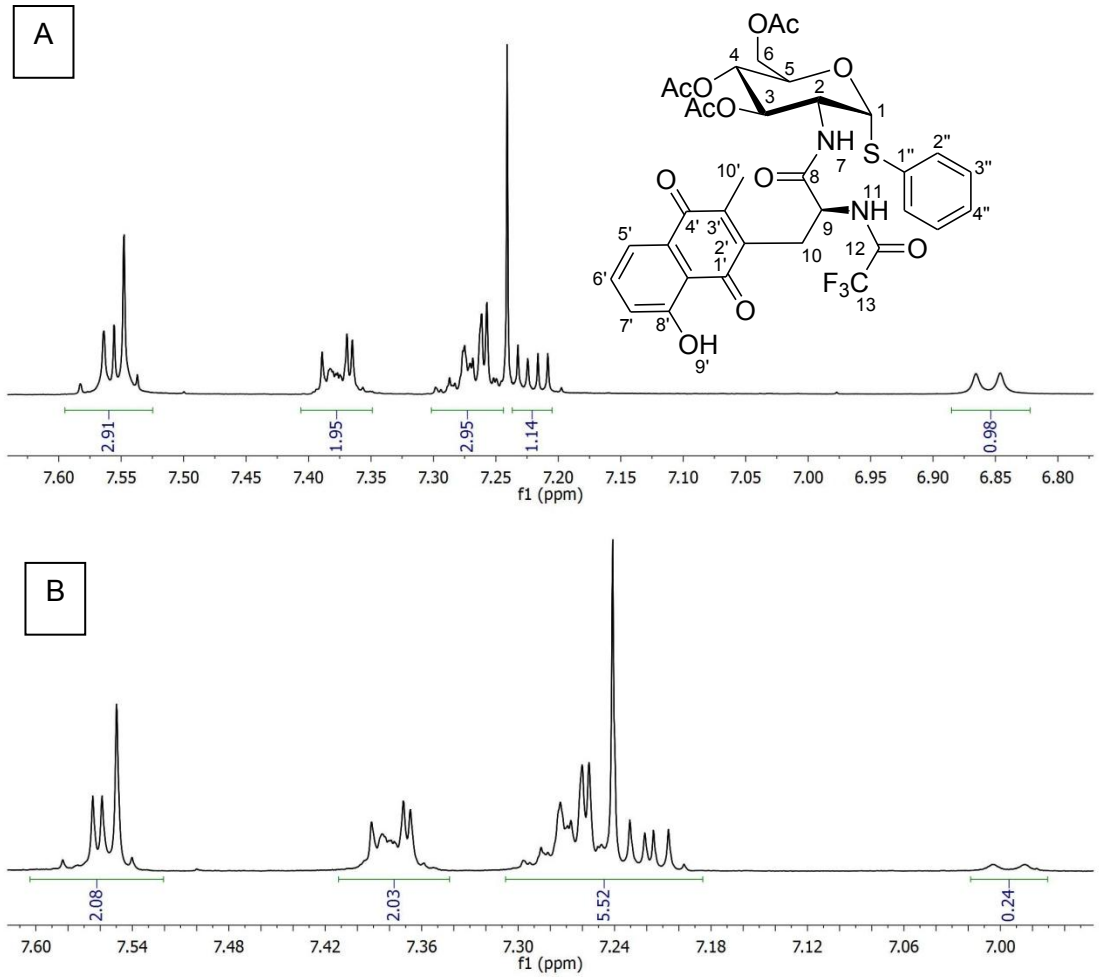

Figure 5. ^{1}H NMR spectrum indicating the aromatic region before (A) and after (B) D_2O wash. The reduction in the integration of the multiplet at 7.55 ppm by one hydrogen is noted.

Consequently, this unexpected reaction is revised as in Scheme 19 below. Although there was some degradation during the reaction, a considerable yield of 70 % was obtained.

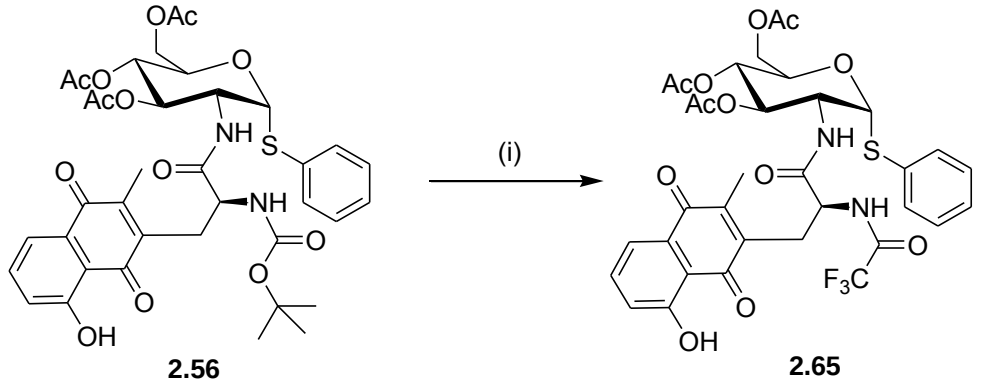

2.56 **2.65**

Scheme 19. Removal of Boc protecting group from aspartic derivative and subsequent acetylation by TFA: (i) TFA, anisole, CH_2Cl_2, r.t., 4 h, 70 %.

Despite this unexpected result, it seemed prudent to complete the synthesis by deprotecting the sugar to obtain the TFA derivative of the target molecule. Due to the similar atomic size of fluorine (van der Waals radius = 1.35 Å)[58] to hydrogen (van der Waals radius = 1.20 Å)[58,59], the trifluoromethyl group is similar in size to the methyl group of a conventional acetate (van der Waals volume of CF_3 = 39.8 Å^3; van der Waals volume of CH_3 = 21.6 Å^3),[58] and does not therefore significantly alter the topology of the molecule. In fact, fluorine is a known bioisostere of hydrogen and there have been numerous examples in medicinal chemistry where a hydrogen atom has been substituted by a fluorine to enhance the biological or physicochemical properties of a molecule without significantly altering its chemical structure.[60,61] Some of these effects include fluorine/hydrogen substitution to enhance membrane permeability,[62] reduce lipophilicity,[63] modulate metabolism,[64] modulate basicity of adjacent amide groups,[65] and influence conformation *via* intramolecular electrostatic interactions with dipolar bonds.[66]

The deprotection of the glucosamine acetates was carried out utilising the standard Zemplén conditions of catalytic sodium methoxide (20 mol %) in methanol (Scheme 20). After 2 h of reaction time, there were two products evident from TLC, which remained after a further 6.5 h of reaction. After 8.5 h, despite the reaction not proceeding to completion, TLC indicated that decomposition was under way, and the reaction was therefore stopped and worked up. Purification was attempted by automated flash chromatography, but the products appeared to decompose during the chromatography while a considerable portion of material remained strongly adhered to the silica. This was eluted after the addition of 1 % AcOH to the mobile phase. Unfortunately, a considerable amount of material was lost during the purification and two products were obtained in small quantities (3 mg and 7 mg, respectively). Neither of the two products showed characteristics of the desired product in their ^{1}H or ^{13}C NMR spectra. The less polar product was submitted for an overnight quantitative ^{13}C experiment in the hope of identifying the characteristic quartets for the trifluoromethyl acetate group. However, these signals were missing, suggesting that the deacetylation had cleaved the trifluoroacetate. The more polar product decomposed in solution and was not identifiable by ^{1}H NMR spectroscopy. This lack of stability in solution precluded the possibility of testing its activity in the enzyme assays, and it was therefore not pursued further.

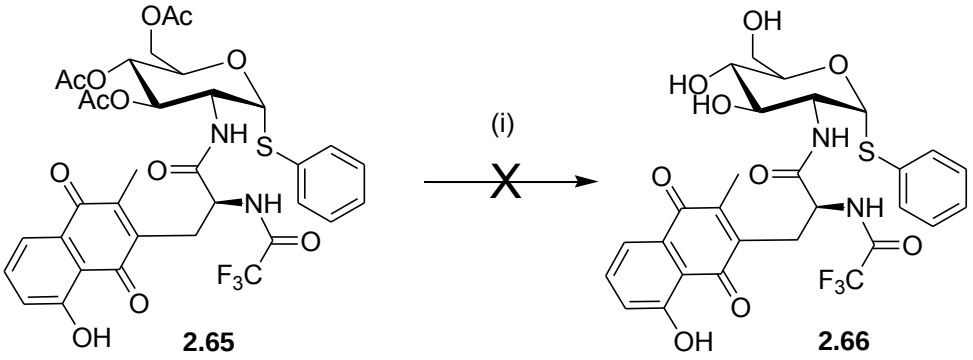

Scheme 20. Attempted Zemplén deacetylation to form the trifluoro bioisostere of the final target aspartic molecule. (i) NaOMe (20 mol %), MeOH/CH_2Cl_2, r.t., 8.5 h.

Attention then turned to the deprotection of the glutamic acid derivative **2.57**, which appeared to proceed with greater success than the aspartic derivative. Treatment of **2.57** with TFA in CH_2Cl_2 resulted in the formation of a product that was at first difficult to characterise, but migrated as a single spot on TLC [R_f (EtOAc:hexane, 6:4) product 0.37; starting material 0.61]. The ^{1}H NMR spectrum indicated that the Boc group had been successfully removed, as seen by the disappearance of the *tert*-butyl signal at 1.44 ppm. The signals for the glucosamine ring as well as the phenylthio substituent were present, as were the expected naphthoquinone proton signals (two doublets of doublets and a triplet); however, the expected methylene signals for the alkyl linker were missing and there was an unexpected aromatic A-B system present as indicated by the signal at ~8.2 ppm, indicating the presence of a cis double bond (two doublets, J = 8.6 Hz). Other noted differences from the starting material were a downfield shift of the phenolic OH singlet (from 12.02 to 13.75 ppm) and a shuffling around of the naphthoquinone signals in the aromatic region. The ^{13}C spectrum indicated the disappearance of the quinone carbonyl signals at 189.9 and 184.1 ppm, with the most downfield carbonyl signal appearing at 172.6 ppm (corresponding to an ester C=O). This suggested that a reduction of the quinone ring had taken place.

Combining this evidence, it appeared that the glutamic side chain had undergone a condensation-elimination sequence, resulting in the formation of a cis double bond in a fused aromatic system, and consequently the loss of the quinone carbonyl signals in the ^{13}C spectrum. Such a condensation/cyclisation would be expected to have an influence on the chemical shifts of all the ^{1}H signals on the naphthoquinone ring, including the methyl and hydroxyl substituents. A benzo[*h*]quinoline structure **2.67** was thus proposed for the reaction product (Scheme 21).

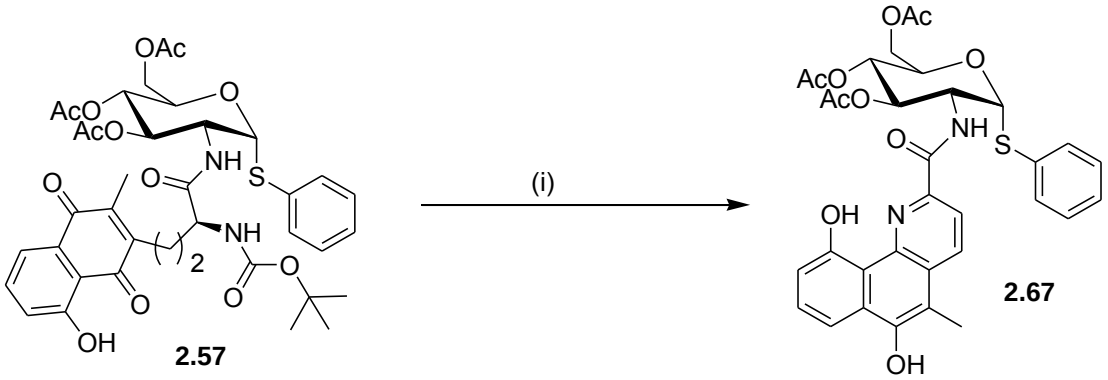

Scheme 21. Removal of the Boc protecting group and resulting cyclised product: (i) TFA, CH_2Cl_2, r.t., 2.5 h, 85 %.

Expansions of the ^{1}H NMR spectrum are given below in Figure 6 and Figure 7, and provide the graphical representation of the above-mentioned results. The A-B system at 8.2 ppm (subsequently assigned as $H_{3'}$ and $H_{4'}$) can be clearly seen in Figure 6. The other aromatic signals include a multiplet at 7.58 ppm, assigned as the ortho H's on the thiophenyl ring and the amide H_7 (confirmed by a coupling in the COSY spectrum to C_2), two doublets of doublets at 7.50 and 7.18 ppm (assigned as $H_{7'}$ and $H_{9'}$), a triplet at 7.46 ppm (assigned as $H_{8'}$) and a multiplet at 7.28 ppm (assigned as the meta and para H's on the thiophenyl ring). These benzoquinoline signals appear at similar chemical shifts to those of the corresponding H's on the naphthoquinone ring (see Figure 5 for comparison).

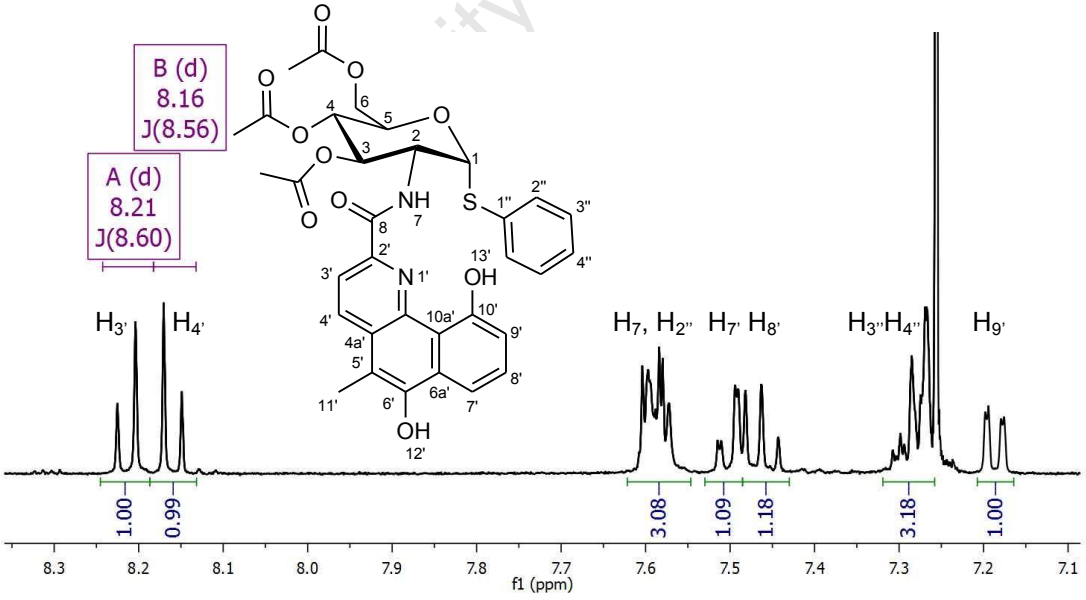

Figure 6. ^{1}H NMR spectrum of aromatic region of the cyclised glutamic product indicating the A-B system at 8.2 ppm

The disappearance of the signals corresponding to the *tert*-butyl (1.44 ppm) and methylene groups (2.65, 1.95 and 1.75 ppm) of the side chain can be seen in the ^{1}H NMR spectra of starting material (A) and product (B) in Figure 7 below. The change in chemical shift of the quinone methyl ($H_{10'}$) from 2.09 ppm in A to 2.53 ppm in B ($H_{11'}$) is also confirmed.

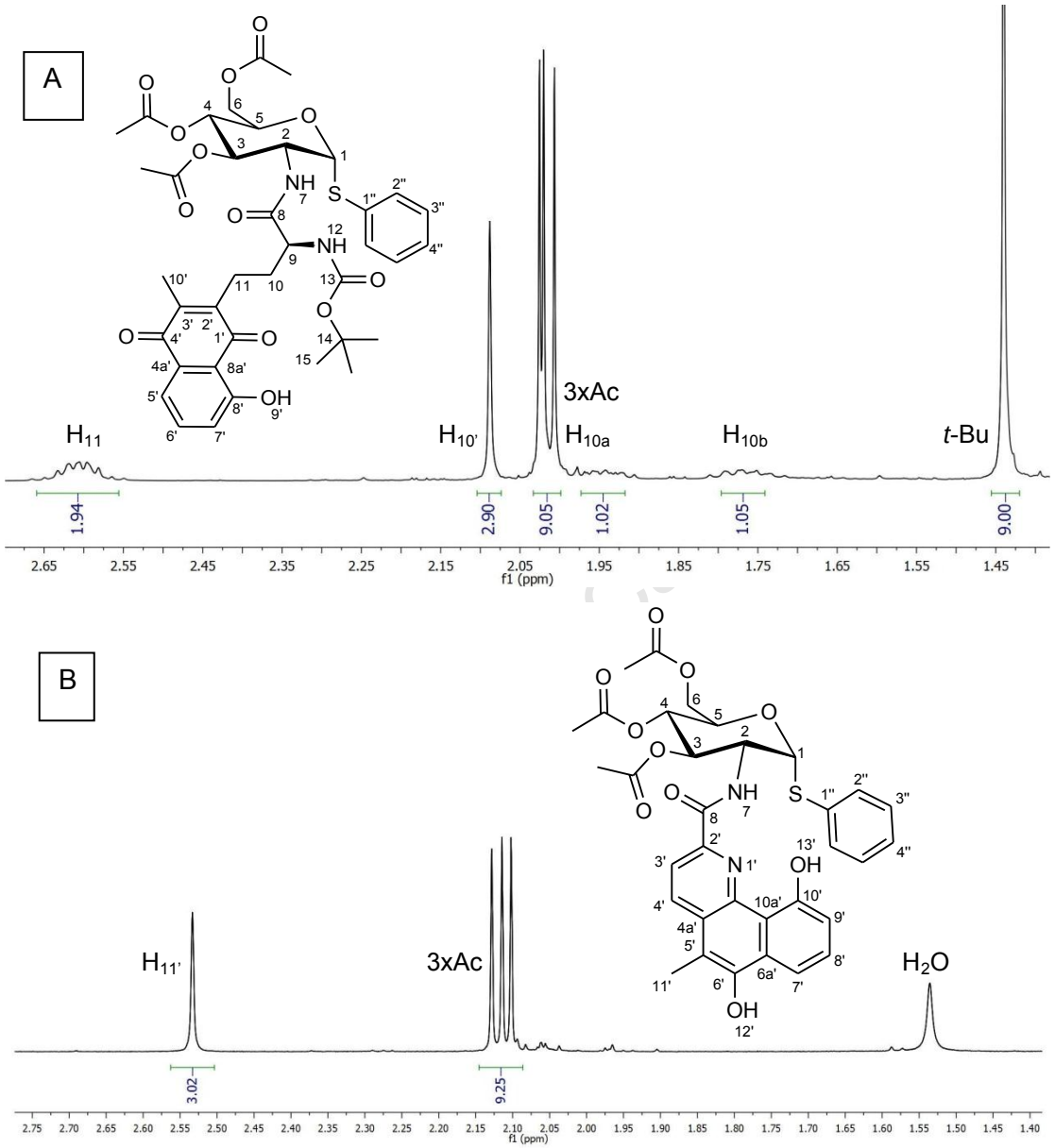

Figure 7. ^{1}H NMR spectra of the aliphatic regions of the Boc-protected (A) and Boc deprotected (B) glutamic conjugates. The disappearance of the *tert*-butyl signal at 1.44 ppm and the methylene signals at 2.65, 1.95 and 1.75 ppm is demonstrated.

An attempt was made to deacetylate the glucosamine ring in order to obtain the benzo[*h*]quinoline conjugate of thiophenyl glucosamine. However, deprotection under standard Zemplén conditions resulted in a product with very poor solubility. In fact, as the deacetylation reaction progressed, the product precipitated out of solution and could not be

dissolved again in any solvent except DMSO. The precipitate was washed with EtOAc and MeOH in order to remove any remaining starting material, and submitted for ^{1}H NMR analysis in deuterated DMSO, but this gave a spectrum that could not be unambiguously assigned. This suggested that the precipitate consisted of a range of partially deprotected acetates, and with such poor solubility, was unlikely to be a suitable candidate for biological evaluation. However, the novelty of the reaction prompted further investigations, both into its applicability to other substrates, and into the structure of the final product.

In order to further investigate the cyclisation reaction, samples of **2.48** and **2.49** were subjected to treatment with TFA, followed by acetylation, to explore the generality of this methodology for the preparation of fused heterocycles.

In the case of the aspartic acid derivative, it was hoped that it could be established whether appropriate conditions would result in deprotection without trifluoroacetylation, and that either the desired *N*-acetylation could be achieved, or alternatively cyclization to substituted benzoindoles.

When **2.48** was treated with TFA in CH_2Cl_2 a compound with an almost identical R_f on TLC was formed, and was only identified as a new product after the staining reagent was changed from anisaldehyde (or CAS) to ferric chloride (in the same way that the aspartic derivative coupled to the glucosamine was identified). Once again, the anisaldehyde and CAS stained both spots black, whereas ferric chloride stained the starting material black and the product dark brown.

After work up and purification, the product was subjected to acetylation (acetic anhydride in pyridine), and isolation and characterisation of this product revealed that the *tert*-butyl group of the Boc was missing, suggesting that deprotection had been successful. However, the NH signal integrated for just 1 hydrogen in the ^{1}H NMR spectrum, suggesting that *N*-acetylation had taken place. In addition, the phenolic OH signal was missing, suggesting initially that it too had been acetylated. However, there were only two methyl singlets in the ^{1}H spectrum, at 2.39 and 2.15 ppm respectively, and since one of these methyl signals corresponded to the methyl substituent at C_3 of the naphthoquinone, the other had to correspond to either the phenolic or amine acetate, but could not be both. The presence of the two quinone carbonyl signals in the ^{13}C spectrum suggested that imine condensation had not taken place, precluding that as a possibility for the lower than expected amine proton integration. Once again the ^{13}C spectrum was carefully examined and provided the clue to the structure of the product. There were two quartets present, one at 157.1 ppm (J = 38.0

Hz) and one at 115.6 ppm (J = 287.6 Hz), each integrating for 1 carbon (in the spectrum of a quantitative ^{13}C experiment). This indicated that the amine had been acetylated by the TFA to produce a trifluoromethyl amide **2.68** (Scheme 22).

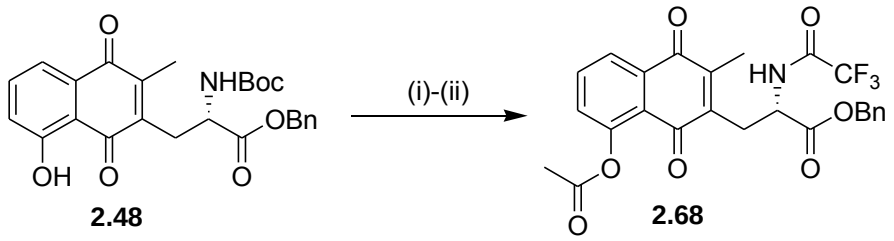

2.48 **2.68**

Scheme 22. Synthesis of trifluoromethyl amide under Boc deprotection conditions. (i) TFA, anisole, CH_2Cl_2, 3.5 h, 0 °C – r.t.; (ii) Ac_2O, pyridine, 17 h, r.t.

Confirmation that the amine, and not the phenolic OH, had been acetylated by the TFA was provided by an HMBC 2D spectrum (Figure 8). This spectrum clearly shows a ^2J through-bond coupling between the C_5 carbonyl carbon and the H_4 proton on the nitrogen, as well as a ^3J through-bond coupling between the C_5 and the H_2 proton. These couplings would not be present if the TFA was on the phenolic OH and the amine was acetylated by a non-fluorinated acetate.

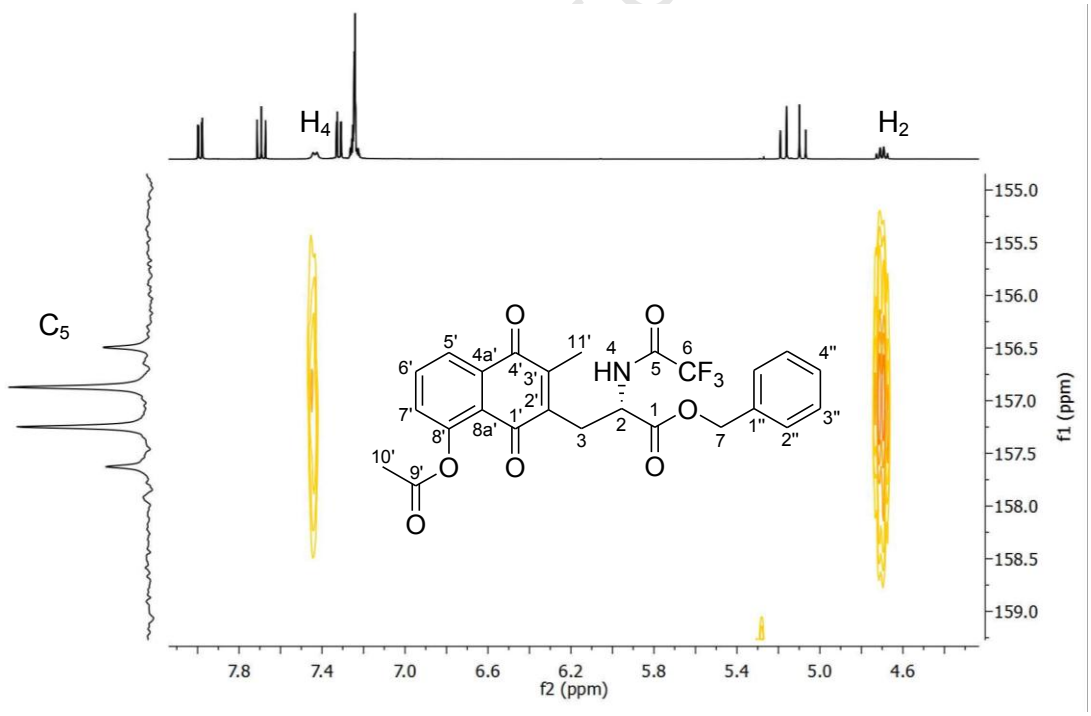

Figure 8. Expansion of the HMBC spectrum of the TFA-acetylated Plum-Asp-OBzl indicating a ^2J and ^3J through-bond coupling between the TFA carbonyl carbon and the NH and CH protons, respectively.

The second product (R_f 0.12, EtOAc:hexane, 1:4) that formed during the reaction of **2.48** with TFA appeared at a considerably lower R_f on the TLC than the starting material (R_f 0.52,

EtOAc:hexane, 1:4), and was highly fluorescent under UV. Unfortunately, this product degraded with time in solution, making full characterisation difficult. After chromatography, a relatively pure fraction (by TLC) was collected and subjected to NMR spectroscopic analysis, and an assignable ^{1}H spectrum obtained (Figure 9). The ^{1}H NMR experiment was run in CD_3OD, which resulted in none of the exchangeable proton signals being visible (due to H-D exchange with the NMR solvent). However, this solvent was preferred over $CDCl_3$ since it allowed the singlet at 7.27 ppm, which was assigned as H_3 on the proposed newly-formed indole ring (Figure 9), to be clearly seen without interference from a $CHCl_3$ signal at 7.25 ppm. The rest of the ^{1}H spectrum supported the hypothesis that an imine condensation/cyclisation to the benzo[*g*]indole, in a similar mechanism to the benzo[*h*]quinoline described earlier, had taken place. The molecule appeared to be achiral, as evidenced by the appearance of the signal for the benzylic methylene group appearing as a singlet at 5.4 ppm, and the signals corresponding to the aspartic alkyl chain were also absent, suggesting a similar reduction/aromatisation had taken place.

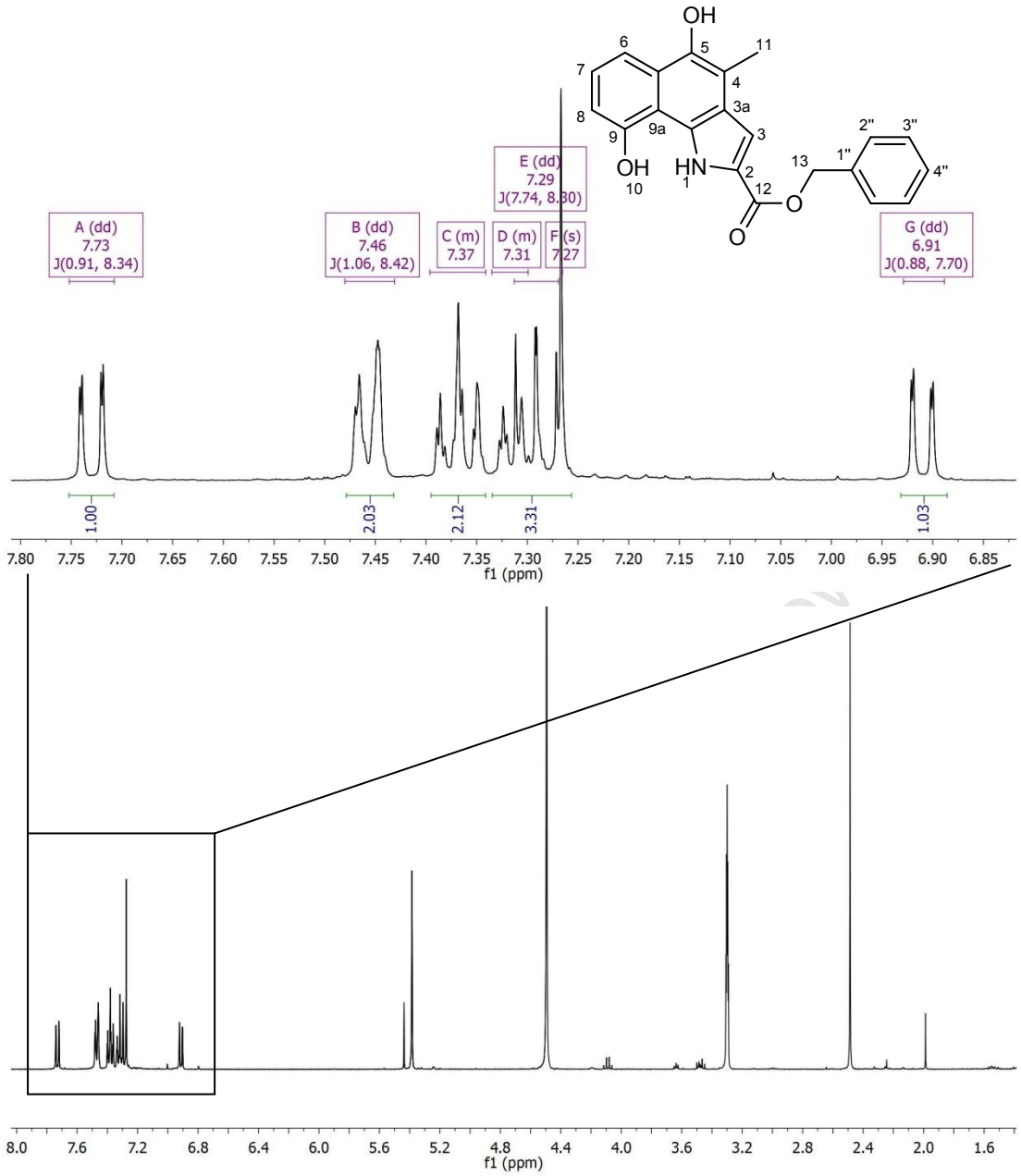

Figure 9. Expansion of the ^{1}H NMR aromatic region of the cyclised benzo[*g*]indole product. The NMR experiment was run in CD_3OD to allow identification of the newly-formed indole by the presence of a singlet at 7.27 ppm.

The poor quality of the ^{13}C spectrum (due to compound degradation) precluded a complete assignment, despite the likely product structure given in Figure 10.

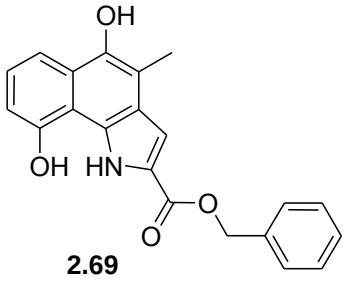

2.69

Figure 10. Chemical structure of the benzo[*g*]indole product formed by TFA-mediated cyclisation.

In an attempt to gain further evidence for this structure, a fraction of this semi-purified product (18 mg) was then subjected to acetylation in acetic anhydride and pyridine. A more stable product was indeed isolated, and full characterisation of the doubly acetylated benzo[*g*]indole product was possible. The ^{1}H NMR spectrum confirmed the structure of the product as a di-acetyl benzo[*g*]indole (Figure 11), and this was supported by the presence of an exchangeable NH signal at 10 ppm and three methyl signals at 2.5 ppm.

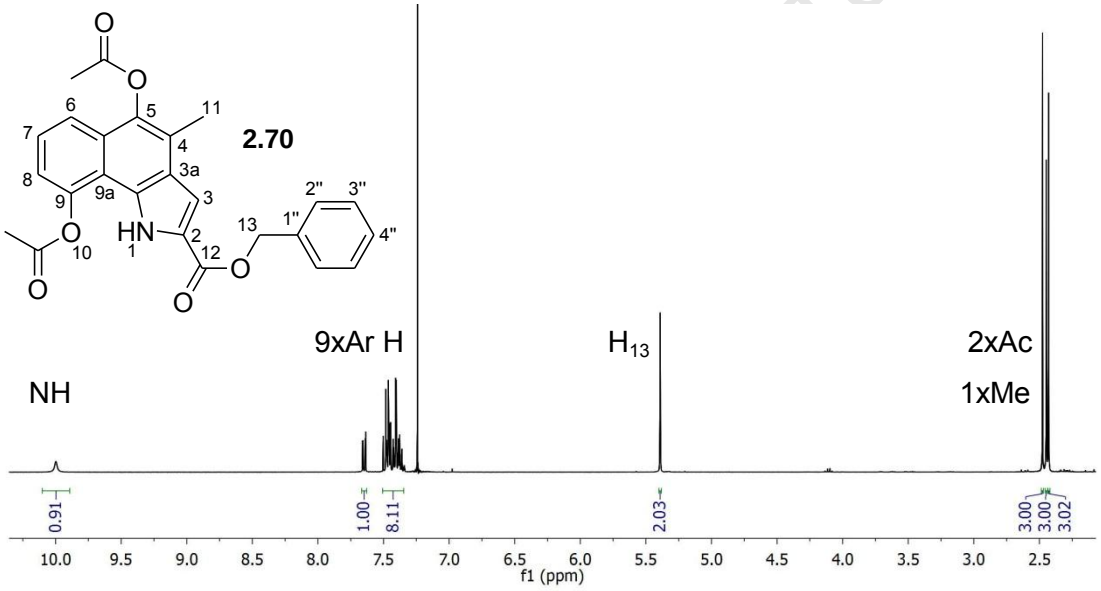

Figure 11. 1H NMR spectrum and chemical structure of acetylated benzo[*g*]indole

The expansion of the aromatic region (Figure 12) shows that, in keeping with the proposed structure, there are nine aromatic protons. Due to considerable overlap, unambiguous assignment of all the signals was difficult, although a general assignment was possible. Using the expansion of the aromatic region of the HSQC it was possible to identify the signals corresponding to protons H_6, H_7 and H_8, as well as the aromatic benzyl protons (Ar_{Bn}), which appear in close proximity to one another in the ^{13}C spectrum. The signal at 108.6 ppm in the ^{13}C and 7.40 ppm in the ^{1}H, is the H_3 singlet, which appears at a considerably different chemical shift to the other signals, and gives a small, well resolved signal in the HSQC.

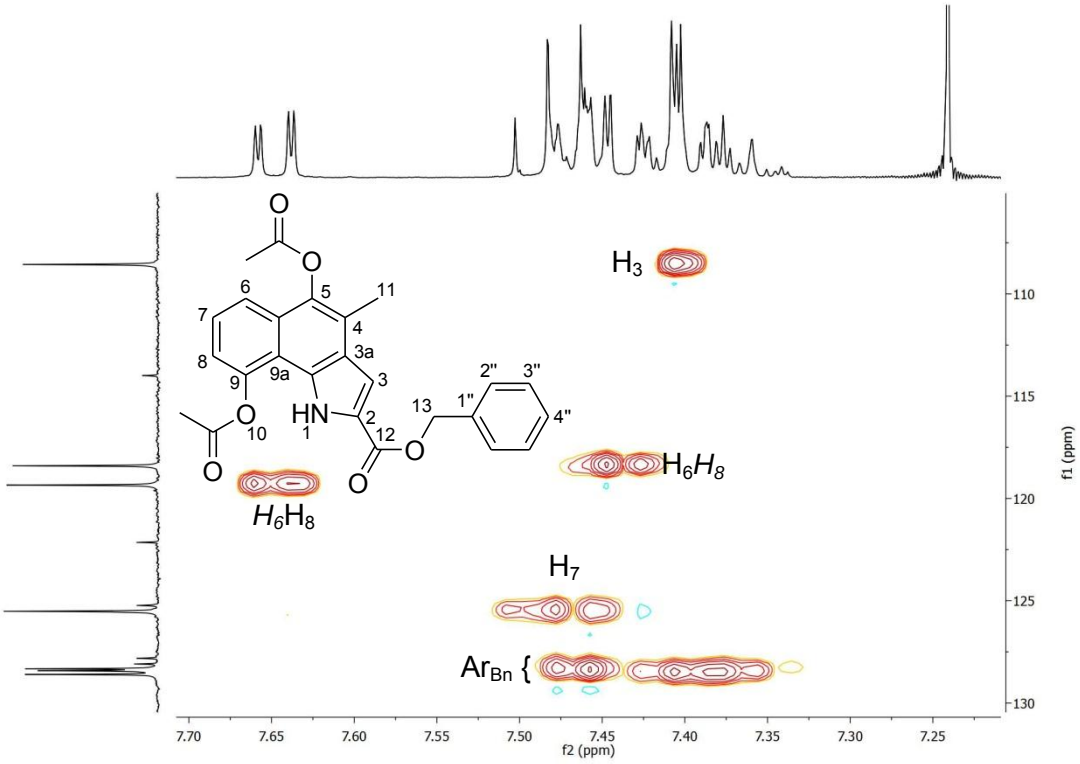

Figure 12. Expansion of the aromatic region of the HSCQ spectrum of the benzo[*g*]indole identifying the likely position of the characteristic aromatic singlet at H_3

The proposed reaction mechanism giving rise to the product is given below in Scheme 23. The Boc deprotection proceeds in the standard manner, with protonation of the carbamate carbonyl leading to loss of the tertiary butyl cation (which is mopped up by the anisole additive). Decarboxylation leads to the free amine with a loss of CO_2. Under the acidic conditions, the quinone carbonyl is protonated, thereby promoting condensation with the free amine, and after loss of H_2O the imine is formed. Reduction of the quinone followed by a proton transfer gives rise to the dihydroxylated benzo[*g*]indole, which is acetylated in the following reaction by acetic anhydride in pyridine.

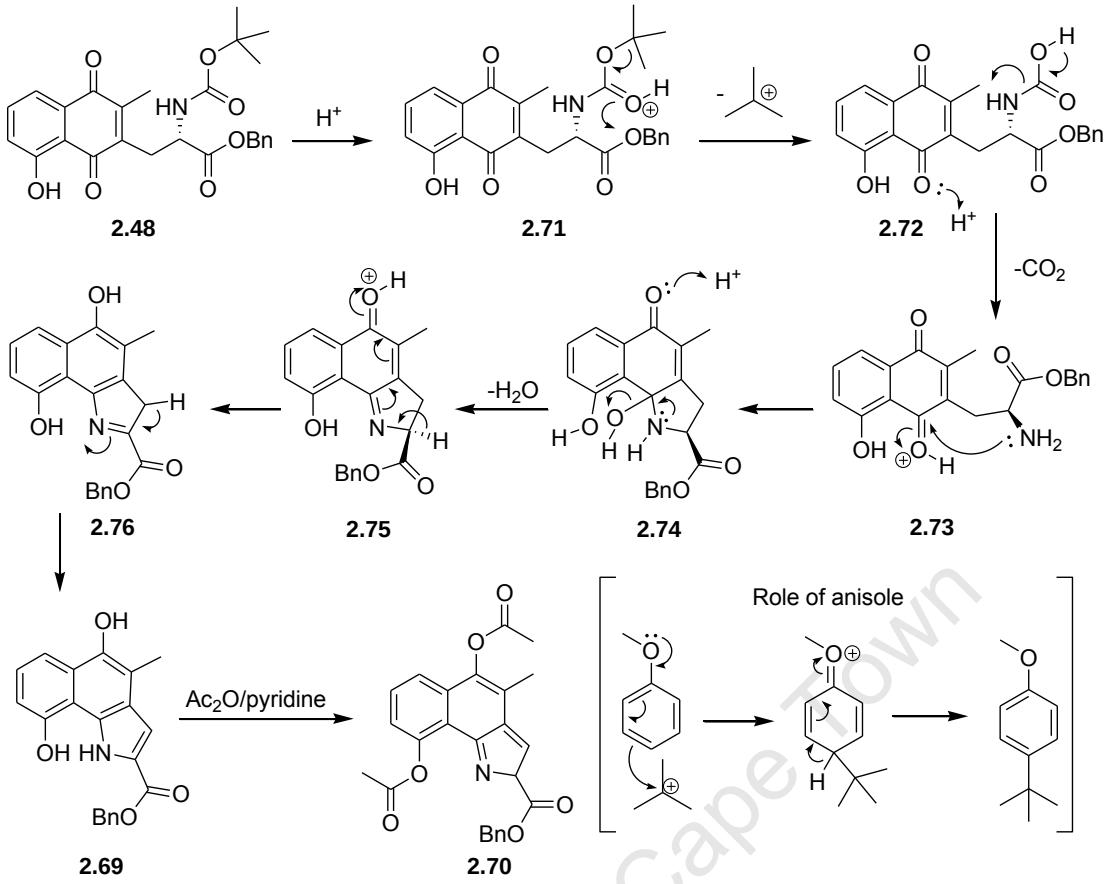

Scheme 23. Proposed mechanism for the formation of the benzo[*g*]indole under acid-catalysed conditions. The role of anisole in mopping up the liberated *tert*-butyl cation is given.

Having demonstrated the intramolecular condensation-aromatization sequence for the aspartic acid derivative, the glutamic derivative **2.49** was subjected to the same Boc deprotection conditions of trifluoroacetic acid and anisole in CH_2Cl_2 at 0 °C, with warming to room temperature, followed by acetylation with acetic anhydride in pyridine. Treatment with TFA in CH_2Cl_2 resulted in the formation of a product migrating as a single new spot on TLC, and after complete consumption of starting material, the reaction was worked up. The crude product was then subjected to acetylation before being purified and analysed. The reaction proceeded in a good yield of 85 % over the two steps. Characterisation of the product demonstrated that cyclisation had successfully taken place and the benzo[*h*]quinoline had formed.

The ^{1}H NMR spectrum (Figure 13) indicated once again that alkyl chain signals were missing and that there was a new cis double bond system as indicated by coupled doublets at 8.51 and 8.36 ppm (J = 8.54 Hz). Other notable differences from the starting material were a downfield shift of the phenolic OH singlet (from 12.08 to 14.70 ppm) and a shuffling around of the naphthoquinone signals in the aromatic region. Acetylation appeared to have

taken place at one of the phenolic hydroxyls, since there were two methyl signals at 2.50 and 2.52 ppm (once again indicating a downfield shift of the naphthoquinone methyl signal from 2.06 ppm). Apart from the change to the benzylic CH_2 signals, the aromatic benzyl signals remained largely unchanged.

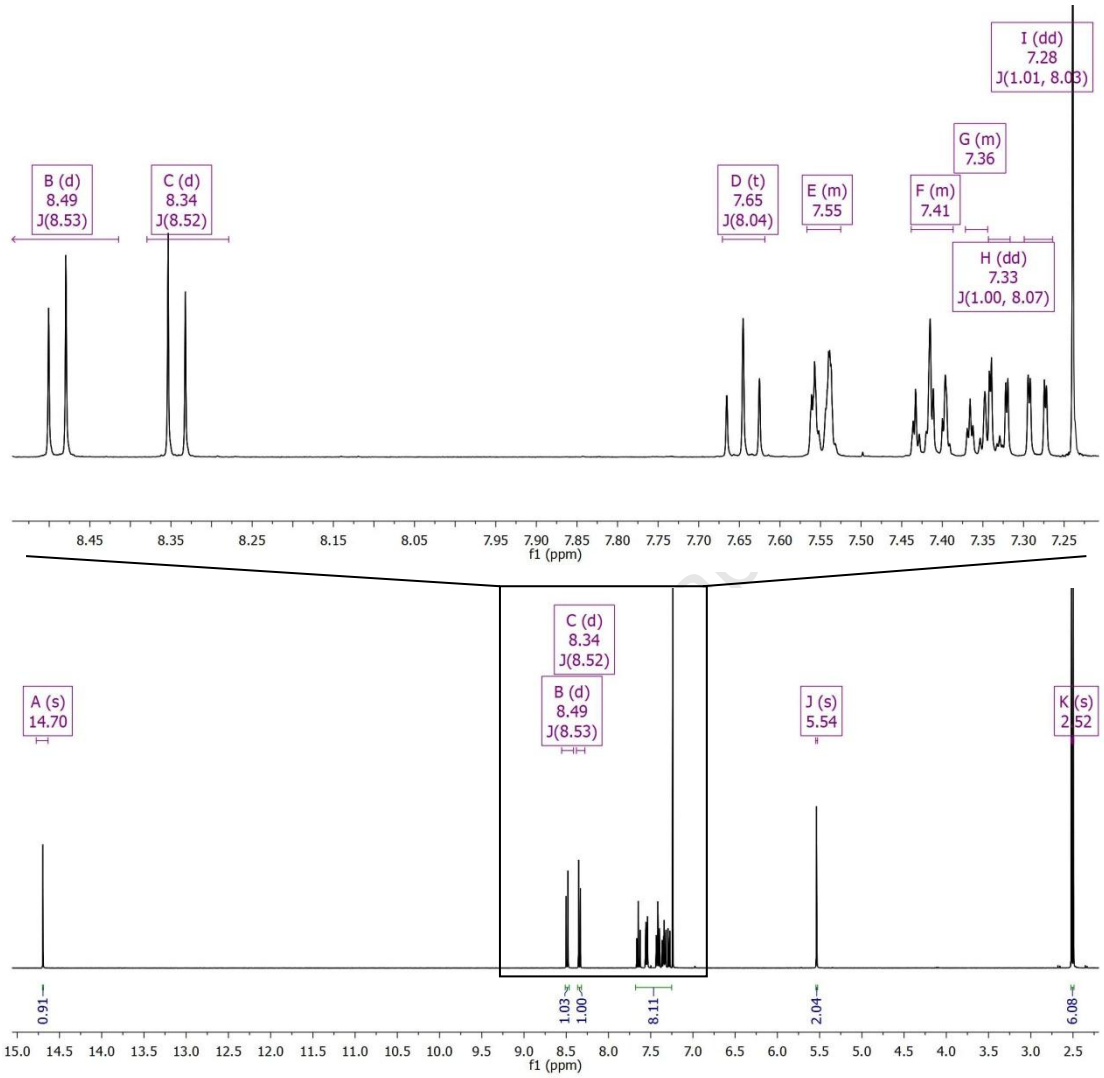

Figure 13. 1H NMR spectrum of the glutamic product of the Boc deprotection and acetylation reaction

Combining the above NMR spectroscopic evidence, a product structure **2.77** was proposed, shown in Figure 14 below.

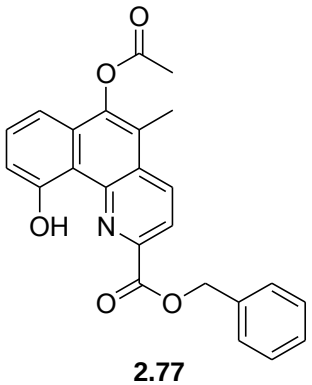

2.77

Figure 14. Chemical structure of novel benzo[*h*]quinoline synthesised by reaction of **2.49** with TFA, then Ac_2O/pyridine. Acetylation is proposed to have occurred at the 6-position.

Unambiguous assignment of the spectra proved difficult, however, since the position of the single acetate could not be confirmed. It was likely to have occurred at the 6-position since the phenolic signal in the ^1H spectrum (14.70 ppm) is closer in position to the phenolic signal (12.08 ppm) of the starting material than that of the 6-position (6.13 ppm) of the cyclised glucosamine-coupled product **2.67** described above. Consequently, crystals of the product were grown and the structure analysed by single crystal X-ray diffraction. This provided unambiguous proof of the tricyclic benzo[*h*]quinoline structure as illustrated in Figure 15 below.

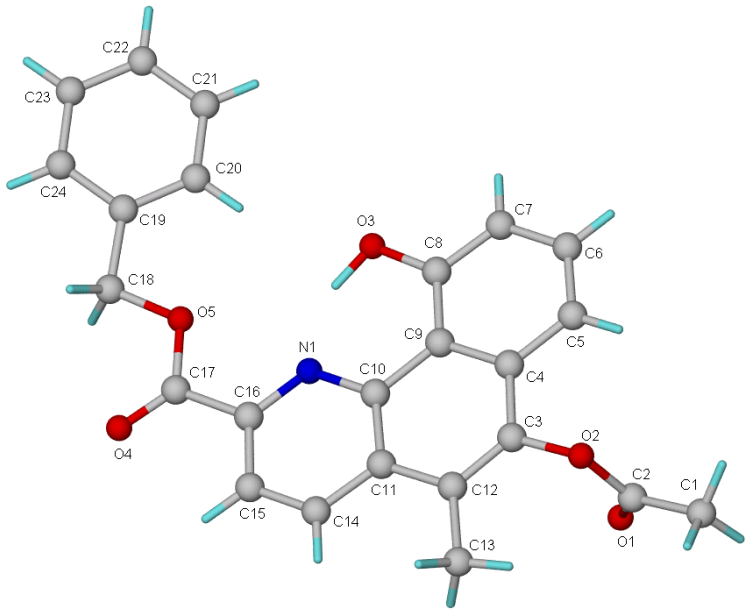

Figure 15. Chemical structure of synthesised benzo[*h*]quinoline derived from crystal structure determination

The data collection and refinement parameters are given in Table 3 below.[67]

Table 3. Data collection and refinement parameters for **2.77**

Crystal system	Monoclinic
Space group	*C*2/c
Unit cell constants	
a (Å)	31.457(3)
b (Å)	7.8845(7)
c (Å)	20.492(2)
β (°)	129.843 (1)
Volume ($Å^3$)	3902.4(6)
Z	8
$Density_{calc}$ ($g.cm^{-3}$)	1.366
F (000)	1680
Temperature of data collection (K)	173(2)
Crystal size (mm)	0.13 x 0.09 x 0.07
Range scanned θ (°)	1.69 – 30.56
Index ranges	h: -44, 44; k: -11, 11; l -29, 25
Total no. of reflections collected	20089
No. of independent reflections	5968
No. of reflections with I > 2σ(I)	4053
No. of parameters	277
S	1.022
R_1 [I > 2σ(I)]	0.0463
wR_2	0.1310
Max. and Av. Shift/Error	0.00, 0.00
Min. and Max. Resd. Dens. [$e/Å^3$]	-0.207, 0.376

Fusion of the benzene ring with the quinoline was confirmed to have taken place at the eighth side of the quinoline ring, and is hence designated “h”. The crystal structure indicates that acetylation took place at the phenolic OH generated by the reduction of the quinone (6-position, C3 in crystal structure diagram), and not at the phenolic OH present of the starting material (10-position). Presumably this is due to its enhanced nucleophilicity as a result of electronic induction by the nitrogen para to the OH. The alkyl side chain was found to be subjected to elimination, with the drive to aromaticity promoting that reaction. The stable, sterically-favoured 6-membered ring that forms as a result of the imine condensation drives the reaction to take place initially, with aromatisation following that initial step.

A proposed mechanism for the formation of **2.77** is presented in Scheme 24 below. The initial mechanism follows the standard Boc deprotection pathway, but once the amine is liberated it condenses with the nearest carbonyl group under the acidic conditions, liberating water and resulting in cyclisation to the 3,4-dihydrobenzo[*h*]quinoline. The drive to aromaticity promotes elimination of hydrogen resulting in the fully aromatic benzo[*h*]quinoline. Acetylation of the newly-formed hydroxyl takes place in the second reaction to form the final acetylated compound.

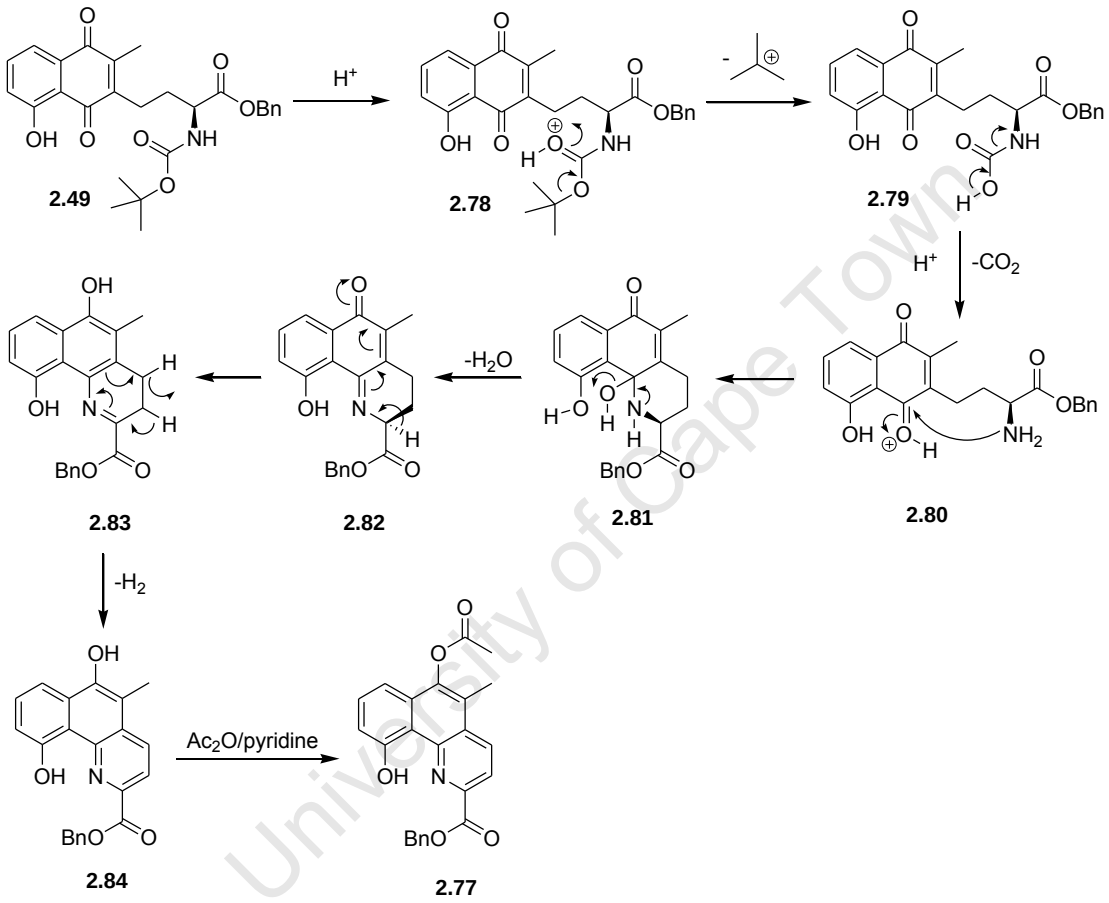

Scheme 24. Mechanism of TFA-mediated cyclisation to benzo[*h*]quinoline

A study of the literature provided a possible reason for this unexpected TFA acetylation of the aspartic acid-derived intermediates. Prior to using the TFA, it was purified by distillation over P_2O_5. However, a paper published by Tojo *et al*[68] reported that the symmetric anhydride of TFA can be prepared by stirring TFA over P_2O_5 in a dehydration reaction. The preparation they report contained a mixture of the acid and anhydride, which would account for the one-pot removal of the Boc and acetylation of the liberated amine by TFA anhydride. Subsequent attempts to remove the Boc protecting group of the aspartic derivative with fresh, untreated TFA resulted in exclusive cyclisation to the benzoindole. It is interesting to note that deprotection of the glutamic derivative with the mixture of TFA and TFA anhydride

did not yield any detectable *N*-acyl product. It would appear that the cyclisation to the benzoquinoline is a faster reaction than the cyclisation to the benzoindole, presumably due to the high stability of the aromatic tricyclic ring system. Obviously this full aromaticity is not possible with the benzoindole due to the presence of the NH in the ring, and this allows a fraction of the free amine to be trapped by the TFA anhydride.

2.4.6 Attempts Towards the Preparation of an N-Acetylated Amino Acid

Following the failure to convert the *N*-Boc to the *N*-acetate group as described above, several attempts were made to install the acetate on the amine of the amino acid starting material prior to oxidative coupling with the naphthoquinone in order to circumvent the reductive cyclisation reaction (Scheme 25).

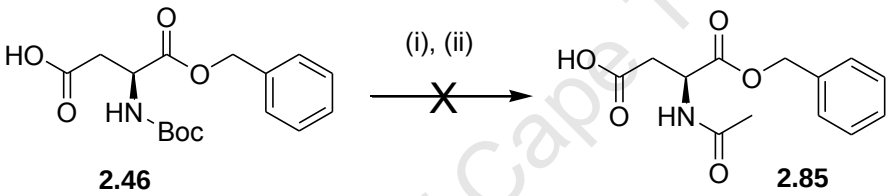

2.46 **2.85**

Scheme 25. Proposed synthesis of the *N*-acetylated amino acid. (i) TFA, anisole, CH_2Cl_2, 0 °C – r.t., 4 h; (ii) Ac_2O, pyridine, r.t., overnight.

This proved to be problematic for several reasons. Firstly, it was difficult to visualise the amino acid on the TLC plate. Despite the presence of a benzyl ester, the UV visibility was poor, and several staining agents, including anisaldehyde, ceric ammonium sulfate, ferric chloride, vanillin and iodine were unable to stain the substrate. Ninhydrin provided a moderately suitable staining agent, but the product migrated as very broad, diffuse spots making it difficult to accurately monitor the progression of the reaction. None-the-less, in the first attempt the Boc removal step was carried out under similar conditions to those described above. The Boc-protected amino acid was stirred in 20 % TFA in CH_2Cl_2 for 4 h before the solvent was removed and the residue dissolved in Ac_2O and pyridine and stirred overnight. After removal of the solvent under reduced pressure attempts were made to purify the residue by chromatography. However, there were no pure fractions isolated that could be identified as a possible product. It appeared that at some stage in the process considerable degradation took place, precluding this route as a potential pathway to the target molecule.

As an alternative, the possibility of acetylating the Boc-protected amine was explored, with a view to selectively removing the Boc group from the *N*-acetyl-*N*-Boc derivative. This proposed synthetic route is outlined below in Scheme 26.

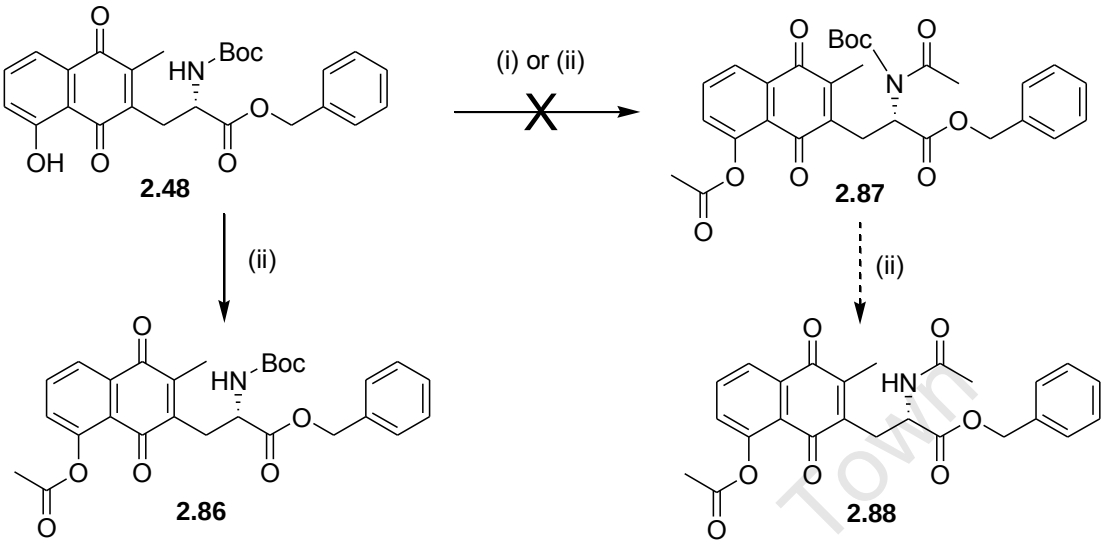

Scheme 26. Proposed synthetic route to prepare the acetylated Boc-protected amine. (i) Ac_2O, pyridine, r.t., 2 - 4 days; (ii) AcCl, dry CH_2Cl_2, Et_3N, 0 °C – r.t., 27 h; (iii) TFA, anisole, CH_2Cl_2, 0 °C – r.t., 4 h.

In the first attempt of this sequence, acetic anhydride in pyridine was employed, and after 4 days in the presence of these reagents at r.t. under argon, considerable degradation of the starting material was visible by TLC, and no major product was isolable.

In the second attempt, the *N*-Boc substrate was treated with acetyl chloride and triethylamine in anhydrous methylene chloride under argon, and a single product was obtained and identified as the *O*-acetate **2.86**. Despite a reaction time of 27 h, double acetylation did not take place.

2.5 Discussion and Conclusion

The inability to generate the final conjugate of naphthoquinone derivative and 2-amino-1-thioglucoside or related glycerol glycoside unfortunately precludes verification of the proposed target molecules as potential subversive substrates/inhibitors. The failure to prepare the glycerol glycoside and the problems associated with the NHAc substituent on the linker were the two most significant challenges in this study. The failure to achieve a successful glycosylation, despite numerous careful attempts and a variety of strategies,

appears to be due to a combination of poor reactivity of the glycerol-derived acceptor, and possible "disarming" of the glycosyl donor by the protecting groups. Future attempts of this reaction might be successful if a more reactive donor was used bearing a closer resemblance to the benzylated trichloroacetimidate donor that was successfully employed by Wu *et al*.[40] The acetate protecting groups on the protected glucoside used in this project would have deactivated the anomeric position and increased the energy requirement for glycosylation. The failure of glycosylation with the glycosyl fluoride and phenylthioglycoside donors is difficult to rationalise based on the structures of the reactants, since high-yielding glycosides have been achieved with analogous compounds. Problems such as these are not unprecedented in carbohydrate chemistry, and may simply point to a limited understanding of subtle steric, conformational and stereoelectronic factors which combine to affect reactivity.

However, this study has been successful in other respects. Firstly, conditions have been established for reproducible application of the oxidative decarboxylation route to 2-alkyl-1,4-naphthoquinones, including the preparation of a potentially useful series of naphthoquinonyl amino acids. Several factors influencing the outcome of this reaction, in particular, the reactivity of the alkyl radical, are described in further detail in Chapter 3. Secondly, the serendipitous discovery of the new route to benzo[*g*]indoles and benzo[*h*]quinolines has suggested a novel approach to these important classes of biologically-active heterocycles,[69,70,71,72,73] and illustrated the differences in reactivity of analogues with differing length of the side chain. This methodology differs from the classical Friedländer synthesis of quinolines,[74,75,76] which uses 2-aminobenzaldehydes and ketones in a condensation reaction to construct the *N*-heterocycle, or the related Niementowski approach,[77,78] or Camps cyclisation.[78,79] These methods all employ an aniline-type amine, with the N-C bond established in the starting material. The Fischer indole synthesis[80] similarly generates the cyclisation from an aryl hydrazine, with the N-C aryl bond extant in the starting material. Our approach is different in that the imine condensation generates the N-C aryl bond from the tethered amine. Other reported syntheses of benzoquinolines and benzoindoles include electroreductive coupling of phthalimides followed by rearrangement of the resulting silyl ketene acetals,[81] *N*-heterocyclisation of naphthylamines with diols catalysed by an iridium chloride/BINAP system,[82] and irradiation of aryl-substituted 3-amino-2-alkene imines to effect cyclisation to benzoquinolines.[83] Soleiman *et al*[84] used a 1,4-naphthoquinone and glycine to generate a benzo[*f*]indole, which they erroneously describe as a benzo[*g*]indole. However, this approach produced the 5-membered *N*-heterocycle on the quinone C=C, rather than through an imine condensation, which conserved the quinone structure and resulted in a considerably different substitution pattern to that observed with our approach.

Treatment of the glutamic derivatives (**2.49** and **2.57**) with the mixture of TFA and TFAA gave the cyclised product exclusively, with no detectable *N*-acylated product, whereas treatment of the aspartic derivatives (**2.48** and **2.56**) with this mixture resulted in the formation of both the linear *N*-acylated product and the cyclised benzo[*g*]indole product. This difference in reactivity can be rationalised by the enhanced stability of the fully conjugated benzo[*h*]quinoline ring system relative to the less conjugated benzo[*g*]indole. It appears that in the formation of the benzo[*h*]quinoline the rate of cyclisation is greater than the rate of acylation of the liberated amine with TFAA, whereas in the formation of the benzo[*g*]indole the rate of cyclization is considerably slower.

It is clear therefore that a revised strategy will be necessary in order to obtain the desired conjugates with an *N*-acetyl group in the linker. An obvious variation to consider in future work is to avoid using the acid-labile *N*-boc protecting group in the starting amino acid so as to avoid the acidic deprotection step which leads to the inadvertent cyclisation. While there are no doubt other viable ways of preparing the desired naphthoquinone derivatives, it might also be worth considering a quite different class of redox cycling subversive substrates, where the quinone unit is replaced by a ferrocenyl unit. Ferrocene derivatives have been reported to be effective redox cyclers and could in principle operate in a similar manner to that of the quinone redox cyclers.[85,86,87,88] A general approach to these such as that proposed in Scheme 27 below from commercially-available amino acid derivatives **2.90** (n = 1, 2) and ferrocene could give access to subversive substrates with the desired NHAc substituent appropriately positioned in the linker between redox-active ferrocene and the MSH-like scaffold.

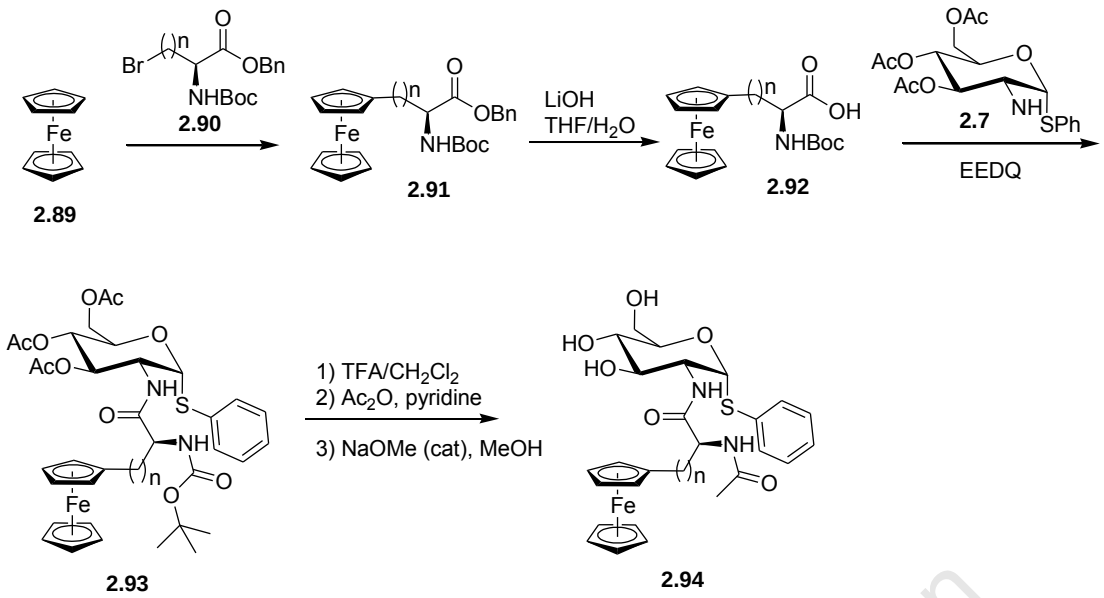

Scheme 27. Proposed synthetic scheme of ferrocene conjugate of phenylthioglucosamine with linker containing the desired NHAc substituent. Synthetic steps include alkylation of the ferrocene by amino acid derivatives **2.90**, followed by saponification and amide coupling to the phenylthioglucosamine, and then Boc removal, amine acetylation and acetate deprotection.

References

1. P.J. O'Brien, *Chem. Biol. Interact*., **1991**, *80*, 1-41
2. L. Salmon-Chemin, E. Buisine, V. Yardley, S. Kohler, M.-A. Debreu, V. Landry, C. Sergheraert, S.L. Croft, R. L. Krauth-Siegel and E. Davioud-Charvet, *J. Med. Chem.*, **2001**, *44,* 548-565
3. T. Tran, E. Saheba, A.V. Arcerio, V. Chavez, Q.-y. Li, L.E. Martinez and T.P. Primm, *Bioorg. Med. Chem.*, **2004**, *12*, 4809-4813
4. T. Iyanagi and I. Yamazaki, *Biochim. Biophys. Acta*, **1970**, *216*, 282-294
5. S.L. Croft, A.T. Evans and R.A. Neal, *Ann. Trop. Med. Parasitol.*, **1985**, *79*, 651-653
6. S.L. Croft, J. Hogg, W.E. Gutteridge, A.T. Hudson and A.W. Randall, *J. Antimicrob. Chemother*., **1992**, *30*, 827-832
7. A. Boveris, R. Docampo, J.F. Turrens, A.O.M. Stoppani, *Biochem. J*., **1978**, *175*, 431-439
8. S.L. Oza, M.P. Shaw, S. Wyllie and A.H. Fairlamb, *Mol. Biochem. Parasitol*., **2005**, *139*, 107-116
9. C.H. Faerman, S.N. Savvides, C. Strickland, M.A. Breidenbach, J.A. Ponasik, B. Ganem, D. Ripoll, R.L. Krauth-Siegel and P.A. Karplus, *Bioorg. Med. Chem*., **1996**, *4*, 1247-1253

10. M.C. Jockers-Scherübl, R.H. Schirmer and R.L. Krauth-Siegel, *Eur. J. Biochem*. **1989**, *180*, 267-272
11. R.H. Schirmer, J.G. Müller and R.L. Krauth-Siegel, *Angew. Chem. Int. Ed*., **1995**, *34*, 141-154
12. G.B. Henderson, P. Ulrich, A.H. Fairlamb, I. Rosenberg, M. Pereira, M. Sela and A. Cerami, *Proc. Natl. Acad. Sci. U.S.A.*, **1988**, *85*, 5374-5378
13. N.K. Cenas, D. Arscott, C.H. Williams and J.S.Blanchard, *Biochemistry*, **1994**, *33*, 2509-2515
14. D.A. Bironaite, N.K. Cenas, J.J. Kulys, *Z. Naturforsch. C*, **1991**, *46*, 966-968; R.M. Lüöng, J.H. McKie, K.T. Douglas, M.J. Dascombe and J. Vale, *J. Enzymol. Inhib.*, **1998**, *13*, 327-345
15. R.M. Lüöng, J.H. McKie, K.T. Douglas, M.J. Dascombe and J. Vale, *J. Enzymol. Inhib.*, **1998**, *13*, 327-345
16. A. Mahapatra, S.P.N. Mativandlela, B. Binneman, P.B. Fourie, C.J. Hamilton, J.J.M. Meyer, F. van der Kooy, P. Houghton and N. Lall, *Bioorg. Med. Chem*., **2007**, *15*, 7638-7646
17. V.K. Jothivasan and C.J. Hamilton, *Nat. Prod. Rep*., **2008**, *25*, 1091-1117
18. D.W. Gammon, D.J. Steenkamp, V. Mavumengwana, M.J. Marakalala, T.T. Mudzunga, R. Hunter and M. Munyololo, *Bioorg. Med. Chem.*, **2010**, *18*, 2501-2514
19. M.P. Patel and J.S. Blanchard, *Biochemistry*, **2001**, *40,* 5119-5126
20. G.L. Newton, N. Buchmeier and R.C. Fahey, *Microbiol. Mol. Biol. Rev.*, **2008**, *72*, 471–494
21. G.L. Newton, P. Ta and R.C. Fahey, *J. Bacteriol*., **2005**, *187*, 7309–7316
22. (a) M.A. Jardine, H.S.C. Spies, C.M Nkambule, D.W. Gammon and D.J. Steenkamp, *Bioorg. Med. Chem.*, **2002**, *10*, 875-881; (b) D.J.R. Massy and P. Wyss, *Helv. Chim. Acta,* **1990**, *73*, 1037–1057; G.R. Baker, D.C. Billington and D. Gani, *Tetrahedron,* **1991**, *47*, 3895–3908; (c) S. Koto, M. Hirooka, T. Yoshida, K. Takenaka, C. Asai, T. Nagamitsu, H. Sakuma, M. Sakurai, S. Masuzawa, M. Komiya, T. Sato, S. Zen, K. Yago and F. Tomonaga, *Bull. Chem. Soc. Jpn*, **2000**, *73*, 2521–2529; (d) C.M. Nkambule, N.W. Kwezi, H.H. Kinfe, M.G. Nokwequ, D.W. Gammon, S. Oscarson and E. Karlsson, *Tetrahedron*, **2011**, *67*, 618-623; (e) S. Lee and J.P.N. Rosazza, *Org. Lett*., **2004**, *6*, 365-368
23. B.B. Metaferia, S. Ray, J.A. Smith and C. Bewley, *Bioorg. Med. Chem. Lett.*, **2007**, *17*, 444-447
24. M.J.G. Stewart, V.K. Jothivasan, A.S. Rowan, J. Wagg and C.J. Hamilton, *Org. Biomol. Chem.*, **2008**, *6*, 385-390
25. S. Knapp, S. Gonzalez, D.S. Myers, L.L. Eckman and C.A. Bewley, *Org. Lett.*, **2002**, *4*, 337-339
26. B.B. Metaferia, B.J. Fetterolf, S. Shazad-ul-Hussan, M. Moravec, J.A. Smith, S. Ray, M.-T. Gutierrez-Lugo and Carole A. Bewley, *J. Med. Chem.*, **2007**, *50*, 6326-6336

27. G.M. Nicholas, L.L. Eckman, P. Kováč, S. Otero-Quintero and C.A. Bewley, *Bioorg. Med. Chem.*, **2003**, *11*, 2641-2647
28. A. Titz, Z. Radic, O. Schwardt and B. Ernst, *Tetrahedron Lett.*, **2006**, *47*, 2383-2385
29. M. Martìn-Lomas, M. Flores-Mosquera and J. Luis Chiara, *Eur. J. Org. Chem.*, **2000**, *8*, 1547-1562
30. P.B. Alper, S.-C. Hung and C.-H. Wong, *Tetrahedron Lett*., **1996**, *37*, 6029-6032
31. P.T. Nyffeler, C.-H. Liang, K.M. Koeller and C.-H. Wong, *J. Am. Chem. Soc.*, **2002**, *124*, 10773-10778
32. P. Brandt, M.J. Söergren, P.G. Andersson and P.-O. Norrby, *J. Am. Chem. Soc.*, **2000**, *122*, 8013-8020
33. (a) T.J. Boltje, J.-H. Kim, J. Park and G.-J. Boons, *Org Lett*., **2011**, *13*, 284-287; (b) D.R. Mootoo, P. Konradsson, U. Udodong and B. Fraser-Reid, *J. Am. Chem. Soc.*, **1988**, *110*, 5583–5584; (c) B. Fraser-Reid, Z. Wu, U.E. Udodong and H. Ottosson, *J. Org. Chem.*, **1990**, *55*, 6068–6070; (d) L.K. Mydock and A.V. Demchenko, *Org. Lett*., **2008**, 10, 2107-2110; (e) Y. Zeng, Z. Wang, D. Whitfield and X. Huang, *J. Org. Chem.*, **2008**, *73*, 7952-7962
34. (a) B. Wegmann and R.R. Schmidt, *J. Carb. Chem.*, **1987**, 6, 357-375; (b) R.R. Schmidt and W. Kinzy, *Adv. Carbohydr. Chem. Biochem.,* **1994**, *50*, 21-123
35. G.-J. Boons and K.J. Hale, *Organic Synthesis with Carbohydrates*, **2000**, Sheffield Academic Press, Pp. 105-107
36. S. Cottaz, J.S. Brimacombe and M.A.J. Ferguson, *J. Chem. Soc. Perkin Trans.*, **1993**, *1*, 2945-2951
37. P. Fügedi, P.J. Garegg, H. Lönn and T. Norberg, *Glycoconjugate J.*, **1987**, *4*, 97-108
38. P.J. Garegg, *Adv. Carbohydr. Chem. Biochem.*, **1997**, 52, 179-205
39. A.V. Demchenko, *Curr. Org. Chem.*, **2003**, *7*, 35-79
40. H.-J. Wu, C.-X. Li, G.-P. Song and Y.-X. Li, *Chin. J. Chem.*, **2008**, *26*, 1641-1646
41. H.H. Kinfe, PhD Thesis, **2006**, University of Cape Town
42. S.K. Madhusudan, G. Agnihotri, D.S. Negi and A.K. Misra, *Carbohydrate Res*., **2005**, *340*, 1373–1377
43. D.W. Gammon, R. Hunter, D.J. Steenkamp and T.T. Mudzunga, *Bioorg. Med. Chem. Lett.*, **2003**, *13*, 2045-2049
44. M. Palme and A. Vasella, *Helv. Chim. Acta*, **1995**, *78*, 959-969
45. G.-J. Boons and K.J. Hale, *Organic Synthesis with Carbohydrates*, **2000**, Sheffield Academic Press, Pp. 113
46. G.-J. Boons and K.J. Hale, *Organic Synthesis with Carbohydrates*, **2000**, Sheffield Academic Press, Pp. 118-119
47. D. Vourloumis, G.C. Winters, M. Takahashi, K.B. Simonsen, B.K. Ayida, S. Shandrick, Q. Zhao and T. Hermann, *ChemBioChem*, **2003**, *4*, 879-885
48. S. Yamago, M. Hashidume and J.-I. Yoshida, *Tetrahedron*, **2002**, *58*, 6805–6813
49. A.I. Tsai, Y.-L.Wu and C.-P. Chuang, *Tetrahedron,* **2001**, *57*, 7829-7837

50. (a) D.H.R. Barton, D Crich and W.B. Motherwell, *J. Chem. Soc. Chem Commun*., **1983**, *17*, 939-941; (b) D.H.R. Barton, D. Crich and W.B. Motherwell, *Tetrahedron Lett*., **1983**, *24*, 4979-4982; (c) D.H.R. Barton, D. Crich and W.B. Motherwell, *Tetrahedron*, **1985**, *41*, 3901-3924
51. M.F. Saraiva, M.R.C. Couri, M.L. Hyaric, *Tetrahedron*, **2009**, *65*, 3563-3572
52. T. Ling, E. Poupon, E.J. Rueden, E.A. Theadorakis, *Org. Lett.,* **2002**, *4*, 819-822
53. S. Debre, R. Duval, G. Roue, A. Garofano, E. Poupon, U. Brandt, S.A. Susin, R. Hocquemiller, *ChemMedChem*, **2006**, *1*, 118–129
54. C. Commandeur, C. Chalumeau, J. Dessolin and M. Laguerre, *Eur. J. Org. Chem.*, **2007**, *18*, 3045–3052
55. J.M. Anderson and J.K. Kochi, *J. Am. Chem. Soc*., **1970**, *92*, 2450–2460
56. (a) F. Minisci, R. Bernardi, F. Bertini, R. Galli and M. Perchinummo, *Tetrahedron*, **1971**, *27*, 3575-3579; (b) F. Minisci, *Synthesis*, **1973**, *1*, 1-24; (c) F. Minisci, *Acc. Chem. Res.*, **1983**, *16*, 27-32
57. D.J. Cremin, A.F. Hegarty and M.J. Begley, *J. Chem. Soc., Perkin Trans.*, **1980**, *2*, 412-420
58. F. Leroux, *ChemBioChem*, **2004**, *5*, 644-649
59. A. Bondi, *J. Phys. Chem*., **1964**, *68*, 441-451
60. N.A. Meanwell, *J. Med. Chem*., **2011**, *54*, 2529–2591
61. (a) J.-P. Bégué and D. Bonnet-Delpon, *Bioorganic and Medicinal Chemistry of Fluorine*, **2008**, John Wiley & Sons: Hoboken, NJ; (b) K. Müller, C. Faeh and F. Diederich, *Science*, **2007**, *317*, 1881–1886; (c) S. Purser, P.R. Moore, S. Swallow and V. Gouverneur, *Chem. Soc. Rev*., **2008**, *37*, 320–330; (d) P. Shah and A.D. Westwell, *J. Enzyme Inhib*. *Med. Chem*., **2007**, *22*, 527–540
62. (a) D.J.P. Pinto, M.J. Orwat, S. Wang, J.M. Fevig, M.L. Quan, E. Amparo, J. Cacciola, K.A. Rossi, R.S. Alexander, A.M. Smallwood, J.M. Luettgen, L. Liang, B.J. Aungst, M.R. Wright, R.M. Knabb, P.C. Wong, R.R. Wexler and P.Y.S. Lam, *J. Med. Chem*., **2001**, *44*, 566–578; (b) M.L. Quan, P.Y.S. Lam, Q. Qi Han, D.J.P. Pinto, M.Y. He, R. Li, C.D. Ellis, C.G. Clark, C.A. Teleha, J.-H. Sun, R.S. Alexander, S. Bai, J.M. Luettgen, R.M. Knabb, P.C. Wong and R.R. Wexler, *J. Med. Chem*., **2005**, *48*, 1729–1744
63. H.-J. Böhm, D. Banner, S. Bendels, M. Kansy, B. Kuhn, K. Müller, U. Obst-Sander and M.Stahl, *ChemBioChem*, **2004**, *5*, 637–643
64. J. W. Clader, *J. Med. Chem*., **2004**, *41*, 1–9
65. W. K. Hagman, *J. Med. Chem*., **2008**, *51*, 4359–4369
66. D. O'Hagan, *Chem. Soc. Rev*., **2008**, *37*, 308–319
67. (a) COLLECT, Data Collection Software, Nonius, Delft, The Netherlands, **1999**; (b) Z. Otwinowski, W. Minor, DENZO and SCALEPACK, in International Tables of Crystallography, ed. M.G. Rossman, E. Arnold, Kluwer, Dordrecht, **2000**, vol. F.; (c) G.M. Sheldrick, SHELXS-97 and SHELXL-97, Programs for crystal structure determination and refinement, University of Göttingen, Germany, **1997**; (d) L.J. Barbour, *J. Supramol. Chem*., **2001**, *1*, 189-191; (e) A.L. Spek, *J. Appl. Crystallogr*., **2003**, *36*, 7-13

68. M. Tojo, S. Fukuoka and H. Tsukube, *J. Fluorine Chem*., **2010**, *131*, 29-35
69. A. Detsi, V. Bardakos, J. Markopoulos and 0. Igglessi-Markopoulos, *J. Chem Soc., Perkin Trans.*, **1996**, *1*, 2909-2913
70. N. Tagmatarchis, K. Thermos and H.E. Katerinopoulos, *J. Med. Chem.*, **1998**, *41*,4165-4170
71. W.F. Michne and N.F. Albertson, *J. Med. Chem.*, **1970**, *13*, 522-525
72. M. Maftouh, R. Besselievre, B. Monsarrat, P. Lesca, B. Meunier, H.P. Husson and C. Paoletti, *Eur. J. Med. Chem.*, **2002**, *28*, 261-266
73. R.C. Oslund, N. Cermak and M.H. Gelb, *J. Med. Chem.*, **2008**, *51*, 4708-4714
74. P. Friedländer, *Chem. Ber*., **1882**, *15*, 2572-2575
75. F.W. Bergstrom, *Chem. Rev*., **1944**, *35*, 77-277
76. C.C. Cheng and S.J. Yan, *Org. React*., **1982**, *28*, 37-201
77. S. Niementowski, *Chem. Ber*., 1894, 27, 1394-1403
78. R.H. Manske, *Chem. Rev*., **1942**, *30*, 113-144
79. R. Camps, *Chem. Ber*., **1899**, *22*, 3228-3234
80. B. Robinson, *Chem. Rev*., **1969**, *69*, 227–250
81. N. Kise, S. Isemoto and T. Sakurai, *Org. Lett.*, **2009**, *11*, 4902-4905
82. H. Aramoto, Y. Obora and Y. Ishii, *J. Org. Chem.*, **2009**, *74*, 628–633
83. P.J. Campos, E. Añón, M.C Malo, C.-Q. Tan and M.A. Rodríguez, *Tetrahedron*, **1998**, *54*, 6929-6938
84. H.A. Soleiman, A.K. Khalafallah and H.M. Abdelzaher, *J. Chin. Chem. Soc.*, **2000**, *47*, 1267-1272
85. T. Kijima, T. Suzuki and T. Izumi, *J. Biosci. Bioeng.*, **2003**, *96*, 585-587
86. L. Soulère and J. Bernard, *Bioorg. Med. Chem. Lett*., **2009**, *19*, 1173–1176
87. M. Vaillancourt, J.W. Chen, G. Fortier and D. Bélanger, *Electroanal.*, **1999**, *11*, 23-31
88. J. Razumiene, A. Vilkanauskyte, V. Gureviciene, V. Laurinavicius, N.V. Roznyatovskaya, Y.V. Ageeva, M.D. Reshetova and A.D. Ryabov, *J. Organomet. Chem*., **2003**, *668*, 83-90

Chapter 3
Carbazole-1,4-Quinone-derived Target Molecules

3.1 Introduction

Carbazole alkaloids have been isolated from a wide range of biological sources, including higher plants, microbes, marine cyanophyta as well as bovine urine and human pathogenic yeast. The most abundant source of carbazoles is the Rutaceae family of plants from which carbazoles have been isolated from the genera *Murraya*, *Glycosmis*, *Clausena* and *Micromelum*.[1] These alkaloids have been reported to display a range of biological activities, including anti-inflammatory, antioxidant, mosquitocidal, antimicrobial,[2,3] anticancer,[4] and antimalarial,[5] among others.[6] Within the context of tuberculosis drug research, the carbazole alkaloid clausine K (or clauszoline J) (Figure 1), which has been isolated from various sources,[7,8,9] was shown to display weak antituberculosis activity (MIC of 100 μg.ml^{-1} against the H_{37}Ra strain),[10,11] and micromeline (Figure 1), isolated from the bark of *Micromelum hirsutum*, was also found to have anti-TB activity (MIC of 31.5 μg.ml^{-1} against *M. tuberculosis* H_{37}Rv).[12]

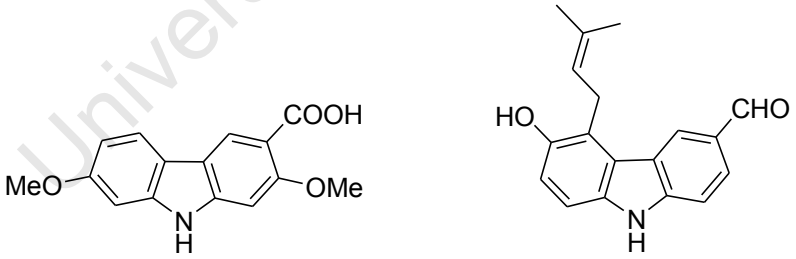

3.1 clausine K (or clauszoline J) **3.2** micromeline

Figure 1. Chemical structures of the carbazole alkaloids, clausine K (or clauszoline J) and micromeline

Based on these preliminary results, Knölker and co-workers[13] screened a series of carbazole alkaloids for their *in vitro* anti-TB activity and established several trends in the substitution patterns that affected the observed activities. It appeared that activity was highly sensitive to subtle changes in substitution about the tricyclic ring system. Using the general carbazole numbering scheme illustrated in Figure 2, substituents at the nitrogen atom were found not

to contribute to antitubercular activity, although the presence of a nitrogen-containing substituent at either the 3- or 7-position resulted in a substantial increase in activity. 3,6-Dibromo, 2-hydroxy, 2-hydroxy-3-methyl and 1-methoxy substitutions gave little or no activity, and neither did the 2,7- or 3,6-dioxygenated derivatives.

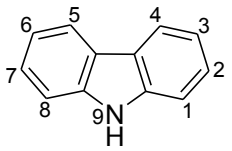

Figure 2. General chemical structure of carbazoles

An example of the subtlety in substitution differences having a marked bearing on activity was seen with the furo[3,2-a]carbazole alkaloid furoclausine A (**3.3**) which was found to show anti-TB activity, whereas its corresponding methyl ether (**3.4**) was inactive (Figure 3).

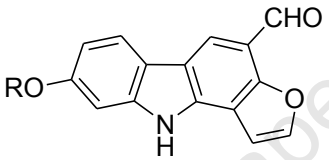

3.3 R = H
3.4 R = Me

Figure 3. Carbazole alkaloids with slight structural differences but considerable differences in MIC (**3.3**: 55 μM; **3.4**: >128 μM)

The greatest activity was observed with the 3,4-dioxygenated carbazole derivatives **3.5** - **3.7**, indicated below in Figure 4.

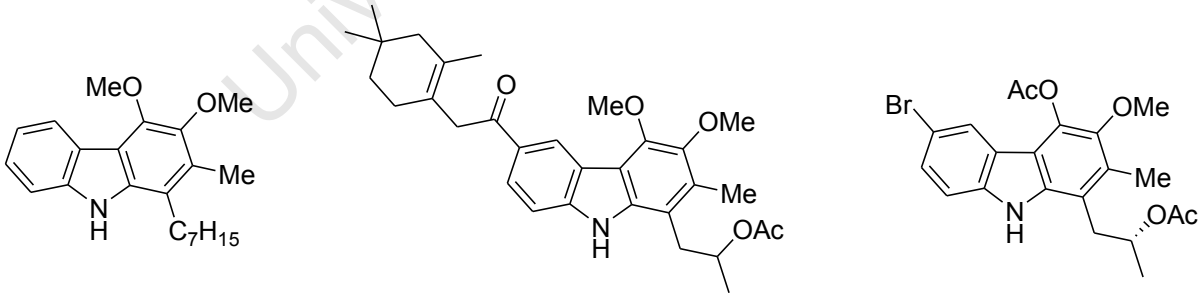

MIC = 11 μM
3.5

MIC = 8 μM
3.6

MIC = 55 μM
3.7

Figure 4. Chemical structures of 3,4-dioxygenated carbazole derivatives with good antitubercular activity

The study was then extended to include the carbazole quinones and quinols. Precedent for quinone analogues displaying anti-tuberculosis activity was given by the investigation of

Tran *et al*[14] that identified low to moderate activity in a number of quinone derivatives. The carbazole-1,4-quinol alkaloids evaluated were found to be inactive against TB, and although carbazole-1,4-quinone **3.8** was inactive as well, carbazole-1,4-quinone **3.9** displayed one of the lowest MIC values of the study (9 μM; 2.2 μg.ml^{-1}). It was noted that this derivative was a 3,4-dioxygenated carbazole, which this investigation seemed to suggest was a requirement for anti-TB activity.

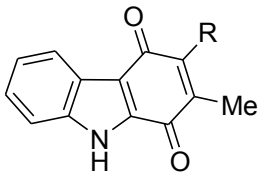

3.8 R = C_7H_{15}
3.9 R = OMe

Figure 5. Chemical structures of carbazole quinones. Derivative **3.9** demonstrated the highest anti-TB activity of all the carbazoles evaluated in the study with an MIC of 9 μM. Derivative **3.8** displayed poor activity with an MIC of 117 μM.

In a continuation of the findings of Knölker and co-workers,[13] several carbazole-1,4-quinones with structural similarity to **3.9** were coupled to a mycothiol-type phenylthio glucosamine scaffold in order to evaluate such conjugates as potential antitubercular compounds. The biological target of **3.9** has not yet been determined, and since the quinone functionality overlaps with that of the 1,4-naphthoquinone conjugates that were developed in our group and shown to have inhibitory activity against the mycothiol enzymes, MshB and Mca,[15] it seemed plausible that similar conjugates with carbazole-1,4-quinones might display comparable activities against these or other mycothiol enzymes. Consequently, a range of substituted carbazoles were considered for coupling to a phenylthio glucosamine unit.

3.2 Target Molecule Design

It was envisaged that the carbazole-1,4-quinone would be alkylated or acylated with a carbon chain of variable length, terminating in a carboxylic acid to allow for formation of an amide linkage to the glucosamine unit. Potential linker sites on the carbazole quinone structure were proposed and evaluated. These proposals were largely directed by the Knölker strategy for assembly of carbazole quinones and included attaching the linker at either the carbazole nitrogen, or the 2- or 3-position of the quinone. The nitrogen site was selected for attachment, despite the possibility that it may reduce the activity of the derivative, as suggested by the Knölker study,[13] since it provided a relatively facile point of

attachment synthetically, and also since substitution at that position would still afford a 3,4-dioxygenated derivative, which was suggested would enhance anti-TB activity. Substituting the 2- and 3-positions was not shown to negatively affect the activity, and in keeping with the findings by Knölker and co-workers, these derivatives were prepared such that the 3,4-dioxygenated carbazole pharmacophore was retained.

The retrosynthetic analysis for the proposed target molecules is outlined below in Scheme 1. The final carbazole-1,4-quinone conjugates of phenylthio glucosamine were envisaged to be prepared by amide coupling of the tethered carbazole with the glucosamine nitrogen, followed by deprotection of the acetate protecting groups. The 3-substituted carbazole derivatives **IV** with the required terminal carboxylic acid functionality were proposed to be prepared from terminal diols **III** by oxidation following an addition-elimination-type substitution at the vinylogous ester 3-position by alkyl diols to generate **III**.

The 2-substituted derivatives **VI** were proposed to originate from the nor-methyl carbazole quinone **3.10** under similar conditions to those used for the substituted naphthoquinone derivatives, namely, oxidative decarboxylation to generate the C-C bond. Since the chemistry required to functionalise a quinone at such an unsubstituted position was known, it seemed a suitable approach to follow.

Generation of *N*-alkylated carbazole quinones **VIII** could conceivably be prepared from starting material **3.11** by a Finkelstein-type alkylation of an alkyl halide. Attachment at the nitrogen could also conceivably be achieved by *N*-acylation. Intermediate **X** could be generated from starting material **3.11** by amide coupling with an alkyl acid chloride.

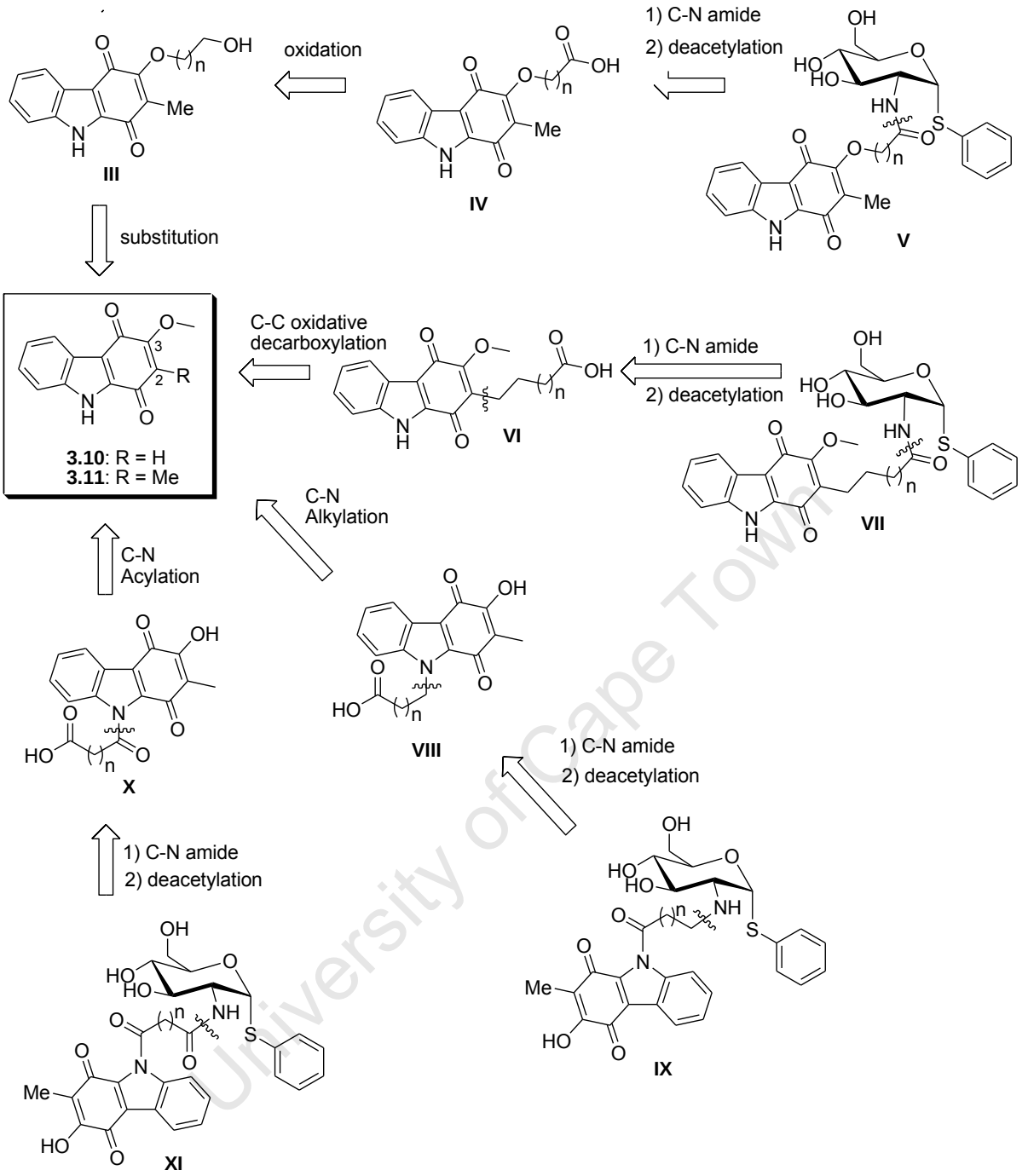

Scheme 1. Retrosynthetic analysis of proposed carbazole-1,4-quinone phenylthio glycosyl conjugates

Starting carbazoles **3.10** and **3.11** were prepared in the laboratory of Prof Knölker (Technische Universität Dresden, Germany) according to a published synthetic procedure,[16] and supplied for use in this project as part of a research collaboration.

3.3 Results

3.3.1 Substitution at the 3-Position

Generation of a 3-substituted carbazole quinone was attempted with dihydroxy alkanes (of differing chain lengths) and NaH as base. Ethane-1,2-diol, propane-1,3-diol and pentane-1,5-diol linkers were selected for this approach with differing outcomes. In the first attempt, **3.11** and NaH were dissolved in ethane-1,2-diol and heated at 50 °C overnight (Scheme 2). This afforded a single product in 74 % yield, identified by GC/MS as having the expected M^+ = 271.1, and the reaction was found to be reproducible on a 100 mg scale under milder conditions (r.t. for 3 h15 min).

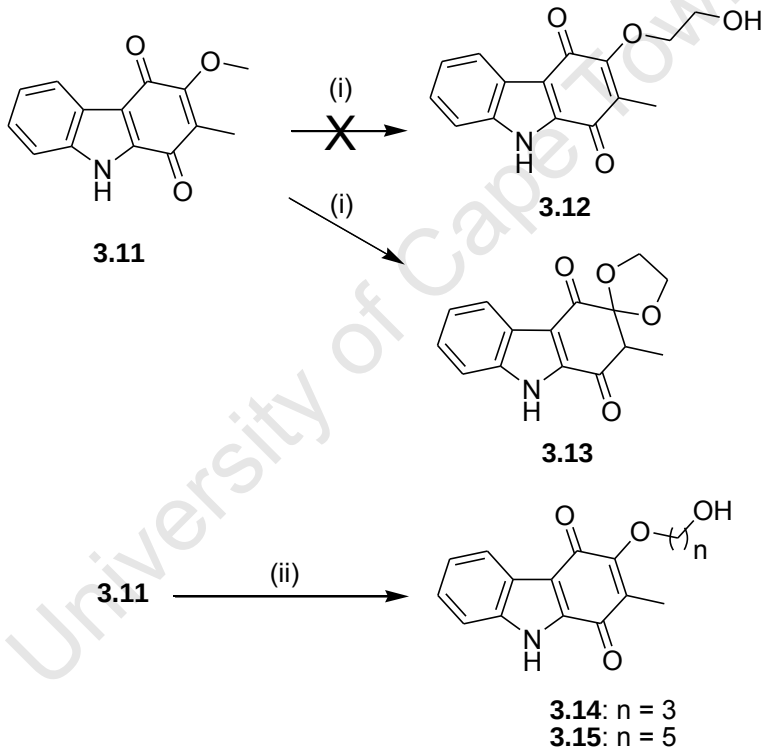

Scheme 2. Synthesis of the 3-substituted carbazole quinone derivatives. (i) NaH, ethylene glycol, r.t, 3 h, 69 %; (ii) NaH, alkyl diol, 50 °C, 18 – 42 h, **3.14**: 65 %, **3.15**: 74 %.

However, the ^{1}H NMR spectrum was not consistent with the expected 3-*O*-alkylated carbazole quinone. The carbazole methyl group appeared as a doublet at 1.2 ppm, instead of the expected singlet at ~2.0 ppm, and there were signals corresponding to five aliphatic protons, instead of the expected two multiplets corresponding to the methylene signals of the alkyl chain. The differentiation of the methylene signals indicated that they were in different

chiral environments. The analysis of the analytical data led to the proposed structure indicated in Figure 6, incorporating an ethylene ketal at C-3'.

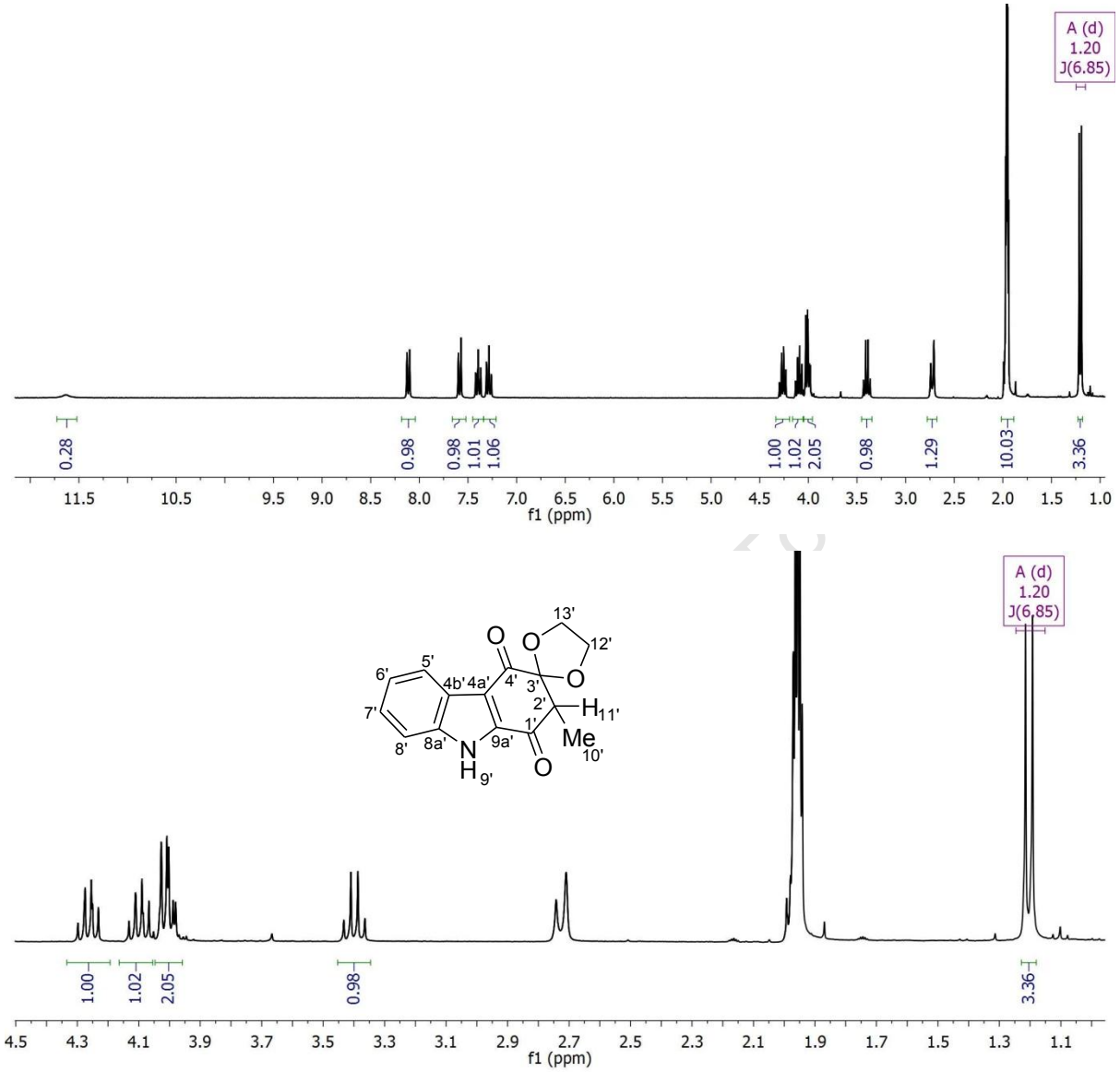

Figure 6. 1H NMR spectrum (top) and expansion of the aliphatic region (bottom) indicating the splitting of the carbazole quinone methyl and differentiation of the methylene signals in the ethyl chain. The signals at 1.95 and 2.70 ppm correspond to the acetone solvent and water signals, respectively.

A plausible mechanism for the formation of **3.13** involves two sequential additions to the vinylogous ester (Scheme 3). After deprotonation of the diol by NaH to form the alkoxide, the first addition-elimination step takes place at C-3' with loss of MeO^-. The terminal alkoxide (generated by excess NaH) then adds at the same position to form the dioxolane enolate, which is quenched during aqueous workup.

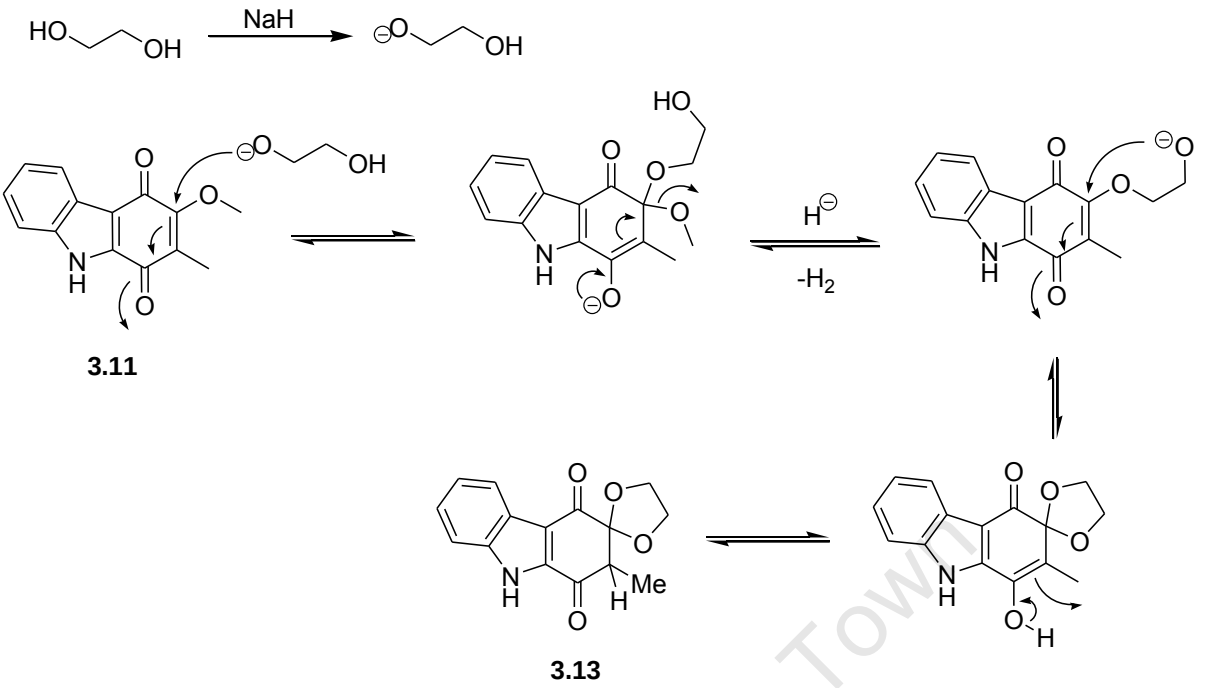

Scheme 3. Mechanism of formation of the dioxolane product by treatment of the carbazole quinone with the dialkoxide of ethylene glycol.

A possible strategy for obtaining controlled addition to the desired terminal alcohol product would be to use 1 eq of NaH and ethylene glycol.

The propane diol and pentane diol derivatives were prepared in the same manner as the ethane diol (Scheme 2), but despite GC/MS evidence supporting their formation, ^{1}H NMR spectroscopy indicated considerable contamination by the diol which was not readily removed by aqueous workup and chromatography. These derivatives were not pursued further.

3.3.2 Substitution at the 2-Position

Since the carbazole quinone bears a resemblance to plumbagin, the possibility of attaching a tethered carboxylic acid at the quinone in an oxidative decarboxylation reaction similar to that achieved with the naphthoquinone was explored. This approach was found to be successful, but low yielding. For this reaction, the nor-2-methyl carbazole quinone derivative **3.10** (Scheme 4) was used for the reaction with glutaric and adipic acid, respectively. The same conditions were employed for the oxidative decarboxylation, namely, the use of

ammonium persulfate as oxidant and silver (I) nitrate as catalyst in a 60 % acetonitrile/water mix. Due to the successive low pressure cycles used to degas the solvent, which resulted in evaporation of some CH_3CN, a solvent mixture containing a slightly higher ratio of CH_3CN to water was used to arrive at a mixture of approximately 60 %.

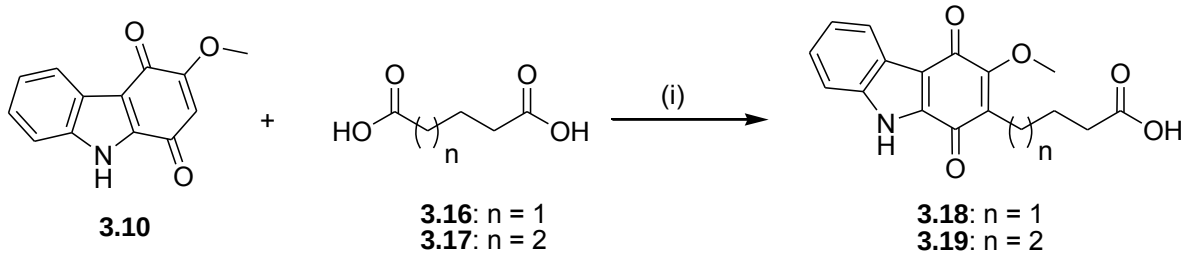

3.10 **3.16**: n = 1 **3.17**: n = 2 **3.18**: n = 1 **3.19**: n = 2

Scheme 4. Oxidative decarboxylation reaction to attach the tethered carboxylic acid at the 2-position of the carbazole quinone. (i) $(NH_4)_2S_2O_8$, $AgNO_3$, 60 % (aq) CH_3CN, 65 – 70 °C, 4 h, **3.18**: 31 %, **3.19**: 38 %.

The reaction resulted in a yield of 31 % for the glutaric and 38 % for the adipic derivatives, respectively, with unreacted starting material recycled for use in subsequent reactions. This afforded a stable carboxyalkyl carbazole quinone in a single step, in a form allowing for direct amide-coupling to the glucosamine thioglycoside.

3.3.3 Substitution at the Carbazole Nitrogen

Attachment of a linker *via* the carbazole nitrogen was initially attempted by reacting the free carbazole quinone **3.11** with an acid chloride. The glutaric and adipic acid-derived derivatives **3.22** and **3.23** (Scheme 5) were prepared from their respective acid chlorides in dry THF with Et_3N, and obtained in 74 and 44 % yield, respectively. The reactions were difficult to monitor due to the product and starting material having similar R_f values on TLC, and purification by chromatography appeared to result in some conversion of the product back to the starting carbazole-1,4-quinone **3.11**.

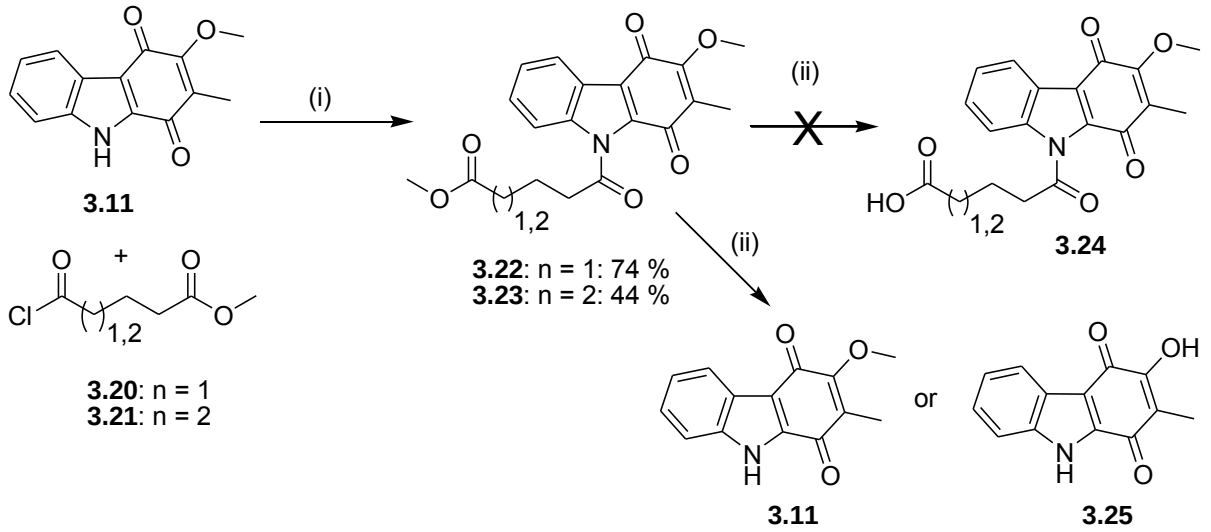

Scheme 5. Synthesis of the *N*-acyl substituted carbazole quinone. (i) Et_3N, THF, r.t., 2-5 h; (ii) LiOH, THF:H_2O (1:1), 47 h.

The labile nature of this amide bond is due to the fact that the carbazole quinone amine can be considered to be part of a vinylogous amide that extends into the quinone (Figure 7). This results in low reactivity of the amine towards acylation, and also causes any subsequent acyl bond to be highly labile and easily cleaved during chromatography due to the electron-withdrawing character of the quinone on the amine.

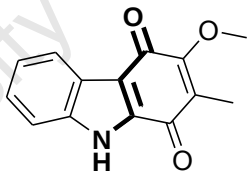

Figure 7. Chemical structure of carbazole quinone with the vinylogous amide bond given in bold.

This high lability was realised in the subsequent reaction where the methyl ester was treated with LiOH in order to effect saponification (Scheme 5). The reaction was unsuccessful and resulted in conversion back to starting material **3.11**, and in one case even resulted in demethylation of the 3-methoxy substituent (to form **3.25**). The difficulties in this approach prompted the use of a benzyl ester as protecting group, to allow for a milder, non-basic hydrogenolytic deprotection step.

Monobenzylated glutaric acid **3.27** was thus prepared by reacting glutaric anhydride and benzyl alcohol in the presence of Et_3N and DMAP in dry CH_2Cl_2 (Scheme 6). The product was obtained in quantitative yield, and used in the subsequent step without further purification. The benzylglutaric acid chloride **3.28** was prepared by treatment of a CH_2Cl_2

solution of the carboxylic acid with oxalyl chloride and a drop of DMF, and the acid chloride was then added by canula to a solution of the carbazole quinone in dry THF. Once the product **3.29** was formed, attempted purification by flash chromatography once again resulted in reversion to the original carbazole quinone. A small fraction of partially purified product was, however, subjected to hydrogenation using Pearlman's catalyst (palladium hydroxide on carbon) to remove the benzyl protecting group, but once again, attempted purification resulted in formation of the carbazole quinone. It was thus clear from these attempts that *N*-acyl derivatives, even if they could be formed, would be too labile for their intended further use, and an alkylation strategy was pursued instead.

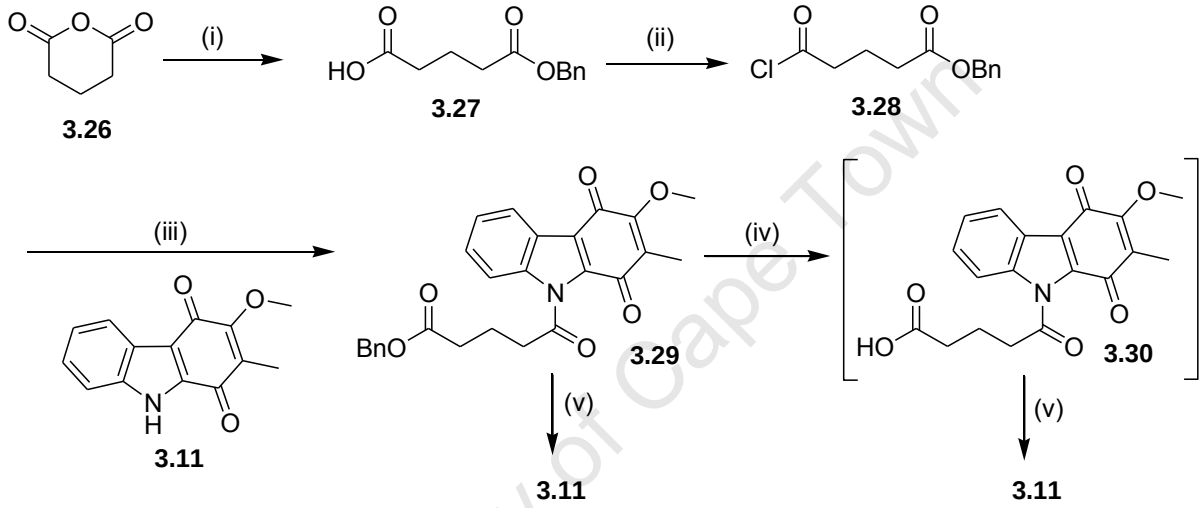

Scheme 6. Synthesis of the benzyl-protected glutaric acid tether, and unsuccessful debenzylation. (i) Benzyl alcohol, Et_3N, DMAP, dry CH_2Cl_2, 0 °C – r.t., 20 h, quant.; (ii) $(COCl)_2$, dry CH_2Cl_2, DMF, 0 °C – r.t., 2 h; (iii) dry THF, Et_3N, 0 °C – r.t.,1 h, <7 %; (iv) H_2, $Pd(OH)_2/C$, EtOAc, r.t.; (v) chromatography.

Alkylation of the carbazole nitrogen with benzyl 6-bromohexanoate and NaI (under Finkelstein conditions) was achieved in the laboratory of Prof Knölker and supplied as the debenzylated carboxylic acid **3.33** (see Scheme 7) for coupling to the glucosamine thioglycoside.

3.3.4 Amide Coupling and Acetate Deprotection

Coupling of the tethered carbazole quinones to the glucosamine thioglycoside was achieved using EDC.HCl as coupling agent in dry THF containing 1-hydroxybenzotriazole (HOBt) and

diisopropylethylamine (DIEA). The yields were quite varied, with the glutaric derivative **3.31**[i] obtained in 72 %, the adipic derivative **3.32** in 14 %, and the *N*-hexanoic derivative **3.34** in 68 % yield (Scheme 7).

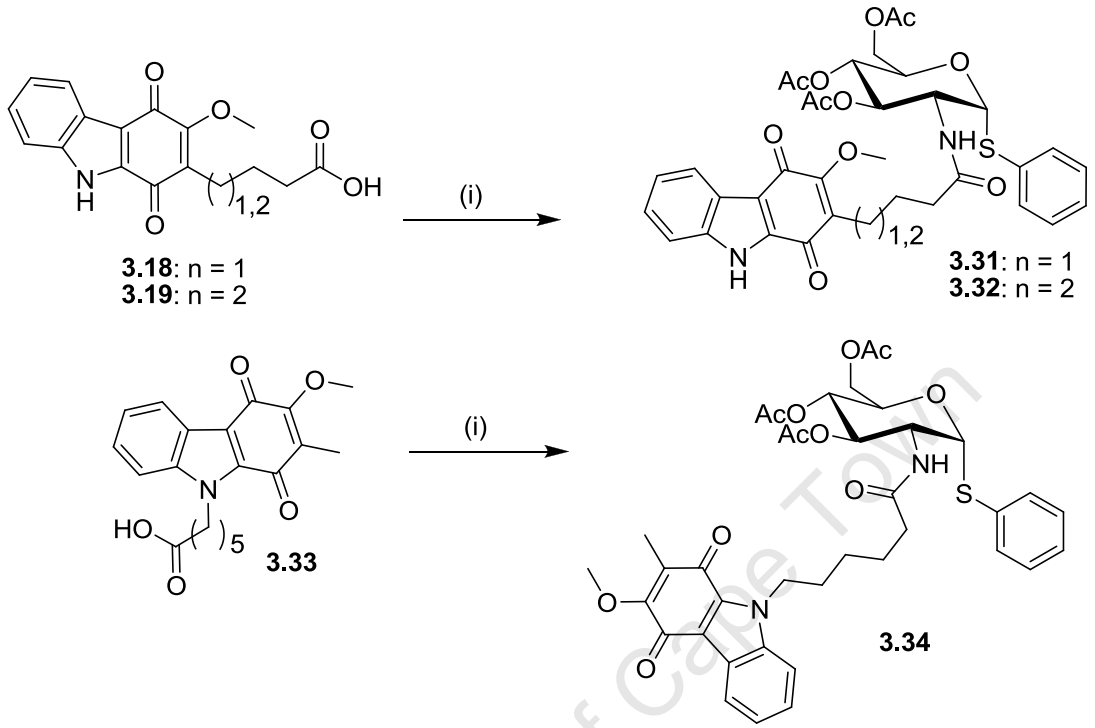

Scheme 7. Coupling of the tethered carbazole quinones to the glucosamine thioglycoside. (i) EDC.HCl, HOBt, DIEA, dry THF, r.t., **3.31**: 67 %, **3.32**: 14 %, **3.34**: 68 %.

Following successful coupling of the carbazole-1,4-quinones to the glucosamine thioglycoside, final deprotection was accomplished using sodium methoxide in methanol (Scheme 8). Due to poor solubility of the deprotected product and the partially deprotected intermediates, non-catalytic quantities of methoxide were required to effect complete deprotection, and various reaction conditions were explored. The glutaric derivative was deprotected using 2.6 eq of methoxide, with the reaction complete after 45 min. This quantity was initially reduced to 0.3 eq methoxide for the adipic derivative, however, conversion to the product was slow and after 24 h an additional 0.5 eq was added and the temperature increased to 50 °C (in order to improve solubility) and the reaction left to continue for a further 16 h before complete consumption of the starting material. For the *N*-hexylated product, 0.2 eq NaOMe was used and the reaction required 10 days to reach complete consumption of the starting material. In all cases, the poor solubility of the deacetylated product was evident by the formation of a precipitate upon addition of the NaOMe. Purification of the deprotected conjugates proved to be difficult and required

[i] Prepared by Prof Knölker's laboratory

combinations of polar solvents for the chromatography as well as recrystallization from methanol to eventually afford the purified products in moderate yields of 68 %, 37 % and 48 % for the glutaric, adipic and *N*-hexylated derivatives, respectively.

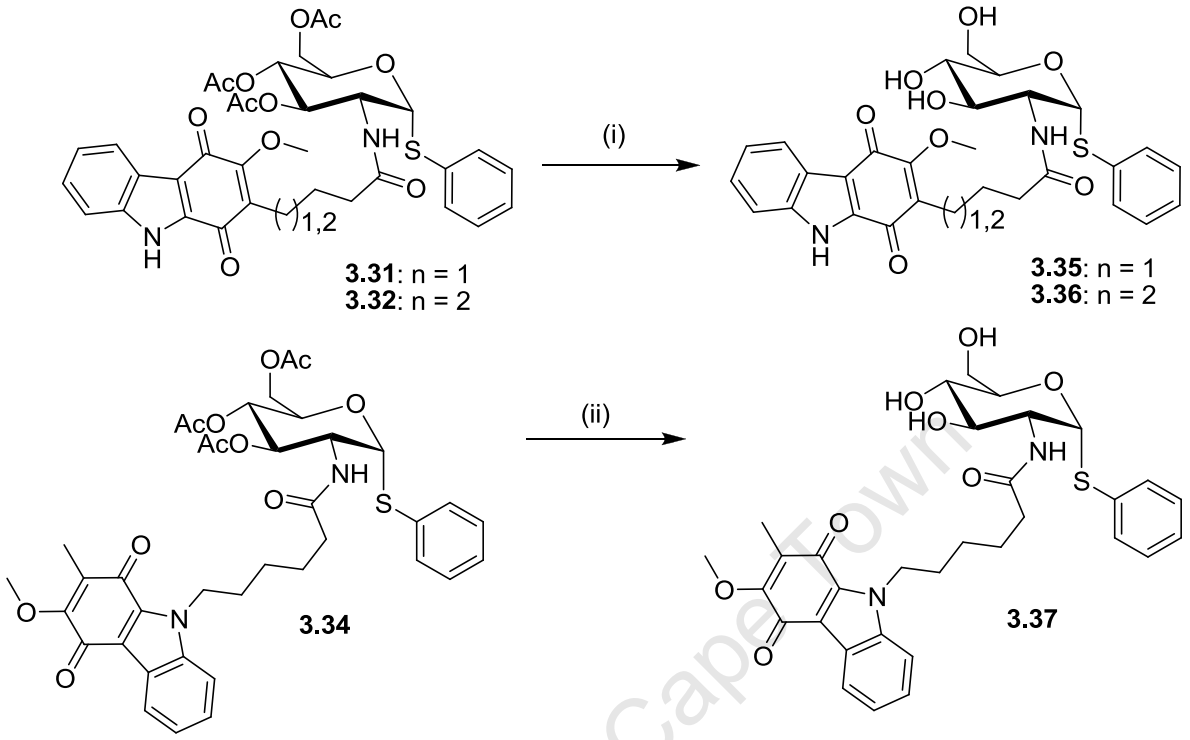

Scheme 8. Deacetylation to form the final carbazole-glucosamine conjugates. (i) NaOMe, (0.8 - 2.6 eq), MeOH, r.t. – 50 °C, 45 min – 36 h, n = 1: 68 %, n = 2: 37 %; (ii) NaOMe (0.2 eq), MeOH, r.t., 10 d, 48 %.

3.4 Discussion and Conclusion

The two main challenges were encountered in substitutions of the 3-methoxy group on the carbazole ring using diols: preventing the addition of the second hydroxyl to form spiro dioxanes, and separation of unreacted diol from the product. Potential solutions to the first challenge could be to use a mono-protected diol, with only one of the alcohol groups available for deprotonation and subsequent addition-elimination, as long as the protecting group was base-resistant, with examples being silyl, alkyl, alkoxymethyl and allyl ethers. A potential solution to the separation problem would be to use fewer equivalents of diol and sodium hydride reagent (~1.5 eq). It was in fact established that excess diol was not required for the reaction to proceed, and the use of an anhydrous solvent as substitute for the excess diol would be a better option. Future attempts towards generating these types of 3,4-dioxygenated derivatives would have to consider such modifications to the synthetic protocol to be successful.

The radical conjugate addition to the quinone to generate the C-C bond was found to be a low-yielding reaction, both with the carbazole-1,4-quinones and 1,4-naphthoquinones, although the reaction was reproducible, the unreacted starting material recoverable, and was able to generate the desired coupled product in a single step. This is in keeping with literature findings on this type of reaction.[15,17,18] The reason for the low yield has not yet been fully evaluated, although there are a number of likely reasons for this phenomenon. One possible reason could be that the quinone is poorly reactive. Once the alkyl radical has been generated, it can react further *via* a number of competing reaction pathways (Scheme 9).[19] Ideally the radical would undergo selective conjugate addition to the quinone. However, the radical could also be oxidised by a second equivalent of Ag(II) to generate the corresponding carbocation, which could then undergo one of several reactions including elimination to the terminal olefin, protonation to the alkane, hydroxylation by water to form a primary alcohol, and esterification in the presence of the acid. Evidence for these side reactions was reported by Anderson and Kochi.[19]

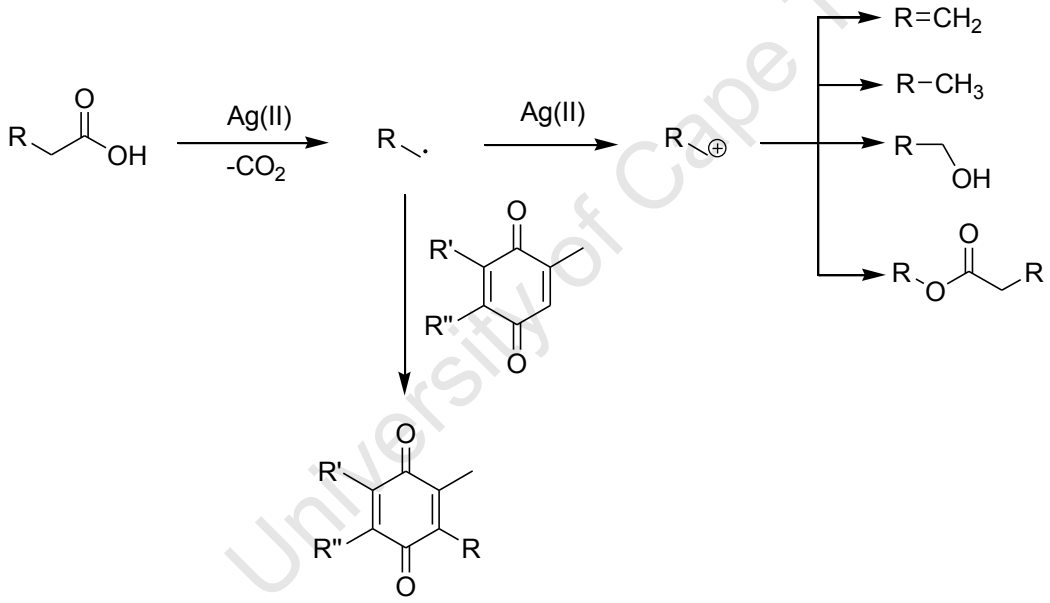

Scheme 9. Competing reaction of the alkyl radical generated by Ag(II)-mediated oxidative decarboxylation. Oxidation by a second equivalent of Ag(II) generates the carbocation which can then undergo one of several reactions including elimination, protonation, hydroxylation or esterification.[19] Successful alkylation of the quinone requires trapping of the radical by the quinone substrate in order to prevent oxidation to the carbocation.

Since in our experience a large proportion of the unreacted quinone was recovered from the reaction, and since extended periods of stirring beyond the usual reaction time of 4 h did not result in a higher yield, it is likely that a considerable quantity of alkyl radical was inactivated by further oxidation by subsequent conversion to one of the products indicated in Scheme 9.

If the alkyl radicals were still present during the additional reaction time, they should have added to the quinone. Consequently, in order to increase the yield of this reaction the reactivity of the quinone would have to be increased so that conjugate addition at this site is the energetically-favoured reaction pathway rather than oxidation of the alkyl radical to the carbocation. This could be achieved by the addition of a catalyst or by a modification to the quinone structure to enhance its electrophilicity. Attempts to slow the addition of APS to the reaction mixture did not result in a higher yield, suggesting that the additional oxidation was not preventable by slowing down the rate of formation of Ag(II), although perhaps a different strategy to achieve this may be possible.

Employing a different synthetic route could potentially increase the yield of alkylated product, although achieving selective addition to the "soft" conjugate position on the quinone rather than 1,2-addition to the "hard" carbonyl carbon would be a considerable challenge to overcome. Nucleophiles such as Grignard reagents, lithiated species and alkoxides would all tend to add predominantly to the carbonyl centre and generate an alcohol or hemiketal, as reported by Knölker and co-workers.[16] However, the use of nitrogen or cuprate nucleophiles might be able to overcome this problem and facilitate addition of an appropriate linker to the 2-position of the quinone (Scheme 10). The overall yield for such a strategy would have to be weighed against the low-yielding single step reaction of the oxidative decarboxylation reaction to evaluate whether such an alternative pathway would result in a product in superior overall yield.

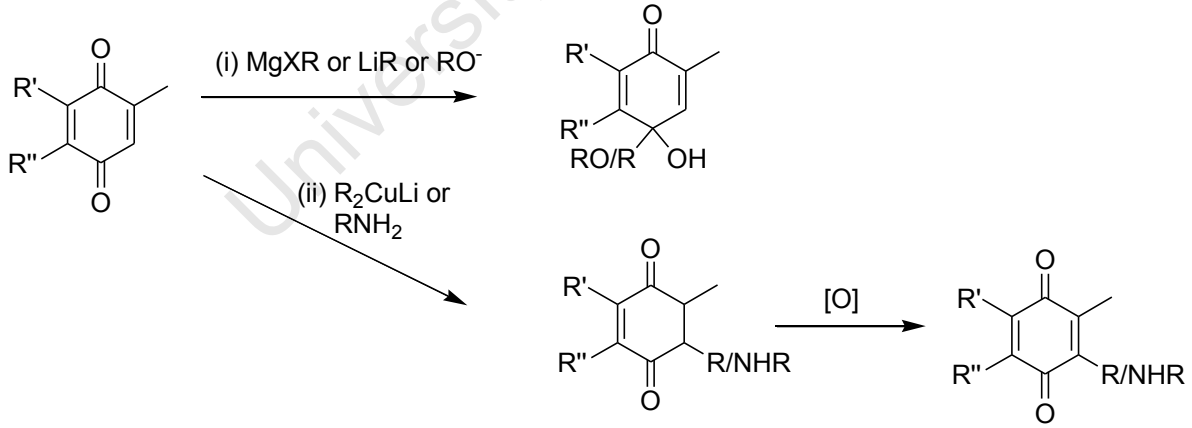

Scheme 10. Addition of nucleophiles to a quinone - potential alternative pathways to substituting the quinone. (i) Addition of Grignard or lithiated species and alkoxides leads to 1,2-addition; (ii) addition of cuprates and nitrogen nucleophiles may generate the 2-substituted derivative, although this pathway also requires an additional oxidation step to regenerate the quinone.

The failure of the *N*-acylation reactions is easy to rationalise based on the identification of the carbazole quinone nitrogen as part of a vinylogous amide. The *N*-alkyl product was far

more stable than its *N*-acyl counterpart, since the C-N bond is less easily cleaved during chromatographic purification. This position on the carbazole provides a facile site for the attachment of a linker to the phenylthioglycoside, and it would be interesting to investigate the impact that differing the chain length would have on subversive substrate/inhibitory activity.

Further sites for the attachment of the linker could be the 6-position, based on the observation that carbazole derivative **3.6** had the lowest MIC of all the compounds evaluated in the Knölker study. A synthetic target for ongoing studies might therefore have a structure such as **3.38** (Figure 8), with the glucosamine incorporated at the 6-position *via* an amide.

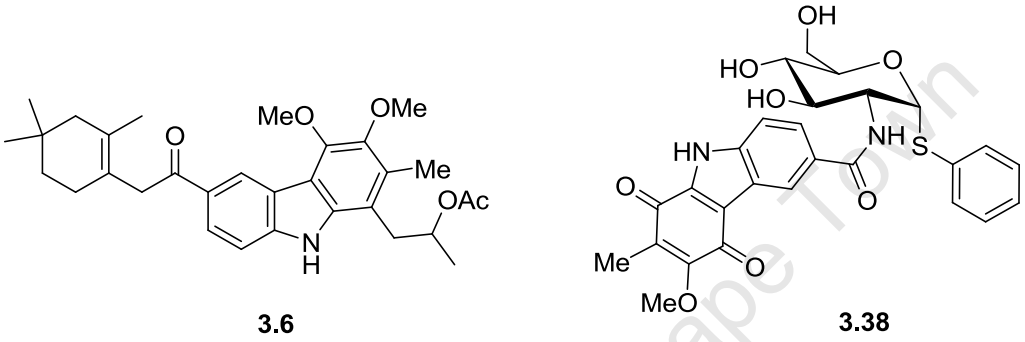

3.6 **3.38**

Figure 8. Chemical structures of the active carbazole **3.6** and a proposed derivative **3.38**

A considerable problem with the final compounds prepared in this study was the poor solubility properties they displayed, which presents significant challenges to their further development as lead compounds. An attempt to address this by incorporating a glycerol unit at the anomeric position to replace the hydrophobic phenylthio group was described in Chapter 2, and incorporation of other polyhydroxylated inositol surrogates such as pentaerythritol[20] or some other polyhydroxylated derivative might be advantageous. It would indeed be interesting to evaluate the extent to which the inhibitory activity is related to the anomeric substituent, and whether the free glycose (OH at the anomeric position) has similar activity. Furthermore, the contribution of the linker itself could be evaluated by considering alternatives such as a polyethylene glycol chain (see **3.40** in Figure 9) that would enhance hydrophilicity. A further alternative would be to consider incorporating a protonatable nitrogen substituent on the carbazole, allowing for the preparation of a salt, and consequent enhancing of the aqueous solubility. It is interesting to note in this regard that enhanced anti-TB activity was observed for the amino-carbazole **3.39** in the Knölker study.

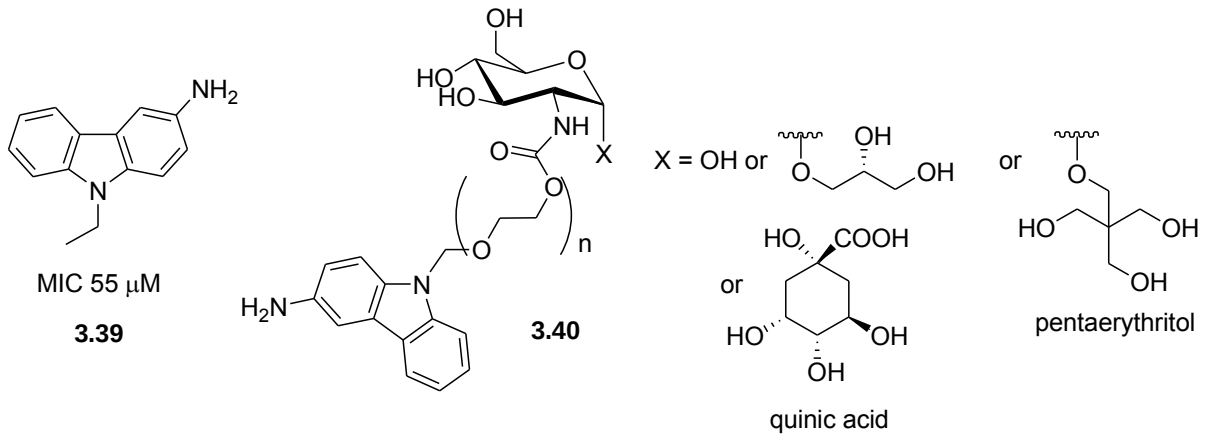

Figure 9. Chemical structures of the ant-TB compound **3.39** and a potential derivative **3.40** with modifications that may enhance the solubility of this conjugate. These include incorporating a protonatable nitrogen at the 3-position of the carbazole, using a polyethylene glycol linker, and substituting the anomeric substituent with a hydroxylated alternative.

References

1. H.-J. Knölker and K.R. Reddy, *Alkaloids Chem. Biol*., **2008**, *65*, 1-410
2. R.S. Ramsewak, M.G. Nair, G.M. Strasburg, D.L. De Witt and J.L. Nitiss, *J. Agric. Food Chem*., **1999**, *47*, 444-447
3. K.C. Das, D.P. Chakraborty and P.K. Bose, *Experientia*, **1965**, *21*, 340-343
4. C. Sánchez, C. Méndez and J.A. Salas, *Nat. Prod. Rep.*, **2006**, *23*, 1007-1045
5. C. Yenjai, S. Sripontan, P. Sriprajun, P. Kittakoop, A. Jintasirikul, M. Tanticharoen and Y. Thebtaranonth, *Planta Med.*, **2000**, *66*, 277-279
6. H.-J. Knölker, *Top. Curr. Chem*., **2005**, *244*, 115-148
7. T.-S. Wu, S.-C. Huang, P.-L. Wu and C.-M. Teng, *Phytochemistry*, **1996**, *43*, 133-140
8. C. Ito, S. Katsuno, H. Ohta, M. Omura, I. Kajiura and H. Furukawa, *Chem. Pharm. Bull*., **1997**, *45*, 48-52
9. C. Yenjai, S. Sripontan, P. Sriprajun, P. Kittakoop, A. Jintasirikul, M. Tanticharoen and Y. Thebtaranonth, *Planta Med*., **2000**, *66*, 277-279
10. A.L. Okunade, P.F. Elvin-Lewis and W.H. Lewis, *Phytochemistry*, **2004**, *65*, 1017-1032
11. A. Sunthitikawinsakul, N. Kongkathip, B. Kongkathip, S. Phonnakhu, J.W. Daly, T.F. Spande, Y. Nimit, S. Rochanaruangrai, *Planta Med*., **2003**, *69*, 155-157
12. C. Ma, R.J. Case, Y. Wang, H. Zhang, G.T. Tan, N.V. Hung, N.M. Cuong, S.G. Franzblau, D.D. Soejarto, H.H.S. Fong and G.F. Pauli, *Planta Med*., **2005**, *71*, 261-267
13. T.A. Choi, R. Czerwonka, W. Fröhner, M.P. Krahl, K.R. Reddy, S.G. Franzblau and H.-J. Knölker, *ChemMedChem*, **2006**, *1*, 812-815

14. T. Tran, E. Saheba, A.V. Arcerio, V. Chavez, Q.-y. Li, L.E. Martinez and T.P. Primm, *Bioorg. Med. Chem.*, **2004**, *12*, 4809-4813
15. D.W. Gammon, D.J. Steenkamp, V. Mavumengwana, M.J. Marakalala, T.T. Mudzunga, R. Hunter and M. Munyololo, *Bioorg. Med. Chem.*, **2010**, *18*, 2501-2514
16. H.J. Knölker, W. Frohner and K.R. Reddy, *Eur. J. Org. Chem.*, **2003**, *4*, 740-746
17. L. Salmon-Chemin, E. Buisine, V. Yardley, S. Kohler, M.-A. Debreu, V. Landry, C. Sergheraert, S.L. Croft, R. L. Krauth-Siegel and E. Davioud-Charvet, *J. Med. Chem.*, **2001**, *44,* 548-565
18. C. Commandeur, C. Chalumeau, J. Dessolin and M. Laguerre, *Eur. J. Org. Chem.*, **2007**, *18*, 3045–3052
19. J.M. Anderson and J.K. Kochi, *J. Org. Chem.*, **1970**, *35*, 986-989
20. A. Smith, Design and Synthesis of Carbohydrate Based Derivatives as Antimicrobial Compounds, Doctoral Thesis, Dublin Institute of Technology, **2008**

Chapter 4
Cloning, Expression and Purification of *Mycobacterium tuberculosis* Mycothiol Disulphide Reductase

4.1 Introduction

Among the disulfide reductase class of flavoproteins are glutathione reductase (GR), trypanothione reductase (TryR), lipoamide dehydrogenase (LipDH), thioredoxin reductase (TrxR), and the mycobacterial mycothiol disulfide reductase[i] (Mtr).[1,2,3] Mtr was first described by Patel and Blanchard in 1998,[4] who subsequently cloned, expressed, purified and characterised the enzyme.[1,5] Similar to its glutathione and trypanothione homologues, Mtr is a 100 kDa dimeric complex containing a single FAD cofactor per monomer adjacent to the redox-active disulfide. During NAD(P)H-dependent reduction of the substrate, the active-site disulfide is reduced to the dithiol in a two-electron transfer process resulting in the formation of a dithiol-FAD charge-transfer complex.[1] The mechanistic details of the reaction were described previously in Chapter 1.

The potential for Mtr to act as a viable target for antitubercular chemotherapy is heightened by the finding that it displays no overlapping activity with the disulfides of GSH and coenzyme A (CoA) found in humans.[1,4] This provides potential for the development of an inhibitor that is selective for the bacterial reductase over the human GR. The enhanced sensitivity to oxidative stress that MSH-deficient mycobacteria display further supports the targeting of this enzyme system for potential antitubercular chemotherapy.[6]

The biological importance of Mtr and its reported ability to react with naphthoquinones in a subversive substrate mechanism prompted the creation of this project in order to investigate the potential for naphthoquinone- and carbazole-derived conjugates of a MSH-like scaffold to display subversive substrate activity against Mtr.[7] Consequently, the cloning, expression

[i] Also referred to as mycothione reductase in earlier papers, based on the nomenclature of the related disulfide reductases of glutathione and trypanothione.

and purification of this disulfide reductase was carried out in order to generate purified enzyme for the study.

4.2 Reagent Suppliers

Kanamycin and Protease Inhibitor Cocktail set III were obtained from Calbiochem. β-NADPH, Tween® 80, acrylamide, HPLC grade acetonitrile (Chromasolv®) and TFA were obtained from Sigma-Aldrich. *N*,*N'*-methylenebisacrylamide was purchased from Fluka. Ammonium persulfate, sodium dodecyl sulphate and TEMED were acquired from BDH. Middlebrook 7H9 Broth was exclusively obtained from Difco.

4.3 Materials and Methods Utilised in the Isolation of Mycothiol From *M. smegmatis*

Neither mycothiol (MSH), nor any of its later precursors, are commercially available (due largely to the low yield and high cost of their chemical synthesis[8,9]). This lack of commercial availability poses a challenge to the study of enzymes that have MSH as a co-factor, since it is required for their assays. The high reactivity of the sulphydryl group of MSH makes extraction from mycobacterial cells difficult, since it readily reacts with other thiols to form disulphides, with aldehydes and activated double bonds to form conjugates, and is irreversibly oxidised to sulphinic acid.[10] Consequently, these side reactions need to be controlled in order to successfully extract MSH from cells in a reasonable yield.

In order to obtain MSH for use in this study, extraction from cultured cells of *M. smegmatis*, using a modification to the procedure reported by Steenkamp and Vogt,[10] was performed. This protocol minimises side reactions by rapidly derivatising MSH with the mixed disulphide, 2-*S*-(2'-thiopyridyl)-6-hydroxynaphthyldisulphide, to form the heterodisulphide, MSSNaph (Scheme 1) upon cell lysis. MSH reacts preferentially with the sulphydryl group of 2-thio-6-hydroxynaphthalene rather than that of the 2-thiopyridine for two reasons. Firstly, the 2-thiopyridine has a lower energy of ionization than the 2-thio-6-hydroxynaphthalene, and secondly, the delocalization of charge from the thiolate anion into the pyridine ring renders the resultant pyridine-2-thione a more stable side product than the 2-thio-6-hydroxynaphthalene which does not have this extra resonance ability. The pH required for this reaction is intermediate between the p*K*a of the 2-thio-6-hydroxynaphthyl thiol and that

of the 2-thiopyridine, and under such conditions the reaction is strongly biphasic. The reaction is outlined in Scheme 1 below.

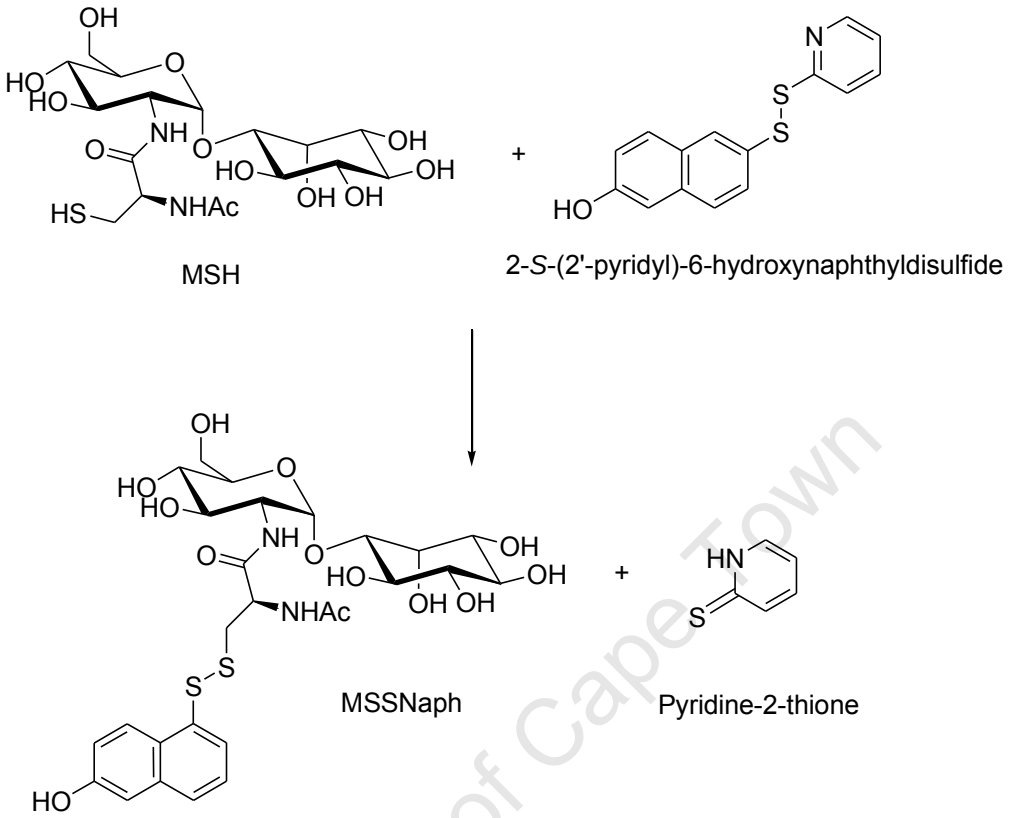

Scheme 1. Derivatisation of MSH with 2-*S*-(2'-thiopyridyl)-6-hydroxynaphthyldisulphide

The isolation and purification of the mixed disulphide product, MSSNaph, is achieved by its adsorption onto reversed-phase materials. After the removal of impurities, the MSH can be recovered by reduction of the disulphide with dithiothreitol (DTT) or 2-mercaptoethanol.

4.3.1 Synthesis of 2-*S*-(2'-thiopyridyl)-6-hydroxynaphthyl-disulphide

The procedure used for the synthesis of the heterodisulphide involved dissolving 6-hydroxynaphyldisulphide (2.00 g, 5.71 mmol) in 1000 ml of a 1:1 (v/v) mixture of acetonitrile and water. The disulphide was reduced by the addition of sodium borohydride (1.50 g, 39.65 mmol) at room temperature, resulting in the appearance of a yellow colour in solution due to the formation of the thiolate anion. Excess borohydride was destroyed by the addition of glacial acetic acid (~5 ml) and the pH of the resulting solution increased to 4.6 by the addition of dipotassium phosphate. This pH was chosen to be considerably lower than the p*K*a of 6.4 of the 2-thio-6-hydroxynaphthalene in order to keep the thiol in its protonated form

and minimise oxidation back to the disulphide.[10] The 2-thio-6-hydroxynaphthalene solution was then added drop-wise over 20 min to a stirred solution of 2,2'-dithiodipyridine (Aldrithiol®) (4.74 g, 21.52 mmol) in 500 ml 1:1 (v/v) acetonitrile/water. The mixture was left stirring for a further 60 min after which 3 volumes of water (4.5 L) were added to reduce the acetonitrile concentration to ~12 %. The solution was cooled to 4 °C overnight and the resulting precipitate, consisting of primarily 6-hydroxy-2-naphthyl disulphide and 2-*S*-(2'-thiopyridyl)-6-hydroxynaphthyl disulphide, was collected by centrifugation. These components were separated on a Vydac TP1022 C18 reversed-phase preparative HPLC column (250 x 22 mm), using an isocratic mobile phase of 65 % acetonitrile and 35 % of 0.1 % trifluoroacetic acid in water, at a flow rate of 10 ml/min, and monitored at 280 nm.

A small aliquot of the mixture was analysed by HPLC on a Phenomenex phenyl hexyl C18 HPLC analytical column (250 x 4.6 mm) using Method 1 (Table 1) as the mobile phase gradient programme, and the effluent monitored at 280 nm.

Table 1. Method 1 gradient programme

Time (min)	0	5	35	40	45
% A	95	95	10	10	95
% B	5	5	90	90	5

5μl injected, flow rate = 0.8 ml/min. Solvents: A = 0.1 % TFA; B = 100 % CH_3CN

The 2-*S*-(2-thiopyridyl)-6-hydroxynaphthyl disulfide eluted at 31 min while the unreacted 6-hydroxy-2-naphthyl disulfide eluted at 34 min, as shown by the elution profile in Figure 1. Impurities were negligible.

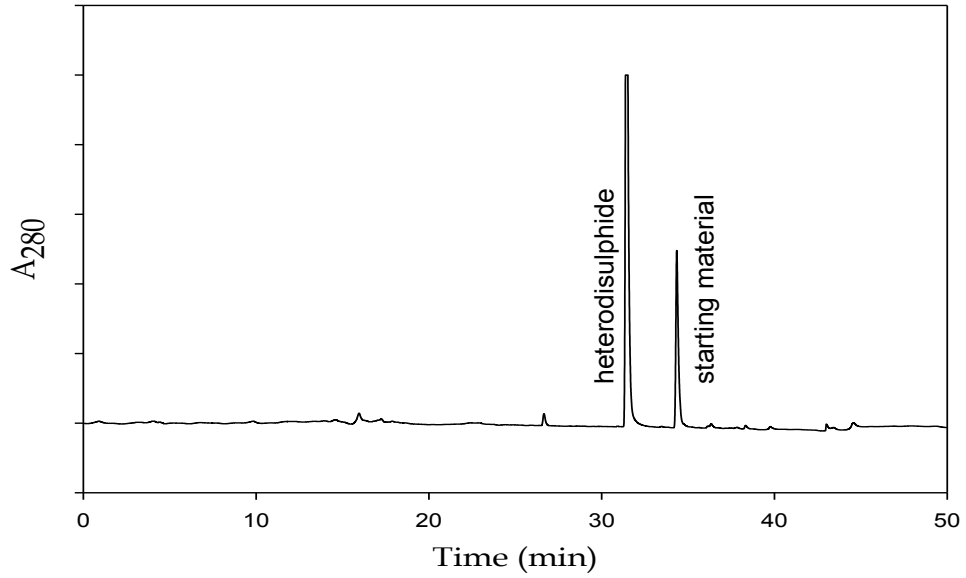

Figure 1: Analytical HPLC elution profile of the heterodisulphide, 2-*S*-(2'-thiopyridyl)-6-hydroxynaphthyl disulphide (31 min), and the starting material, 6-hydroxy-2-naphthyl disulphide (34 min)

Quantification of the desired 2-*S*-(2'-thiopyridyl)-6-hydroxynaphthyl disulphide was determined spectrophotometrically (Ocean Optics mini diode-array USB2000 spectrometer) at a wavelength of 298 nm using an extinction coefficient of 11,184 $M^{-1}.cm^{-1}$. A 20 μl aliquot of the heterodisulphide was mixed with 980 μl of 25 mM potassium phosphate buffer (pH 8) in a 1 ml cuvette and the OD_{298} determined. The eluted heterodisulphide solution was obtained at a concentration of 1.27 mM in 1.1 L (0.399 g, 1.397 mmol) with a yield of 24 %.

4.3.2 Reaction between heterodisulphide and mycothiol-containing cell lysates

A solution of 0.25 M perchloric acid containing 2 mM EDTA in water was prepared, and diluted in a 1:1 ratio with 40 % acetonitrile/water. This solution (500 ml) was added to 250 g of packed *M. smegmatis* cells (wet weight), and the mixture sonicated until a homogeneous mixture was obtained (~15 min). This was then centrifuged at 10,000 x g for 15 min. The supernatant was decanted and its thiol concentration estimated by reaction with 4,4'-dithiodipyridine (DTDP). Reaction mixtures contained 24.25 μmoles of potassium phosphate buffer, pH 8, and 0.2 μmoles of DTDP in a volume of 980 μl. To this was added 20 μl of the sample and its thiol concentration was determined by following the resultant absorbance

change at 325 nm ($\Delta\epsilon_{325}$ = 19.8 $mM^{-1}cm^{-1}$). Total thiol content was estimated to be 849 μmoles (in 510 ml).

The pHs of both the cell lysate and heterodisulphide solutions were increased to 4.6 by the drop-wise addition of Et_3N at room temperature, after which the cell lysate solution was added drop-wise to the heterodisulphide over a period of 30 min with stirring. The reaction leading to the formation of 2-*S*-(mycothiolyl)-6-hydroxynaphthyldisulfide (MSSNaph) was monitored by HPLC analysis of aliquots of the reaction mixture (Figure 2).

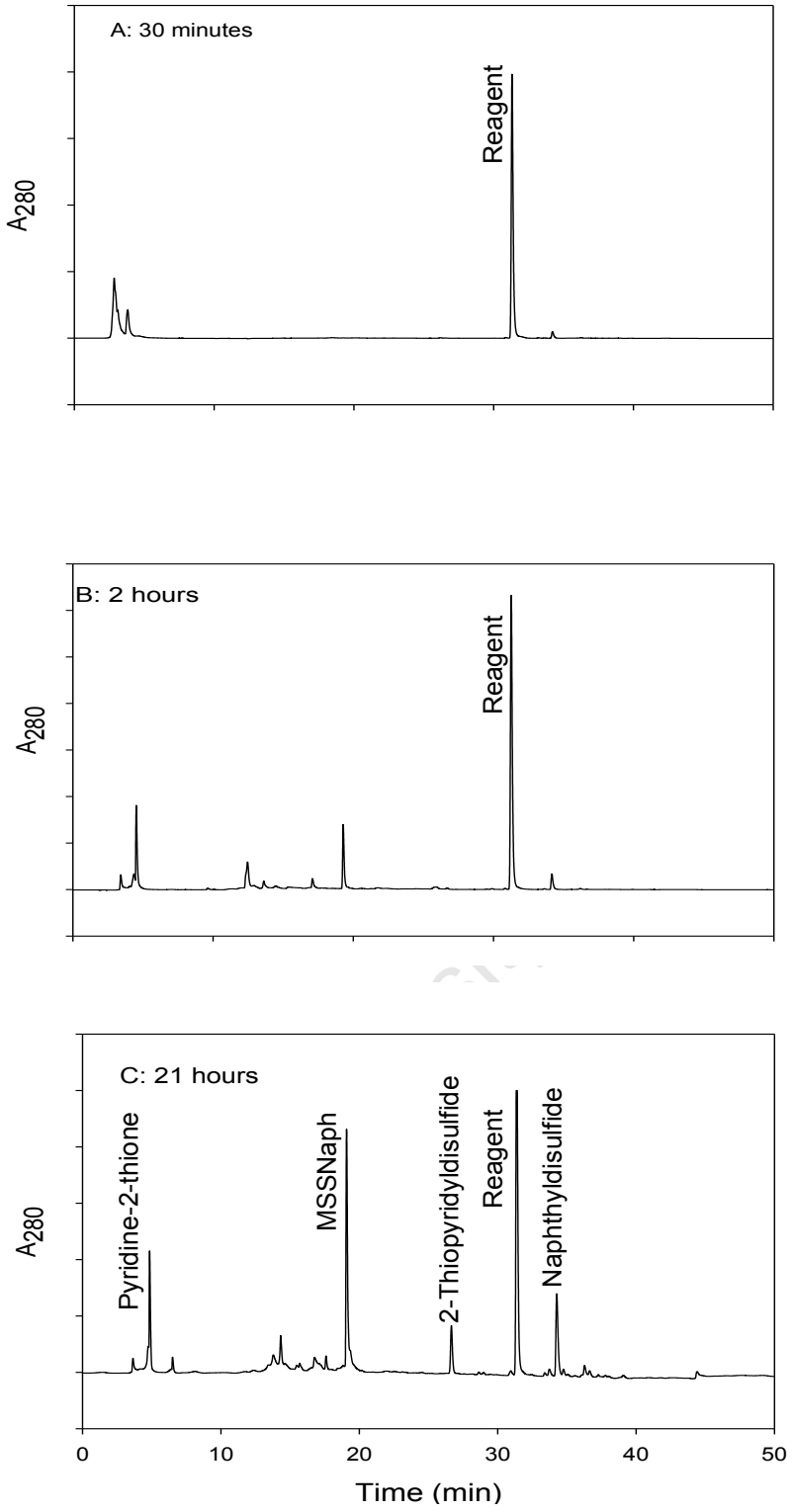

Figure 2. Analytical HPLC elution profile of the cell lysate/heterodisulphide reaction mixture. Reaction progress was monitored after 30 min (A), 2 h (B), and 21 h (C). The product, MSSNaph, eluted after 19 min. Method 1 was used for the analysis.

After 48 h there remained a significant excess of heterodisulphide over MSSNaph, and it was decided that more cell lysate should be added in order to increase the yield of MSSNaph. Consequently, a further 115 g of *M. smegmatis* cells were lysed and prepared as described above, and added to the reaction mixture. The thiol content of this second lysate mixture was estimated to be 412 μmoles (in 240 ml), based on reaction with DTDP.

Upon consumption of all MSH in the cell lysate, the resultant MSSNaph solution was diluted with 2 volumes of distilled water (3.7 L) to reduce the acetonitrile concentration to ~10 %. This solution was then loaded onto a C18 silica gel column, and pure MSSNaph product was eluted in 30 % acetonitrile/water. The acetonitrile was removed under reduced pressure, and dry MSSNaph obtained after lyophilisation in a final yield of 140 mg (0.212 mmoles; 17 % of an initial total thiol content of 1.261 mmoles).

2-*S*-(2-thiopyridyl)-6-hydroxynaphthyldisulfide clearly has high specificity for MSH as there is but one prominent peak in the chromatogram corresponding to the MSSNaph conjugate (at 19 min, see Figure 3), with minor uncharacterised side-products. Even after an extended incubation time of 48 h, no other thiol present in the *M. smegmatis* cell extract formed a disulphide with the heterodisulphide reagent to a notable extent. Other major characterised peaks in the HPLC trace included pyridine-2-thione (eluted at 5 min), 2-thiopyridyldisulfide (eluted at 27 min), excess 2-*S*-(2-thiopyridyl)-6-hydroxynaphthyldisulfide (eluted at 31 min) and 6-hydroxy-2-naphthyldisulfide (eluted at 34 min).

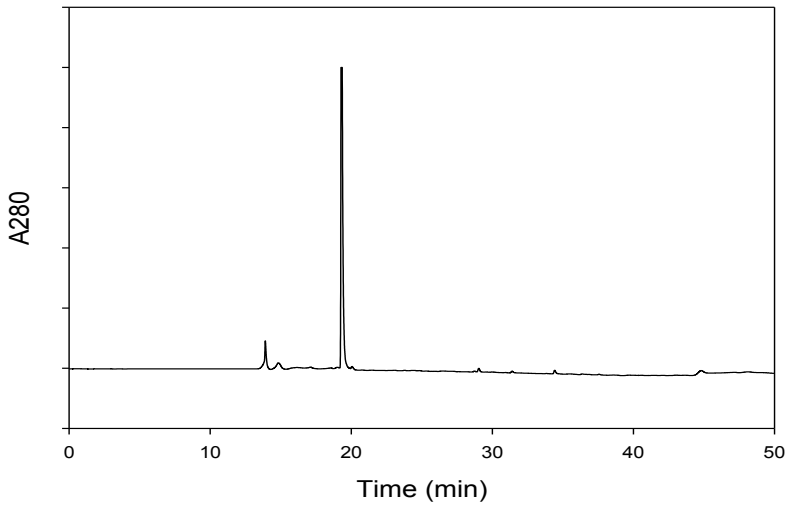

Figure 3. Analytical HPLC elution profile of purified MSSNaph.

The excellent chromatographic properties provided by the naphthalene chromophore, allowed for comparison of the relative quantities of naphthyl heterodisulphides, including MSSNaph, to be done by measuring the peak areas in the HPLC profiles.

4.3.3 Conclusion

It is indicated in the literature that an expected yield of MSH from *M. smegmatis* cells is 100 mg from 250 g cells.[10] In this isolation, 140 mg MSSNaph was obtained from 365 g cells, which could yield a maximum of 103 mg of MSH - approximately 70 % of the expected value. This lower-than-expected result could be due to scale-up factors, which are often known to influence the yield of chemical reactions. While this value is lower than that reported by Steenkamp and Vogt,[10] it is significantly greater than that achieved by chemical synthesis, and permits the acquisition of significant amounts of MSH needed for enzyme assays in a comparatively short period of time.

4.4 Materials and Methods Used in the Cloning, Expression and Purification of Mtr

4.4.1 Introduction

The cloning, expression and purification of Mtr was carried out using a procedure that was based on the approach reported by Patel and Blanchard,[11] involving transformation of *M. smegmatis* cells with a heat-shock inducible plasmid containing the *Mtr* gene. Purification was envisaged to proceed by nickel immobilised metal affinity chromatography (IMAC) since the construct included a hexahistidyl tag (His_6-tag) at the carboxyl terminus.

4.4.2 Preparation of Middlebrook Medium

Cultures of *M. smegmatis* cells that had been transformed with the construct containing the *Mtr* gene and heatshock inducible promotor region were grown in Bacto Middlebrook 7H9 broth prepared as follows: the powdered medium (18.8 g) was dissolved in H_2O (3.6 L) and the mixture autoclaved at 121 $^{\circ}$C and 15 psi for 20 min. 360 ml aliquots of this stock were

added to each of 10 x 1 L conical flasks. To each of these 10 flasks was added 40 ml of ADS (Albumin, Dextrose, Sodium chloride) mix, which was prepared separately as follows: Bovine serum albumin (20 g), glucose (8 g), NaCl (3.4 g), glycerol (20 ml, to a final concentration of 0.5 %) and Tween 80 (2 ml, to a final concentration of 0.05 %) were dissolved in Millipore®-purified water (400 ml) and filter sterilized through Minisart® sterile cartridges. Where bovine serum albumin was unavailable, casein digest (tryptone powder) was used as an amino acid source in its place. Kanamycin (final concentration: 15 µg/ml) was added as antibiotic to each flask (concentration greater than that was found to be toxic to the *M. smegmatis* cells).

4.4.3 Ni^{2+} Immobilised Metal Affinity Chromatography

Iminodiacetic acid 6 % agarose resin was charged with 0.2 M $NiSO_4$ solution, followed by washing and equilibration of the column with KH_2PO_4 (20 mM; pH 7.6) buffer, prior to being loaded with the clarified cell extract. After sample loading, the column was washed in a step-wise gradient of NaCl (200 ml each of 50 mM, 100 mM, 200 mM), to remove cellular impurities bound by non-specific ionic attraction. When the column eluent had an A_{280} < 0.05, a low concentration of imidazole (100 ml, 10 mM, pH 7.6) in column buffer was added to elute any weakly bound impurities. However, this had the surprising result of causing the bound $(His)_6$-tagged enzyme to elute. Due to the bound flavin, the enzyme fraction was bright yellow in colour, which allowed it to be monitored as it moved down the column. The eluent was collected by automated fraction collector, and the active fractions identified by their yellow colour and by spectrophotometric enzyme assay.

.

4.4.4 2',5'-Adenosine Diphosphate-Sepharose Affinity Chromatography

The 2',5'-ADP resin was suspended in binding buffer (20 mM KH_2PO_4, 50 mM NaCl, pH 7.6), poured into the column, and washed with additional buffer. The enzyme sample was then added allowing for a fraction (8 %) of the protein to bind, although a considerable quantity (92 %) eluted without binding. When this active, unretained fraction was reloaded onto the column, it again failed to bind, and eluted in the binding buffer. The fraction that did bind was purified by washing with binding buffer, and then eluted in a step-wise gradient of NaCl (75 mM, 0.2 M, 1.0 M).

4.4.5 Anion Exchange Chromatography

A Q-Sepharose High Performance (Q-HP) column (column volume of 30 ml) was used in conjunction with a Gilson 321 pump (at a flow rate of 2.5 ml/min), Waters 484 tunable absorbance detector (set at 280 nm) and a Gilson FC 204 fraction collector. The data was transferred to a computer using a Gilson 506C system interface and was interpreted using Gilson Unipoint software, version 5.11.

The Q-HP column was first reversed and washed with 2 column volumes (CV) 2 M NaCl, 2 CV distilled water, 2 CV 1 M NaOH and again with 2 CV distilled water. The column was then returned to the normal direction and equilibrated with 5 CV of 20 mM Tris-HCl, 300 mM NaCl, pH 7.6. The pre-column sample was passed through a 0.45 µm filter and loaded onto the Q-HP column using a 50 ml GE healthcare superloop. The sample was loaded onto the pre-equilibrated column, and cycled three times in order to increase enzyme interaction with the resin. Thereafter, the column was washed with binding buffer (20 mM Tris-HCl, 300 mM NaCl, pH 7.6) and once the A_{280} < 0.05, a gradient elution was run (300 mM to 1 M NaCl) over 10 CV. Fractions of 5 ml were collected in 60 tubes over 120 min. Activity assays revealed active enzyme to be found in all collected fractions, with the greatest activity found in test tubes 6 – 24.

4.4.6 Absorbance Spectrophotometry

The eluents from the chromatographic columns used in the purification of Mtr were monitored at 280 nm in order to follow the progression of purification. Impurities were assumed to have been eluted when the A_{280} < 0.05.

4.4.7 SDS-Polyacrylamide Gel Electrophoresis

4.4.7.1 Preparation of materials

Resolving gel buffer: Prepared by dissolving Tris (18.18 g; 0.75 M) and SDS (0.4 g; 0.2 %) in 200 ml distilled water and adjusting the pH to 8.8 with concentrated HCl.

Stacking gel buffer: Prepared by dissolving Tris (6.06 g; 0.25 M) and SDS (0.8g 0.4 %) in 200 ml distilled water. The pH was adjusted to 6.8 with concentrated HCl.

30 % Acrylamide-bis-acrylamide stock solution: Prepared by dissolving acrylamide (30.0 g) and bis-acrylamide (0.8 g) in 100ml distilled water. The solution was filtered and stored at 4 °C in a foil-covered bottle.

10 % Ammonium persulfate solution (APS): Prepared by dissolving APS (0.05 g) in 500 µl distilled water. The solution was stored at -20 °C.

N,*N*,*N*',*N*'-tetramethyl-1,2-diaminoethane(TEMED): The TEMED catalyst was used without dilution.

Electrophoresis tank buffer: Prepared by dissolving Tris (3.03 g; 0.025 M), glycine (14.40 g; 0.192 M) and SDS (1.00 g; 0.1 %) in distilled water (1.00 L). This solution, at pH 8.3, was stored at 4 °C.

Sample treatment buffer: Solution composed of stacking gel buffer (2.5 ml), 10 % (w/v) SDS solution (4 ml), glycerol (2 ml), 2-mercaptoethanol (1 ml), bromophenol blue, and 0.5 ml distilled water. Stored at -20 °C.

Coomassie blue staining solution: Coomassie Brilliant Blue (1.25 g) was dissolved in 227 ml methanol, 227 ml water and 46 ml glacial acetic acid, and the solution filtered.

Destaining solution: The destaining solution was composed of ethanol, acetic acid and water in a ratio of 2:1:7.

4.4.7.2 Preparation of the Gel

SDS-polyacrylamide gel electrophoresis was performed on vertical slab gels.[12] The resolving gel was prepared according to the recipe given in Table 2. After combining the buffer, water, acrylamide solution and APS, the TEMED catalyst was added and the solution gently mixed, before being poured between the 2 glass plates in the gel assembly apparatus. A 0.5 cm layer of water was carefully applied to the top of the gel solution to ensure a flat upper surface. The gel was left to polymerise for approximately 45 min. The stacking gel was prepared in the same way using the recipe given in Table 2, and was

added over the resolving gel. A comb was added and the gel allowed to set over 1 h. Once set, the comb was removed and the top tank assembled and filled with electrophoresis buffer.

Table 2. SDS Polyacrylamide Gel Electrophoresis Composition

Solutions	**Resolving gel** **10 % electrophoresis gel**	**Stacking gel**
Resolving buffer	20.00 ml	-
Stacking buffer	-	6.00 ml
Distilled Water	6.70 ml	4.20 ml
30 % Acrylamide solution	10.25 ml	2.25 ml
APS	15 mg	7.5 mg
TEMED	15 µl	7.5 µl

4.4.7.3 Sample preparation and loading

Protein samples were mixed in a 1:1 ratio with sample treatment buffer (typically 100 µl + 100 µl) and heated at 90 °C for 5 min, prior to loading. The apparatus was connected and electrophoresis carried out at 30 mA. An unstained protein molecular weight marker (Fermentas) was used to estimate protein size.

4.4.7.4 Visualisation of Proteins Separated by SDS PAGE

Gels were stained in the Coomassie blue staining solution and destained in the destaining solution, both processes carried out overnight with shaking to ensure uniform staining/destaining.

4.4.8 Mtr Assay

Mycothiol disulfide reductase (Mtr) activity was determined spectrophotometrically by monitoring the oxidation of NADPH at 340 nm (molar extinction coefficient, ε_{340} = 6220 $M^{-1}cm^{-1}$) using an Ocean Optics spectrophotometer. Since MSSNaph has been shown to be a suitable substrate for Mtr (unpublished results from our group), and since a method for its preparation from *M. smegmatis* extracts has also been developed in our group, it was used as a substitute for MSSM in the assay mixture. The standard 1 ml assay mixture contained

0.110 mM NADPH, 0.034 mM MSSNaph and 2 µl of enzyme sample in 50 mM Tris-HCl buffer, pH 7.6, containing 2 mM EDTA. These conditions were used to determine the specific activity of Mtr at each stage of purification.

4.4.9 Biorad Protein Determination

Standard protein samples of bovine serum albumin (BSA) were prepared containing 1.5, 3.0, 5.0, 7.5 and 10 µg/ml. An 800 µl aliquot of each standard was pipetted into a microcentrifuge tube, in duplicate. To each sample, 200 µl of the dye reagent concentrate was added and the tube vortexed. Samples were incubated at room temperature for the duration of time it took to prepare all samples (5-10 min), and their absorbance at 595 nm recorded. The cuvette was washed with methanol and rinsed with water after each determination. A standard curve (Figure 4) was then plotted and used to determine the protein concentration of Mtr at each stage of purification. Samples that were out of range of the standard curve were appropriately diluted before protein concentrations were determined by the procedure.

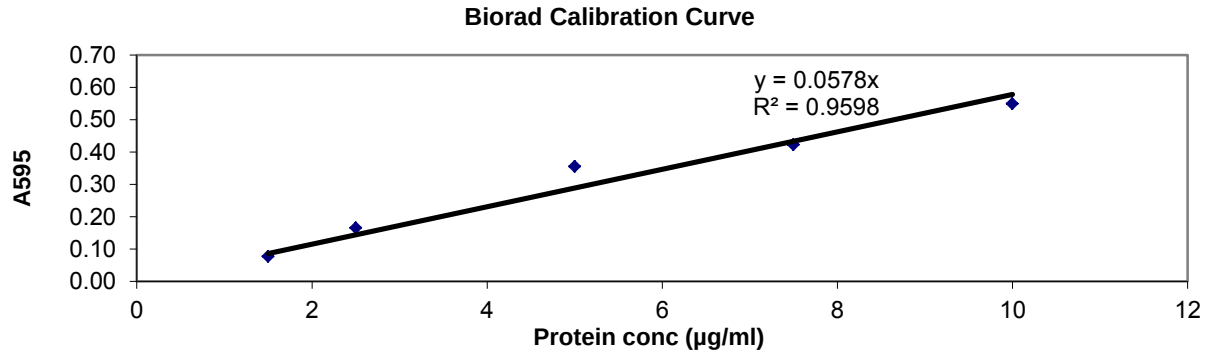

Figure 4. Biorad calibration curve determined from the absorbance of standard solutions of BSA at 595 nm, and used to estimate the protein concentrations at each stage of Mtr purification

4.5 Results

4.5.1 Cloning and Expression of Mtr

The heat-shock promotor Hsp60 containing the *Mtr* gene was cloned into the plasmid pMV261 (donated by Annelise Williamson, UCT Division of Medical Virology). In keeping with the published procedure of Patel and Blanchard,[1] *M. smegmatis* was used as the bacterial expression system, and cells were successfully transformed with the plasmid by electroporation, followed by spreading on LB-agar plates containing kanamycin (15 μg/ml), to yield successfully-transformed colonies.

A selected colony was inoculated into 200 ml of Middlebrook/ADS medium under aseptic conditions and was incubated with shaking at 37 °C for 3 days, then 30 °C for 2 days, after which 20 ml of this inoculum was added to each 10 x 1 L flasks containing 400 ml of Middlebrook/ADS medium per flask. The lower temperature of 30 °C was used for growth of the cells to create a large temperature jump for the heat-shock induction step. Once the flasks had reached an OD_{600} = 1.2, the temperature in the incubator was increased to 42 °C. It took approximately 1.5 h for the internal temperature of the medium to reach the required 42 °C. Incubation was continued for a further 3.5 h until the OD_{600} = 1.8. Cells were then collected by centrifugation at 8000 g at 4 °C for 15 min (wet weight of expressed cells = 9.22 g), and resuspended in 40 ml of 20 mM KH_2PO_4, 50 mM NaCl buffer (pH 7.6) containing DNAse (final concentration = 20 μg/ml) and 200 μL EDTA-free protease inhibitor cocktail (set III, Calbiochem). The resuspended cells were sonicated (Branson Sonifier 250) on ice for 10 x 2 min bursts, such that the temperature of the solution did not exceed 10 °C. The cell extract was then clarified by centrifugation (Beckman J2-21 centrifuge, JA14 rotor) at 22,000 rpm, 4 °C, for 45 min.

4.5.2 Chromatographic Purification

Purification of the expressed protein was envisioned to proceed *via* a similar method to that of Patel and Blanchard,[5] namely, immobilised metal ion affinity chromatography (IMAC) utilising the His_6 tag on the carboxyl terminus. However, binding of the enzyme to the IMAC resin was weak and minor traces of imidazole were sufficient to induce elution of the bound protein. This suggested that the His_6-tag was not present, or that it was truncated (through protease activity or irregular transcription), or otherwise had folded in such an orientation

that it had restricted access to the resin (possibly as a result of post-translational modification). The partially purified enzyme solution was concentrated in an Amicon® pressure filtration cell at 400 kPa using a 30 kDa cut-off membrane. The volume was reduced from 900 ml to 20 ml, and a 100 μl sample run on a 10 % acrylamide gel. The resulting gel indicated some degree of purification, despite the presence of numerous impurities. Consequently, focus was then switched to a procedure that had been successfully employed to purify non-His-tagged Mtr.[1] The reported procedure used a combination of anion exchange chromatography, 2',5'-adenosine diphosphate (ADP)-sepharose affinity chromatography, and gel filtration chromatography, to isolate a single band of purified Mtr. In a parting from the reported procedure, the 2',5'-ADP-sepharose column was employed first. This affinity resin binds enzymes that use NADPH as a cofactor (2',5'-ADP is a structural analogue of NADP), and it proved to be an effective means of purifying the Mtr extract, although the yield of purified enzyme tended to be low (8 %) due to a large proportion (92 %) of the extract not binding to the resin. Three active fractions were obtained, each eluting at a different NaCl concentration. The 75 mM NaCl fraction contained minor impurities, however, the 0.2 M and 1.0 M NaCl fractions were found to be pure by SDS-PAGE analysis (Figure 5). Protein concentrations of each fraction were determined by the Bradford dye-binding assay (Bio-Rad) using bovine serum albumin (BSA) as a standard.

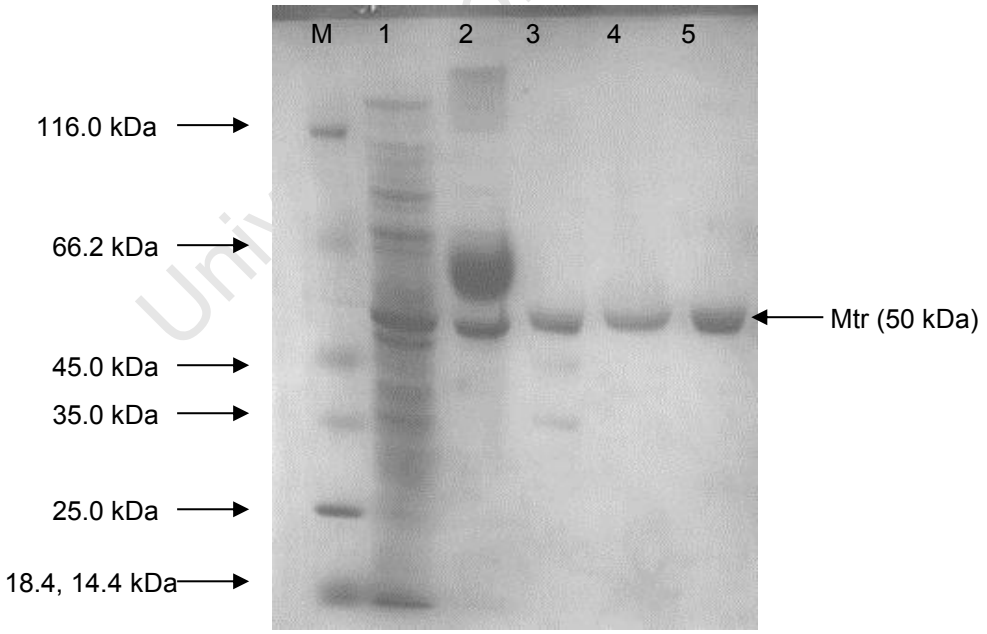

Figure 5. SDS-PAGE of ADP-Sepharose purification of Mtr. (M) Marker; (1) Crude cell extracts after expression of Mtr; (2) partially purified fraction obtained from the IMAC column; (3) active fraction of Mtr with minor impurities eluting in 75 mM NaCl from ADP-sepharose column; (4) pure, active fraction of Mtr eluting in 0.2 M NaCl from ADP-Sepharose column; (5) pure, active fraction of Mtr eluting in 1 M NaCl from ADP-Sepharose column.

Despite the high degree of purity, the ADP-sepharose method had a low yield of protein. Anion exchange chromatography (Q-Sepharose High Performance column) was therefore used as an alternate means of purification of the eluted IMAC enzyme fractions in the hope that it would achieve higher yields. The sample was dialysed against 20 mM Tris-HCl, pH 7.6, containing 300 mM NaCl. According to the results of Patel and Blanchard[1] the enzyme eluted at 0.45 and 0.5 M NaCl (for the constitutively expressed *M. smegmatis* and recombinant *M. tuberculosis* Mtr, respectively) in 20 mM triethylamine hydrochloride (TEA-HCl) (pH 7.6). However, it was discovered that this buffer system does not act as a buffer at pH 7.6. Consequently, Tris-HCl was instead used at the same concentration and pH. The sample was loaded onto the pre-equilibrated column, and cycled three times in order to increase enzyme interaction with the resin. Thereafter, the column was washed with binding buffer (20 mM Tris-HCl, 300 mM NaCl, pH 7.6) and once the $A_{280} < 0.05$, a gradient elution was run (300 mM to 1 M NaCl). SDS-PAGE analysis (Figure 6) revealed poor purification of the desired protein. It was noted that the mobile phase buffer was different to that used by Patel and Blanchard[1] in their purification procedure, and the different buffer system with different ionic properties might alter the NaCl concentration required for protein elution to that which was reported. However, the presence of an extended gradient of eluted enzyme between test tubes 6 and 24 suggested that there was a degree of binding to the stationary phase. This negates the possibility that the initial NaCl concentration was above the threshold level for binding, since this would have resulted in the entire enzyme fraction eluting in the first few tubes. In the selection of an alternate purification strategy, it was decided not to proceed to gel filtration as this is generally a polishing step in purification protocols.

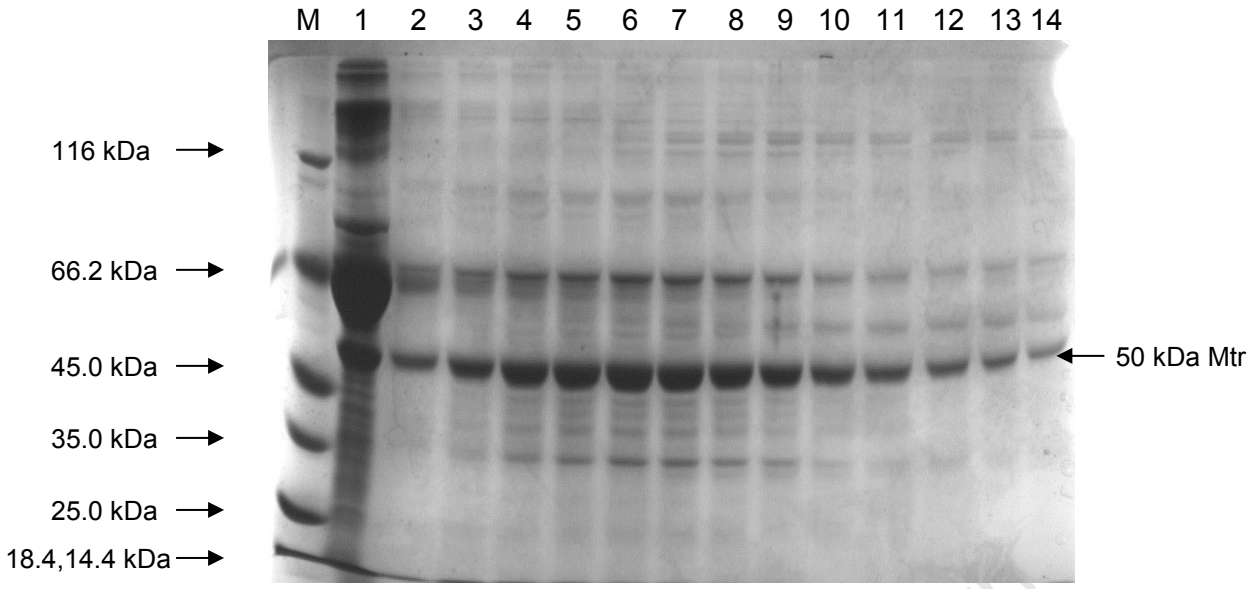

Figure 6. SDS-PAGE analysis of anion exchange chromatography fractions. (M) Marker; (1) fraction unretained by column; (2) – (14) collected fractions eluted in test tubes 6 and every second tube up to and including 30.

Rather than using gel filtration, the ADP-sepharose technique was revisited with an alteration to the protocol that was hoped would increase the yield of purified protein. The active samples from the anion exchange method (tubes 6-24) were pooled, concentrated in an Amicon® apparatus, and dialysed against 20 mM KH_2PO_4, pH 7.6 buffer. This sample was then stirred overnight in a suspension of the 2',5'-ADP-sepharose resin at 4 °C, before being poured into a column and purified in the manner described above. By this stage, a significant proportion of the enzyme had become inactive and precipitated, and the quantity of purified, active protein obtained from the ADP-sepharose column was negligible. A likely reason for this loss was the handling of the enzyme samples, which were run, stored during the run, and transported from the anion exchange apparatus, all at room temperature. This elevated temperature is likely to have denatured a significant proportion of the sample over this period of time. Extended interaction with the resin could also have been a contributing factor to the loss of activity.

4.6 Discussion and Conclusion

Mycothiol disulfide reductase was purified 4.7-fold in a combined yield of 2.68 %, for the combined ADP-sepharose fractions (yield based on total activity of the fraction relative to the extract, see Table 3). Sequential chromatography on Ni^{2+} IMAC and ADP-sepharose columns yielded two solutions that contained a single band at 50 kDa (indicative of the target

protein monomer) and a third solution with a predominant band at 50 kDa and minor protein impurities of lower molecular weight. A considerable amount of activity was lost after the IMAC column with a yield of just 17 % being recovered. The subsequent purification step resulted in further loss of activity with a combined yield of just 5.98 % for the fractions collected from the ADP-sepharose column. The purified fraction with the greatest specific activity (41.4 μmoles.min^{-1}.mg^{-1}) eluted in 75 mM NaCl, yet contained containing minor impurities. Interestingly, the specific activity decreased by almost an order of magnitude for each subsequent fraction eluting from the ADP-sepharose column, from 75 mM NaCl to 200 mM to 1 M, despite similar protein concentrations for each of the solutions. This is likely due to inactivation of a considerable amount of protein over the course of the chromatography. It is also likely that as a result of handling and several concentration steps in the Amicon apparatus, a substantial amount of enzyme activity was lost. The sensitive nature of Mtr was already established during the attempted purification by anion exchange chromatography when a considerable portion of the enzyme became inactive.

Table 3. Purification of recombinant *M. tuberculosis* mycothiol disulfide reductase

Purification Stage	Protein Conc (mg/ml)	Vol of Fraction (ml)	Total Protein Content (mg)	Specific Activity (SA) (μmols/mg/min)	Total Activity (nmols/min)	Yield (%)	Purification Factor SA/SA-extract
Extract	7.68	55	422.4	9.99	4219.77	100	1
IMAC	3.45	55	189.5	3.78	716.31	17	0.378
ADP-U[a]	7.66	18	137.9	1.01	139.28	3.3	0.101
ADP-1[b]	0.21	10	2.1	41.4	86.94	2	4.14
ADP-2[c]	0.48	10	4.8	5.02	24.1	0.6	0.50
ADP-3[d]	0.52	10	5.2	0.67	3.48	0.08	0.35

[a] Pooled fraction unretained by the ADP-sepharose column

[b] Pooled fraction eluting from the ADP-sepharose column in 75 mM NaCl

[c] Pooled fraction eluting from the ADP-sepharose column in 200 mM NaCl

[d] Pooled fraction eluting from the ADP-sepharose column in 1.0 M NaCl

The separation of active enzyme into different fractions during the ADP-sepharose purification step was surprising and suggested that post-translational modification of the protein structure may have taken place. This could give rise to a variety of protein morphologies with divergent ionic properties resulting in differing degrees of adsorption to the stationary phase. In particular, the lack of binding of the major fraction of protein (12.1 mg retained vs 137.9 mg unretained) suggested that this particular affinity chromatography

technique is inefficient for this enzyme and an alternate method will have to be employed for larger scale preparations. The poor adhesion of the enzyme to the IMAC stationary phase could be explained by a possible mutation having occurred in the gene that give rise to a truncated His_6-tag with a lower affinity for the bound Ni^{2+}. Alternatively, it is possible that protease activity resulted in different degrees of protein cleavage, giving rise to a range of protein sizes. An attempt to establish the molecular weight of each eluted protein fraction by matrix-assisted laser desorption/ionisation time-of-flight (MALDI-TOF) mass spectrometry was carried out on a purified Mtr fraction. The analysis gave inconclusive results, however, since it appeared that the protein and matrix did not co-crystallise. This precluded a satisfactory analysis being carried out, and a molecular ion signal was not obtained.

References

1. M.P. Patel and J.S. Blanchard, *Biochemistry*, **1999**, *38*, 11827-11833
2. L. Zhong, E.S.J. Arnér, L. Ljung, F. Aslund and A. Holmgren, *J. Biol. Chem*., **1998**, *273*, 8581-8591
3. L.D. Arscott, S. Gromer, R.H. Schirmer, K. Becker and C.H. Williams, Jr., *Proc. Natl. Acad. Sci. U.S.A*., **1997**, *94*, 3621-3626
4 M.P. Patel and J.S. Blanchard, *J. Am. Chem. Soc.*, **1998,** *120,* 11538-11539
5. M.P. Patel and J.S. Blanchard, Biochemistry, **2001**, *40*, 5119-5126
6. (a) M. Rawat, G.L. Newton, M. Ko, G.J. Martinez, R.C. Fahey and Y. Av-Gay, *Antimicrob. Agents Chemother.*, **2002**, *46*, 3348-3355; (b) G.L. Newton, M.D. Unson, S.J. Anderberg, J.A. Aguilera, N.N. Oh, S.B. del Cardayre, Y. Av-Gay and R.C. Fahey, *Biochem. Biophys. Acta, Res. Commun*., **1999**, *255*, 239-244
7. A. Mahapatra, S.P.N. Mativandlela, B. Binneman, P.B. Fourie, C.J. Hamilton, J.J.M. Meyer, F. van der Kooy, P. Houghton and N. Lall, *Bioorg. Med. Chem*., **2007**, *15*, 7638-7646
8. H.S.C. Spies and D.J. Steenkamp, *Eur. J. Biochem*., **1994**, *224*, 203–213
9. M.A. Jardine, H.S.C. Spies, C.M. Nkambule, D.W. Gammon, D.J. Steenkamp, *Bioorg. Med. Chem*., **2002**, *10*, 875–881
10. D.J. Steenkamp and R.N. Vogt, *Anal. Biochem*., **2004**, *325*, 21-27
11. M.P. Patel and J.S. Blanchard, *Biochemistry*, **2001**, *40*, 5119-5126
12. U.K. Laemmli, *Nature*, **1970**, *227*, 680-685

Chapter 5
Cloning and Expression of *Mycobacterium tuberculosis* Glyoxalase I

5.1 Introduction

The glyoxalase system (GlxI and GlxII)[i] (Scheme 1) has been promoted as a potential drug target for a number of diseases, including malaria,[1,2] leishmaniasis and trypanosomiasis,[3,4,5] bacterial infections,[6] and cancer, for which the greatest body of literature has been published.[7,8,9,10,11,12] Inhibition of this enzyme system as a means of generating cell death is based upon the associated accumulation of the toxic by-product of glycolysis, methyl glyoxal (MG). MG is toxic because its high reactivity allows is to form adducts with numerous biological targets, including proteins and nucleic acids, forming glycation end-products such as hydroimidazolones and imidazopurinones.[13] In general, it is the first glyoxalase enzyme that is targeted for drug development since it is involved in isomerising the glutathione (GSH) conjugate of MG (Scheme 1), and therefore its inhibition would have a direct result on the accumulation of MG, whereas inhibition of GlxII would result largely in the accumulation of *S*-D-lactoyl glutathione. It is, however, also likely that there would be overlapping activity between the two enzymes since the substrate structures are so similar, which has in fact been reported.[14] Within the context of cancer research, GlxII activity has been shown to be substantially lower than GlxI in some types of cancer cells, which has also contributed to the focus being on GlxI.[15]

[i] The abbreviations for glyoxalase, Glx and Glo, are used interchangeably in the literature

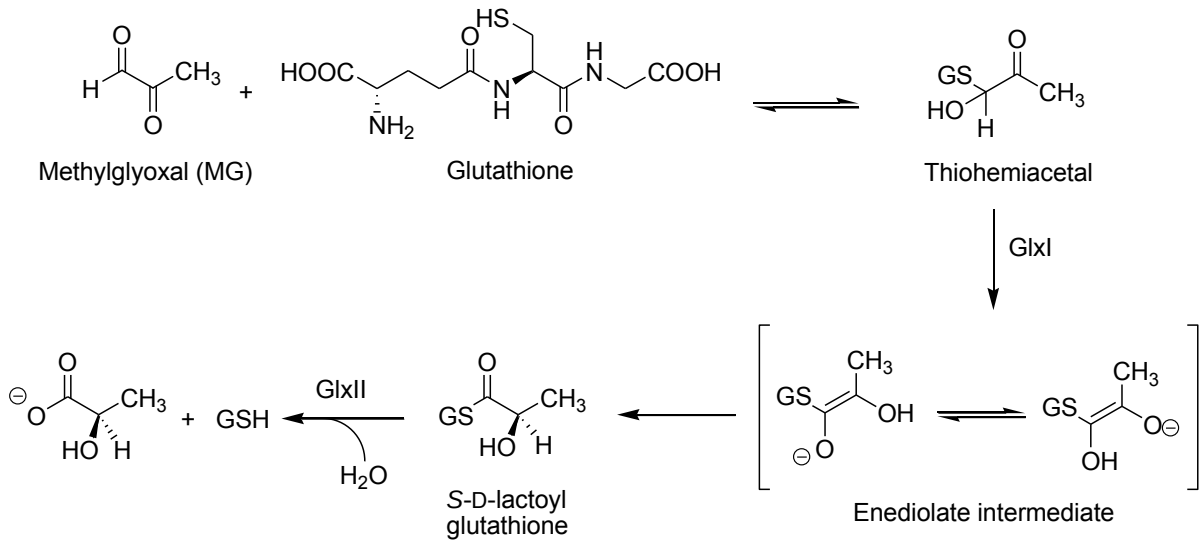

Scheme 1. The glutathione-dependent glyoxalase enzyme system, comprising GlxI and GlxII, responsible for the detoxification of MG

Several polyphenols and flavonoids have been shown to display inhibitory activity against GlxI, including curcumin and derivatives thereof,[9,16] 10-ethylisoalloxazine,[17] kojic acid,[18] the naphthoquinone, lapachol,[18,19] quercetin,[19] delphinidin,[20] and a thiazole developed from computational modelling of the enediolate intermediate and termed TLSC702.[21] (Figure 1).

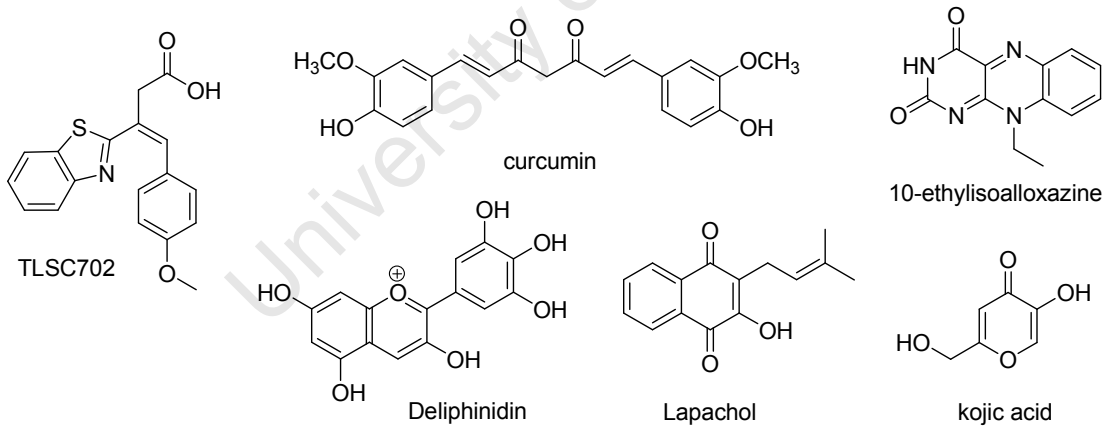

Figure 1. Chemical structures of selected polyphenols and flavonoids with inhibitory activity against GlxI

In addition to these classes of active compounds, several glutathione *S*-conjugates have been shown to be good inhibitors of GlxI, with the most active derivatives being (i) *S*-*p*-bromobenzyl glutathione (**5.1**),[22,23,24,25] and (ii) *S*-hydroxamic acid glutathione (**5.2**)[15] (see Figure 2), with the combination of these two pharmacophores (**5.3**) shown to generate a nanomolar inhibitor of yeast GlxI.[14,26,27]

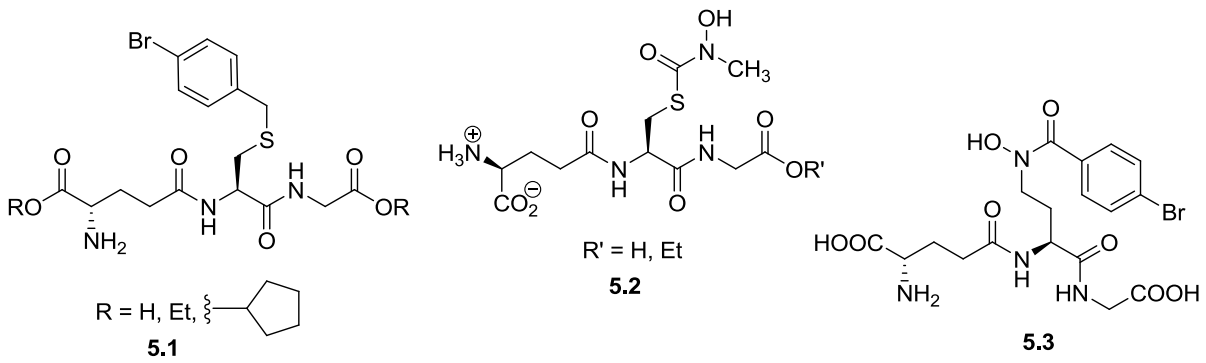

Figure 2. Chemical structures of *S*-conjugate glutathione illustrating the two most active pharmacophores, *S*-*p*-bromobenzyl (**5.1**) and *S*-(*N*-methyl-*N*-hydroxycarbamoyl) glutathione (**5.2**), and the combination of the two into a single molecule (**5.3**)

Within the context of *Mycobacterium tuberculosis*, although the presence of a mycobacterial glyoxalase system has been suggested, to date there has not been a published report of its identification, although the production of *S*-lactoylmycothiol, the hypothetical reaction product of the enzyme, in extracts of *M. smegmatis,* was noted but not published by Nobel lauteate, Irwin Rose.[28] However, it does seem to be likely that this enzyme system exists, and that instead of GSH-mediated detoxification of MG, this process would be carried out instead by a MSH-dependent glyoxalase system. Such a MSH-dependent GlxI system is worthwhile investigating as a potential drug target due to the importance of detoxification of MG to the integrity of a cell. Also, the large structural difference that exists between GSH and MSH creates the possibility of generating an inhibitor that is selective for the mycobacterial protein over the mammalian one. Based on the reported activity of the flavonoid-type inhibitors described above, and the reported activity derived from *S*-conjugation of GSH, it seemed plausible that the naphthoquinone and carbazole-1,4-quinone conjugates described in Chapters 2 and 3 might display inhibitory activity against the hypothetical mycobacterial GlxI, since they consist of a MSH-type functionality substituted with a quinone at a similar position to the thiol of MSH. This could potentially increase the number of enzymes targeted by the synthesised derivatives and thus increase their overall activity against TB.

5.2 Glyoxalase I: Cloning, Transformation and Expression Methods

The first step in the planned process towards identifying and then cloning and expressing a potential mycobacterial GlxI protein involved performing a sequence homology search of the *M. tuberculosis* genome to identify the gene candidate. This was followed by PCR amplification of the putative gene and then cloning into a suitable vector, in this case, pET17b (Novagen), to generate the expression vector. This construct was then used to transform the bacterial expression system, namely, BL21(DE3) Rosetta pLysS *E. coli* cells (Novagen), in which the protein was expressed. Precedent for this approach was given by the published work of Fairlamb and co-workers[29,30] who cloned, expressed and characterised the related trypanothione-dependent *Leishmania Major* and *Trypanosoma cruzi* GlxI enzymes from BL21(DE3)pLysS *E. coli* cells transformed with a pET15b construct. Induction was carried out by treatment of the transformed cells with IPTG.

5.2.1 Material Suppliers

M. tuberculosis H37Rv, was obtained as a gift from Dr Ian Wiid at the Department of Medical Biochemistry at the University of Stellenbosch, South Africa. Blue/Orange Loading Dye (Agarose Gel), 1kb DNA ladder and Pfu DNA polymerase were obtained from Promega. pET17b vector and BL21 (DE3) Rosetta, pLysS competent *E. coli* cells were obtained from Novagen. Fastdigest® BamHI and Fastdigest® NdeI restriction enzymes, isopropyl β-D-1-thiogalactopyranoside (IPTG), agarose, and T4 DNA ligase (as part of a "Rapid DNA ligation kit") were all purchased from Fermentas. The antibiotics, carbenicillin and kanamycin were obtained from Calbiochem, whereas chloramphenicol was obtained from Boehringer Mannheim. Protease Inhibitor Cocktail set III was also obtained from Calbiochem. One Shot Top 10™ competent *E. coli* cells and Zero Blunt® PCR cloning kit were obtained from Invitrogen. QiAprep® Spin Miniprep kits were acquired from Qiagen. DNA extraction from agarose gel was employed utilising a number of kits from different suppliers: DNA Gel Extraction Kit (Fermentas), NucleoSpin® Extract II (Macherey-Nagel), GELase™ Agarose Gel Digesting Preparation (Epicentre Biotechnologies), Zymoclean Gel DNA Recovery (Zymo Research Corporation) and TaKaRa RECOCHIP (Takara Bio Inc.). Methyl glyoxal and 4,4'-dithiodipyridine were purchased from Sigma Aldrich. *N*,*N'*-methylenebisacrylamide was purchased from Fluka. Ammonium persulfate, sodium dodecyl sulphate and TEMED were acquired from BDH. Tryptone, yeast extract and agar were purchased either from Difco, Biolab, Fluka or Oxoid.

5.2.2 Identification of *M. tuberculosis* GlxI Gene Candidate

The search for a mycobacterial *glxI* gene product in the *M. tuberculosis* H_{37}Rv genome (NCBI Protein database)[31] using the functionally homologous *E. coli* GlxI (accession number U57363.1)[32] as a protein database query, resulted in a match with 88 % sequence homology, and with 78 % sequence homology with both the related trypanothione-dependent GlxI of *Trypanosoma cruzi* CL Brener (accession no. XP_810268) and *Leishmania major* Friedlin (accession no. XP_843406). There was little detectable overlap with the glutathione-dependent human GlxI (accession no. AAH11365).

The amino acid sequence of the putative *M. tuberculosis* GlxI protein is indicated below:

MEILASRMLL RPADYQRSLS FYRDQIGLAI AREYGAGTVF FAGQSLLELA GYGEPDHSRG PFPGALWLQV RDLEATQTEL VSRGVSIARE PRREPWGLHE MHVTDPDGIT LIFVEVPEGH PLRTDTRA

Mol Wt: 14.35 kDa

The nucleotide sequence of the identified gene Rv0546c was obtained from the BioCyc[33] *M. tuberculosis* genome database as:

ATGGAAATCC TGGCCAGCCG GATGCTACTT CGGCCGGCGG ACTATCAGCG GTCGCTGAGC TTCTACCGTG ACCAGATCGG GCTGGCGATT GCCCGTGAAT ACGGGGCCGG CACAGTGTTT TTCGCCGGTC AGTCACTGCT CGAACTGGCC GGTTACGGCG AGCCGGACCA TTCGCGGGGA CCTTTTCCCG GCGCGCTGTG GCTGCAGGTG CGCGACCTCG AGGCTACCCA GACCGAGCTG GTCAGCCGAG GCGTGTCGAT CGCTCGCGAG CCCCGCCGCG AACCGTGGGG CCTGCACGAG ATGCATGTGA CCGACCCAGA CGGGATCACA CTGATATTCG TCGAGGTTCC CGAGGGTCAC CCGCTGCGTA CAGACACCCG GGCGTGA

The identified open reading frame was used to design oligonucleotide primers containing restriction enzyme sites for NdeI (forward primer) and BamHI (reverse primer). The gene was amplified by PCR from *M. tuberculosis* H_{37}Rv template DNA using the forward primer: 5' cacagggcatatgaaatcctg 3' with the NdeI site underlined, and the reverse primer: 5' ggatccgcgttttgcggagttcacgcccg 3' with the BamHI site underlined. The expected PCR product with restriction sites underlined is indicated below:

CACAGGGCAT ATGGAAATCC TGGCCAGCCG GATGCTACTT CGGCCGGCGG ACTATCAGCG
GTCGCTGAGC TTCTACCGTG ACCAGATCGG GCTGGCGATT GCCCGTGAAT ACGGGGCCGG
CACAGTGTTT TTCGCCGGTC AGTCACTGCT CGAACTGGCC GGTTACGGCG AGCCGGACCA
TTCGCGGGGA CCTTTTCCCG GCGCGCTGTG GCTGCAGGTG CGCGACCTCG AGGCTACCCA
GACCGAGCTG GTCAGCCGAG GCGTGTCGAT CGCTCGCGAG CCCCGCCGCG AACCGTGGGG
CCTGCACGAG ATGCATGTGA CCGACCCAGA CGGGATCACA CTGATATTCG TCGAGGTTCC
CGAGGGTCAC CCGCTGCGTA CAGACACCCG GGCGTGAACT CCGCAAAACG CGGATCC

5.2.3 PCR Conditions

The putative gene identified from the BLAST search of the mycobacterial genome was amplified by PCR from *M. tuberculosis* H_{37}Rv template DNA using the forward primer: 5' ggatccgcgttttgcggagttcacgcccg 3' which contained a BamHI restriction site (underlined), and the reverse primer: 5' cacagggcatatgaaatcctg 3' with an incorporated NdeI restriction site incorporated (underlined). The PCR conditions employed are given below in Table 1.

Table 1. PCR conditions employed for the amplification of the putative *M. tuberculosis* GlxI gene

Time (min)	Temperature (°C)	
5	98	
1	98	
1	50	35 cycles
2	72	
10	72	
Store at 4 °C		

The PCR mixture contained the following components:
Pfu buffer (5 µl), dNTP mix (2 mM, 5 µl), primers (100-fold diluted, 2 µl), template DNA (*M. tuberculosis* H37Rv; 2 µl), pfu DNA polymerase (1.25 µl), water (32 µl).

5.2.4 DNA Digestion

Fastdigest® BamHI and NdeI restriction enzymes (Fermentas) were used for digestion of the pET-17b plasmid (Novagen). According to the manufacturer, 1 µl of each enzyme is capable of digesting 1 µg of plasmid DNA in 5 – 15 min. A typical reaction involved

combining the following reagents (in the order indicated) in a 1.5 ml microcentrifuge tube in ice:

	Vol (µl)
Nuclease-free water	15
10x Fastdigest® buffer	2
DNA	2
Fastdigest® BamHI	1
Fastdigest® NdeI	1
Total volume	21

After mixing, the contents of the tube was spun down and incubated at 37 °C for 15 min in a thermostated waterbath. Upon completion of the reaction, the restriction enzymes were inactivated by incubating at 80 °C for 5 min. Successful plasmid digestion was confirmed by agarose gel electrophoresis.

5.2.5 Agarose Gel Electrophoresis

TAE Buffer: A working solution of 1x TAE (Tris-acetate, EDTA) was prepared by diluting an aliquot of 50x stock solution with deionised water. The final solute concentration was 40 mM Tris-acetate and 1 mM EDTA.

Agarose Gel Preparation: The 1 % agarose gel was prepared by mixing 500 mg agarose gel powder in 50 ml TAE buffer, and heating in a microwave until complete dissolution. Ethidium bromide (0.5 µg/ml) was added and the liquid gel poured into a mould containing a sample comb and left to set at room temperature. Once set, the sample comb was removed and the gels submerged in TAE buffer in the electrophoresis apparatus in preparation for sample loading.

Sample Preparation: DNA products of restriction enzyme digest reactions were typically loaded in 5 µl aliquots and combined with 1 µl blue/orange loading dye. DNA products from PCR or large scale plasmid digestion reactions, which required purification by electrophoresis, were loaded in 50 µl aliquots and combined with 5 µl blue/orange loading dye. An additional end lane containing a low concentration of the product was also prepared in order to identify the position of the bulk DNA band during visualisation (see description below). The prepared samples were then added to the sample wells and the gel run at 80 – 100 mA until the dye front was approximately 2 cm from the end of the gel.

Visualisation: For small-scale restriction enzyme digest products, the gel was placed on a transilluminator (UV light at 254 nm) after completion of the run and photographed. In order to prevent exposure of purified PCR or large-scale plasmid digestion products to harmful UV light, which can damage DNA and negatively influence subsequent ligation reactions, the end lane was cut off and visualised under UV (Figure 3). The DNA band was marked, and the excised lane aligned with the remainder of the gel. The position of the bulk DNA product band was estimated using the marked band, and excised without exposure to the UV lamp.

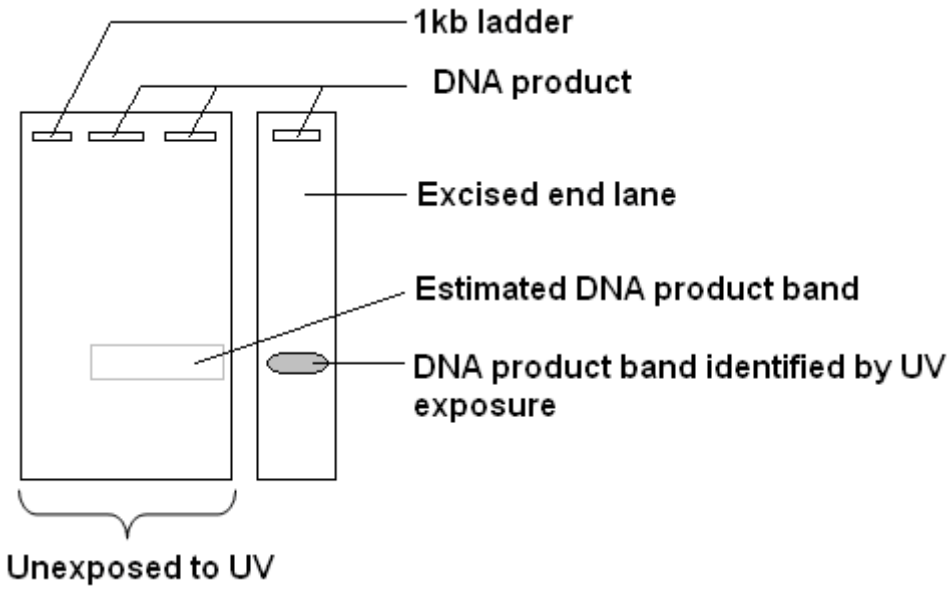

Figure 3. Diagram indicating method of identification of agarose gel product band

5.2.6 DNA Purification and Recovery

DNA was extracted from the agarose gel using one of three methods: Nucleospin® Extract II, Zymoclean Gel DNA Recovery kit, or TaKaRa Recochip.

5.2.6.1 NucleoSpin® Extract II (Macherey-Nagel)

The published protocol for DNA purification using NucleoSpin Extract II was used.[34]
Briefly, DNA was bound to a silica membrane in the presence of a chaotropic salt solution, which was added to the sample as a binding buffer (buffer NT). The mixture was added to a Nucleospin® column and centrifuged on a bench-top microcentrifuge (11,000 x g; 30 s). Contaminants (including salts and macromolecular components) were removed by elution

with an ethanolic buffer (buffer NT3) (11,000 x g; 30 s). Finally, pure DNA was obtained by eluting with an alkaline, low ionic strength buffer (buffer NE) (11,000 x g; 1 min).

Small fragments of DNA can be removed from a sample by diluting an aliquot of buffer NT with sterile water. Diluting buffer NT in a specified range lowers the binding efficiency of small DNA fragments without compromising the recovery of larger DNA strands. The degree of dilution depends on the size of the DNA fragment to be purified, i.e. the smaller the fragment, the less buffer NT has to be diluted. This method was used particularly for purifying linearised pET17b vector in preparation for ligation with a sticky ended insert. Since the fragment of pET17b to be removed was 63 bp in size, a dilution of 5 volumes of water was used (calculation based on the manufacturer's agarose gel result showing size of fragment removed at each level of dilution).

5.2.6.2 Zymoclean Gel DNA Recovery Kit

This agarose gel DNA recovery kit provided a method of extraction of DNA from agarose gel slices excised after electrophoresis. The system used a single buffer system (Agarose Dissolving Buffer - ADB™) to dissolve the agarose gel slice, which was then passed through the Zymo-Spin I™ column by spinning on a microcentrifuge allowing adsorption of the DNA onto the column matrix. After washing, the DNA was eluted in a small volume of water (6-10 µl). According to the manufacturers, DNA purified by this method is suited for use in DNA ligation reactions, sequencing and PCR. The protocol is available online.[35]

5.2.6.3 TaKaRa RECOCHIP

The protocol is available online from the manufacturer.[36] The technology involves binding DNA to a cellulose membrane during electrophoresis. The band of interest is identified by UV illumination after the gel has been run, and the chip containing the cellulose membrane is inserted into the agarose gel directly in front of the band of interest. Electrophoresis is then continued and the DNA is trapped by the membrane as it travels along the electrical gradient. The DNA is removed from the chip by centrifugation on a benchtop microcentrifuge.

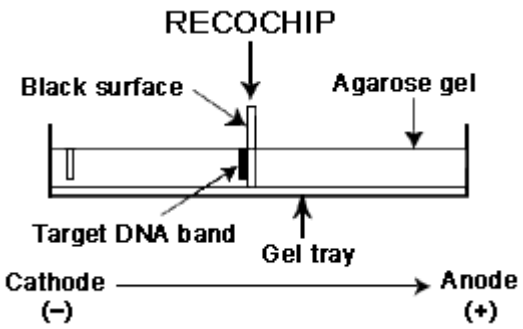

Figure 4. Diagram indicating collection of DNA by RECOCHIP during electrophoresis[36]

5.2.7 Determination of DNA Concentration

The concentration of DNA in solution was determined by a NanoDrop (Thermo Scientific) spectrophotometer. Typically 1-2 µl samples were measured at A_{260} to give a DNA concentration in ng/µl, which was used to calculate the quantities of vector and insert for ligation reactions, and the amount of DNA product from miniprep extractions.

5.2.8 Ligation of PCR Product into ZeroBlunt Vector and Transformation of Top10 Cells

Ligation of the PCR product into a pCR-Blunt® vector was carried out using T4 DNA ligase (1 µl; 4U/µl) in a solution of ligation buffer (total volume 10 µl). The mixture was incubated at 16 °C (optimal temperature for ligation) for 1 h. A 2 µL aliquot was added to an ice-thawed 50 µl vial of One Shot® TOP10 cells and the mixture gently stirred with the pipette tip and incubated on ice for 30 min, before being subjected to a 45 sec heat shock at 45 °C followed by cooling on ice for 2 min. SOC medium (250 µl) was added and the vials shaken at 225 rpm at 37 °C for 1 h. The transformation mix was then spread on 1 % LB agar plates containing 50 µg/ml kanamycin and incubated overnight at 37 °C.

5.2.9 Preparation of plates

LB medium (200 ml) was added to 2 x 500 ml Schott bottles (labelled “1” and “2”) containing bactoagar (2.00 g). The bottles were autoclaved at 121 °C and 15 psi for 20 min. Upon cooling to 45 °C, chloramphenicol (final concentration 30 µg/ml) was added to each bottle and carbenicillin (final concentration 50 µg/ml) added to bottle “1”. After mixing, 20 ml agar

plates of each solution were poured, covered, labelled and left to set in a laminar flow cabinet.

5.2.10 Preparation of Luria-Bertani (LB) Medium

A 1 L solution of LB medium was prepared by mixing tryptone powder (10 g), yeast extract (5 g) and NaCl (10 g) in deionised water (1 L) and autoclaving at 121 °C and 15 psi for 20 min. Upon cooling, appropriate antibiotic was added.

5.2.11 Miniprep

Harvesting of plasmids was achieved using the QIAprep Spin Miniprep kit according to the manufacturer's protocol.[37]

5.2.12 Transformation of BL21 (DE3) Rosetta, pLysS Cells

The vial of BL21 (DE3) Rosetta, pLysS cells was thawed on ice before 4 µl of ligation mix was added and the mixture gently stirred with the pipette tip. The vial was then incubated on ice for 20 min before being subjected to a 30 sec heat shock at 42 °C, and then returned to the ice. 250 µl of room temperature SOC medium was added and the mixture shaken horizontally at 37 °C for 1 h at 225 rpm. The mixture was then plated on a 1 % LB agar plate containing carbenicillin (50 µg/ml) and chloramphenicol (34 µg/ml), and incubated overnight at 37 °C.

5.2.13 Induction with IPTG

Into each of two 2 L conical flasks was placed 500 ml of freshly autoclaved LB medium containing chloramphenicol (34 µg/ml) and carbenicillin (50 µg/ml). Each flask was inoculated with a portions of the same colony and incubated and shaken at 37 °C until each flask had an OD_{600} = 0.5. A 10 ml sample from each flask was removed, prior to the addition of IPTG to a final concentration of 0.4 mM, and incubation and shaking was continued at 25 °C. Subsequent 10 ml samples were removed from each flask after 1 h, 2.5 h and 3.5 h.

Samples from equivalent times were combined and centrifuged at 4000 rpm for 15 min at 4 °C. The cells in the bulk medium after 3.5 h were collected by centrifugation under the same conditions, and stored at -80 °C. The supernatant of each sample was then discarded and the cells resuspended in Tris-HCl buffer (2 ml, 0.75 M, pH 8.8). DNAse (final conc. 20 μg/ml), to reduce viscosity due to DNA, and a protease inhibitor tablet, to prevent protease digestion of the expressed enzyme, was added to each sample. The samples were then successively frozen in liquid N_2 and thawed 3 times in order to break open the cells (the BL21 pLysS cells contain T7 lysozyme which leaks out during freeze/thaw cycles and digests the cell wall). This approach was employed in an attempt to maintain a low sample temperature and reduce loss of enzyme activity, however, several additional mild sonication cycles were required to complete cell lysis. Samples were then clarified by centrifugation at 5000 rpm and 4 °C in preparation for SDS-PAGE.

5.2.14 Glyoxalase I Assay

The assay used for the determination of glyoxalase I activity measured the rate of formation of the isomerised thiohemiacetal-MSH adduct, which has an absorbance peak at 240 nm.[38] The assay protocol employed was adapted from a published procedure that was used for a trypanothione-dependent glyoxalase I from *Leishmania major*.[29] The first step involved preparation of lactoylmycothiol by combining 3.2 µl of 55.5 mM methyl glyoxal (final conc. 200 µM) with 26 µl of 5.2 mM MSH (final conc. 150 mM) in 870 µl of 100 mM Na_2HPO_4 (pH 7.0) and incubating at 27 °C for 10 min. This provided the substrate for glyoxalase I. The second step involved the addition of 5 µl of enzyme sample, and recording the time-dependent increase of absorbance at A_{240} as the isomerised thiohemiacetal-MSH product was formed.

5.2.15 Recovery of MSH from MSSNaph

Pure MSH was obtained for the GlxI assay from MSSNaph after reduction of the disulphide by 2-mercaptoethanol using the following procedure:

The required amount of MSSNaph (typically ~1 mg) was suspended in a 2:1:1 mixture of water: acetonitrile: EtOAc. A slight excess of 2-mercaptoethanol was added to reduce MSSNaph to its constituent thiols, and the mixture vortexed. Under these conditions, mycothiol will partition into the aqueous phase, while 2-thio-6-hydoxynaphthalene and most

of the 2-mercaptoethanol will partition into the organic phase. The pH was lowered to <5.0 by the addition of glacial acetic acid to stabilize the protonated forms of the thiols. This improved the extraction of 2-thio-6-hydroxynaphthalene and 2-mercaptoethanol into the organic phase. The residual 2-mercaptoethanol was removed by repeated extraction of the aqueous phase using water saturated EtOAc.

5.2.16 Absorbance Spectrophotometry

To determine the mycothiol content of a sample resulting from the reduction of MSSNaph, a 5 µl aliquot was added to a solution containing 10 µl of 19.27 mM DTDP and 985 µl Hepes buffer (50 mM; pH 7). The absorbance change, due to the formation of pyridine-4-thione ($\Delta\varepsilon_{325}$ = 19800 $M^{-1}cm^{-1}$), at 325 nm was recorded on an Ocean Optics USB2000 spectrophotometer and was used to calculate the MSH concentration.

5.3 Results

DNA amplification by PCR was carried out under the conditions described above. The PCR product was run on a 1 % agarose gel in TAE buffer to confirm that it was the predicted size, 416 bp (Figure 5)

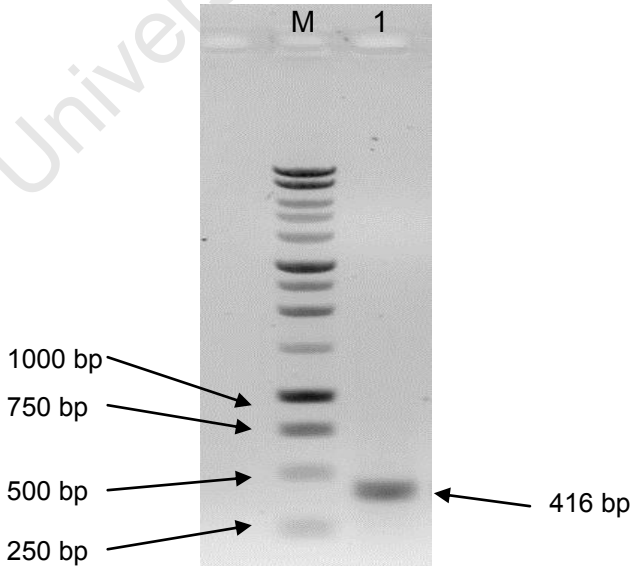

Figure 5. Agarose gel indicating required size of PCR product at 416 bp. (M) Marker; (1) PCR product.

The plasmid into which the PCR product was cloned was Novagen's pET17b. This vector is 3,306 base pairs (bp) in length, contains an ampicillin resistance gene, and in the multiple cloning region has BamHI and NdeI restriction sites. pET plasmids have been used to clone a wide range of enzymes, including many found in mycobacteria,[39,40] and their ease of use and wide-spread application rendered pET17b a suitable candidate for the cloning experiment. Linearisation of the vector with BamHI and NdeI restriction enzymes removed a 63 bp section of the cloning region (Figure 6).

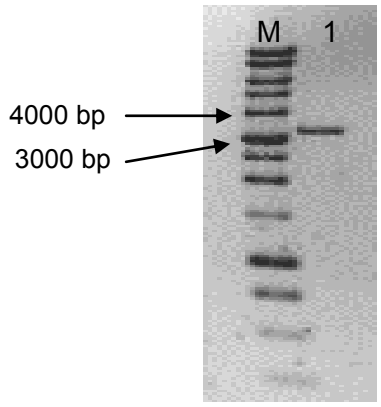

Figure 6. (M) Marker; (1) pET17b plasmid linearised by digestion with BamHI and NdeI to give a product consistent with the expected length of 3243 bp.

Several gel extraction kits were unsuccessfully employed in attempts to extract pure pET17b digestion and PCR products from agarose gels run by electrophoresis. These included the DNA Gel Extraction Kit (Fermentas), the NucleoSpin® Extract II (Macherey-Nagel) kit and the GELase™ Agarose Gel Digesting Preparation (Epicentre Biotechnologies). In all cases, and regardless of the scale-up, insufficient plasmid DNA (<20 ng/ml) was obtained to proceed with the ligation.

The Zymoclean Gel DNA Recovery kit was then used to purify the PCR product. From an initial 50 μL of product (conc. = 427 ng/μL), 10 μL of 50 ng/μL pure PCR product were obtained from the excised agarose gel band.

Ligation of the purified blunt-ended PCR product into the ZeroBlunt® vector containing the lethal control of cell death B (*ccdB*) gene was then attempted by incubating the ligation mix at 16 °C for 2 h.[41] This gene reduces non-recombinant background clones since ligation of a blunt PCR fragment disrupts expression of the *ccdB* gene permitting exclusive growth of positive recombinants during transformation. Cells containing non-recombinant vector die due to expression of the ccdB protein, which interferes with bacterial topoisomerase II, an essential enzyme catalysing negative supercoiling of DNA. Inhibition of topoisomerase II results in DNA breakage and ultimately cell death.[42]

Transformation of Top10™ cells was then attempted using the manufacturer's protocol, and followed by spreading on 1 % LB agar plates containing kanamycin (50 μg/ml). After overnight incubation at 37 °C, no colonies were formed.

The ligation procedure was then repeated with a modified incubation time of 5 min at 16 °C (as proposed in the manufacturer's manual) for the ligation experiment. Transformation of Top10™ cells was then attempted, and followed by spreading on 1 % LB agar plates containing kanamycin (50 μg/ml). Once again, after overnight incubation at 37 °C, no colonies were formed.

In order to rule out the possibility that the lack of successful transformation was due to poor cell competency, transformation of the Top10™ cells was attempted with undigested pET17b vector. After following the same protocol, and spreading on 1 % LB agar plates containing carbenicillin (50 μg/ml), several colonies were formed, although a "lawn" of colonies was not obtained. The cells appeared to be moderately competent.

The ligation of the PCR product into the ZeroBlunt® vector was then repeated, with a modification to the incubation conditions. The incubation time was extended from 5 min to overnight, and the incubation temperature was raised from 16 °C to room temperature. Transformation of Top10 cells was then performed utilising the same procedure as in previous attempts, and was followed by spreading of the mixture on 1 % LB agar plates containing kanamycin (50 μg/ml). After overnight incubation at 37 °C, 3 colonies were obtained. These were inoculated into 5 ml LB medium containing kanamycin (50 μg/ml) and incubated overnight at 37 °C with shaking. The plasmids in each sample were harvested by miniprep, with good yields ranging from 261 – 311 ng/μl (as determined by Nanodrop spectrophotometry), and digested with BamHI and NdeI restriction enzymes at 37 °C for 90 min. The presence of the desired insert in the plasmids was confirmed by agarose gel (1 % in TAE buffer) electrophoresis. The gel indicated the presence of a band of the required size at 404 bp, as indicated in Figure 7 below.

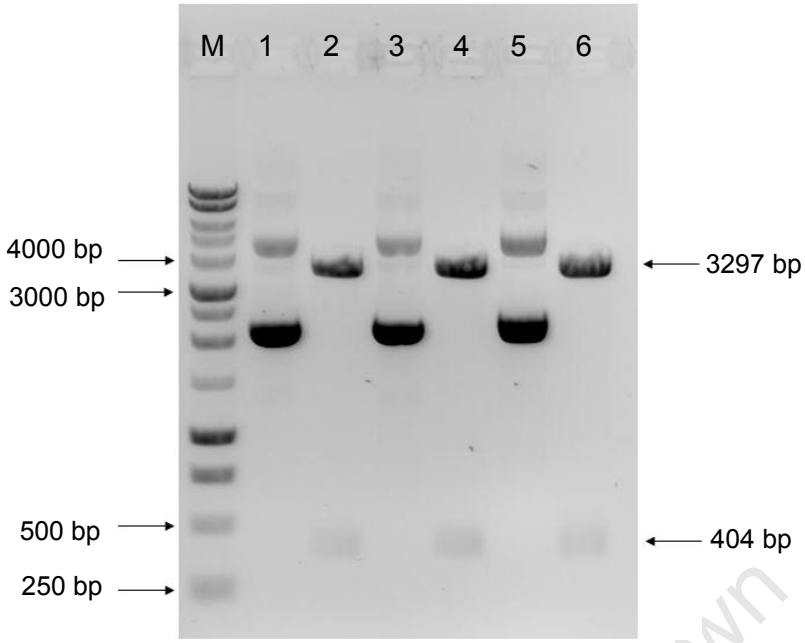

Figure 7. Digested plasmid from TOPO transformation. (M) Marker; (1), (3), (5) undigested plasmid isolated by miniprep from three different colonies 1,2,3 respectively. The two bands correspond to the supercoiled and non-supercoiled circular plasmids. (2), (4), (6) Plasmid samples isolated from colonies 1,2,3, respectively, digested by BamHI and NdeI restriction enzymes. The gene can be seen faintly appearing at 404 bp.

A large-scale digestion (13.5 μg) of the ZeroBlunt plasmid was then performed to isolate the insert in bulk. The Fastdigest™ BamHI and NdeI restriction enzymes were used as before, and the reaction mixture incubated at 37 °C for 2 h. The insert was purified by agarose gel electrophoresis, and extracted using the Zymoclean gel DNA recovery kit.

In preparation for ligation with the insert, 5 μg of the pET17b vector was digested with the Fastdigest™ BamHI and NdeI restriction enzymes at 37 °C for 2 h, and purified by agarose gel electrophoresis, with extraction by means of the Zymoclean kit. The amount of linearized pET17b vector isolated from the agarose gel was 680 ng (14 % yield), and the amount of insert obtained was 960 ng (5 % yield from an initial volume of 45 μL at a concentration of 427 ng/μL).

Once the purified, correctly digested insert and plasmid were obtained, ligation was once again attempted. The two components were combined with ligation buffer and T4 DNA ligase, and incubated at room temperature overnight. Transformation was attempted with both Top10 cells and pLysS BL21 cells utilising the same protocol for each as outlined above. The transformation mixes were spread on 1 % LB agar plates containing carbenicillin (50 μg/ml), in the case of the Top10 cells, and chloramphenicol (34 μg/ml) and

carbenicillin (50 μg/ml) in the case of the pLysS BL21 cells. After overnight incubation at 37 °C, only colonies of transformed Top10 cells had formed. Several of these colonies were inoculated into 5 ml aliquots of LB medium containing carbenicillin (50 μg/ml), and incubated overnight at 37 °C with shaking. The plasmids of each of the samples were harvested by miniprep, and digested with the previously-used restriction enzymes to confirm the presence of the insert. The digested samples were analysed by 1 % agarose gel electrophoresis. As indicated by Figure 8, all but one sample contained a band of the required insert length.

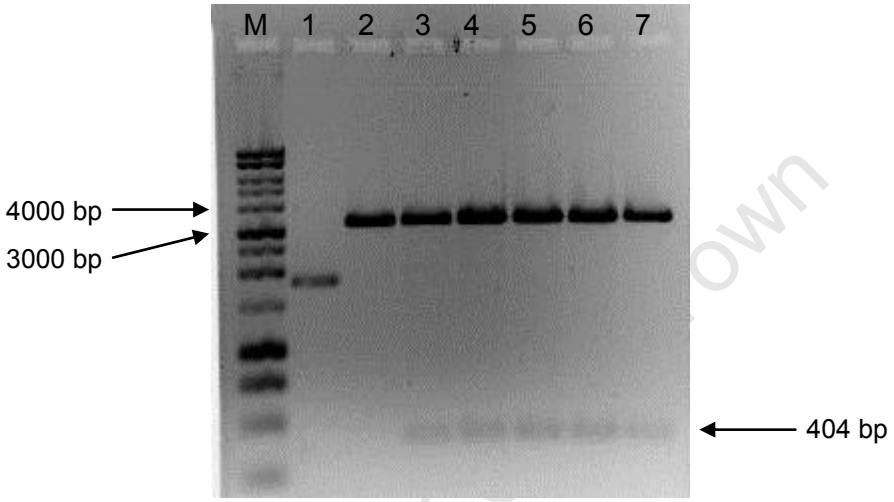

Figure 8. Successful transformation as indicated by presence of insert at 404 bp. (M) Marker; (1) undigested plasmid isolated from colony of transformed Top10 cells; (2) – (7) plasmid samples isolated from colonies of transformed Top10 cells after culturing and miniprep. Digested by BamHI and NdeI restriction enzymes. The presence of the insert at 404 bp in all but sample (2) indicates successful transformation of samples (3) – (7).

Plasmid isolated from one of the samples containing the correctly-sized insert band, was used for transformation of BL21 (DE3) Rosetta, pLysS cells. These cells are designed to enhance the expression of proteins that contain codons rarely used in *E. coli*, and provide the tRNAs for the 6 rare codons, AUA, AGG, AGA, CUA, CCC, GGA, on a chloramphenicol-resistant plasmid that also codes for T7 lysozyme.[43] This is of importance since *Mycobacteria* are rich in guanine and cytosine,[44,45] whereas *E. coli* is not, and this difference could impact on its ability to express mycobacterial proteins. Rosetta cells have been used to express various mycobacterial enzymes.[46,47,48] The protocol described above was used to effect the transformation, which was followed by plating of the cell mixture on 1 % LB agar plates containing chloramphenicol (34 μg/ml) and carbenicillin (50 μg/ml). Colonies were successfully grown, and several were inoculated into 5 ml aliquots of LB medium containing chloramphenicol (34 μg/ml) and carbenicillin (50 μg/ml). The plasmids of the grown colonies were extracted by miniprep and samples digested (BamHI and NdeI) in order to confirm the

presence of the insert. The digested samples were run on a 1 % agarose gel, which when visualised, indicated the presence of the insert at 404 bp (Figure 9).

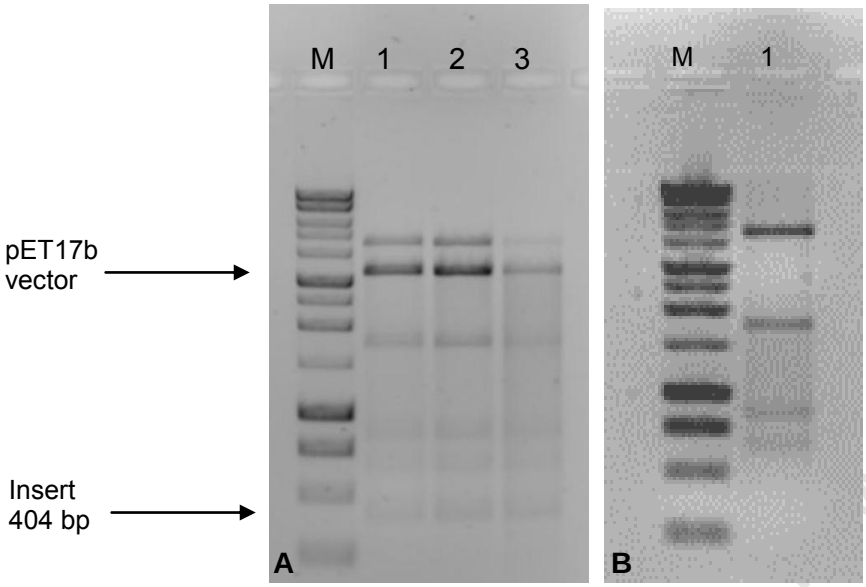

Figure 9. A: Digest of plasmids isolated from transformed Rosetta cells. (M) Marker; (1) – (3) three different colonies that were cultured, cells collected and plasmids isolated and digested by restriction enzymes BamHI and NdeI. The multiple bands correspond to the ligated plasmid and the resident pLysS plasmid that were both cleaved by the restriction enzymes. The gene of interest corresponds to the faint band at 404 bp. The bands corresponding to the pLysS plasmid are identified in **B**: (M) Marker; (1) Resident pLysS plasmid isolated by miniprep of untransformed Rosetta cells and digested by BamHI and NdeI restriction enzymes.

Since the gel indicated that the insert was present, expression of the enzyme was attempted next. Colony 1 (see above gel image) was inoculated into 500 ml of freshly autoclaved LB medium containing chloramphenicol (34 μg/ml) and carbenicillin (50 μg/ml) in a 2 L conical flask, and incubated with shaking at 37 °C until the medium had an OD_{600} = 0.6. At that point, a 10 ml sample was removed (to provide a pre-induction sample for SDS-PAGE), and IPTG added to the bulk mixture to a final concentration of 0.4 mM. Incubation and shaking was then continued at 25 °C. Subsequent 10 ml samples were removed from the flask 1 h, 2 h, 3 h and 4 h post-induction. Samples were centrifuged at 4000 rpm for 15 min at 4 °C, the supernatant discarded, and the cell pellet resuspended in 2 ml lysis buffer (50 mM NaCl in 50 mM Hepes, pH 7.5). A protease inhibitor cocktail (set III, Calbiochem) was added to each sample, followed by DNAse (final conc. 20 μg/ml) to reduce viscosity due to DNA, before being sonicated on ice for 10 min (5 x 2 min; 30 % duty cycle). The mixture was clarified at 15,000 g for 30 min at 4 °C, and the supernatant removed for analysis by SDS-PAGE (sodium dodecyl sulphate polyacrylamide gel electrophoresis).

The running and stacking gels were prepared as outlined in Chapter 4, with the running gel being composed of 15 % acrylamide. The small size (14.35 kDa) of the target protein, which would cause it to run rapidly near the gel front, necessitated a high acrylamide percentage in the gel. 100 μL of each sample was treated with 10 μl of sample treatment buffer and heated at 80 °C for 5 min in order to denature and linearise the protein prior to loading, as well as increase the density of the sample so that it would sink in the gel sample well.
Samples were loaded into the wells, the buffer poured into the reservoir, and the gel run at 30 mA for 5 h. The visualised gel is given in Figure 10 below:

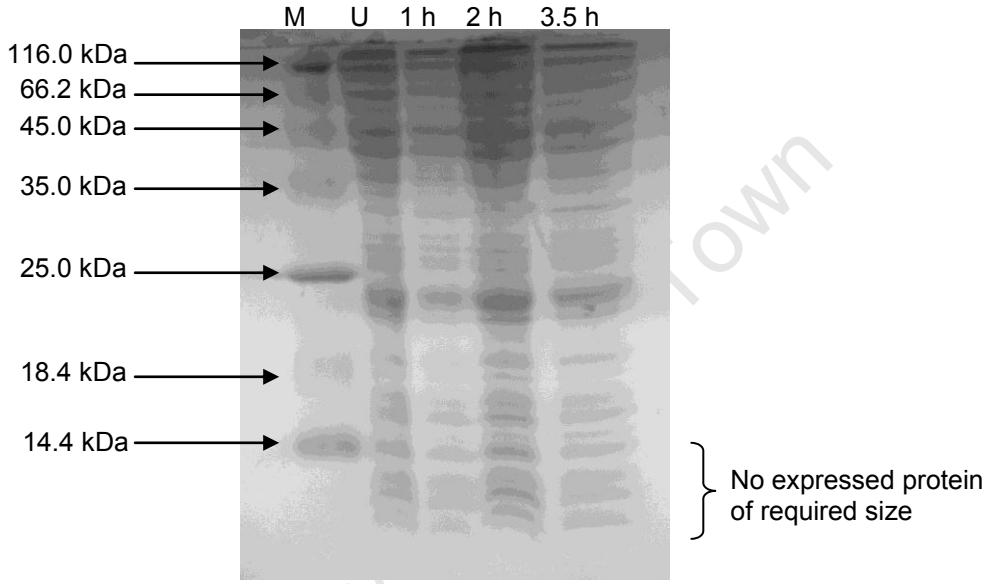

Figure 10. SDS-PAGE of first attempted expression. (M) Marker; (U) uninduced cells; 1 h, 2 h, 3.5 h = time after addition of IPTG at 25 °C.

The lack of an increase in intensity in any of the protein bands in the gel indicated that either expression was too low to be observed on the gel, or was unsuccessful. Consequently, the plasmid used for the expression was sequenced and analysed for errors. The sequence is given below:

```
Score =  728 bits (394),  Expect = 0.0  Identities = 399/401 (99%), Gaps =
1/401 (0%) Strand=Plus/Minus

Query  45      ATGGAAATTCTGGCCAGCCGGATGCTACTTCGGCCGGCGGACTATCAGCGGTCGCTGAGC
104            |||||||| ||||||||||||||||||||||||||||||||||||||||||||||||||||
Sbjct  296062  ATGGAAATCCTGGCCAGCCGGATGCTACTTCGGCCGGCGGACTATCAGCGGTCGCTGAGC
296003

Query  105     TTCTACCGTGACCAGATCGGGCTGGCGATTGCCCGTGAATACGGGGCCGGCACAGTGTTT
164             ||||||||||||||||||||||||||||||||||||||||||||||||||||||||||||
Sbjct  296002  TTCTACCGTGACCAGATCGGGCTGGCGATTGCCCGTGAATACGGGGCCGGCACAGTGTTT
295943

Query  165     TTCGCCGGTCAGTCACTGCTCGAACTGGCCGGTTACGGCGAGCCGGACCATTCGCGGGGA
224             ||||||||||||||||||||||||||||||||||||||||||||||||||||||||||||
Sbjct  295942  TTCGCCGGTCAGTCACTGCTCGAACTGGCCGGTTACGGCGAGCCGGACCATTCGCGGGGA
295883

Query  225     CCTTT-CCCGGCGCGCTGTGGCTGCAGGTGCGCGACCTCGAGGCTACCCAGACCGAGCTG
283             |||||||||||||||||||||||||||||||||||||||||||||||||||||||||||||
Sbjct  295882  CCTTTTCCCGGCGCGCTGTGGCTGCAGGTGCGCGACCTCGAGGCTACCCAGACCGAGCTG
295823

Query  284     GTCAGCCGAGGCGTGTCGATCGCTCGCGAGCCCCGCCGCGAACCGTGGGGCCTGCACGAG
343             ||||||||||||||||||||||||||||||||||||||||||||||||||||||||||||
Sbjct  295822  GTCAGCCGAGGCGTGTCGATCGCTCGCGAGCCCCGCCGCGAACCGTGGGGCCTGCACGAG
295763

Query  344     ATGCATGTGACCGACCCAGACGGGATCACACTGATATTCGTCGAGGTTCCCGAGGGTCAC
403             ||||||||||||||||||||||||||||||||||||||||||||||||||||||||||||
Sbjct  295762  ATGCATGTGACCGACCCAGACGGGATCACACTGATATTCGTCGAGGTTCCCGAGGGTCAC
295703

Query  404     CCGCTGCGTACAGACACCCGGGCGTGAACTCCGCAAAACGC  444
                ||||||||||||||||||||||||||||||||||||||||
Sbjct  295702  CCGCTGCGTACAGACACCCGGGCGTGAACTCCGCAAAACGC  295662
```

Two errors were found in the sequence, namely a mutation at position 9 of the gene from a C to a T, as well as a single nucleotide deletion at position 230. The mutation of the wobble base as position 9 is not significant, since the resulting ATT codon will code for the same amino acid as ATC (isoleucine). However, the deletion at position 230 is likely to have a dramatic effect on the sequence, since each three consecutive nucleotides in the DNA sequence comprise a codon, which codes for a single, specific amino acid. Consequently, the deletion of one nucleotide (a frameshift mutation) would disrupt each subsequent codon, thereby preventing the correct amino acids from being inserted. In addition, the stop codon will be misread resulting in a different stop codon being used and a different sized protein being produced. The deletion is therefore a possible reason for the protein not being expressed.

In order to remove any doubt that the error had occurred at the PCR stage, the PCR product was also sequenced, and was found to be correct. It was then decided to repeat the entire

process from the PCR ligation stage since it was known that the PCR product was correct and unmutated. Consequently, ligation into the ZeroBlunt plasmid was carried out by incubation of 4 μl of the PCR product with 1 μl of ZeroBlunt vector at 16 °C for 1 h in a reaction mix containing 1 μl of 10X ligation buffer, 1 μl T4 DNA ligase and 3 μl of water. Top10 cells were then transformed according to the protocol described above, before being spread on LB-agar plates containing kanamycin (50 μg/ml). After incubation overnight at 37 °C, colonies were obtained, 6 of which were inoculated into 5 ml LB medium containing kanamycin (50 μg/ml) and incubated with shaking overnight at 37 °C. The plasmids in each sample were isolated by miniprep using the Qiaprep kit (Qiagen). 2 μl Samples of each were digested (Fastdigest BamHI and NdeI) and run on a 1 % agarose gel to check for the presence of the insert. The gel image (Figure 11) confirmed that all of the colonies but one contained the insert.

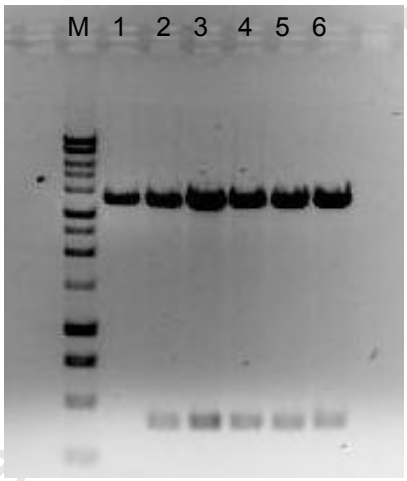

Figure 11. Digest of ligated Zeroblunt plasmid to confirm presence of insert. (M): ladder; (1) – (6): six colonies that were cultured in LB medium, cells collected, plasmids isolated by miniprep and digested by restriction enzymes BamHI and NdeI. The absence of the insert in colony (1) and its presence in colonies (2) – (6) is noted.

Miniprep 3 was selected and digested in large scale (45 μl, 242 ng/μl, 10.8 μg), to liberate the sticky ended insert, in a mix containing 12 μl each of BamHI, NdeI and 10X Fastdigest buffer. The digestion mix was incubated at 37 °C for 1 h, before being run on a 1 % agarose gel. The DNA was extracted using the Takara chip extraction kit, to yield 50 μl of 13 ng/μl purified sticky ended insert. Ligation was performed using 1 μl of the linearized pET17b vector previously prepared with 15 μl of the insert in 2 μl of 5X rapid ligation buffer and 2 μl T4 DNA ligase (Fermentas, “Rapid DNA ligation kit”). 4 μl of the ligation product was used to transform Rosetta cells, which were subsequently spread on LB-agar plates containing

carbenicillin (50 μg/ml) and chloramphenicol (34 μg/ml). After overnight incubation at 37 °C, many colonies were obtained, 7 of which were inoculated into LB medium containing the above antibiotics and cultured at 37 °C overnight with shaking. The plasmids in each sample were isolated by miniprep and aliquots of each digested with BamHI and NdeI to confirm the presence of the insert, following the protocol described above. Agarose gel electrophoresis identified colonies 2, 4, 6 and 7 to have bands of equivalent size to that of the desired insert, as depicted in Figure 12 below. Because Rosetta cells contain a resident pLysS plasmid with restriction sites that are digested by the enzymes, a reference agarose gel of untransformed, digested Rosetta cells was required to unambiguously identify the band corresponding to the insert. To do this, untransformed Rosetta cells were inoculated into 5 ml of LB broth and grown up overnight at 37 °C. The plasmid was then isolated by miniprep and digested with the same enzymes and run on a 1 % agarose gel to provide a comparison to the transformed cells' digested plasmids. The gel is indicated below:

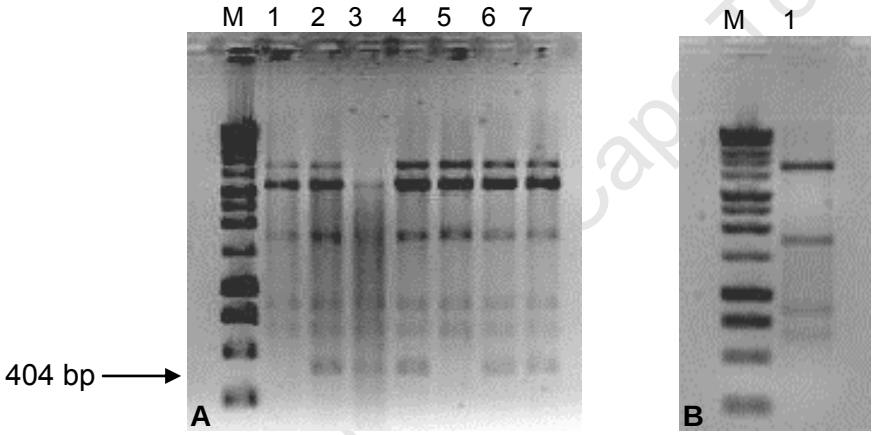

Figure 12. A: Digest of plasmid from transformed Rosetta cells. (M) Marker; (1) – (7) seven colonies of transformed Rosetta cells that were cultured in LB medium, plasmids isolated by miniprep and digested by restriction enzymes BamHI and NdeI. The absence of the insert in colonies (1) and (5) and its presence in colonies (2), (4), (6) and (7) is noted. Colony (3) appears to be lacking the resident pLysS plasmid. **B**: (M) Marker; (1) resident pLysS plasmid isolated from cultured Rosetta cells, digested by BamHI and NdeI restriction enzymes. The corresponding four plasmid fragment bands can be assigned in lanes (1) – (7) of **A** to the pLysS plasmid, and by deduction the remaining two bands assigned to the recombinant pET17b vector containing the GlxI gene.

The gel confirmed that the insert of appropriate length was still present in the cells, and so expression of the enzyme was attempted next. This was carried out according to the protocol described previously in section 5.2.12.

A 13 % polyacrylamide gel was prepared for the electrophoresis in order to evaluate whether expression had been successfully achieved. This gel concentration was chosen after

evaluating the pattern of the previously-run polyacrylamide gel. To this end, 17.3 ml of the 30 % acrylamide/bis-acrylamide solution was diluted with 2.7 ml water, and mixed with 20 ml of running gel buffer, 15 μl TEMED and 15 mg $(NH_4)_2S_2O_8$, to produce the running gel. The stacking gel consisted of 1.5 ml 30 % acrylamide/bis-acrylamide, 3.75 ml stacking gel buffer, 9.6 ml water, 12 μl TEMED and 9.5 mg $(NH_4)_2S_2O_8$ (Figure 13).

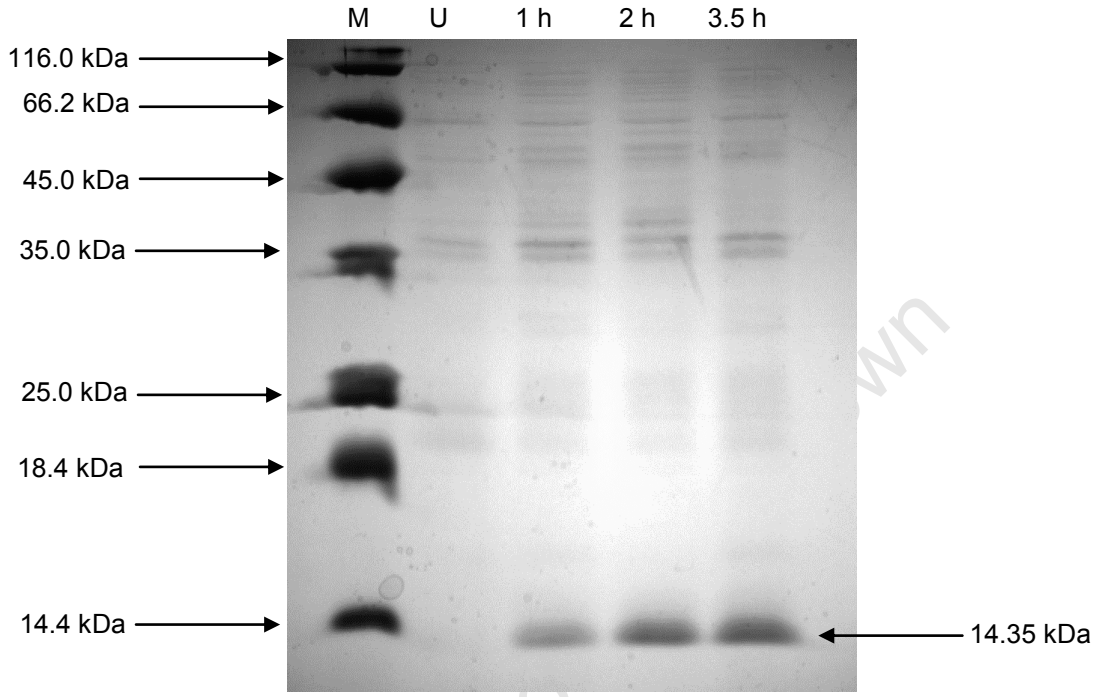

Figure 13. SDS-PAGE gel indicating successful expression. (M) Protein marker; (U) uninduced cells; 1 h – 3.5 h: time after addition of IPTG. The increase in concentration of the protein band at 14.35 kDa indicates successful expression of the protein.

The gel indicated that expression was successful. This was an encouraging result, and the bulk cells were retrieved from the -80 °C storage, defrosted on ice, and lysed by sonication (10 x 2 min, 30 % duty cycle). The mixture was then clarified by centrifugation at 30,000 g for 30 min at 4 °C. The supernatant containing the expressed protein was then stored at -20 °C in preparation for assaying to determine activity.

The assay was carried out according to the protocol described in section 5.2.13, and surprisingly it was revealed that there was no change in absorption at 240 nm, suggesting a lack of enzyme activity.

In order to confirm the validity of the assay, clarified cell extracts of *E. coli* (BL21, pLysS) were assayed as a positive control, using glutathione instead of MSH. Since *E. coli* has been proven to possess a glutathione-dependent glyoxalase system, which also generates an

isomerised thiohemiacetal product with an absorbance peak at 240 nm, it seemed reasonable to assume that it would be able to validate the MSH-based assay.[49] Unfortunately, the results were inconclusive and no obvious peak at 240 nm was generated during the reaction. This could be due to the presence of GlxII in the clarified cell extracts which may have converted the *S*-D-lactoyl glutathione to D-lactate and GSH immediately it was formed, thus preventing its visualisation on the spectrophotometer. Similar difficulties were reported in a previous study using this approach.[50]

The plasmid was then sequenced and found to contain two mutations: a C to T (position 9) and a C to A (position 344). The mutation at position 9 resulted in a codon for the same amino acid, isoleucine, whereas the mutation at 344 would have altered the amino acid coded for from asparagine to histidine, which may have affected activity. The positions of these mutations are indicated below.


```
Score =  730 bits (395),  Expect = 0.0 Identities = 399/401 (99%), Gaps =
0/401 (0%) Strand=Plus/Minus

Query  50      ATGGAAATTCTGGCCAGCCGGATGCTACTTCGGCCGGCGGACTATCAGCGGTCGCTGAGC
109            |||||||| ||||||||||||||||||||||||||||||||||||||||||||||||||
Sbjct  637969  ATGGAAATCCTGGCCAGCCGGATGCTACTTCGGCCGGCGGACTATCAGCGGTCGCTGAGC
637910

Query  110     TTCTACCGTGACCAGATCGGGCTGGCGATTGCCCGTGAATACGGGGCCGGCACAGTGTTT
169            ||||||||||||||||||||||||||||||||||||||||||||||||||||||||||||
Sbjct  637909  TTCTACCGTGACCAGATCGGGCTGGCGATTGCCCGTGAATACGGGGCCGGCACAGTGTTT
637850

Query  170     TTCGCCGGTCAGTCACTGCTCGAACTGGCCGGTTACGGCGAGCCGGACCATTCGCGGGGA
229            ||||||||||||||||||||||||||||||||||||||||||||||||||||||||||||
Sbjct  637849  TTCGCCGGTCAGTCACTGCTCGAACTGGCCGGTTACGGCGAGCCGGACCATTCGCGGGGA
637790

Query  230     CCTTTTCCCGGCGCGCTGTGGCTGCAGGTGCGCGACCTCGAGGCTACCCAGACCGAGCTG
289            ||||||||||||||||||||||||||||||||||||||||||||||||||||||||||||
Sbjct  637789  CCTTTTCCCGGCGCGCTGTGGCTGCAGGTGCGCGACCTCGAGGCTACCCAGACCGAGCTG
637730

Query  290     GTCAGCCGAGGCGTGTCGATCGCTCGCGAGCCCCGCCGCGAACCGTGGGGCCTGAACGAG
349            |||||||||||||||||||||||||||||||||||||||||||||||||||| |||||
Sbjct  637729  GTCAGCCGAGGCGTGTCGATCGCTCGCGAGCCCCGCCGCGAACCGTGGGGCCTGCACGAG
637670

Query  350     ATGCATGTGACCGACCCAGACGGGATCACACTGATATTCGTCGAGGTTCCCGAGGGTCAC
409            ||||||||||||||||||||||||||||||||||||||||||||||||||||||||||||
Sbjct  637669  ATGCATGTGACCGACCCAGACGGGATCACACTGATATTCGTCGAGGTTCCCGAGGGTCAC
637610

Query  410     CCGCTGCGTACAGACACCCGGGCGTGAACTCCGCAAAACGC  450
               |||||||||||||||||||||||||||||||||||||||
Sbjct  637609  CCGCTGCGTACAGACACCCGGGCGTGAACTCCGCAAAACGC  637569
```

5.4 Discussion and Conclusion

It is surprising that the mutations occurred and the poor degree of transformation of the Rosetta cells with the ligated plasmid seems to suggest that perhaps the expressed protein is toxic to *E. coli*, and/or perhaps the selected gene from the BLAST search did not, in fact, code for GlxI. Low expression levels could be indicative of inherent toxicity of the expressed protein to the host bacterium.[51] This phenomenon has been reported in relation to the expression of a range of proteins including membrane proteins,[52] cytoplasmic proteins,[53] cell division proteins,[54,55] and other toxic proteins such as DNAse.[56] Since few colonies were obtained it is possible that the only viable cells were those that did not express active enzyme, with those that did succumbing to the associated toxicity. This would result in the formation of mutated, inactive enzyme in the post-induction clarified cell extract.

A final possibility is that the gene selected from the BLAST search was not the mycobacterial Glx I. Glyoxalase is a member of the vicinal oxygen chelate (VOC) metalloenzyme superfamily.[57] VOC proteins can be difficult to differentiate from one another as they have similar amino acid sequences despite having differing enzymatic functions.[58,59] Diverse members of this group include the fosfomycin resistance protein FosA, several extradiol dioxygenases and methylmalonyl-CoA epimerase, among others.[60] Consequently it is possible that the incorrect gene, possibly another VOC protein, was selected for cloning and expression, and as a result did not display glyoxalase I activity.

References

1. P.J. Thornalley, M. Strath and R.J.M. Wilson, *Biochem. Pharmacol.*, **1994**, *47*, 418-420
2. M. Urscher, R. Alisch and M. Deponte, *Semin. Cell Dev. Biol.*, **2011**, *22*, 262-270
3. (a) N. Greig, S. Wyllie, T.J. Vickers and A.H. Fairlamb, *Biochem. J.*, **2006**, *400*, 217-223; (b) S. Wyllie and A.H. Fairlamb, *Semin. Cell Dev. Biol.*, **2011**, *22*, 271-277
4. S.C. Chauhan, P.K. Padmanabhan and R. Madhubala, *Curr. Drug. Targets*, **2008**, *9*, 957-965
5. S. Wyllie and A.H. Fairlamb, *Semin. Cell Dev. Biol.*, **2011**, *22*, 271-277
6. U. Suttisansanee and J.F. Honek, *Semin. Cell Dev. Biol.*, **2011**, *22*, 285-292

7. D.J. Creighton, Z.B. Zheng, R. Holewinski, D.S. Hamilton and J.L. Eiseman, *Biochem*. *Soc. Trans.*, **2003**, *31*, 1378-1382
8. D. Hamilton and G. Batist, *Curr. Oncol. Rep.*, **2004**, *6*, 116-122
9. T. Santel, G. Pflug, N.Y.A. Hemdan, A. Schäfer, M. Hollenbach, M. Buchold, A. Hintersdorf, I. Lindner, A. Otto, M. Bigl, I. Oerlecke, A. Hutschenreuter, U. Sack, K. Huse, M. Groth, C. Birkemeyer, W. Schellenberger, R. Gebhardt, M. Platzer, T. Weiss, M.A. Vijayalakshmi, M. Krüger and G. Birkenmeier, *PLoS ONE*, **2008**, *3*, e3508
10. K.D. Tew, *Drug Resist. Updat.*, **2000**, *3*, 263-264
11. D. Burg and G.J. Mulder, *Drug Metab. Rev.*, **2002**, *34*, 821-863
12. P.J. Thornalley and N. Rabbani, *Semin. Cell Dev. Biol.*, **2011**, *22*, 318-325
13. N. Rabbani and P.J. Thornalley, *Semin. Cell Dev. Biol.*, **2011**, *22*, 261
14. N.S.R.K. Murthy, T. Bakeris, M.J. Kavarana, D.S. Hamilton, Y. Lan and D.J. Creighton, *J. Med. Chem*., **1994**, *37*, 2161–2166
15. D.S. Hamilton and D.J. Creighton, *J. Biol. Chem.*, **1992**, *267*, 24933-24936
16. M. Yuan, M. Luo, Y. Song, Q. Xu, X. Wang, Y. Cao, X. Bu, Y. Ren and X. Hua, *Bioorg. Med. Chem.*, **2011**, *19*, 1189-1196
17. K.T. Douglas, A.J. Quilter, S. Shinkai and K. Ueda, *Biochim*. *Biophys*. *Acta*, **1985**, *829*, 119–126
18. K.T. Douglas, D.I. Gohel, I.N. Nadvi, A.J. Quilter and A.P. Seddon, *Biochim. Biophys. Acta.*, **1985**, *829*, 109–118
19. P.K. Padmanabhan, A. Mukherjee, S. Singh, S. Chattopadhyaya, V.S. Gowri, P.J. Myler, N. Srinivasan and R. Madhubala, *Biochem. Biophys. Res. Comm*., **2005**, *337*, 1237–1248
20. R. Takasawa, K. Saeki, A. Tao, A. Yoshimori, H. Uchiro, M. Fujiwara and S.-I. Tanuma, *Bioorg. Med. Chem.*, **2010**, *18*, 7029-7033
21. (a) R. Takasawa, S. Takahashi, K. Saeki, S. Sunaga, A. Yoshimori and S.-I. Tanuma, *Bioorg. Med. Chem.*, **2008**, *16*, 3969–3975; (b) R. Takasawa, A. Tao, K. Saeki, N. Shionozaki, R. Tanaka, H. Uchiro, S. Takahashi, A. Yoshimori and S.-I. Tanuma, *Bioorg, Med. Chem. Lett.* 2011, *21*, 4337–4342
22. T.W.C. Lo and P.J. Thornalley, *Biochem. Pharmacol,*, **1992**, *44*, 2357-2363
23. P.J. Thornalley, L.G. Edwards, Y. Kang, C. Wyatt, N. Davies, M.J.Ladan and J. Double, *Biochem. Pharmacol.*, **1996**, *51*, 1365-1372
24. H. Sakamoto, T. Mashima, S. Sato, Y. Hashimoto, T. Yamori and T. Tsuruo, *Clin. Cancer Res*., **2001**, *7*, 2513-2518
25. R. Vince, S. Daluge and W.B. Wadd, *J. Med. Chem.*, **1971**, *14*, 402-404
26. S.S. More and R. Vince, *Bioorg. Med. Chem. Lett*., **2006**, *16*, 6039–6042
27. S.S. More and R. Vince, *J. Med. Chem*., **2009**, *52*, 4650–4656
28. http://nobelprize.org/nobel_prizes/chemistry/laureates/2004/rose-autobio.html
29. T.J. Vickers, N. Greig and A.H. Fairlamb, *PNAS*, **2004**, *101*, 13186-13191

30. N. Greig, S. Wyllie, T.J. Vickers and A.H. Fairlamb, *Biochem. J.*, **2006**, *400*, 217-223
31. http://www.ncbi.nlm.nih.gov/protein
32. S.L. Clugston, J.F.J. Barnard, R. Kinach, D. Miedema, R. Ruman, E. Daub and J.F. Honek, *Biochemistry*, **1998**, *37*, 8754–8763
33. http://biocyc.org/MTBRV/sequence-rc?type=GENE&object=RV0546C
34. Macherey-Nagel, PCR Clean-Up Gel Extraction, NucleoSpin® Extract II User Manual, http://www.mn-net.com/Portals/8/attachments/Redakteure_Bio/Protocols/DNA%20clean-up/UM_PCRcleanup_Gelex_NSExII.pdf
35. Zymoclean DNA Gel Recovery Kit, protocol available online: http://www.zymoresearch.com/zrc/pdf/D4001d.pdf, accessed 22/02/2010
36. http://www.takara-bio.com
37. www.qiagen.com/hb/qiaprepminiprep
38. E. Racker, *J. Biol. Chem.*, **1951**, *190*, 685-696
39. S.S. Poletto, I.O. da Fonseca, L.P.S. de Carvalho, L.A. Basso and D.S. Santos, *Protein Expression Purif.*, **2004**, *34*, 118-125
40. L.W. Tremblay, J.-E. Hugonnet and J.S. Blanchard, *Biochemistry*, **2008**, *47*, 5312-5316
41. Invitrogen Zero Blunt PCR Cloning Manual, **2006**
42. http://tools.invitrogen.com/content/sfs/manuals/zeroblunt_man.pdf
43. http://www.novagen.com/SharedImages/Novagen/ccOrigamiSWF.html
44. L.R. Hill, *J. Gen. Microbiol.*, **1966**, *44*, 419-437
45. L.G. Wayne and W.M. Gross, *J. Bacteriol.*, **1968**, *96*, 1915-1919
46. F. Ely**,** J.E.S. Nunes**,** E.K. Schroeder**,** J. Frazzon**,** M.S. Palma**,** D.S. Santos and L..A. Basso, *BMC Biochem*., **2008**, *9*, 13
47. A. Singh, L. Guidry, K.V. Narasimhulu, D. Mai, J. Trombley, K.E. Redding, G.I. Giles, J.R. Lancaster Jr. and A.J.C. Steyn, *PNAS*, **2007**, *104*, 11562-11567
48. A. Castell, P. Johansson, T. Unge, T.A. Jones and K. Bäckbro, *Protein Sci.*, **2005**, *14*, 1850-1862
49. S.L. Clugston, J.F.J. Barnard, R. Kinach, D. Miedema, R. Ruman, E. Daub, J.F. Honek, *Biochemistry*, **1998**, *37*, 8754-8763
50. C.E. Hand, Investigations into Intracellular Thiols of Biological Importance, PhD Thesis, **2007**, University of Waterloo, Ontario, Canada
51. B. Miroux and J.E. Walker, *J. Mol. Biol.*, **1996**, *260*, 289-298
52. M.M. Klepsch, J.O. Persson and J.-W.L. de Gier, *J. Mol. Biol*., **2011**, *407*, 532–542
53. H. Dong, L. Nilsson and C.G. Kurland, *J. Bacteriol.*, **1995**, *177*, 1497–1504
54. P.A.J. de Boer, R.E. Crossley and L.I. Rothfield, *J. Bacteriol*., **1988**, *170*, 2106–2112
55. L.M. Gutzman, J.J. Barondess and J. Beckwith, *J. Bacteriol*., **1992**, *174*, 7716–7728
56. A.J. Doherty, B.A. Connolly and A.F. Worrall, *Gene*, **1993**, *136*, 337–340
57. J.A. Gerlt and P.C. Babbitt, *Curr. Opin. Mol. Biol*., **1998**,*2*, 607-612
58. I. Mulako, J.M. Farrant, H. Collett and N. Illing, *J. Exp. Bot.*, **2008**, *59*, 3885-3901

59. A.D.Cameron, B. Olin, M. Ridderström, B. Mannervik and T.A. Jones, *EMBO J.*, **1997**, *16*, 3386-3395

60. P. He and G.R. Moran, *J. Inorg. Biochem.*, **2011**, *105*, 1259-1272

Chapter 6
Biological Evaluation of Synthetic Conjugates

6.1 Naphthoquinone Conjugates

As noted previously, completion of the synthesis of the naphthoquinone conjugates was not achieved within the time-frame of this study, and since the advanced intermediates bearing a structural resemblance to the designed target molecules were also not obtained, evaluation of the inhibitory/subversive substrate activity of this class of molecules against Mtr or one of the other mycothiol enzymes was not possible.

6.2 Carbazole Quinone Conjugates

The successful synthesis of the carbazole quinone conjugates afforded three target molecules for biological evaluation. Through a collaboration with Prof Hans-Joachim Knölker (TU Dresden, Germany) the compounds were analysed for their anti-tuberculosis activity using the same assays applied to the parent carbazole quinone derivatives as reported in a published study,[1] with assays being performed in the lab of Prof Scott Franzblau (Institute for Tuberculosis Research, University of Illinois at Chicago). Activity was evaluated against *M. tuberculosis* strain H37Rv in *in vitro* assays to determine minimum inhibitory concentration (MIC) using the microplate alamar blue assay (MABA).[2,3,4] Conjugates **3.35**, **3.36** and **3.37** were tested and found to be inactive, with MIC values >128 μm (see Table 1), and with Rifampicin used as a positive control.

Table 1. Anti-TB Results obtained from MABA assay

Compound code	Structure	MABA Results
3.35	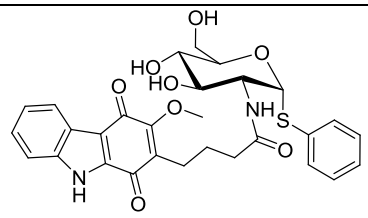	>128 μM
3.36	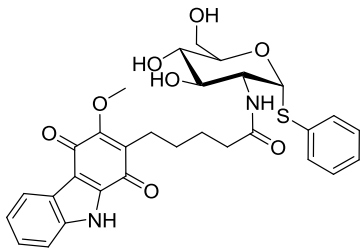	>128 μM
3.37	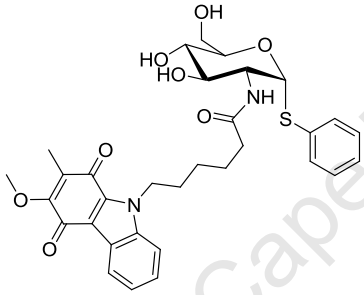	>128 μM
3.9[†]	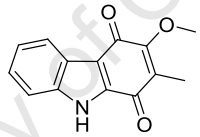	9 μM

[†] Prepared and assayed in a prior study by Knölker and co-workers[1]

The results suggest that addition of the linker and phenylthioglucosamine unit to the carbazole quinone **3.9** significantly reduces the anti-TB activity of the parent carbazole quinone. This is consistent with the earlier findings of Knölker *et al.* that further substitution of the carbazole-quinone nucleus tends to dampen the anti-TB activity. While the mechanism of action of the carbazole-1,4-quinones is not known, these results seem to disprove our initial hypothesis, that they may target enzymes involved in the mycothiol biosynthetic pathway, or be subversive substrates for the enzyme Mtr and therefore that coupling to substrate mimics in this pathway may deliver them to their target. However, it remained important to test the compounds for inhibitory activity against the enzymes, or for activity as subversive substrates of Mtr. The low activity of the Mtr prepared during this study necessitated finding alternative assays, and samples were submitted to the group of Dr Chris Hamilton (University of East Anglia, UK). Unforeseen problems in his lab have delayed the assays, and the results are not available at this time. In addition, it was decided to evaluate the conjugates as inhibitors of the MSH biosynthetic enzyme, MshB, since

similar plumbagin-derived analogues (described in Chapter 2 and prepared in a previous study)[5] displayed good activity against the enzyme. The compounds were submitted to the group of Prof Trevor Sewell at the University of Cape Town but similar delays have been encountered, with results of these assays not yet available.

6.3 Discussion and Conclusion

Although the enzyme assay results were not obtained within the timeframe of the project, the valuable anti-TB results provided a useful indication of the likelihood of this class of inhibitors eventually being developed into active pharmaceutical agents. It appears that addition of the elaborate substituents on either the nitrogen or C-3 of the carbazole-quinone shuts down the anti-TB activity, while the effect on the enzyme-inhibitory activity is yet to be determined. Since the carbazole quinone **3.9** displayed the best activity in the assay, it is clear that further systematic study of the structure-activity of analogues of this needs to be carried out, and is indeed under investigation in on-going studies. Some possible variations in the structure of the conjugate in relation to the carbohydrate and linker functionalities are as suggested at the end of Chapters 2 and 3.

References

1. T.A. Choi, R. Czerwonka, W. Fröhner, M.P. Krahl, K.R. Reddy, S.G. Franzblau and H.-J. Knölker, *ChemMedChem*, **2006**, *1*, 812-815
2. K. Falzari, Z. Zhu, D. Pan, H. Liu, P. Hongmanee and S.G. Franzblau, *Antimicrob. Agents Chemother.*, **2005**, *49*, 1447-1454
3. G.F. Pauli, R.J. Case, T. Inui, Y. Wang, S. Cho, N.H. Fischer and S.G. Franzblau, *Life Sci*., **2005**, *78*, 485-494
4. L.A. Collins and S.G. Franzblau, *Antimicrob. Agents Chemother*., **1997**, *41*, 1004-1009
5. D.W. Gammon, D.J. Steenkamp, V. Mavumengwana, M.J. Marakalala, T.T. Mudzunga, R. Hunter and M. Munyololo, *Bioorg. Med. Chem.*, **2010**, *18*, 2501-2514

Chapter 7
Experimental

7.1 General

All commercial chemicals were purchased from Merck (South Africa) or Sigma-Aldrich. All solvents were freshly distilled and dried by appropriate techniques with the exception of analytical grade absolute ethanol (EtOH), methanol, methylene chloride and acetone. Reactions were monitored by thin layer chromatography (TLC) using Merck F254 silica gel plates and were visualised by ultraviolet light or staining with acidic ethanolic solutions of anisaldehyde, ceric ammonium sulfate or ninhydrin, or ferric chloride ethanol/water. Silica gel chromatography was performed using Merck silicagel 60. Automated flash chromatography was performed on a Biotage Isolera system, using prepacked columns, or in the case of the carbazole quinone derivatives, on a Buchi Sepacore flash chromatography system using self-packed silica gel columns. Melting points were determined on a Reichert-Jung Thermovar hot-stage microscope and are uncorrected. Infrared spectra were recorded on a Perkin-Elmer Spectrum 100 FT-IR spectrometer in the range 4000 – 600 cm^{-1} using thin films of compound on NaCl disks. Microanalyses were determined using a Fisons EA 1108 CHNS-O instrument. GC/MS results for the carbazole quinone derivatives were obtained using an Agilent 6890N GC/5973N MSD gas chromatography/mass spectrometry system. HRMS data were obtained using a Waters Synapt G2 with direct injection (1 µl) into a stream into a stream of 80% acetonitrile, 0.1% formic acid using a Waters UPLC at flow rate of 0.1ml/min. Source: Electrospray positive/negative, Capillary voltage 3 kV, Cone Voltage 25 V. ^{1}H, ^{13}C and 2D NMR spectra were recorded on a Varian Mercury 300 MHz Spectrometer, a Varian Unity 400 MHz Spectrometer or a Bruker Advance III with Ultra Shield 400 Plus magnet. In the case of the carbazole quinone derivatives, ^{1}H, ^{13}C and 2D spectra were recorded on an Avance 300 or 400 MHz, or DRX-500 spectrometer. All spectra were recorded in deuterochloroform, deuterodimethylsulfoxide, deuteroacetone, deuteromethanol or deuterium oxide. All chemical shifts were recorded in ppm with reference to TMS as internal standard.

The numbering scheme given for each compound is for assignment purposes only and not necessarily consistent with the IUPAC naming convention used in the title. ^{1}H NMR spectra

are provided as mark of purity, in accordance with Journal of Organic Chemistry Guidelines for Authors,[1] and are attached in the appendix.

7.2 Synthesis of the Glucosamine-Derived Thioglycoside

Trifluoromethanesulfonyl azide, 2.2

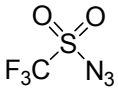

Sodium azide (39.00 g; 600 mmol) was dissolved in water (100 ml) before toluene (100 ml) was added and the mixture stirred at 0 °C. Triflic anhydride (40 ml; 238 mmol) was added drop-wise and stirring continued for 30 min, after which the temperature was raised to 10 °C and the biphasic mixture stirred for a further 2 h. Saturated $NaHCO_3$ was added until effervescence ceased. The organic phase was separated and the aqueous phase extracted with toluene (2 x 50 ml). The extracts were combined to form the stock solution of triflic azide (maximum possible concentration ~ 1.15 M). Note: this reagent is shock-sensitive and should be handled with care.

1,3,4,6-Tetra-O-acetyl-2-azido-2-deoxy-β-D-glucopyranoside,[2,3] 2.5

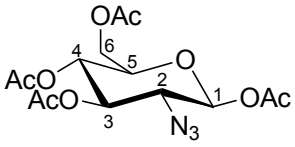

Protocol adapted from a reported procedure.[4] Glucosamine hydrochloride (30.00 g; 139 mmol), $NaHCO_3$ (46.71 g; 556 mmol) and $CuSO_4.5H_2O$ (1.40 g; 5.6 mmol) were dissolved in H_2O (92.4 ml). Triflic azide **2.2** stock solution (157 ml) was added, followed by the addition of MeOH (609.5 ml) to yield a homogeneous mixture that was stirred at room temperature for 15 h. Over the course of the reaction, the colour of the solution changed from blue to green. The solvents were removed under reduced pressure, and the residue left to dry on a high vacuum pump for 3 days. The residue was then dissolved in dry pyridine (100 ml) and cooled to 0 °C. Acetic anhydride (100 ml) was added drop-wise to the solution, which was stirred for 30 min at 0 °C before being warmed to room temperature and left to stir for a further 17 h until complete consumption of the starting material. The solvents were removed under reduced pressure, and the crude residue dissolved in EtOAc (1 L) and washed with H_2O (2 x 500 ml). The aqueous fractions were extracted with EtOAc (2 x 500 ml), and the combined organic fractions were dried (Na_2SO_4) and reduced under reduced pressure. The syrupy residue was purified by column chromatography (silica gel, eluting in

EtOAc:petroleum ether, 3:7) to obtain the product as a white precipitate of α/β isomers (46.28 g; 124 mmol; 89 %). The β isomer was obtained by recrystallisation of the purified product mixture in EtOAc/Pet Ether and used for analysis. R_f (EtOAc:Petroleum Ether, 3:7) 0.25; m.p. 93-94 °C (β-isomer); lit.[5] m.p. 96-97 °C; IR (NaCl, dry film) v_{max} (cm^{-1}): 2115 (N_3), 1756 (C=O).

^{1}H NMR (300 MHz, $CDCl_3$) β-isomer: δ 5.55 (d, *J* = 8.6, 1H, H_1), 5.06 (m, 2H, H_3, H_4), 4.29 (dd, *J* = 4.6, 12.5, 1H, H_{6a}), 4.08 (dd, *J* = 2.2, 12.5, 1H, H_{6b}), 3.83 – 3.77 (m, 1H, H_5), 3.70 – 3.61 (m, 1H, H_2), 2.18 (s, 3H, CH_3), 2.08 (s, 3H, CH_3), 2.06 (s, 3H, CH_3), 2.01 (s, 3H, CH_3).

^{13}C NMR (75 MHz, $CDCl_3$) β-isomer: δ 170.5 (C=O), 169.7 (C=O), 169.6 (C=O), 168.5 (C=O), 92.6, 72.8, 72.7, 67.8, 62.6, 61.4, 20.8 (CH_3), 20.6 (CH_3), 20.6 (CH_3), 20.5 (CH_3).

Anal. Calcd for $C_{14}H_{19}N_3O_9$: C, 45.04; H, 5.13; N, 11.26. Found: C, 45.33; H, 5.26; N, 10.91.

Phenyl 3,4,6-Tri-O-acetyl-2-azido-2-deoxy-1-thio-α-D-glucopyranoside,[6] 2.6a

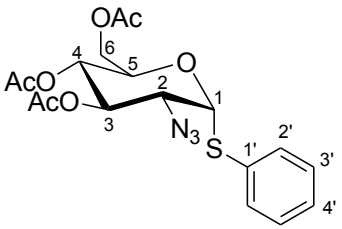

1,3,4,6-Tetra-*O*-acetyl-2-azido-2-deoxy-D-glucopyranoside **2.5** (10.003 g; 26.80 mmol) was dissolved in dry CH_2Cl_2 (40 ml) and cooled to 0 °C. To this solution, $BF_3.OEt_2$ (15.28 ml; 120.60 mmol) was added drop-wise and the solution left stirring for 30 minutes to form the oxocarbenium ion intermediate. Thiophenol (4.13 ml; 40.20 mmol) was then added drop-wise and the solution allowed to warm to room temperature, before the temperature was increased and the solution refluxed for 14 hours until the reaction was complete (determined by TLC). After cooling to room temperature, crushed ice was added and the reaction mixture extracted with CH_2Cl_2 (2 x 150 ml). The CH_2Cl_2 extract was washed with water (150 ml), dried (Na_2SO_4), and purified by column chromatography (EtOAc:Pet Ether, 2:8) to yield the product as a mixture of isomers (9.029 g; 21.32 mmol; 80 %). Pure crops of the α-thioglycoside were isolated by crystallisation from EtOH and obtained as white needles (5.185 g; 12.24 mmol; 46 %), however, further separation of the isomers was not possible and the mother liquor remained as a mixture. R_f (EtOAc:Pet Ether, 3:7) 0.45; m.p. 93-95 °C; IR (NaCl, dry film) v_{max} (cm^{-1}): 3440, 2111 (N_3), 1750 (C=O).

^{1}H NMR (400 MHz, $CDCl_3$) δ 7.45 – 7.40 (m, 2H, Ph), 7.28 – 7.21 (m, 3H, Ph), 5.56 (d, *J* = 5.6, 1H, H_1), 5.26 (dd, *J* = 9.2, 10.6, 1H, H_3), 4.96 (dd, *J* = 9.2, 10.3, 1H, H_4), 4.52 (ddd, *J* = 2.2, 5.0, 10.3, 1H, H_5), 4.21 (dd, *J* = 5.2, 12.4, 1H, H_{6a}), 3.99 (dd, *J* = 5.6, 10.6, 1H, H_2), 3.96 (dd, *J* = 2.3, 12.3, 1H, H_{6b}), 2.02 (s, 3H, CH_3), 1.98 (s, 3H, CH_3), 1.95 (s, 3H, CH_3).

^{13}C NMR (101 MHz, CDCl3) δ 170.4 (C=O), 169.7 (2 x C=O), 132.5 ($C_{1'}$), 132.2 (2 x $C_{2'3'}$), 129.2 (2 x $C_{2'3'}$), 128.1 ($C_{4'}$), 86.6 (C_1), 72.1 (C_3), 68.9 (C_4), 68.6 (C_5), 62.0 (C_6), 61.7 (C_2), 20.6 (2 x CH_3), 20.6 (CH_3).

EI-MS *m/z*: Calcd for $C_{18}H_{21}N_3O_7S$, 423.11; Found 423.06 [M].

Anal.Calcd for $C_{18}H_{21}N_3O_7S$: C, 51.06; H, 5.00; N, 9.92; S, 7.57. Found: C, 52.08; H, 5.07; N, 9.78; S, 7.56.

Phenyl 3,4,6-Tri-O-acetyl-2-amino-2-deoxy-1-thio-α-D-glucopyranoside, 2.7

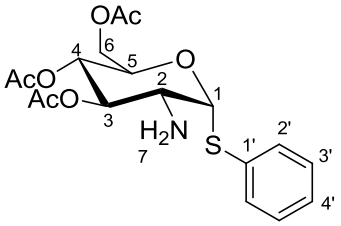

Ethanol (50 ml) was added to a round-bottomed flask, followed by 10 wt % palladium on carbon (0.499 g). The walls of the flask were washed with a further 250 ml of ethanol to ensure full wetting of the palladium. Phenyl 3,4,6-tri-*O*-acetyl-2-azido-2-deoxy-1-thio-D-glucopyranoside **2.4** (4.751 g; 11.22 mmol) was dissolved in this mixture before the flask was subjected to successive purging and filling with hydrogen. The flask was then fitted with a hydrogen-filled balloon, and the mixture stirred for 16 h at room temperature until complete consumption of the starting material. The mixture was then filtered through a celite plug, evaporated to dryness, and the residue purified by silica gel chromatography (eluting in EtOAc:petroleum ether, 6:4). The purified product was then crystallised from EtOAc/Pet Ether and obtained as colourless needles (3.368 g; 8.47 mmol; 75 %). R_f (EtOAc/Petroleum Ether, 6:4) 0.40; m.p. 83-85 °C; IR (NaCl, dry film) v_{max} (cm^{-1}): 3392 (NH), 1742 (C=O), 1632 (C=C).

Alternate synthesis:

Pd/C (10 wt %; 125 mg) was added to a round-bottomed flask before the sides of the flask were washed down with Et_2O (5 ml). **2.4** (500 mg; 1.181 mmol) was added to the suspension, and the atmosphere of the flask flushed with H_2 gas. The solution was stirred at room temperature under a H_2 atmosphere (provided by a balloon) for 24 h. The mixture was filtered through a plug of Celite and the solvent removed at room temperature under reduced pressure. The product (482 mg; 1.212 mmol) was obtained in quantitative yield as a syrup, which was then crystallised from EtOAc/Pet Ether and obtained as colourless needles.

^{1}H NMR (300 MHz, CDCl3) δ 7.60 – 7.43 (m, 2H, Ph), 7.38 – 7.20 (m, 3H, Ph), 5.56 (d, *J* = 5.2, 1H, H_1), 5.10 – 4.95 (m, 2H, H_3, H_4), 4.56 (ddd, *J* = 2.2, 5.0, 9.7, 1H, H_5), 4.32 (dd, *J* = 5.1, 12.3, 1H, H_{6a}), 4.07 (dd, *J* = 2.3, 12.3, 1H, H_{6b}), 3.32 (dd, *J* = 5.2, 10.2, 1H, H_2), 2.09 (s, 3H, CH_3), 2.04 (s, 6H, 2 x CH_3).

^{13}C NMR (75 MHz, CDCl3) δ 170.7 (C=O), 170.6 (C=O), 169.8 (C=O), 133.5 ($C_{1'}$), 131.9 (2C, $C_{2'}$), 129.1 (2C, $C_{3'}$), 127.8 ($C_{4'}$), 91.3 (C_1), 74.7 (C_3), 69.0 (2C, C_4C_5), 62.3 (C_6), 55.2 (C_2), 20.8 (CH_3), 20.7 (2 x CH_3).

EI-MS *m/z*: [M^+] Calcd for $C_{18}H_{23}NO_7S$, 397.12; Found 397.14

HRMS (ESI-TOF): Calcd for $C_{18}H_{23}NO_7S$, 397.1195; Found 398.1265 [M+H], 420.1087 [M+Na].

7.3 Attempts Toward the Synthesis of a Glycerol Glycoside

3,4,6-Tri-O-acetyl-2-azido-2-deoxy-α/β-D-glucopyranose,[7] 2.18

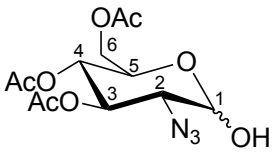

Using a method adapted from Zhang and Kováč,[8] glacial acetic acid (1.50 ml; 26.03 mmol) was added drop-wise to a stirring solution of ethylene diamine (1.50 ml; 22.31 mmol) in THF (400 ml) at 0 °C. A solution of 1,3,4,6-tetra-*O*-acetyl-2-azido-2-deoxy-α/β-D-glucopyranose **2.5** (6.942 g; 18.595 mmol) in THF (64 ml) was added drop-wise to the protonated ethylene diamine solution, and the reaction continued for 24 h. Upon consumption of the starting material (as indicated by TLC), water (200 ml) was added and the product extracted into

CH_2Cl_2. The organic layer was washed sequentially with 1 M HCl (3x 100 ml), saturated aqueous $NaHCO_3$ (2 x 100 ml) and brine (100 ml), and dried (Na_2SO_4). The solvent was removed under reduced pressure and the crude syrup purified by silica gel chromatography (EtOAc:hexane, 3:7 – 1:1) to afford the product (6.2045 g) in quantitative yield as an inseparable mixture of anomers (α:β = 1.59:1 by ^{1}H NMR) and as a colourless syrup. R_f (EtOAc:hexane, 4:6) 0.18.

α Anomer:
^{1}H NMR (400 MHz, $CDCl_3$) δ 5.50 (dd, *J* = 10.5, 9.3 Hz, 1H, H_3), 5.37 (d, *J* = 3.4 Hz, 1H, H_1), 5.07 – 5.01 (m, 1H, H_4), 4.32 – 4.18 (m, 2H, H_5, H_{6a}), 4.16 – 4.07 (m, 2H, H_{6b}), 3.93 (bs, 1H, OH), 3.41 (dd, *J* = 10.5, 3.4 Hz, 1H, H_2), 2.07 (s, 3H, C*H*$_3$COO), 2.07 (s, 3H, C*H*$_3$COO), 2.02 (s, 3H, C*H*$_3$COO).

^{13}C NMR (101 MHz, $CDCl_3$) δ 171.0 (C=O), 170.2 (C=O), 169.9 (C=O), 92.1 (C_1), 70.6 (C_3), 68.7 (C_4), 67.6 (C_5), 62.1 (C_6), 61.6 (C_2), 20.7 (2C, 2 x *C*H$_3$COO), 20.6 (*C*H$_3$COO).

β Anomer:
^{1}H NMR (400 MHz, $CDCl_3$) δ 5.01 – 4.96 (m, 2H, H_3, H_4), 4.71 (d, *J* = 8.0 Hz, 1H, H_1), 4.42 (bs, 1H, OH), 4.32 – 4.18 (m, 1H, H_{6a}), 4.16 – 4.07 (m, 1H, H_{6b}), 3.74 – 3.65 (m, 1H, H_5), 3.51 – 3.43 (m, 1H, H_2), 2.07 (s, 3H, C*H*$_3$COO), 2.07 (s, 3H, C*H*$_3$COO), 2.00 (s, 3H, C*H*$_3$COO).

^{13}C NMR (101 MHz, $CDCl_3$) δ 171.0 (C=O), 170.2 (C=O), 169.9 (C=O), 96.3 (C_1), 72.7 (C_3 or C_4), 72.0 (C_5), 68.5 (C_4 or C_3), 65.0 (C_2), 62.1 (C_6), 20.7 (2C, 2 x *C*H$_3$COO), 20.6 (*C*H$_3$COO).

HRMS (ESI-TOF): Calcd for $C_{12}H_{17}N_3O_8$, 331.1016; Found 354.0909 [M+Na].

3,4,6-Tri-O-acetyl-2-azido-2-deoxy-α/β-D-glucopyranosyl trichloroacetimidate, 2.19

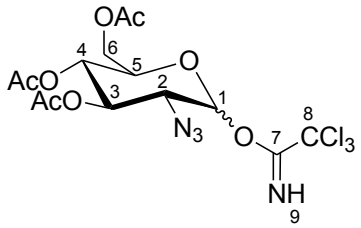

A suspension of 3,4,6-tri-*O*-acetyl-2-azido-2-deoxy-α/β-D-glucopyranose **2.18** (1.50 g; 4.53 mmol) and furnace-dried K_2CO_3 (2.56 g; 18.52 mmol) in anhydrous CH_2Cl_2 (15 ml) was stirred at r.t. before trichloroacetonitrile (2.31 ml; 3.26 g; 22.58 mmol) was added and the

mixture stirred for 2 h. Upon completion of the reaction, as determined by TLC, the reaction mixture was diluted with CH_2Cl_2, filtered through a plug of celite, and concentrated. The oily residue was purified by automated flash chromatography (EtOAc:hexane, 3:7 – 4:6) to afford the product (1.64 g; 3.45 mmol) as a mixture of anomers in 76 % yield. R_f (EtOAc:hexane, 4:6) 0.77.

α-Anomer:

^{1}H NMR (400 MHz, $CDCl_3$) δ 8.81 (s, 1H, H_9), 6.47 (d, *J* = 3.6 Hz, 1H, H_1), 5.49 (dd, *J* = 10.5, 9.4 Hz, 1H, H_3), 5.12 (dd, *J* = 10.2, 9.4 Hz, 1H, H_4), 4.25 (dd, *J* = 12.2, 4.3 Hz, 1H, H_{6a}), 4.19 (ddd, *J* = 10.3, 4.4, 2.0 Hz, 1H, H_5), 4.08 (dd, *J* = 12.2, 2.1 Hz, 1H, H_{6b}), 3.75 (dd, *J* = 10.5, 3.6 Hz, 1H, H_2), 2.08 (s, 3H, C*H*$_3$COO), 2.03 (s, 3H, C*H*$_3$COO), 2.03 (s, 3H, C*H*$_3$COO).

^{13}C NMR (101 MHz, $CDCl_3$) δ 170.4 (C=O), 169.8 (C=O), 169.6 (C=O), 160.6 (C_7), 94.0 (C_1), 90.5 (C_8), 70.7 (C_5), 70.2 (C_3), 68.0 (C_4), 61.4 (C_6), 60.7 (C_2), 20.6 (*C*H$_3$COO), 20.6 (*C*H$_3$COO), 20.5 (*C*H$_3$COO).

β-Anomer:

^{1}H NMR (400 MHz, $CDCl_3$) δ 8.78 (s, 1H, H_9), 5.69 (d, *J* = 8.4 Hz, 1H, H_1), 5.12 – 5.03 (m, 2H, H_3, H_4), 4.28 (dd, *J* = 12.5, 4.5 Hz, 1H, H_{6a}), 4.09 (dd, *J* = 12.9, 2.8 Hz, 1H, H_{6b}), 3.83 – 3.76 (m, 1H, H_5), 3.77 (dd, *J* = 9.9, 8.5 Hz, 1H, H_2), 2.06 (s, 3H, C*H*$_3$COO), 2.03 (s, 3H, C*H*$_3$COO), 1.99 (s, 3H, C*H*$_3$COO).

^{13}C NMR (101 MHz, $CDCl_3$) δ 170.5 (C=O), 169.8 (C=O), 169.5 (C=O), 160.7 (C_7), 96.4 (C_1), 90.2 (C_8), 72.7 (C_3 or C_5), 72.7 (C_5 or C_3), 68.0 (C_4), 63.3 (C_2), 61.5 (C_6), 20.6 (*C*H$_3$COO), 20.6 (*C*H$_3$COO), 20.5 (*C*H$_3$COO).

Attempt to Convert the Protecting Groups of 5.28 From Acetates to Benzyl Ethers

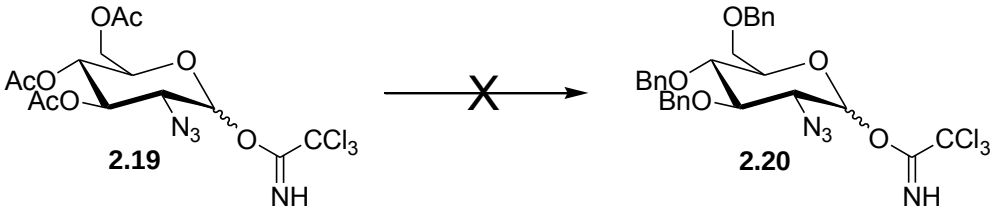

A suspension of **2.19** (662 mg, 1.39 mmol), TBAI (100 mg; 0.27 mmol) and powdered NaOH (757 mg; 18.92 mmol) in THF (12 ml) was stirred for 30 min at r.t. before BnBr (2.206 g; 3.17 ml; 12.9 mmol) was added and the mixture stirred for an additional 1 h. At this stage it was

clear that decomposition was taken place (based on TLC analysis) and the reaction was not continued.

Glycosylation Attempts with Trichloroacetimidate 2.28

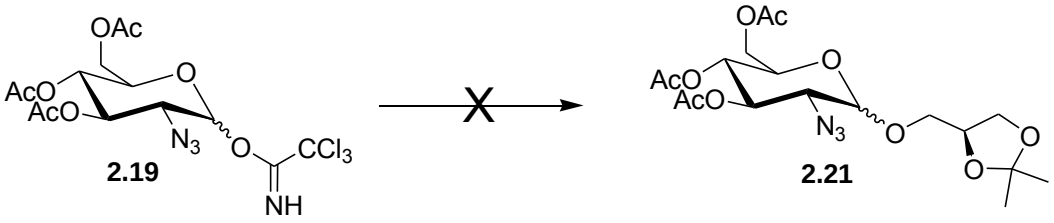

i) A solution of **2.19** (75 mg; 0.157 mmol), isopropylidene glycerol **2.15** (14.5 mg; 0.110 mmol) and TMSOTf (2.9 mg; 23 µl; 0.129 mmol)) in anhydrous Et_2O (5 ml) was stirred at r.t. for 1h15min, by which time there was no discernible reaction product (as determined by TLC).

ii) A solution of **2.19** (602 mg; 1.274 mmol) and **2.15** (811 mg; 6.137 mmol) in anhydrous CH_2Cl_2 (10 ml) containing furnace-dried 4 Å powdered molecular sieves was stirred under nitrogen at 0 °C before a 46.5% solution of BF_3 in Et_2O (2.089 ml; 6.128 mmol) was added. The reaction was continued for 3 h by which stage the starting material had been consumed (according to TLC). The reaction was quenched by the addition of solid $NaHCO_3$ and then filtered through a plug of Celite. After concentration under reduced pressure, the residue was purified by automated flash chromatography (MeOH:CH_2Cl_2, 1:20 – 1:4) to afford a pure fraction of the product, which was subsequently analysed by ^{1}H NMR spectroscopy and found to be the starting material 3,4,6-tri-*O*-acetyl-2-azido-2-deoxy-α/β-D-glucopyranose **2.18**.

3,4,6-Tri-O-acetyl-2-azido-2-deoxy-α/β-D-glucopyranosyl fluoride,[9] 2.30

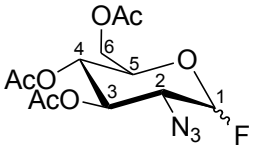

Using a protocol adapted from Posner and Haines,[10] a solution of 3,4,6-tri-O-acetyl-2-azido-2-deoxy-α/β-D-glucopyranose **2.18** (0.8953 g; 2.702 mmol) in anhydrous THF (20 ml) under argon was cooled to 0 °C before diethylaminosulfur trifluoride (DAST) (1.00 ml; 8.106 mmol) was added drop-wise over a period of 5 minutes. The solution was allowed to warm to room temperature and gradually turned yellow with time. After 45 min the starting material had

been consumed (according to TLC) and MeOH (1 ml) was added to quench the DAST. After removal of the solvents under reduced pressure, the residue was purified by silica gel chromatography (eluting in EtOAc:hexane, 2:8 – 4:6) to afford the glycosyl fluoride (768 mg; 2.304 mmol) as an inseparable mixture of anomers (α:β = 1:2.2 by ^{1}H NMR) and as a colourless syrup in 85 % yield. R_f (EtOAc:hexane, 4:6) 0.39.

α-Anomer: ^{1}H NMR (400 MHz, $CDCl_3$) δ 5.72 (dd, *J* = 51.9, 2.7 Hz, 1H, H_1), 5.45 (dd, *J* = 10.5, 9.4 Hz, 1H, H_3), 5.10 (t, *J* = 9.72 Hz, 1H, H_4), 4.31 (dd, *J* = 11.8, 3.6 Hz, 1H, H_{6a}), 4.23 – 4.20 (m, 1H, H_5), 4.14 (dd, *J* = 12.5, 2.2 Hz, 1H, H_{6b}), 3.51 (ddd, *J* = 25.5, 10.5, 2.7 Hz, 1H, H_2), 2.10 (s, 3H, C*H*$_3$COO), 2.09 (s, 3H, C*H*$_3$COO), 2.05 (s, 3H, C*H*$_3$COO).

β-Anomer: ^{1}H NMR (400 MHz, $CDCl_3$) δ 5.14 (dd, *J* = 51.5, 7.3 Hz, 1H, H_1), 5.12 – 5.03 (m, 2H, H_3, H_4), 4.28 (dd, *J* = 11.8, 4.5 Hz, 1H, H_{6a}), 4.18 (dd, *J* = 12.1, 2.3 Hz, 1H, H_{6b}), 3.85 – 3.76 (m, 1H, H_5), 3.71 – 3.61 (m, 1H, H_2), 2.10 (s, 3H, C*H*$_3$COO), 2.09 (s, 3H, C*H*$_3$COO), 2.03 (s, 3H, C*H*$_3$COO).

HRMS (ESI-TOF): Calcd for $C_{12}H_{16}FN_3O_7$, 333.0972; Found 356.0866 [M+Na].

Glycosylation Attempts with Glycosyl Fluoride

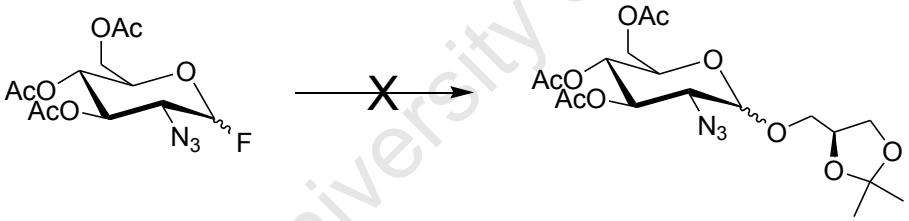

i) A solution of 3,4,6-tri-*O*-acetyl-2-azido-2-deoxy-α/β-D-glucopyranosyl fluoride **2.30** (67 mg; 0.201 mmol) and (S)-*O*-isopropylidene glycerol **2.15** (40 mg; 0.302 mmol) in anhydrous THF (3 ml) containing powdered, furnace-dried molecular sieves (4 Å) was stirred under argon at room temperature for 30 min (to ensure anhydrous conditions) before $BF_3.OEt_2$ (29 mg; 25 µl; 0.201 mmol) was added drop-wise. Stirring was continued for 2 h, by which stage no product spot was visible by TLC. Consequently, additional $BF_3.OEt_2$ (0.1 ml; 4 equiv.) was added. The reaction was left to stir overnight, but there was still no evidence for formation of any product. Consequently the reaction was quenched with Et_3N (1 ml), filtered through Celite and extracted into EtOAc. The work up yielded the unreacted starting material.

ii) A solution of 3,4,6-tri-*O*-acetyl-2-azido-2-deoxy-α/β-D-glucopyranosyl fluoride **2.30** (254 mg; 0.762 mmol) and **2.15** (67 mg; 0.508 mmol) in anhydrous THF (6 ml) containing powdered, furnace-dried molecular sieves (4 Å) was stirred under argon at room temperature for 30 min (to ensure anhydrous conditions) before $BF_3.OEt_2$ (433 mg; 368 µl; 3.049 mmol) was added drop-wise. Stirring was continued for a further 2 hours by which stage the colour had changed from light yellow to colourless. No product was detectable by TLC, and the temperature was then raised to 40 °C. After 2.5 h at this temperature there was still no product evident from TLC, and the temperature was raised further to 50 °C and stirring continued overnight. The starting material appeared to have been consumed (TLC), and the reaction was thus quenched with Et_3N (0.4 ml), filtered though Celite, extracted into EtOAc and then washed sequentially with saturated aqueous $NaHCO_3$ (2 x 30 ml), saturated aqueous NH_4Cl (2 x 30 ml) and brine. After drying (Na_2SO_4) and removal of the solvent under reduced pressure, the residue was purified by silica gel chromatography (eluting in MeOH:CH_2Cl_2, 0:100 – 5:95). The chromatography yielded a thick colourless gel, which after ^{1}H NMR analysis, was found to be polymerised THF (only two signals were present: a multiplet at 3.40 ppm and one at 1.60 ppm).

iii) Change of solvent to CH_2Cl_2: A solution of 3,4,6-tri-*O*-acetyl-2-azido-2-deoxy-α/β-D-glucopyranosyl fluoride **2.30** (71 mg; 0.213 mmol) and **2.15** (29 mg; 0.219 mmol) in anhydrous CH_2Cl_2 (5 ml) containing powdered, furnace-dried molecular sieves (4 Å) was stirred under argon at room temperature for 30 min (to ensure anhydrous conditions) before $BF_3.OEt_2$ (120 mg; 0.l0 ml; 0.852 mmol) was added drop-wise and the solution stirred at r.t. The solution turned from colourless to light orange after 20 min. After 5 h the reaction was incomplete, therefore additional (S)-*O*-isopropylidene glycerol (2 drops) was added. The starting material was consumed after 22 h (by TLC) and the TLC evidence for a more polar product was noted (R_f 0.18 vs. R_f 0.38 for the glycosyl fluoride). The reaction was quenched by the addition of Et_3N (0.4 ml) and stirred for 5 min. After filtration through a plug of Celite, the reaction product was extracted into EtOAc, washed successively with saturated aqueous $NaHCO_3$ (2 x 30 ml), saturated aqueous NH_4Cl (30 ml) and brine (30 ml), and dried (Na_2SO_4). The solvent was removed under reduced pressure and the residue purified by silica gel chromatography (eluting in EtOAc:hexane, 4:6). A pure fraction (20 mg) of the reaction product was isolated and characterised (^{1}H and ^{13}C NMR spectroscopy) and shown to be 3,4,6-tri-*O*-acetyl-2-azido-2-deoxy-α/β-D-glucopyranose **2.18**, in the ratio α:β = 2:1 (by ^{1}H NMR). R_f (EtOAc:hexane, 4:6) 0.18.

iv) Change of solvent to Et_2O: An anhydrous Et_2O (10 ml; dried over CaH_2) solution of 3,4,6-tri-*O*-acetyl-2-azido-2-deoxy-α/β-D-glucopyranosyl fluoride **2.30** (140 mg; 0.420 mmol) and **2.15** (94 mg; 0.711 mmol) containing furnace-dried molecular sieves was stirred under argon at room temperature for 30 minutes before $BF_3.OEt_2$ (144 mg; 129 µl; 1.26 mmol) was added drop-wise and the solution stirred for 19 h. By this stage a considerable amount of starting material remained although a component with a lower R_f was visible below it on the TLC. The reaction was quenched by the addition of Et_3N (0.3 ml), and after stirring for 5 minutes was filtered through a plug of Celite and washed with EtOAc. The crude reaction mixture was washed successively with $NaHCO_3$ (2 x 30 ml), NH_4Cl (2 x 30 ml) and brine (30 ml), dried (Na_2SO_4) and solvent removed under reduced pressure. The residue was purified by silica gel chromatography (eluting in EtOAc:hexane, 4:6) to afford the starting material (63 mg; 45 %) as a mixture of inseparable anomers (α:β = 1.8:1, by ^1H NMR) and 3,4,6-tri-*O*-acetyl-2-azido-2-deoxy-α/β-D-glucopyranose **2.18** (33 mg; 0.100 mmol; 24 %) also as a mixture of inseparable anomers (α:β = 1.7:1, by ^1H NMR).

Glycosylation Attempts by Activation of a Phenyl-thioglycoside [11]

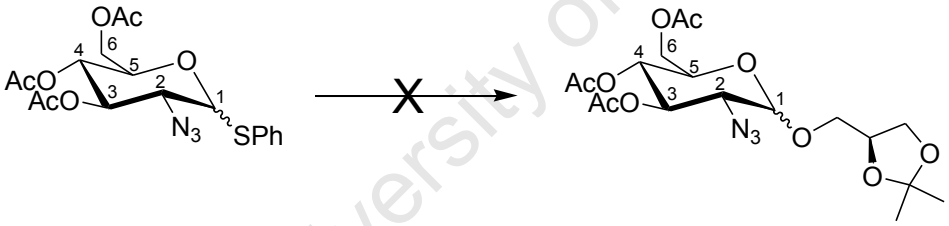

A mixture of the acetylated phenyl 3,4,6-tri-*O*-acetyl-2-azido-2-deoxy-1-thio-D-glucopyranoside **2.6** (112 mg; 0.265 mmol), NIS (119 mg; 0.529 mmol) and molecular sieves (4 Å) in anhydrous CH_2Cl_2 (20 ml) was cooled to -40 °C (acetonitrile/liq. N_2 slurry) under nitrogen before (*S*)-1,2-isopropylidene glycerol (52 mg; 0.397 mmol) was added. The mixture was stirred for 4 h whilst being allowed to warm to 0 °C, whereafter there was no detectable product (TLC), and the temperature was raised to 50 °C and the reaction left overnight. After this treatment, there was still no evidence for product formation, and the reaction was worked up and starting material recovered.

3,4,6-Tri-O-benzyl-2-azido-2-deoxy-α/β-D-glucopyranose, 2.34

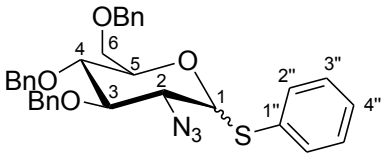

Using an adapted from a literature procedure,[12] a solution of phenyl 3,4,6-tri-O-acetyl-2-azido-2-deoxy-1-thio-D-glucopyranoside **2.6** (440 mg; 1.039 mmol; α:β = 1:9) in MeOH (10 ml) was cooled to 0 °C (ice bath) before a solution of 4.62 M NaOMe (0.07 ml; 0.312 mmol) in MeOH was added. The solution was allowed to warm to r.t. before being left to stir overnight (16 h). DOWEX (H^+ form) ion exchange resin was added and the mixture stirred for 10 min. The resin was removed by filtration and the solvent removed under reduced pressure, before the product mixture was purified by automated flash chromatography (MeOH:CH_2Cl_2, 0:100 – 1:4). The deacetylated phenyl 2-azido-2-deoxy-1-thio-D-glucopyranoside (297 mg; 0.999 mmol) was obtained in 96 % yield, and directly subjected to benzylation. Thus, a solution of the phenyl 2-azido-2-deoxy-1-thio-D-glucopyranoside (297 mg; 0.999 mmol), TBAI (74 mg; 0.200 mmol) and NaOH (544 mg;13.60 mmol) was stirred in THF (4 ml) for 30 min before BnBr (1.08 ml; 9.00 mmol) was added and the mixture stirred at r.t. for 2.5 h. Water was added and the product extracted into CH_2Cl_2. The organic layer was washed with water and dried (Na_2SO_4) before the solvent was removed under reduced pressure. The residue was purified by automated flash chromatography (EtOAc:hexane, 3:97 – 1:4) to obtain phenyl 3,4,6-tri-*O*-benzyl-2-azido-2-deoxy-1-thio-α/β-D-glucopyranose **2.34** (448 mg; 0.789 mmol; α:β = 1:9) in 79 % yield as a colourless syrup which solidified upon standing to form a white solid. R_f (EtOAc:hexane, 1:9) 0.37.

β Anomer (in agreement with reported characterisation)[13]

^{1}H NMR (400 MHz, $CDCl_3$) δ 7.64 – 7.59 (m, 2H), 7.39 – 7.18 (m, 18H), 4.87 (d, *J* = 10.6 Hz, 1H), 4.83 (d, *J* = 10.6 Hz, 1H), 4.80 (d, *J* = 11.0 Hz, 1H), 4.62 (d, *J* = 11.9 Hz, 2H), 4.60 (d, *J* = 10.9 Hz, 2H), 4.55 (d, *J* = 11.9 Hz, 1H), 4.43 (d, *J* = 10.1 Hz, 1H), 3.79 (dd, *J* = 11.0, 2.2 Hz, 1H), 3.74 (dd, *J* = 11.0, 4.0 Hz, 1H), 3.63 (t, *J* = 9.3 Hz, 1H), 3.52 (t, *J* = 9.1 Hz, 1H), 3.48 (ddd, *J* = 9.7, 4.0, 2.0 Hz, 1H), 3.35 (dd, *J* = 10.1, 9.3 Hz, 1H).

Literature: ^{1}H NMR (500 MHz, $CDCl_3$) δ 7.60 (m, 2H), 7.35-7.19 (m, 18H), 4.86 (d, *J* = 10.5, 1H), 4.83 (d, *J*= 10.5, 1H), 4.79 (d, *J*= 11.0, 1H), 4.62 (d, *J* = 12.0, 1H), 4.58 (d, *J*= 10.5, 1H), 4.54 (d, *J* = 12.0, 1H), 4.41 (d, *J* = 10.0, 1H), 3.78 (dd, *J* = 2.0, 11.0, 1H), 3.74 (dd, *J* = 4.0, 11.0, 1H), 3.61 (dd, *J* = 9.5, 9.5, 1H), 3.51 (dd, *J*= 9.5, 9.5, 1H), 3.47 (ddd, *J* = 2.0, 4.0, 9.5, 1H), 3.34 (dd, *J* = 9.5, 9.5, 1H).

HRMS (ESI-TOF): Calcd for $C_{33}H_{33}N_3O_4S$, 567.2192; Found 590.2092 [M+Na].

Glycosylation Attempt with Phenyl 3,4,6-tri-O-benzyl-2-azido-2-deoxy-1-thio-D-glucopyranoside (2.34) as Donor

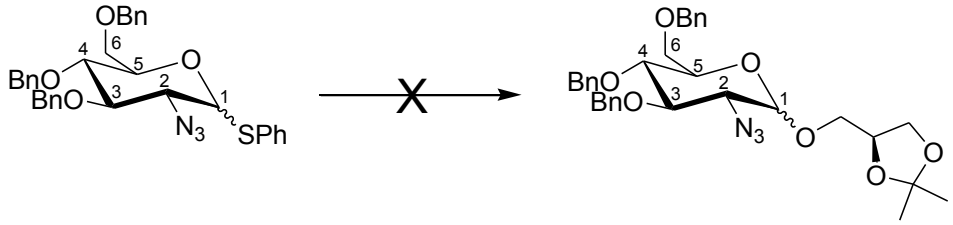

A mixture of **2.34** (235 mg; 0.414 mmol), NIS (186 mg;0.828 mmol) and furnace-dried molecular sieves (4 Å) was stirred under vacuum for 30 min before being suspended in anhydrous CH_2Cl_2 (3 ml) and anhydrous Et_2O (6 ml). The suspension was cooled to -30 °C (acetonitrile/liq N_2 slurry) and stirred for 30 min (to allow the molecular sieves to absorb any residual water), before a solution of (s)-isopropylidene glycerol (82 mg; 0.621 mmol) in anhydrous Et_2O (6 ml) was added drop-wise over 10 min (to generate a solution of 0.03 M concentration with respect to the glycoside donor). The solution was stirred under argon at between -40 and -30 °C for 1 h, then allowed to warm to 0 °C. After 2 h, no product was detectable by TLC, and the reaction was therefore allowed to warm to r.t. and was left stirring overnight. At this stage there was still no product detectable, and the reaction was worked up and starting material recovered.

7.4 General Procedure for Oxidative Decarboxylation and Coupling of Carboxylic acids to Naphthoquinones

The general synthesis is adapted from a reported procedure.[14] A degassed 100 ml solution of 30 % acetonitrile in water containing naphthoquinone (1 eq), carboxylic acid (5 eq) and $AgNO_3$ (0.3 eq) was stirred at 65 °C for 1 hr under an inert atmosphere (Ar or N_2). A second degassed solution of 30 % acetonitrile in water (50 ml) containing $(NH_4)_2S_2O_8$ (2.5 eq) under argon was added drop-wise to the first solution over a period of 2 h. The reaction was allowed to stir for a further 2 h, by which time maximum conversion of the starting materials to product had taken place. The reaction was removed from heat, evaporated under reduced pressure to remove the acetonitrile, and crude mixture partitioned between EtOAc and water. The water layer was washed with EtOAc (3 x 50 ml), and the combined organic fractions dried (Na_2SO_4), concentrated under reduced pressure, and purified by column

chromatography (silica gel). Unreacted naphthoquinone was recovered and used in subsequent reactions.

Benzyl (S)-2-(tert-butoxycarbonylamino)-3-(8-hydroxy-3-methyl-1,4-dioxo-1,4-dihydronaphthalen-2-yl)propanoate, 2.48

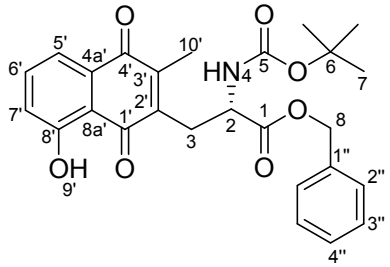

Compound **2.48** was prepared from plumbagin (379 mg; 2.13 mmol) and (*S*)-benzyl 2-(tert-butoxycarbonylamino)-3-(8-hydroxy-3-methyl-1,4-dioxo-1,4-dihydronaphthalen-2-yl)butanoate (3.263 g; 10.65 mmol) using the general procedure described above. Purification by column chromatography (silica gel, eluting in EtOAc:pentane, 2:8) provided **2.48** as an orange powder (355 mg; 0.763 mmol; 36 %). R_f (EtOAc:pentane, 2:8) 0.47; m.p. 139-142 °C; IR (NaCl, dry film) ν_{max} (cm^{-1}): 3435 (NH), 1744 (C=O), 1712 (C=O), 1660 (C=O), 1635 (C=C).

^{1}H NMR (500 MHz, $CDCl_3$) δ 12.01 (s, 1H, $H_{9'}$), 7.60 – 7.53 (m, 2H, $H_{5'}$, $H_{6'}$), 7.29 – 7.25 (m, 5H, $H_{2''}$, $H_{3''}$, $H_{4''}$), 7.20 (dd, *J* = 7.5, 1.6 Hz, 1H, $H_{7'}$), 5.27 (d, *J* = 7.7 Hz, 1H, H_4), 5.15 (d, *J* = 12.2 Hz, 1H, H_{8a}), 5.12 (d, *J* = 12.2 Hz, 1H, H_{8b}), 4.64 – 4.54 (m, 1H, H_2), 3.15 (dd, *J* = 12.9, 6.6 Hz, 1H, H_{3a}), 3.06 (dd, *J* = 12.9, 8.2 Hz, 1H, H_{3b}), 2.22 (s, 3H, $H_{10'}$), 1.35 (s, 9H, H_7).

^{13}C NMR (126 MHz, $CDCl_3$) δ 189.8 ($C_{1'}$), 184.0 ($C_{4'}$), 171.2 (C_1), 161.2 ($C_{8'}$), 155.0 (C_5), 147.0 ($C_{2'}$ or $C_{3'}$), 141.7 ($C_{3'}$ or $C_{2'}$), 136.0 ($C_{6'}$), 134.8 ($C_{1''}$), 132.1, 128.6 (2C, $C_{2''}$ or $C_{3''}$), 128.5 ($C_{4''}$), 128.2 (2C, $C_{3''}$ or $C_{2''}$), 123.9 ($C_{7'}$), 119.0 ($C_{5'}$), 114.7 ($C_{8a'}$), 80.2 (C_6), 67.5 (C_8), 52.7 (C_2), 30.1 (C_3), 28.2 (3C, C_7), 13.2 ($C_{10'}$).

HRMS (ESI-TOF): Calcd for $C_{26}H_{27}NO_7$, 465.1788; Found 465.1775 [M^+].

Benzyl (S)-2-(tert-butoxycarbonylamino)-4-(8-hydroxy-3-methyl-1,4-dioxo-1,4-dihydronaphthalen-2-yl)butanoate, 2.49

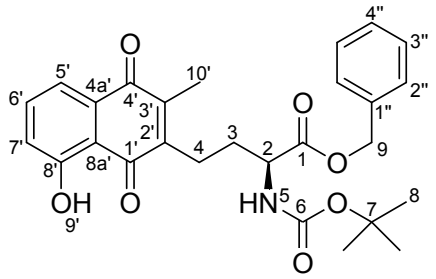

Compound **2.49** was prepared from plumbagin (300 mg; 1.59 mmol) and (*S*)-5-(benzyloxy)-4-(tert-butoxycarbonylamino)-5-oxopentanoic acid (2.192 g; 7.97 mmol) using the general procedure described above. Purification by column chromatography (silica gel, eluting in EtOAc:toluene, 5:95) provided **2.49** as an orange powder (390 mg; 0.813 mmol; 51%). R_f (EtOAc:toluene, 5:95) 0.19; m.p. 101-103 °C; IR (NaCl, dry film) v_{max} (cm^{-1}): 3401 (NH), 1740 (C=O),1716 (C=O), 1660 (C=O), 1632 (C=C).

^{1}H NMR (500 MHz, $CDCl_3$) δ 12.08 (s, 1H, $H_{9'}$), 7.58 (dd, *J* = 7.5, 1.4, 1H, $H_{5'}$), 7.54 (t, *J* = 7.8, 1H, $H_{6'}$), 7.40 – 7.30 (m, 5H, $H_{2''}$, $H_{3''}$, $H_{4''}$), 7.20 (dd, *J* = 8.1, 1.3, 1H, $H_{7'}$), 5.33 (bs, 1H, NH_5), 5.24 (d, *J* = 12.2, 1H, H_9), 5.16 (d, *J* = 12.2, 1H, H_9), 4.44 (bs, 1H, H_2), 2.68-2.58 (m, 2H, H_4), 2.08 (s, 3H, $H_{10'}$), 2.08 – 2.00 (m, 1H, H_3), 1.90 - 1.82 (m, 1H, H_3), 1.45 (s, 9H, H_8).

^{13}C NMR (126 MHz, $CDCl_3$) δ 189.6 ($C_{1'}$), 184.1 ($C_{4'}$), 171.9 (C_1), 161.2 ($C_{8'}$),155.3 (C_6), 145.5 ($C_{2'}$ or $C_{3'}$), 145.2 ($C_{3'}$ or $C_{2'}$), 136.0 ($C_{6'}$), 135.2 ($C_{1''}$), 132.0 ($C_{4a'}$), 128.6 (2C, $C_{2''}$ or $C_{3''}$), 128.6 ($C_{4''}$), 128.5 (2C, $C_{3''}$ or $C_{2''}$), 123.8 ($C_{7'}$), 118.9 ($C_{5'}$), 114.9 ($C_{8a'}$), 80.1 (C_7), 67.3 (C_9), 53.5 (C_2), 30.8 (C_3), 28.3 (3C, C_8), 22.2 (C_4), 12.5 ($C_{10'}$).

HRMS (ESI-TOF): Calcd for $C_{27}H_{29}NO_7$, 479.1944; Found 502.1823 [M+Na].

(S)-2-(tert-butoxycarbonylamino)-3-(8-hydroxy-3-methyl-1,4-dioxo-1,4-dihydronaphthalen-2-yl)propanoic acid, 2.54

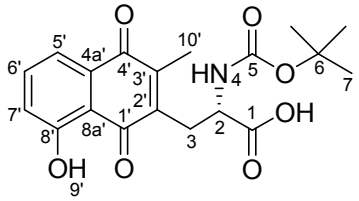

A solution of **2.48** (115 mg; 0.247 mmol) in THF (4 ml) and H_2O (2 ml) was stirred at r.t., before adding $LiOH.H_2O$ (31 mg; 0.741 mmol). There was an instantaneous colour change from yellow to purple due to deprotonation of the phenolic OH. The reaction mixture was

stirred for 4 h before being diluted with EtOAc (40 ml), washed with saturated aqueous NH_4Cl (2 x 30 ml) and brine (30 ml). The aqueous layer was extracted with EtOAc (2 x 10 ml) and the combined organic layers dried (Na_2SO_4) and concentrated under reduced pressure. The residue was purified by silica gel chromatography (eluting in EtOAc:hexane, 1:1, 1 % AcOH), to afford the product (83 mg; 0.221 mmol) as a yellow film in 89 % yield. R_f (MeOH:CH_2Cl_2, 1:9) 0.34; m.p. 93-95 °C; IR (NaCl, dry film) ν_{max} (cm^{-1}): 3431 (NH), 1635 (C=O, C=C).

^{1}H NMR (400 MHz, $CDCl_3$) δ 12.05 (s, 1H, $H_{9'}$), 7.65 – 7.54 (m, 2H, $H_{5'}$, $H_{6'}$), 7.26 – 7.18 (m, 1H, $H_{7'}$), 5.35 – 5.26 (m, 1H, H_4), 4.55 (bs, 1H, H_2), 3.30 – 3.17 (m, 1H, H_{3a}), 3.14 – 2.99 (m, 1H, H_{3b}), 2.26 (s, 3H, $H_{10'}$), 1.33 (s, 9H, H_7).

^{13}C NMR (100 MHz, $CDCl_3$) δ 189.9 ($C_{1'}$), 184.1 ($C_{4'}$), 175.0 (C_1), 161.3 ($C_{8'}$), 155.4 (C_5), 147.2 ($C_{2'}$ or $C_{3'}$), 141.9 ($C_{3'}$or $C_{2'}$), 136.1 ($C_{6'}$), 132.2 ($C_{4a'}$), 123.9 ($C_{7'}$), 119.1 ($C_{5'}$), 114.8 ($C_{8a'}$), 80.5 (C_6), 52.8 (C_2), 29.9 (C_3), 28.1 (C_7), 13.3 ($C_{10'}$).

HRMS (ESI-TOF): Calcd for $C_{19}H_{21}NO_7$, 375.1318; Found 376.1395 [M+H], 398.1212 [M+Na].

(S)-2-(tert-butoxycarbonylamino)-4-(8-hydroxy-3-methyl-1,4-dioxo-1,4-dihydronaphthalen-2-yl)butanoic acid, 2.55

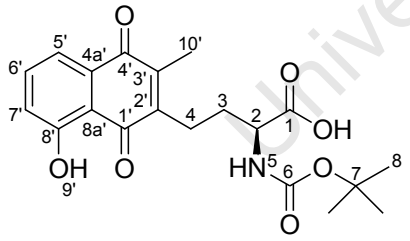

A solution of **2.49** (582; 1.22 mmol) in THF (10 ml) and H_2O (3.5 ml) was stirred at r.t. before adding $LiOH.H_2O$ (153 mg; 3.64 mmol). The reaction mixture was stirred for 4 h and then extracted into EtOAc and the EtOAc extract washed with saturated aqueous NH_4Cl (2 x 50 ml) and brine (30 ml). After drying (Na_2SO_4) and removal of the solvent under reduced pressure, the residue was purified by column chromatography (silica gel, eluting in EtOAc:hexane, 1:1, 1 % AcOH) to give the product as a yellow precipitate (431 mg; 1.108 mmol; 91 %). R_f (MeOH:CH_2Cl_2, 1:9) 0.40; m.p. 66-68 °C; IR (NaCl, dry film) ν_{max} (cm^{-1}): 3414 (NH), 1635 (C=O, C=C).

^{1}H NMR (500 MHz, CD_3OD) δ 7.56 (1H, dd, *J* = 8.2, 7.7 Hz, $H_{6'}$), 7.47 (d, *J* = 7.5 Hz, 1H, $H_{5'}$), 7.15 (dd, *J* = 8.4, 0.9 Hz, 1H, $H_{7'}$), 4.20 – 4.11 (m, 1H, H_2), 2.75 – 2.65 (m, 2H, H_4), 2.13 (s, 3H, $H_{10'}$), 2.11 – 2.00 (m, 1H, H_{3a}), 1.91 – 1.80 (m, 1H, H_{3b}), 1.44 (s, 9H, H_8).

^{13}C NMR (126 MHz, CD_3OD) δ 189.5 ($C_{1'}$), 183.9 ($C_{4'}$), 174.5 (C_1), 160.8 ($C_{8'}$), 156.6 (C_6), 145.6 ($C_{2'}$ or $C_{3'}$), 145.0 ($C_{3'}$or $C_{2'}$), 135.7 ($C_{6'}$), 132.1 ($C_{4a'}$), 123.2 ($C_{7'}$), 118.2 ($C_{5'}$), 114.7 ($C_{8a'}$), 79.2 (C_7), 53.6 (C_2), 30.0 (C_3), 27.4 (3C, C_8), 22.6 (C_4), 11.4 ($C_{10'}$).

HRMS (ESI-TOF), Calcd for $C_{20}H_{23}NO_7Na$, 412.1372; Found 412.1393 [M+Na].

Phenyl-3,4,6-tri-O-acetyl-2-deoxy-2-[(S)-2'-(tert-butoxycarbonyamino)-3'-(8''-hydroxy-3''-methyl-1'',4''-dioxo-1'',4''-dihydronaphthalen-2''-yl)propanamido]-1-thio-α-D-glucopyranoside, 2.56

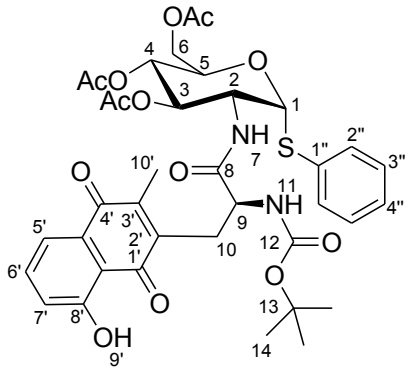

A solution of **2.54** (60 mg; 0.160 mmol), EDC.HCl (34 mg; 0.176 mmol) and HOBt.H_2O (24 mg; 0.176 mmol) in anhydrous THF (10 ml) was cooled to 0 °C. To this was added a solution of **2.7** (100 mg; 0.252 mmol) in dry THF (10 ml), drop-wise over 15 min, followed by DIEA (0.1 ml; 0.574 mmol). There was an instantaneous colour change from dark orange to dark red due to deprotonation of the phenolic OH. The reaction was allowed to warm to room temperature and stirring was continued for 18 h. By this stage TLC showed the reaction to be incomplete, and a spatula tip of EDC.HCl was therefore added and stirring continued for a further 24 h. The reaction mixture was then partitioned between EtOAc (40 ml) and saturated aqueous NH_4Cl (40 ml). The organic layer was washed once again with saturated aqueous NH_4Cl (30 ml) and brine (30 ml). The combined aqueous layers were extracted with EtOAc (3 x 20 ml), and the combined organic layers dried (Na_2SO_4). After removal of the solvent under reduced pressure, the crude residue was purified by column chromatography (silica gel, eluting in EtOAc:petroleum ether, 6:4) to yield the product (40 mg; 0.053 mmol) in 33 % yield. R_f (EtOAc:petroleum ether, 6:4) 0.60; m.p. 210-212 °C; IR (NaCl, dry film) v_{max} (cm^{-1}): 3435 (NH), 1746 (C=O), 1664 (C=O), 1635 (C=C).

Alternate Synthesis Using EEDQ as Coupling Reagent:

Portions of **2.54** (91 mg; 0.242 mmol), phenyl 3,4,6-tri-O-acetyl-2-amino-2-deoxy-1-thio-D-glucopyranoside **2.7** (200 mg; 0.503 mmol) and EEDQ (2-ethoxy-1-ethoxycarbonyl-1,2-dihydroquinoline) (72 mg; 0.290 mmol) were dissolved in anhydrous THF (10 ml) under Ar, and stirred at 40 °C overnight (15 h). The solvent was removed under reduced pressure, and the residue purified by automated flash chromatography (EtOAc:petroleum ether, 1:9 – 1:1 containing 1 % AcOH) to afford the product (179 mg; 0.237 mmol) as a yellow powder in 98 % yield.

^{1}H NMR (400 MHz, $CDCl_3$) δ 12.00 (s, 1H, $H_{9'}$), 7.62 – 7.53 (m, 2H, $H_{5'}$, $H_{6'}$), 7.49 – 7.42 (m, 2H, $H_{2''}$), 7.35 – 7.25 (m, 3H, $H_{3''}$, $H_{4''}$), 7.23 (dd, *J* = 7.2, 2.1 Hz, 1H, $H_{7'}$), 6.80 (d, *J* = 8.3 Hz, 1H, NH_7), 5.74 (d, *J* = 5.2 Hz, 1H, H_1), 5.28 – 5.20 (m, 2H, H_3 or H_4, NH_{11}), 5.17 (t, *J* = 9.6 Hz, 1H, H_4 or H_3), 4.60 – 4.49 (m, 2H, H_2, H_5), 4.40 – 4.32 (m, 1H, H_9), 4.29 (dd, *J* = 12.3, 5.0 Hz, 1H, H_{6a}), 4.09 (broad dd, *J* = 12.4, 1.9 Hz, 1H, H_{6b}), 3.07 (dd, *J* = 13.5, 3.5 Hz, 1H, H_{10a}), 2.92 (dd, *J* = 13.4, 10.0 Hz, 1H, H_{10b}), 2.23 (s, 3H, $H_{10'}$), 2.06 (s, 3H, C*H*$_3$COO), 2.05 (s, 3H, C*H*$_3$COO), 2.04 (s, 3H, C*H*$_3$COO), 1.30 (s, 9H, H_{14}).

^{13}C NMR (101 MHz, $CDCl_3$) δ 190.4 ($C_{1'}$), 183.9 ($C_{4'}$), 171.4 (C=O), 171.0 (C=O), 170.6 (C=O), 169.3 (C=O), 161.4 ($C_{8'}$), 155.3 (C_{12}), 147.2 ($C_{2'}$ or $C_{3'}$), 142.3 ($C_{3'}$ or $C_{2'}$), 136.3 ($C_{6'}$), 132.8 ($C_{1''}$), 132.1 ($C_{4a'}$), 131.6 (2C, $C_{2''}$), 129.2 (2C, $C_{3''}$), 127.9 ($C_{4''}$), 124.0 ($C_{7'}$), 119.2 ($C_{5'}$), 114.8 ($C_{8a'}$), 87.3 (C_1), 80.5 (C_{13}), 71.1 (C_3), 69.0 (C_5), 68.2 (C_4), 62.0 (C_6), 54.1 (C_9), 53.0 (C_2), 30.4 (C_{10}), 28.1 (3C, C_{14}), 20.6 (2 x *C*H$_3$COO), 20.6 (*C*H$_3$COO), 13.3 ($C_{10'}$) .

HRMS (ESI-TOF), Calcd for $C_{37}H_{42}N_2O_{13}S$, 754.2408; Found 755.2495 [M+H], 777.2307 [M+Na].

Phenyl-3,4,6-tri-O-acetyl-2-deoxy-2-[(S)-2'-(tert-butoxycarbonyamino)-4'-(8''-hydroxy-3''-methyl-1'',4''-dioxo-1'',4''-dihydronaphthalen-2''-yl)butanamido]-1-thio-α-D-glucopyranoside, 2.57

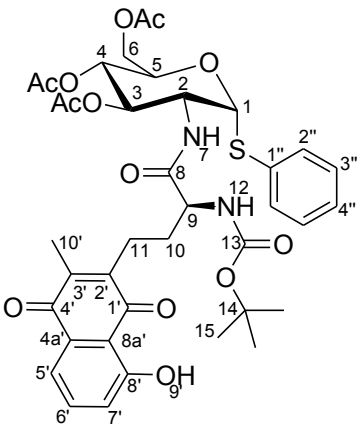

Portions of **2.55** (129 mg; 0.331 mmol) and EEDQ (86 mg; 0.348 mmol) were combined and first placed under reduced pressure for 20 min, then purged with Ar before adding anhydrous THF (5 ml). The resulting solution was stirred for 10 min at r.t. before adding a solution of **2.7** (158 mg; 0.398 mmol) in anhydrous THF (5 ml). The mixture was stirred at r.t. under Ar for 39 h. The reaction mixture was then partitioned between EtOAc and sat. aq. NH_4Cl, and the organic layer washed with additional NH_4Cl (2 x 30 ml) and brine (30 ml). The combined aqueous layers were extracted with additional EtOAc until the yellow product colour was no longer evident. The combined organic fractions were dried (Na_2SO_4), the solvent removed under reduced pressure, and the residue purified by silica gel chromatography (eluting in EtOAc:petroleum ether, 3:7). The purified product was obtained as a yellow solid (217 mg; 0.282 mmol, 85 %). R_f (EtOAc:petroleum ether,1:1) 0.50; m.p. 173-174 °C; IR (NaCl, dry film) ν_{max} (cm^{-1}): 3431 (NH), 1746 (C=O), 1660 (C=O), 1633 (C=C).

^{1}H NMR (400 MHz, $CDCl_3$) δ 12.02 (s, 1H, $H_{9'}$), 7.58 (dd, *J* = 7.5, 1.6 Hz, 1H, $H_{5'}$), 7.57 – 7.52 (m, 1H, $H_{6'}$), 7.42 – 7.37 (m, 2H, $H_{2''}$), 7.25 – 7.17 (m, 4H, $H_{3''}H_{4''}H_{7'}$), 6.79 (d, *J* = 8.1 Hz, 1H, NH_7), 5.73 (d, *J* = 5.3 Hz, 1H, H_1), 5.19 (dd, *J* = 10.7, 9.2 Hz, 1H, H_3 or H_4), 5.16 – 5.10 (m, 2H, H_4 or H_3, NH_{12}), 4.57 – 4.47 (m, 2H, H_2, H_5), 4.26 (dd, *J* = 12.4, 5.0 Hz, 1H, H_{6a}), 4.14 – 4.09 (m, 1H, H_9), 4.06 (dd, *J* = 12.4, 2.3 Hz, 1H, H_{6b}), 2.68 – 2.53 (m, 2H, H_{11}), 2.09 (s, 3H, $H_{10'}$), 2.03 (s, 3H, C*H*$_3$COO), 2.02 (s, 3H, C*H*$_3$COO), 2.01 (s, 3H, C*H*$_3$COO), 1.98 – 1.88 (m, 1H, H_{10a}), 1.82 – 1.69 (m, 1H, H_{10b}), 1.44 (s, 9H, H_{15}).

^{13}C NMR (101 MHz, $CDCl_3$) δ 189.9 ($C_{1'}$), 184.1 ($C_{4'}$), 171.7 (C=O), 171.4 (C=O), 170.6 (C=O), 169.3 (C=O), 161.3 ($C_{8'}$), 155.6 (C_{13}), 145.6 ($C_{2'}$ or $C_{3'}$), 145.3 ($C_{3'}$ or $C_{2'}$), 136.2 ($C_{6'}$), 133.0 ($C_{1''}$), 132.1 ($C_{4a'}$), 131.5 (2C, $C_{2''}$), 129.2 (2C, $C_{3''}$), 127.8 ($C_{4''}$), 123.9 ($C_{7'}$), 119.1 ($C_{5'}$),

114.9 ($C_{8a'}$), 87.4 (C_1), 80.6 (C_{14}), 70.8 (C_3), 69.0 (C_5), 68.3 (C_4), 62.0 (C_6), 54.6 (C_9), 53.0 (C_2), 30.7 (C_{10}), 28.3 (3C, C_{15}), 20.6 (2 x CH_3COO), 20.6 (CH_3COO), 12.7 ($C_{10'}$).

HRMS (ESI-TOF), Calcd for $C_{38}H_{44}N_2O_{13}S$, 768.2564; Found 769.2648 [M+H].

Attempted Removal of Boc Protecting Group in 5.56: Formation of Phenyl-3,4,6-tri-O-acetyl-2-deoxy-2-[(s)-2'-(trifluoroacetamido)-3'-(8''-hydroxy-3''-methyl-1'',4''-dioxo-1'',4''-dihydronaphthalen-2''-yl)propanamido]-1-thio-α-D-glucopyranoside, 2.65

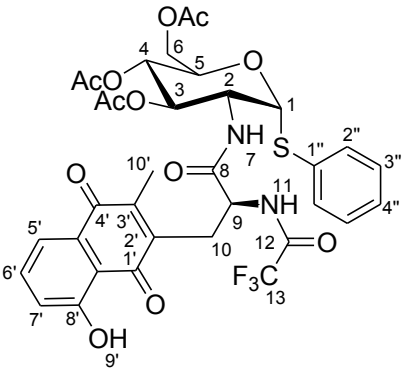

A solution of **2.56** (24 mg; 0.032 mmol) and anisole (7 mg; 0.064 mmol) in CH_2Cl_2 (2 ml) was stirred at r.t. before drop-wise addition of TFA containing TFAA (0.4 ml). The solution was stirred for 4 h at r.t., by which stage the starting material had been consumed (by TLC), and the excess reagents and solvents were then removed by evaporation under a stream of air. The residue was diluted with EtOAc (30 ml) and washed with $NaHCO_3$ (2 x 20 ml) then NH_4Cl (20 ml) before drying (Na_2SO_4) and removing the solvent under reduced pressure, and the residue purified by automated flash chromatography (gradient elution with EtOAc:hexane mixtures, 2:8 – 6:4). The product was obtained as a yellow powder (36.5 mg; 0.049 mmol; 70 %). R_f (EtOAc:hexane, 4:6) 0.35; m.p. 234-236 °C; IR (NaCl, dry film) ν_{max} (cm^{-1}): 3440 (NH), 1725 (C=O), 1635 (C=C).

^{1}H NMR (400 MHz, $CDCl_3$) δ 11.84 (s, 1H, $H_{9'}$), 7.59 – 7.53 (m, 3H, H_{11}, $H_{5'}$, $H_{6'}$), 7.41 – 7.34 (m, 2H, $H_{2''}$), 7.31 – 7.25 (m, 3H, $H_{3''}$, $H_{4''}$), 7.23 – 7.19 (m, 1H, $H_{7'}$), 6.86 (d, *J* = 7.8 Hz, 1H, H_7), 5.77 (d, *J* = 5.4 Hz, 1H, H_1), 5.22 (dd, *J* = 10.5, 9.3 Hz, 1H, H_3 or H_4), 5.17 (t, *J* = 9.4 Hz, 1H, H_4 or H_3), 4.59 (td, *J* = 7.6, 4.7 Hz, 1H, H_9), 4.54 – 4.44 (m, 2H, H_2, H_5), 4.27 (dd, *J* = 12.4, 5.1 Hz, 1H, H_{6a}), 4.05 (dd, *J* = 12.4, 2.3 Hz, 1H, H_{6b}), 3.10 – 2.98 (m, 2H, H_{10}), 2.19 (s, 3H, $H_{10'}$), 2.04 (s, 3H, CH_3), 2.03 (s, 3H, CH_3), 2.02 (s, 3H, CH_3).

^{13}C NMR (101 MHz, $CDCl_3$) δ 191.0 ($C_{1'}$), 183.5 ($C_{4'}$), 172.3 (C=O), 170.7 (C=O), 169.4 (C=O), 169.1, 161.8 ($C_{8'}$), 157.5 (q, 1C, *J* = 37.9 Hz, C_{12}), 148.3, 141.1, 136.9 ($C_{6'}$), 132.5, 132.1, 131.7 (2C, $C_{2''}$), 129.5 (2C, $C_{3''}$), 128.1 ($C_{4''}$), 124.4 ($C_{7'}$), 119.8 ($C_{5'}$), 115.5 (q, 1C, *J* =

287.7 Hz, C_{13}), 114.7, 86.8 (C_1), 71.4 (C_3 or C_4), 69.2 (C_2 or C_5), 68.1 (C_4 or C_3), 62.1 (C_6), 53.8 (C_5 or C_2), 53.3 (C_9), 30.6 (C_{10}), 20.8 (CH_3COO), 20.8 (CH_3COO), 20.7 (CH_3COO), 13.5 ($C_{10'}$).

HRMS (ESI-TOF), Calcd for $C_{34}H_{33}F_3N_2O_{12}S$, 750.1706; Found 751.1776 [M+H], 773.1596 [M+Na].

Phenyl 2-deoxy-2-[(s)-2'-(trifluoroacetamido)-3'-(8''-hydroxy-3''-methyl-1'',4''-dioxo-1'',4''-dihydronaphthalen-2''-yl)propanamido]-1-thio-α-D-glucopyranoside, 2.66

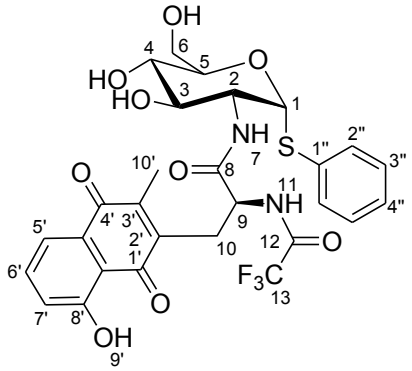

A solution of **2.65** (36.5 mg; 0.049 mmol) in CH_2Cl_2 (5 ml) and MeOH (4 ml) was stirred at r.t. before a solution of NaOMe (0.52 mg; 0.010 mmol) in MeOH (0.26 ml) was added and the solution stirred for 8.5 h. Two product spots were visible by TLC and after 8.5 h they had not converged to a single spot. The starting material had, however, not been completely consumed at this stage, and degradation was evident from products detectable on the baseline of the TLC. Consequently, the reaction was neutralised by the addition of DOWEX ion exchange resin (H^+ form), filtered and the solvent removed under reduced pressure. Purification of the residue was attempted by automated flash chromatography using MeOH:CH_2Cl_2 mixtures (0:100 - 10:90), but the product appeared to adhere to the silica, and 1 % AcOH was added to the mobile phase to encourage elution. However, considerable material was lost during chromatography due to adherence to the silica and due to degradation. Two minor fractions were obtained (3 mg and 7 mg), neither of which had spectroscopic features (^1H or ^{13}C NMR) consistent with the desired product.

Phenyl-3,4,6-tri-O-acetyl-2-deoxy-2-[2'-carboxamido-5'-methyl-6',10'-dihydroxy-benzo[h]quinolinyl)-1-thio-α-D-glucopyranoside, 2.67

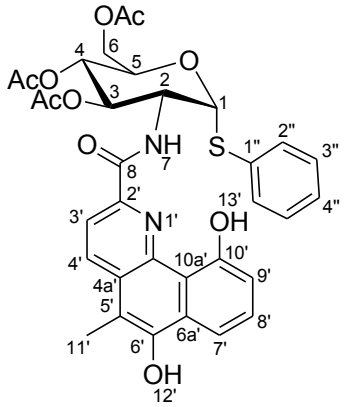

A solution of **2.57** (196 mg; 0.255 mmol) and anisole (55 mg; 0.510 mmol) in CH_2Cl_2 (5 ml) was cooled to 0 °C (ice slurry) before trifluoroacetic acid (1.5 ml) was added drop-wise. The solution was stirred at 0 °C for 2h 30min by which stage the starting material was completely consumed (TLC). The acid was neutralised by drop-wise addition of saturated aq. $NaHCO_3$, and the product extracted into CH_2Cl_2, then the organic phase washed with saturated aqueous NH_4Cl, dried (Na_2SO_4) and the solvent removed under reduced pressure. The residue was purified by silica gel chromatography (EtOAc: hexane, 2:5) to yield the cyclised product as a yellow solid (141 mg; 0.217 mmol; 85 %). R_f (EtOAc:hexane, 6:4) 0.37; m.p. 217-219 °C; IR (NaCl, dry film) ν_{max} (cm^{-1}): 3444 (NH), 1746 (C=O), 1635 (C=C).

^{1}H NMR (400 MHz, $CDCl_3$) δ 13.75 (s, 1H, $H_{13'}$), 8.20 (d, *J* = 8.6 Hz, 1H, $H_{3'}$ or $H_{4'}$), 8.14 (d, *J* = 8.6 Hz, 1H, $H_{4'}$ or $H_{3'}$), 7.63 (1H, bs, H_7), 7.61 – 7.53 (m, 2H, $H_{2''}$), 7.48 (dd, *J* = 8.2, 1.6 Hz, 1H, $H_{7'}$ or $H_{9'}$), 7.44 (t, *J* = 8.0 Hz, 1H, $H_{8'}$), 7.30 – 7.24 (m, 3H, $H_{3''}$, $H_{4''}$), 7.17 (dd, *J* = 7.47, 1.45 Hz, 1H, $H_{9'}$ or $H_{7'}$), 6.13 (bs, 1H, $H_{12'}$), 5.91 (d, *J* = 5.4 Hz, 1H, H_1), 5.49 (dd, *J* = 11.1, 9.2 Hz, 1H, H_3), 5.29 (t, *J* = 9.6 Hz, 1H, H_4), 4.89 (ddd, *J* = 11.1, 8.7, 5.4 Hz, 1H, H_2), 4.68 (ddd, *J* = 10.1, 4.9, 2.2 Hz, 1H, H_5), 4.37 (dd, *J* = 12.3, 5.0 Hz, 1H, H_{6a}), 4.17 (dd, *J* = 12.3, 2.3 Hz, 1H, H_{6b}), 2.52 (s, 3H, $H_{11'}$), 2.11 (s, 3H, C*H*$_3$COO), 2.10 (s, 3H, C*H*$_3$COO), 2.08 (s, 3H, C*H*$_3$COO).

^{13}C NMR (75 MHz, $CDCl_3$) δ 172.6 (C=O), 170.7 (C=O), 169.4 (C=O), 165.3 (C=O), 158.7, 149.1, 143.1, 142.4, 133.1, 132.2 ($C_{3'}$ or $C_{4'}$), 132.0 (2C, $C_{2''}$), 129.9 ($C_{8'}$), 129.4, 129.2 (2C, $C_{3''}$), 128.3, 128.0 ($C_{4''}$), 120.0 ($C_{4'}$ or $C_{3'}$), 114.4, 114.0 ($C_{7'}$ or $C_{9'}$), 111.4 ($C_{9'}$ or $C_{7'}$), 109.3, 88.0 (C_1), 71.8 (C_3), 69.0 (C_5), 68.5 (C_4), 62.2 (C_6), 53.2 (C_2), 20.9 (*C*H$_3$COO), 20.7 (*C*H$_3$COO), 20.6 (*C*H$_3$COO), 10.6 ($C_{11'}$).

HRMS (ESI-TOF), Calcd for $C_{33}H_{32}N_2O_{10}S$, 648.1778; Found 649.1850 [M+H].

Attempted Removal of Boc Protecting Group in 5.48: Formation of Benzyl (S)-2-(trifluoroacetamido)-3-(8-acetoxy-3-methyl-1,4-dioxo-1,4-dihydronaphthalen-2-yl)propanoate, 2.68

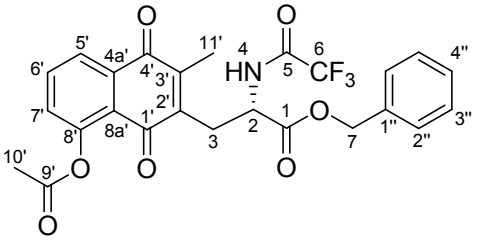

A solution of **2.48** (165 mg; 0.353 mmol) and anisole (76 mg; 0.707 mmol) in CH_2Cl_2 (9 ml) was stirred at room temperature before trifluoroacetic acid (2 ml) was added. The solution was stirred for 3.5 h by which stage the starting material was completely consumed (TLC, staining with ferric chloride). The mixture was then neutralised with saturated aqueous $NaHCO_3$, washed with saturated aqueous NH_4Cl, and the organic fraction dried (Na_2SO_4) before removing the solvent under reduced pressure. The crude mixture was purified by silica gel chromatography (eluting with EtOAc:petroleum ether, 1:9 – 3:17) to afford the deprotected product (146 mg) as a yellow powder in quantitative yield. After confirmation of the disappearance of the *t*-Bu signal in the ^{1}H NMR spectrum, the free amine was subjected to acetylation. A solution of the amine (100 mg; 0.274 mmol) in Ac_2O (1 ml) and anhydrous pyridine (2 ml) was stirred overnight (17 h) at room temperature. The solution was diluted with EtOAc, washed sequentially with 1M HCl (2 x 30 ml), saturated aqueous $NaHCO_3$ (2 x 30 ml) and saturated aqueous NH_4Cl (30 ml), and the organic layer dried (Na_2SO_4). After removal of the solvent removed under reduced pressure, the resulting residue was purified by silica gel chromatography (EtOAc:petroleum ether, 1:5) to afford the acetylated product as a yellow powder (81 mg; 0.161 mmol; 59 %). R_f (EtOAc:hexane, 3:7) 0.35; m.p. 151-152 °C; IR (NaCl, dry film) ν_{max} (cm^{-1}): 3470 (NH), 1746 (C=O), 1725 (C=O), 1660 (C=C).

^{1}H NMR (400 MHz, $CDCl_3$) δ 7.98 (dd, *J* = 7.8, 1.3 Hz, 1H, $H_{5'}$), 7.73 – 7.65 (t, *J* = 7.90 Hz, 1H, $H_{6'}$), 7.46 (d, *J* = 6.7 Hz, 1H, H_4), 7.31 (dd, *J* = 8.1, 1.2 Hz, 1H, $H_{7'}$), 7.27 – 7.21 (m, 5H, $H_{2''}$, $H_{3''}$, $H_{4''}$), 5.17 (d, *J* = 12.1 Hz, 1H, H_{7a}), 5.08 (d, *J* = 12.1 Hz, 1H, H_{7b}), 4.74 – 4.67 (m, 1H, H_2), 3.19 – 3.07 (m, 2H, H_3), 2.39 (s, 3H, CH_3), 2.15 (s, 3H, CH_3).

^{13}C NMR (101 MHz, $CDCl_3$) δ 184.1 ($C_{1'}$), 183.6 ($C_{4'}$), 169.4 (C=O), 169.3 (C=O), 157.1 (q, *J* = 38.0 Hz, C_5), 149.6, 145.6, 141.8, 134.8 ($C_{6'}$), 134.5, 133.7, 129.6 ($C_{7'}$), 128.7 ($C_{4''}$), 128.7 ($C_{2''}$ or $C_{3''}$), 128.4 ($C_{3''}$ or $C_{2''}$), 125.1 ($C_{5'}$), 123.1, 115.6 (q, *J* = 287.6 Hz, C_6), 68.1 (C_7), 51.9 (C_2), 29.2 (C_3), 21.0 (CH_3), 12.9 (CH_3).

Benzyl 5,9-dihydroxy-4-methyl-1H-benzo[g]indole-2-carboxylate, 2.69

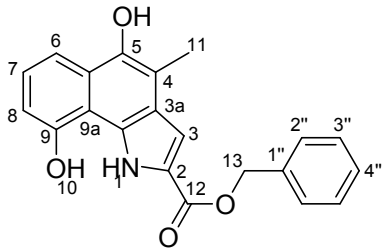

A solution of **2.48** (197 mg; 0.423 mmol) and anisole (few drops) in CH_2Cl_2 (10 ml) and TFA (1ml) was stirred at r.t. for 4 h, by which time the starting material had been consumed. The acid was neutralised with $NaHCO_3$, diluted with additional CH_2Cl_2 (20 ml) and the organic layer washed sequentially with saturated aqueous NH_4Cl and brine. The solvent was removed under reduced pressure and the residue purified by automated flash chromatography (eluting in EtOAc:hexane, 1:4 – 2:3) to afford the cyclised product as a pale yellow solid (73 mg; 0.211 mmol; 50 %). R_f (EtOAc:hexane, 1:4) 0.15; m.p. 191-192 °C.

^{1}H NMR (400 MHz, MeOD) δ 7.73 (dd, *J* = 8.3, 0.9 Hz, 1H, H_6 or H_8), 7.51 – 7.44 (m, 2H, $H_{2''}$), 7.42 – 7.35 (m, 2H, $H_{3''}$), 7.34 – 7.27 (m, 2H, $H_{4''}$, H_7), 7.28 (s, 1H, H_3), 6.91 (dd, *J* = 7.7, 0.8 Hz, 1H, H_8 or H_6), 5.38 (s, 2H, H_{13}), 2.49 (s, 3H, H_{11}).

HRMS (ESI-TOF), Calcd for $C_{21}H_{17}NO_4$, 347.1158; Found 348.1241 [M+H], 370.1115 [M+Na].

Benzyl 5,9-diacetoxy-4-methyl-1H-benzo[g]indole-2-carboxylate , 2.70

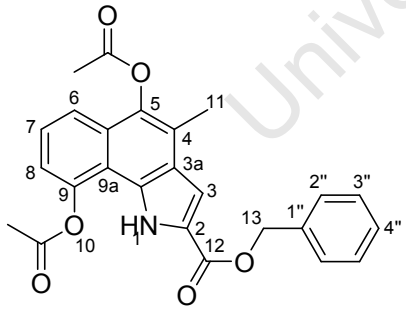

A solution of **2.69** (18 mg; 0.052 mmol) in acetic anhydride (2 ml) and anhydrous pyridine (1.5 ml) was stirred at r.t. under argon for 24 h to allow for complete acetylation. The solution was then diluted with $CHCl_3$ (30 ml) and washed sequentially with 1 M HCl (2 x 50 ml), saturated aqueous $NaHCO_3$ (2 x 50 ml) and saturated aqueous NH_4Cl (20 ml). After drying (Na_2SO_4) and removal of the solvent under reduced pressure, the crude product residue was purified by automated flash chromatography (eluting in EtOAc:hexane, 1:4 –

2:5). The purified product was obtained as an off-white powder (11 mg; 0.025 mmol; 48 %). R_f (EtOAc:hexane, 2:3) 0.64; m.p. 164-166 °C.

^{1}H NMR (400 MHz, $CDCl_3$) δ 10.00 (s, 1H, H_1), 7.65 (dd, *J* = 8.0, 1.3 Hz, 1H, H_6 or H_8), 7.48 (dd, *J* = 8.0, 7.9 Hz, 1H, H_7), 7.48-7.33 (m, 7H, H_8 or H_6, H_3, $H_{2''}$, $H_{3''}$, $H_{4''}$), 5.39 (s, 2H, H_{13}), 2.48 (s, 3H, C*H*$_3$COO), 2.45 (s, 3H, C*H*$_3$COO), 2.43 (s, 3H, H_{11}).

^{13}C NMR (101 MHz, $CDCl_3$) δ 169.1 (C=O), 167.6 (C=O), 161.0 (C=O), 145.7, 138.5, 135.6, 128.6 (Ar_{Bn}), 128.4 (Ar_{Bn}), 128.3 (Ar_{Bn}), 128.1, 127.8, 125.6, 125.5 (C_7), 125.2, 122.2, 119.4 (C_6 or C_8), 118.4 (C_6 or C_8), 114.0, 108.6 (C_3), 66.7 (C_{13}), 21.5 (*C*H$_3$COO), 20.4 (*C*H$_3$COO), 12.8 (C_{11}).

HRMS (ESI-TOF), Calcd for $C_{25}H_{21}NO_6$, 431.1369; Found 432.1448 [M+H], 454.1263 [M+Na].

Benzyl 6-acetoxy-10-hydroxy-5-methylbenzo[h]quinoline-2-carboxylate, 2.77

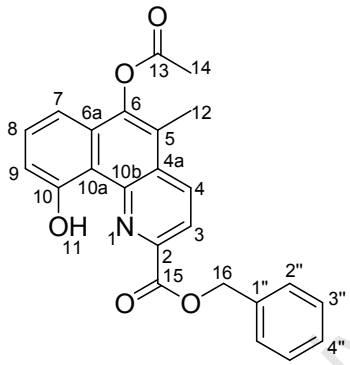

A solution of **2.49** (156 mg; 0.325 mmol) and anisole (70 mg; 0.651 mmol) in CH_2Cl_2 (5 ml) was cooled to 0 °C before TFA (1.5 ml) was added drop-wise. The solution was stirred at 0 °C for 3h 10min at which stage the starting material was completely consumed (according to TLC) and the acid neutralised with saturated aqueous $NaHCO_3$. The mixture was diluted with additional CH_2Cl_2 (20 ml) and the organic layer washed sequentially with saturated aqueous NH_4Cl and brine. The solvent was removed under reduced pressure and the residue dissolved in dry THF (8 ml), pyridine (0.5 ml) and Ac_2O (0.5 ml), and stirred at room temperature for 24 h. The reaction was found to be incomplete after this period, and the temperature was therefore raised to 50 °C, additional Ac_2O (1.2 eq) added and stirring continued for a further 24 h. Reaction was then found to be complete by TLC and the reaction mixture was then diluted with EtOAc, washed successively with 1 M HCl (2 x 90 ml), saturated aqueous $NaHCO_3$ (2 x 100 ml), saturated aqueous NH_4Cl (100 ml) and brine (100

ml). After drying (Na_2SO_4), the organic layer was concentrated under reduced pressure and the residue purified by silica gel chromatography (CH_2Cl_2:EtOAc:hexane, 2:1:7) to afford the product as yellow needles (116 mg; 0.275 mmol; 85 %). R_f (EtOAc:hexane, 3:7) 0.46; m.p. 181-182 °C; IR (NaCl, dry film) ν_{max} (cm^{-1}): 3427 (OH), 1766 (C=O), 1727 (C=O), 1628 (C=C).

^{1}H NMR (400 MHz, $CDCl_3$) δ 14.70 (s, 1H, H_{11}), 8.51 (d, *J* = 8.5 Hz, 1H, H_3 or H_4), 8.36 (d, *J* = 8.5 Hz, 1H, H_4 or H_3), 7.66 (t, *J* = 8.1 Hz, 1H, H_8), 7.58 – 7.54 (m, 2H, $H_{2''}$), 7.46 – 7.40 (m, 2H, $H_{3''}$), 7.39 – 7.33 (m, 1H, $H_{4''}$), 7.35 (dd, *J* = 8.07, 1.01 Hz, 1H, H_7 or H_9) 7.30 (dd, *J* = 8.0, 1.0 Hz, 1H, H_9 or H_7), 5.55 (s, 2H, H_{16}), 2.53 (s, 3H, H_{14}), 2.51 (s, 3H, H_{12}).

^{13}C NMR (101 MHz, $CDCl_3$) δ 168.5 (C_{13}), 163.9 (C_{15}), 159.7 (C_{10}), 146.4, 145.8, 141.9, 135.6, 133.6 (C_3 or C_4), 131.0 (C_8), 129.8, 128.7 (2C, $C_{3''}$), 128.7, 128.5 ($C_{4''}$), 128.2 (2C, $C_{2''}$), 121.4 (C_4 or C_3), 121.3, 115.5 (C_7 or C_9), 115.4, 111.7 (C_9 or C_7), 67.7 (C_{16}), 20.6 (C_{14}), 12.0 (C_{12}).

HRMS (ESI-TOF), Calcd for $C_{24}H_{19}NO_5$, 401.1263; Found 402.1335 [M+H].

Towards the Preparation of an N-Acetylated Amino Acid

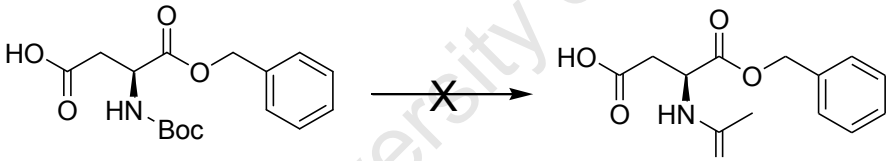

2.46 **2.85**

A solution of **2.46** (244 mg; 0.755 mmol), TFA (1 ml) and anisole (few drops) in CH_2Cl_2 (5 ml) was stirred at r.t. for 4 h before the solvent was removed under reduced pressure and the residue redissolved in CH_2Cl_2 (3 ml), Ac_2O (1 ml) and pyridine (2 ml), before stirring at r.t. overnight (17 h). The crude mixture was then diluted in CH_2Cl_2 (40 ml) and washed sequentially with 1 M HCl (2 x 30 ml), saturated aqueous $NaHCO_3$ (30 ml), and saturated aqueous NH_4Cl (30 ml). The organic layer was dried (Na_2SO_4) and concentrated under reduced pressure before purification by automated flash chromatography (MeOH:CH_2Cl_2, 1:9). The eluted column fractions all contained multiple components suggesting decomposition had taken place.

Attempts Towards the Synthesis of an Acetylated Boc-Protected Amine: Formation of Benzyl (S)-2'-(tert-butoxycarbonyamino)-3'-(8''-acetoxy-3''-methyl-1'',4''-dioxo-1'',4''-dihydronaphthalen-2''-yl)propanoate, 2.86

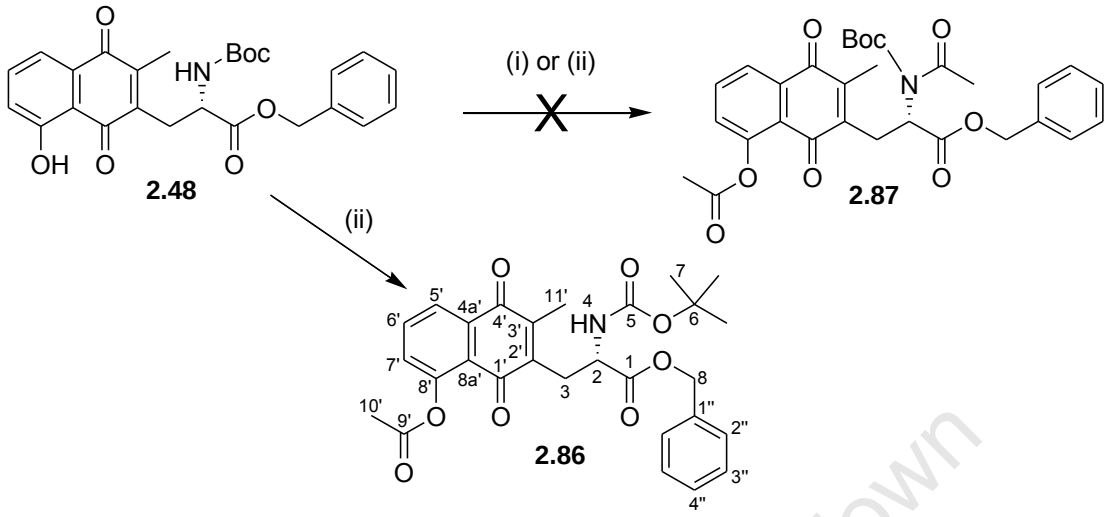

i) A solution of **2.48** (24 mg; 0.516 mmol) in Ac_2O (0.5 ml) and pyridine (0.5 ml) was stirred at r.t. under Ar for 2 days. The product was extracted into CH_2Cl_2 (20 ml), washed sequentially with 1 M HCl (2 x 20 ml), saturated aqueous $NaHCO_3$ (20 ml) and saturated aqueous NH_4Cl (20 ml), and dried (Na_2SO_4). After concentration under reduced pressure, purification of the residue was attempted by automated flash chromatography (EtOAc:hexane, 1:9), however, TLC analysis of the eluted fractions indicated that mulitiple components were present in each, suggesting that decomposition had taken place.

ii) A solution of **2.48** (24 mg; 0.051 mmol) in anhydrous CH_2Cl_2 (5 ml) was stirred at 0 °C (ice bath) before Et_3N (18 µl; 0.128 mmol) and acetyl chloride (9 µl; 0.128 mmol) were added drop-wise. The ice bath was removed and the solution allowed to warm to r.t. and stirred for 24 h. After this extended reaction time no detectable product had formed (TLC) and additional AcCl (0.1 ml) and Et_3N (0.1 ml) were added and stirring continued for an additional 15 min, by which stage the starting material had been consumed. The reaction mixture was diluted with CH_2Cl_2 and the organic layer washed sequentially with saturated aqueous $NaHCO_3$ and saturated aqueous NH_4Cl, and dried (Na_2SO_4). After removal of the solvent under reduced pressure, the residue was purified by automated flash chromatography (EtOAc:hexane, 1:4) to afford a fraction that was analysed by 1H NMR spectroscopy and found to be the phenolic acetate derivative **2.86**. R_f (EtOAc:hexane, 1:4) 0.19.

^{1}H NMR (400 MHz, $CDCl_3$) δ 8.00 (dd, *J* = 7.8, 1.2 Hz, 1H, $H_{5'}$ or $H_{7'}$), 7.68 (t, *J* = 7.9 Hz, 1H, $H_{6'}$), 7.31 (dd, *J* = 8.1, 1.1 Hz, 1H, $H_{7'}$ or $H_{5'}$), 7.28 (bs, 5H, $H_{2''}$, $H_{3''}$, $H_{4''}$), 5.24 (s, 1H, H_4), 5.15 (d, *J* = 12.2 Hz, 1H, H_{8a}), 5.09 (d, *J* = 12.2 Hz, 1H, H_{8b}), 4.57 – 4.44 (m, 1H, H_2), 3.16 – 2.99 (m, 2H, H_3), 2.41 (s, 3H, $H_{11'}$), 2.20 (s, 3H, $H_{10'}$), 1.35 (s, 9H, H_7).

7.5 Carbazole Quinone Derivatives

7.5.1 3-Substituted Carbazole Quinones

2,3-dihydro-3-dioxolanyl-2-methyl-9H-carbazole-1,4-quinone, 3.13

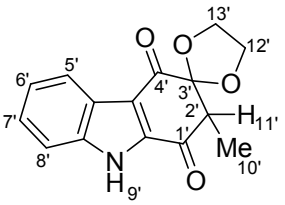

i) A solution of 3-methoxy-2-methyl-*9H*-carbazole-1,4-quinone (53 mg; 0.220 mmol) and NaH (21 mg; 0.880 mmol) in ethane-1,2-diol (7.3 ml) was heated under Ar at 50 °C overnight (17 h). By this time the starting material had been consumed and the reaction mixture was extracted into EtOAc (50 ml), washed with NH_4Cl (2 x 30 ml) and brine (2 x 30 ml) and the organic layer dried (Na_2SO_4). After removal of the solvent under reduced pressure, the residue was purified by automated flash chromatography (A: pentane, B: CH_2Cl_2:EtOAc 5:1; 45 – 50 % B). The purified product was obtained as a yellow solid (44 mg; 0.162 mmol; 74 %).

ii) The reaction was repeated and the procedure modified such that a solution of NaH (30 mg; 1.24 mmol) in ethane-1,2-diol (5 ml) was added dropwise to a solution of the carbazole quinone (100 mg; 0.414 mmol) in ethane-1,2-diol (5 ml) and the mixture stirred under Ar at r.t. for 3h15min. After purification by automated flash chromatography using a less polar mobile phase (30-35 % B), the product was recovered (78 mg; 0.288 mmol; 69 %) and the unreacted carbazole quinone starting material (13 mg; 0.054 mmol; 13 %) recovered for further reaction. R_f (pentane:EtOAc:CH_2Cl_2, 10:5:1) 0.20.

^{1}H NMR (600 MHz, Acetone) δ 11.79 (s, 1H, $H_{9'}$), 8.24 (d, *J* = 8.1 Hz, 1H, $H_{5'}$), 7.71 (d, *J* = 8.3 Hz, 1H, $H_{8'}$), 7.52 (t, *J* = 7.7 Hz, 1H, $H_{7'}$), 7.41 (t, *J* = 7.5 Hz, 1H, $H_{6'}$), 4.39 (td, *J* = 7.2, 6.1 Hz, 1H, $H_{12'}$ or $H_{13'}$), 4.24 – 4.20 (m, 1H, $H_{13'}$ or $H_{12'}$), 4.13 (qt, *J* = 13.6, 6.8 Hz, 2H, $H_{13'}$ or $H_{12'}$), 3.52 (q, *J* = 6.9 Hz, 1H, $H_{11'}$), 1.33 (d, *J* = 6.9 Hz, 3H, $H_{10'}$).

GC/MS *m/z*: Calcd for $C_{15}H_{13}NO_4$, 271.1; Found 271.1 [M]

3-(3-Hydroxypropoxy)-2-methyl-9H-carbazole-1,4-quinone, 3.14

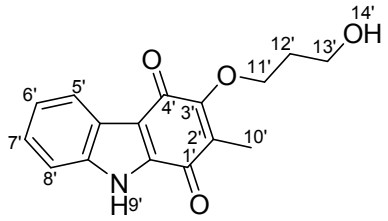

A solution of NaH (15 mg; 0.625 mmol) in propane-1,3-diol (3.9 ml) was added drop-wise over 15 min to a solution of 3-methoxy-2-methyl-*9H*-carbazole-1,4-quinone (52 mg; 0.216 mmol) in propane-1,3-diol (3.2 ml). The reaction mixture was stirred at 40 °C under Ar for 42 h. EtOAc (50 ml) was then added and the solution washed extensively with saturated aqueous NH_4Cl (3 x 30 ml), water (30 ml) and brine (30 ml), and the organic layer dried (Na_2SO_4) and solvent removed under reduced pressure. The crude residue was purified on silica gel by automated flash chromatography (EtOAc:pentane, 3:7 – 4:6) to recover unreacted carbazole quinone (10 mg; 19 %) and the purified product as a solid (40 mg; 0.141 mmol; 65 %). Despite the work up and chromatography, a considerable amount of propane-1,3-diol were present as shown by the NMR spectrum. This compound was not further pursued. R_f (pentane:EtOAc:CH_2Cl_2, 10:4:1) 0.10.

GC/MS *m/z*: Calcd $C_{16}H_{15}NO_4$ 285.1; Found 285.1.

5-(5-Hydroxypentoxy)-2-methyl-9H-carbazole-1,4-quinone, 3.15

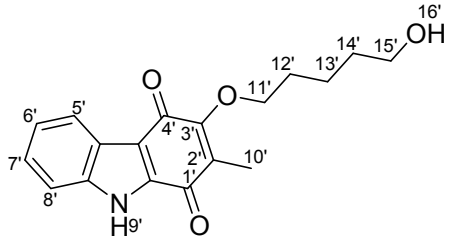

i) A solution of NaH (16 mg; 0.660 mmol) in pentane-1,5-diol (3.9 ml) was added drop-wise over 15 min to a solution of 3-methoxy-2-methyl-*9H*-carbazole-1,4-quinone (53 mg; 0.220 mmol) in pentane-1,5-diol (2.2 ml) and the mixture stirred under Ar at 50

°C overnight (18 h). The reaction mixture was diluted with EtOAc (50 ml), washed with saturated aqueous NH_4Cl (2 x 30 ml) and brine (2 x 30 ml), dried (Na_2SO_4) and solvent removed under reduced pressure. The residue contained a significant amount of pentane-1,5-diol, necessitating two repetitions of the foregoing work up procedure. However, after drying and removal of the solvent under reduced pressure, the product residue still contained a significant quantity of pentane-1,5-diol. This mixture was purified on silica gel by automated flash chromatography (A: pentane, B: CH_2Cl_2:EtOAc 5:1; 45 – 50 % B) to afford the product as an oil (44 mg; 0.162 mmol; 74 %) with a considerable amount of diol starting material present (as evidenced in the ^{1}H NMR spectrum).

The reaction was repeated as follows:

ii) A solution of NaH (90 mg; 3.731 mmol) in pentane-1,5-diol (15 ml) was added to a stirring solution of 3-methoxy-2-methyl-*9H*-carbazole-1,4-quinone (300 mg; 1.244 mmol) in pentane-1,5-diol (12 ml) under Ar at 50 °C. The mixture was stirred at this temperature for 12 h before being extracted into EtOAc (50 ml), washed with saturated aqueous K_2CO_3 (3 x 40 ml), saturated aqueous NH_4Cl (2 x 30 ml) and brine (30 ml). The organic layer was dried (Na_2SO_4) and evaporated before being purified by automated flash chromatography on silica gel (A: pentane, B: EtOAc). After chromatography there still remained a significant amount of pentane-1,5-diol in the product fractions and this was mostly removed by repeatedly washing the organic layer with water (7 x 100 ml), leaving to separate overnight where necessary. The organic layer was then concentrated under reduced pressure and the residue chromatographed once again under the conditions described above to afford the partially purified product (198 mg; 0.632 mmol; 51 %). R_f (pentane:EtOAc:CH_2Cl_2, 10:4:1) 0.10.

ESI-MS *m/z*: Calcd $C_{18}H_{19}NO_4$ 313.1; Found 314.1 [M+H], 336.1 [M+Na]
GC-MS *m/z*: Calcd $C_{18}H_{19}NO_4$ 313.1; Found 313.1

7.5.2 2-Substituted Carbazole Quinones

4-(3-methoxy-9H-carbazole-1,4-quinone-2-yl)-butanoic acid, 3.18

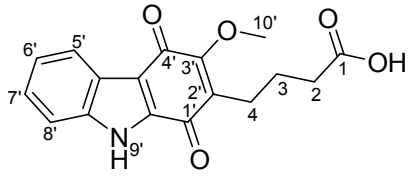

A solution of 3-methoxy-9*H*-carbazole-1,4-quinone (320 mg; 1.408 mmol) and glutaric acid (650 mg; 4.920 mmol) in 66 % CH_3CN/H_2O (20 ml) was heated to 70 °C. Solid $AgNO_3$ (111 mg; 0.653 mmol) was then added and the solution degassed and placed under argon. A degassed solution of $K_2S_2O_8$ (576 mg; 2.131 mmol) in 30 % CH_3CN/H_2O (24 ml) was then added to the reaction mixture drop-wise over 2 h. Once the addition was complete, the mixture was stirred at 70 °C for a further 2 h. By this stage only partial conversion to the product had taken place (possibly due to the poor solubility of the starting material). Therefore, degassed CH_3CN (12 ml) was added, followed by a solution of $K_2S_2O_8$ (200 mg; 0.740 mmol) in degassed H_2O (5 ml) over 1 h, and stirring continued for a further 2 h. The reaction was then stopped by removing the CH_3CN under reduced pressure and extracting the crude aqueous suspension into EtOAc (50 ml). The organic layer was washed with saturated aqueous NH_4Cl (2 x 30 ml) and brine, and the combined aqueous layers extracted with additional EtOAc (3 x 20 ml). The combined organic layers were dried (Na_2SO_4) and the solvent removed under reduced pressure. The residue was purified by automated flash chromatography (silica gel, eluting in MeOH:CH_2Cl_2, 0:100 – 5:95) to recover the unreacted starting material (139 mg; 0.612 mmol; 43 %), and purified product as an orange solid (136 mg; 0.434 mmol; 31 %). M.p. not determined due to presence of glutaric acid impurity.

^{1}H NMR (500 MHz, DMSO/$CDCl_3$) δ 12.84 (s, 1H, $H_{9'}$), 12.01 (s, 1H, COOH), 8.01 (d, *J* = 7.9 Hz, 1H, $H_{5'}$), 7.53 (d, *J* = 8.2 Hz, 1H, $H_{8'}$), 7.39 – 7.33 (m, 1H, $H_{7'}$), 7.30 (t, *J* = 7.1 Hz, 1H, $H_{6'}$), 4.05 (s, 3H, $H_{10'}$), 2.44 (t, *J* = 7.4 Hz, 2H, H_2), 2.24 (t, *J* = 7.4 Hz, 2H, H_4), 1.68 (p, *J* = 7.4 Hz, 2H, H_3).

^{13}C NMR (126 MHz, DMSO) δ 180.3 ($C_{1'}$ or $C_{4'}$), 178.5 ($C_{4'}$ or $C_{1'}$), 174.2 (*C*OOH), 158.2 (C), 137.5 (C), 136.1 (C), 129.3 (C), 125.9 (CH), 123.8 (CH) , 123.5 (C), 121.4 (CH), 113.9 (CH), 113.8 (C), 61.4 ($C_{10'}$), 33.3 (C_2), 23.6 (C_4), 22.1 (C_3).

ESI-MS *m/z*: Calcd for $C_{17}H_{15}NO_5$ 313.1; Found 314.1 [M+H], 336.1 [M+Na], 649.1 [2M+Na].

HRMS *m/z*: Calcd for $C_{17}H_{15}NO_5$ 313.0950; Found 314.1019 [M+H], 336.0848 [M+Na].

5-(3-methoxy-9H-carbazole-1,4-quinone-2-yl)pentanoic acid, 3.19

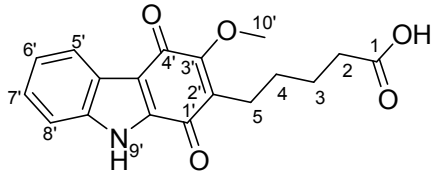

A solution of 3-methoxy-9*H*-carbazole-1,4-quinone (241.5 mg; 1.063 mmol) and adipic acid (465.8 mg; 3.189 mmol) in 70 % CH_3CN/H_2O (10 ml) was degassed (by several cycles of evacuation followed by purging with argon) and heated to 70 °C. $AgNO_3$ (72 mg; 0.425 mmol) was then added and the solution once again degassed. A solution of $K_2S_2O_8$ (374 mg; 1.382 mmol) in degassed 50 % CH_3CN/H_2O (18 ml) was added drop-wise to the reaction mixture over 2 h. After complete addition 10 ml of CH_3CN was added to completely dissolve the starting material, and the reaction mixture maintained at 65 °C for a further 2 h. The product was then extracted into EtOAc (50 ml) and the EtOAc layer washed with saturated aqueous NH_4Cl (3 x 25 ml) and brine. The aqueous layer was extracted with further EtOAc (3 x 20 ml) and the combined organic layers dried (Na_2SO_4). After removal of the solvent under reduced pressure, the residue was purified by automated flash chromatography (silica gel, eluting in MeOH:CH_2Cl_2, 0:100 – 5:95). Unreacted starting material (117.5 mg; 49 %) was recovered, and the purified product obtained as an orange powder (131.5 mg; 0.402 mmol; 38 %). R_f (MeOH:CH_2Cl_2, 5:95) 0.24; m.p. 210-212 °C.

^{1}H NMR (500 MHz, DMSO) δ 12.85 (s, 1H, $H_{9'}$), 11.98 (s, 1H, COOH), 8.01 (d, *J* = 7.9 Hz, 1H, $H_{5'}$), 7.53 (d, *J* = 8.2 Hz, 1H, $H_{8'}$), 7.36 (t, *J* = 7.5 Hz, 1H, $H_{7'}$), 7.31 (t, *J* = 7.4 Hz, 1H, $H_{6'}$), 4.05 (s, 3H, $H_{10'}$), 2.41 (t, *J* = 7.4 Hz, 2H, H_2), 2.24 (t, *J* = 7.2 Hz, 2H, H_5), 1.57 – 1.48 (m, 2H, H_3 or H_4), 1.48 – 1.40 (m, 2H, H_4 or H_3).

^{13}C NMR (126 MHz, DMSO) δ 180.4 ($C_{1'}$ or $C_{4'}$), 178.6 ($C_{4'}$ or $C_{1'}$), 174.4 (C_1), 158.1 (C), 137.6 (C), 136.1 (C), 130.1 (C), 126.1 (CH), 123.9 (CH), 123.5 (C), 121.5 (CH), 114.0 (CH), 113.8 (C), 61.5 ($C_{10'}$), 33.5 (CH_2), 28.0 (CH_2), 24.5 (CH_2), 22.3 (CH_2).

HRMS *m/z*: Calcd for $C_{18}H_{17}NO_5$ 327.1107; Found 328.1194 [M+H], 350.1021 [M+Na].

7.5.3 Substitution at the Carbazole Nitrogen

Methyl 5-(3-methoxy-2-methyl-9H-carbazole-1,4-quinone-9-yl)-5-oxopentanoate, 3.22

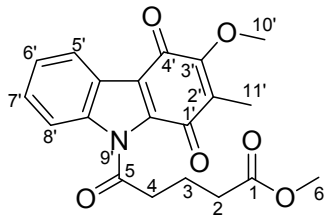

To a stirring solution of 3-methoxy-2-methyl-*9H*-carbazole-1,4-quinone **3.11** (200.5 mg; 0.831 mmol) in anhydrous THF (12 ml) was added Et_3N (126.1 mg; 0.173 ml; 1.247 mmol) followed by glutaric acid monomethylester chloride (205.2 mg; 0.172 ml; 1.247 mmol). The orange solution was left to stir at room temperature under an atmosphere of argon. After 5 min a precipitate had begun to form, and after 2 h the reaction was complete, accompanied by a colour change to red-orange. The crude product was extracted into EtOAc (20 ml), washed with sat. aqueous NH_4Cl (2 x 25 ml) and brine (2 x 25 ml), dried (Na_2SO_4), and adsorbed onto silica gel. Purified product was obtained by automated flash chromatography using a mobile phase gradient of 25 % A in pentane to 30 % A in pentane (A = CH_2Cl_2:EtOAc, 17:83). Separation did prove to be difficult due to the starting material and product having almost identical R_f values. However, a portion of pure product was obtained as a solid (225.8 mg; 0.611 mmol; 74 %). R_f (CH_2Cl_2:EtOAc:pentane, 6:31:63) 0.33; m.p. unstable, decomposition back to carbazole quinone starting material.

^{1}H NMR (500 MHz, $CDCl_3$) δ 8.25 (d, *J* = 7.9 Hz, 1H, $H_{5'}$), 7.84 (d, *J* = 8.5 Hz, 1H, $H_{8'}$), 7.50 – 7.43 (m, 1H, $H_{7'}$), 7.40 (t, *J* = 7.2 Hz, 1H, $H_{6'}$), 4.14 (s, 3H, OCH_3), 3.65 (s, 3H, OCH_3), 3.03 (t, *J* = 7.2 Hz, 2H, H_2 or H_4), 2.47 (t, *J* = 7.2 Hz, 2H, H_4 or H_2), 2.18 – 2.11 (m, 1H, H_3), 2.02 (s, 3H, $H_{11'}$).

^{13}C NMR & DEPT (126 MHz, $CDCl_3$) δ 180.1 ($C_{1'}$ or $C_{4'}$), 179.8 ($C_{4'}$ or $C_{1'}$), 175.0 (C=O), 173.3 (C=O), 156.5 (C), 138.2 (C), 134.7 (C), 128.8 (CH), 128.2 (C), 125.7 (CH), 123.5 (C), 122.9 (CH), 119.6 (C), 114.1 (CH), 61.3 ($C_{10'}$), 51.7 (CH_3), 38.7 (CH_2), 32.6 (CH_2), 20.4 (CH_2), 9.1 (CH_3).

ESI-MS *m/z*: Calcd for $C_{20}H_{19}NO_6$ 369.1; Found 370.2 [M+H], 392.2 [M+Na]

Methyl 6-(3-methoxy-2-methyl-9H-carbazole-1,4-quinone-9-yl)-6-oxohexanoate, 3.23

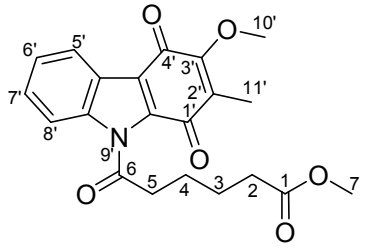

To a stirring solution of 3-methoxy-2-methyl-*9H*-carbazole-1,4-quinone **3.11** (200 mg; 0.829 mmol) in anhydrous THF (24 ml) was added Et_3N (172 µl; 126 mg; 1.244 mmol), and after 5 min of stirring at -10 °C, methyl adipoyl chloride (193 µl; 222 mg; 1.244 mmol) was added. Stirring was continued at this temperature for 1 h, followed by 4 h at room temperature. Similar R_f's for the product and starting material made it difficult to determine by TLC whether the reaction had gone to completion. Crude product was extracted into EtOAc (50 ml), and the EtOAc solution washed with sat. NH_4Cl (2 x 30 ml) and brine (2 x 30 ml), dried (Na_2SO_4) and evaporated under reduced pressure. Purification of the residue was carried out by automated flash chromatography using a mobile phase gradient of 25 % A in pentane to 30 % A in pentane (A = CH_2Cl_2:EtOAc, 17:83) to afford the pure product as a red powder (129 mg; 0.363 mmol; 44 %). R_f (CH_2Cl_2:EtOAc:pentane, 6:31:63) 0.33; m.p. unstable, decomposition back to carbazole quinone starting material.

^{1}H NMR (500 MHz, $CDCl_3$) δ 8.25 (d, J = 7.9 Hz, 1H, $H_{5'}$), 7.84 (d, J = 8.5 Hz, 1H, $H_{8'}$), 7.49 – 7.44 (m, 1H, $H_{7'}$), 7.42 – 7.37 (m, 1H, $H_{6'}$), 4.14 (d, J = 2.2 Hz, 3H, OCH_3), 3.65 (d, J = 5.9 Hz, 3H, OCH_3), 3.01 – 2.93 (m, 2H, H_2 or H_5), 2.34 (dd, J = 9.2, 5.6 Hz, 2H, H_5 or H_2), 2.03 (s, 3H, $H_{11'}$), 1.90 – 1.80 (m, 2H, H_3 or H_4), 1.75 – 1.66 (m, 2H, H_4 or H_3).

^{13}C NMR (126 MHz, $CDCl_3$) δ 180.2 ($C_{1'}$ or $C_{4'}$), 179.8 ($C_{4'}$ or $C_{1'}$), 175.3 (C=O), 173.6 (C=O), 156.5 (C), 138.2 (C), 134.7 (C), 128.8 (CH), 128.2 (C), 125.7 (CH), 123.5 (C), 122.9 (CH), 119.5 (C), 114.2 (CH), 61.3 ($C_{10'}$), 51.6 (CH_3), 39.5 (CH_2), 33.6 (CH_2), 24.9 (CH_2), 24.1 (CH_2), 9.1 ($C_{11'}$).

Attempted Hydrolysis of Methyl Ester 6.5: Formation of 3-Hydroxy-2-methyl-9H-carbazole-1,4-quinone, 3.25

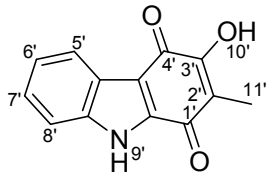

A solution of **3.22** (47 mg; 0.228 mmol) and LiOH (62 mg; 2.566 mmol) in THF (3 ml) and H_2O (3 ml) was stirred at room temperature for 47 h. The product was extracted into EtOAc (50 ml), washed with sat. NH_4Cl (2 x 30 ml) and brine (2 x 30 ml), dried (Na_2SO_4) and evaporated under reduced pressure. Purification was carried out by automated flash chromatography using a mobile phase gradient of 18 % A in pentane to 45 % A in pentane (A = CH_2Cl_2:EtOAc, 17:83) to afford the semi-purified carbazole-1,4-quinone **3.25** as a grey-brown powder (30 mg; 0.134 mmol; 59 %).

^{1}H NMR (300 MHz, DMSO) δ 12.88 (s, 1H, NH), 10.74 (s, 1H, OH), 7.98 (d, *J* = 7.1 Hz, 1H, $H_{5'}$ or $H_{8'}$), 7.53 (d, *J* = 7.3 Hz, 1H, $H_{8'}$ or $H_{5'}$), 7.40 – 7.27 (m, 2H, H_6, H_7), 1.86 (s, 3H, CH_3). (No further characterisation performed – the side product is unwanted).

Monobenzylglutarate, 3.27

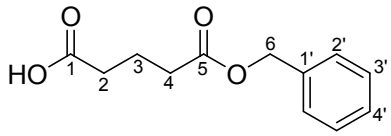

A solution of glutaric anhydride (5.00 g; 43.82 mmol), benzyl alcohol (5.21 g; 4.992 ml; 48.20 mmol), Et_3N (4.877 g; 6.681 ml; 48.20 mmol) and DMAP (100 mg; 0.82 mmol) in dry CH_2Cl_2 (50 ml) was stirred at room temperature under Ar. Due to the exothermic nature of the reaction, the flask was initially immersed in a cold water bath. The reaction was then allowed to stir overnight (20 h) by which time the glutaric anhydride was completely consumed. The solvent was removed under reduced pressure and the residue dissolved in Et_2O (50 ml) and then washed with saturated aqueous $NaHCO_3$ (50 ml). The water layer was acidified to pH 2 with 2 M HCl and extracted with Et_2O (3 x 30 ml). The organic layers were combined, dried (Na_2SO_4) and the solvent removed under reduced pressure to afford the benzylated glutaric acid as a colourless oil (9.855 g; 44.34 mmol) in quantitative yield.

^{1}H NMR (300 MHz, $CDCl_3$) δ 7.44 – 7.32 (m, 5H, $H_{2'}$, $H_{3'}$, $H_{4'}$), 5.15 (s, 2H, H_6), 2.55 – 2.43 (m, 4H, H_2, H_4), 2.08 – 1.95 (m, 2H, H_3).

Literature[15] ^{1}H NMR (200 MHz, DMSO-d6): 7.45 (5H, m, ArH); 5.09 (2H, s, CH_2O); 2.39 (2H, t, *J* = 6.9 Hz, ROOC-CH_2); 2.25 (2H, t, *J* = 6.9 Hz, CH_2COOH); 1.76 (2H, m, *J* = 6.9 Hz, $CH_2CH_2CH_2$).

Attempted Synthesis of 5-(3-methoxy-2-methyl-9H-carbazole-1,4-quinone-9-yl)-5-oxopentanoic acid, 3.30

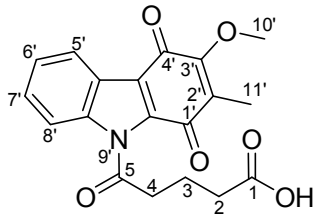

A solution of **3.27** (143 mg; 0.643 mmol) in dry CH_2Cl_2 (2 ml) was stirred at room temperature before oxalyl chloride (2.0 M; 0.42 ml; 0.836 mmol) and a drop of dry DMF (which caused instantaneous effervescence) was added to the reaction mixture which was stirred for a further 2 h at room temperature. This solution was then added dropwise to a solution of **3.11** (105.5 mg; 0.427 mmol) in anhydrous THF (12 ml) at 0 °C, followed by the addition of Et_3N (89 µl; 65 mg; 0.643 mmol) at the same temperature. The reaction was allowed to warm to room temperature and stirring continued for 1 h. By this stage the reaction was complete, as determined by TLC, and the reaction mixture was diluted with EtOAc (40 ml), washed with saturated aqueous NH_4Cl (3 x 20 ml) and brine (20 ml), and dried (Na_2SO_4). The solvent was removed under reduced pressure and the residue purified by automated flash chromatography (A: pentane, B: CH_2Cl_2:MeOH 5:1; 25 – 35 % B). The carbazole quinone (60 mg; 0.270 mmol) starting material was recovered from the column in 60 % yield, suggesting the acylated product was unstable and was converted back to the starting material by interaction with the silica gel. Fractions of the product (21 mg; 0.047 mmol; 7 %) were isolated but found to be impure by ^{1}H NMR. Hydrogenation of the benzyl protecting group was carried out on a crude fraction of the product (30 mg) using $Pd(OH)_2$ on carbon (10 mg) in EtOAc (15 ml). The mixture was stirred at room temperature under a H_2 atmosphere. Upon complete reduction of the benzyl ester, the solution was filtered through a plug of Celite and the solvent removed under reduced pressure. The initially colourless solution turned progressively orange as the reduced quinone was reoxidised in the presence of atmospheric oxygen. An attempt to purify the residue by silica gel chromatography once again resulted in decomposition back to the starting carbazole quinone. No reduction product was isolated.

7.5.4 Amide Coupling and Acetate Deprotection

Phenyl-3,4,6-tri-O-acetyl-2-deoxy-2-[5'-(3"-methoxy-9"H-carbazole-1",4"-quinone-2"-yl)-pentanamido]-1-thio-α-D-glucopyranoside, 3.32

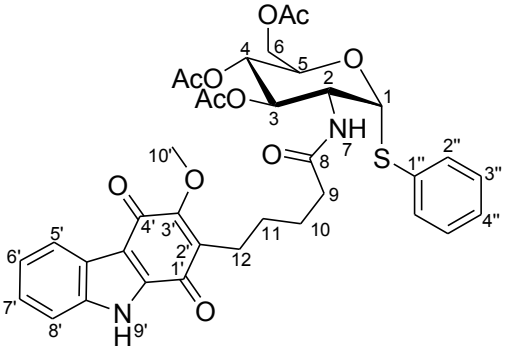

A solution of **3.19** (72 mg; 0.219 mmol), 1-hydroxybenzotriazole (33 mg; 0.241 mmol) and 1-(3-dimethylaminopropyl)-3-ethylcarbodiimide hydrochloride (EDC.HCl) (37 mg; 0.241 mmol) in dry THF was stirred at 0 °C for 30 min. DIEA (41 µl; 31 mg; 0.241 mmol) was added, followed by a solution of **2.7** (87 mg; 0.219 mmol) in dry THF (8 ml). The solution was allowed to warm to r.t. and stirred for 22 h. At this stage the reaction was still incomplete but with much of the amine having been consumed. Additional amine (50 mg; 0.126 mmol) was therefore added and stirring continued for a further 20 h, then additional EDC.HCl (37 mg; 0.241 mmol) and DIEA (41 µl; 0.241 mmol) added and the reaction continued for a further 2 h (total reaction time 44 h). The reaction mixture was then partitioned between EtOAc (50 ml) and saturated aqueous NH_4Cl (40 ml). The organic layer was washed with additional NH_4Cl (40 ml) and brine, and the combined aqueous layers extracted with EtOAc (3 x 30 ml). The combined organic layers were dried (Na_2SO_4) and the solvent removed under reduced pressure. Purification of the residue was achieved by automated flash chromatography (silica gel, eluting in MeOH:CH_2Cl_2, 0:100 – 5:95) to afford the product as an orange solid (21 mg; 0.030 mmol; 14 %). R_f (MeOH:CH_2Cl_2, 5:95) 0.57; m.p. 179-180 °C.

^{1}H NMR (500 MHz, $CDCl_3$) δ 9.71 (s, 1H, $H_{9'}$), 8.15 (d, J = 7.9 Hz, 1H, $H_{5'}$), 7.47 (d, J = 8.2 Hz, 1H, $H_{8'}$), 7.39 – 7.28 (m, 4H, $H_{6'}$, $H_{7'}$, $H_{2''}$), 7.27 – 7.19 (m, 3H, $H_{3''}$, $H_{4''}$), 6.14 (d, J = 8.2 Hz, 1H, H_7), 5.76 (d, J = 5.3 Hz, 1H, H_1), 5.22 – 5.15 (m, 1H, H_3 or H_4), 5.12 (t, J = 9.6 Hz, 1H, H_4 or H_3), 4.60 – 4.53 (m, 1H, H_2), 4.53 – 4.46 (m, 1H, H_5), 4.26 (dd, J = 12.4, 4.9 Hz, 1H, H_{6a}), 4.15 (s, 3H, $H_{10'}$), 4.06 (dd, J = 12.4, 2.2 Hz, 1H, H_{6b}), 2.50 (t, J = 7.4 Hz, 2H, H_9), 2.38 – 2.18 (m, 2H, H_{12}), 2.06 (s, 3H, CH_3COO), 2.06 (s, 3H, CH_3COO), 2.03 (s, 3H, CH_3COO), 1.81 – 1.60 (m, 2H, H_{10} or H_{11}), 1.60 – 1.45 (m, 2H, H_{11} or H_{10}).

^{13}C NMR (126 MHz, $CDCl_3$) δ 181.2 ($C_{1'}$ or $C_{4'}$), 179.1 ($C_{4'}$ or $C_{1'}$), 173.3 (C=O), 172.0 (C=O), 170.7 (C=O), 169.5 (C=O), 158.6 (C), 137.1 (C), 135.7 (C), 132.8 ($C_{1''}$), 131.5 (2C, $C_{2''}$), 129.9 (C), 129.2 (2C, $C_{3''}$), 127.8 ($C_{4''}$), 126.6 (ArCH), 124.3 (ArCH), 124.2 (C), 122.6 (ArCH), 114.9 (C), 113.0 (ArCH), 87.5 (C_1), 71.1 (C_3), 68.8 (C_5), 68.5 (C_4), 62.0 (C_6), 61.8 ($C_{10'}$), 52.6 (C_2), 36.0 (C_9), 27.8 (C_{12}), 25.4 (C_{10} or C_{11}), 21.9 (C_{11} or C_{10}), 20.8 (CH_3), 20.7 (CH_3), 20.7 (CH_3).

ESI-MS *m/z*: Calcd for $C_{36}H_{38}N_2O_{11}S$ 706.2; Found 707.3 [M+H], 729.3 [M+Na].
HRMS *m/z*: Calcd for $C_{36}H_{38}N_2O_{11}S$ 706.2196; Found 707.2257 [M+H], 729.2105 [M+Na].

Phenyl-3,4,6-tri-O-acetyl-2-deoxy-2-[6'-(2''-methyl-3''-methoxy-9''H-carbazole-1'',4''-quinone-9''-yl)-hexanamido]-1-thio-α-D-glucopyranoside, 3.34

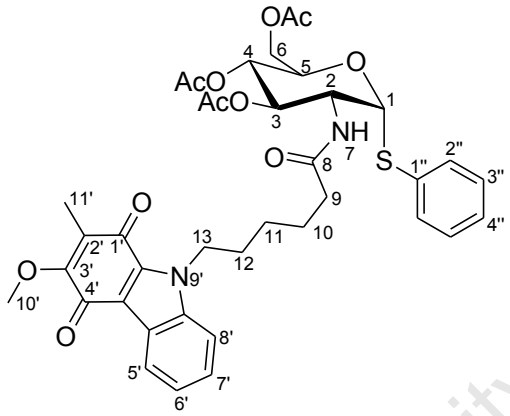

A solution of **3.33** (125 mg; 0.352 mmol), EDC.HCl (82 mg; 0.527 mmol) and HOBt.H_2O (71 mg; 0.527 mmol) in dry THF (12 ml) was cooled to 0 °C. DIEA (0.27 ml; 205 mg; 1.583 mmol) was added followed by a solution of the amine (209 mg; 0.527 mmol) in dry THF (10 ml), and the solution was allowed to warm to r.t. Stirring was continued for 9 h before the reaction mixture was partitioned between EtOAc (50 ml) and sat. aqueous NH_4Cl (30 ml). The organic layer was washed with additional sat. aqueous NH_4Cl (30 ml) and brine (30 ml), and the combined aqueous layers extracted with EtOAc (4 x 20 ml). The combined organic layers were dried (Na_2SO_4) and the solvent removed under reduced pressure, after which the residue was purified by automated flash chromatography (silica gel, eluting in EtOAc:pentane:AcOH, 40:59:1 – 45:54:1). Of the initial acid starting material, 20 % (25 mg) was recovered, and the product obtained as an orange solid (175 mg; 0.240 mmol; 68 %). M.p. 170-172 °C.

^{1}H NMR (500 MHz, $CDCl_3$) δ 8.25 – 8.20 (m, 1H, $H_{5'}$), 7.44 – 7.26 (m, 8H, $H_{6'}$, $H_{7'}$, $H_{8'}$, $H_{2''}$, $H_{3''}$, $H_{4''}$), 5.86 (d, *J* = 8.5 Hz, 1H, H_7), 5.71 (d, *J* = 5.4 Hz, 1H, H_1), 5.18 – 5.09 (m, 2H, H_3H_4),

4.61 – 4.47 (m, 4H, H_2, H_5, H_{13}), 4.27 (dd, *J* = 12.4, 5.0 Hz, 1H, H_{6a}), 4.13 (s, 3H, $H_{10'}$), 4.07 (dd, *J* = 12.4, 2.2 Hz, 1H, H_{6b}), 2.20 – 2.15 (m, 2H, H_9), 2.05 (s, 3H, CH_3COO), 2.05 (s, 3H, CH_3COO), 2.03 (s, 3H, CH_3COO), 2.00 (s, 3H, $H_{11'}$), 1.86 – 1.77 (m, 2H, H_{10} or H_{12}), 1.72 – 1.60 (m, 2H, H_{12} or H_{10}), 1.47 – 1.36 (m, 2H, H_{11}).

^{13}C NMR (126 MHz, $CDCl_3$) δ 181.9 ($C_{1'}$ or $C_{4'}$), 179.1 ($C_{4'}$ or $C_{1'}$), 172.6 (C=O), 171.7 (C=O), 170.6 (C=O), 169.3 (C=O), 157.4 (C), 138.8 (C), 133.7 (C), 132.8 ($C_{1''}$), 131.5 (2C, $C_{2''}$), 129.3 (2C, $C_{3''}$), 127.9 ($C_{4''}$), 127.6 (C), 126.3 (ArCH), 124.4 (ArCH), 123.7 (C), 122.9 (ArCH), 115.3 (C), 111.0 (ArCH), 87.7 (C_1), 71.3 (C_3), 68.9 (C_5), 68.0 (C_4), 62.0 (C_6), 61.3 ($C_{10'}$), 52.6 (C_2), 44.7 (C_{13}), 36.3 (C_9), 29.6 (C_{10} or C_{11} or C_{12}), 26.3 (C_{10} or C_{11} or C_{12}), 25.0 (C_{10} or C_{11} or C_{12}), 20.8 (CH_3), 20.7 (CH_3), 20.6 (CH_3), 8.7 ($C_{11'}$).

ESI-MS *m/z*: Calcd for $C_{38}H_{42}N_2O_{11}S$ 734.3; Found 735.3 [M+H], 757.2 [M+Na].
HRMS *m/z*: Calcd for $C_{38}H_{42}N_2O_{11}S$ 734.2509; Found 735.2587 [M+H], 757.2429 [M+Na].

Phenyl 2-deoxy-2-[4'-(3"-methoxy-9"H-carbazole-1",4"-quinone-2"-yl)-butanamido]-1-thio-α-D-glucopyranoside, 3.35

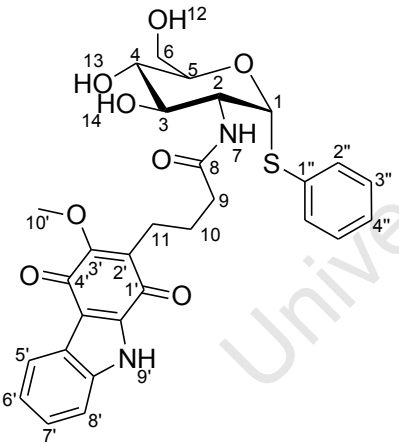

A solution of **3.31** (49 mg; 0.071 mmol) in MeOH (10 ml) was stirred at r.t. before NaOMe (10 mg; 0.185 mmol) was added, causing a red suspension to form. Stirring was continued for 45 min, after which the solution was filtered through a plug of Dowex 50wx2-200 ion exchange resin. After removal of the solvent under reduced pressure, the residue was purified by flash chromatography (silica gel, eluting in CH_2Cl_2:MeOH:Acetone, 4:1:5) and recrystallisation from MeOH afforded the product as an orange solid (27 mg; 0.048 mmol; 68 %). M.p. 243-245 °C.

^{1}H NMR (400 MHz, DMSO) δ 12.81 (m, 1H), 8.01 (dd, *J* = 7.7, 1.2 Hz, 1H, $H_{5'}$), 7.95 (d, *J* = 6.7 Hz, 1H, NH_7), 7.54 (dd, *J* = 8.1, 1.0 Hz, 1H, $H_{8'}$), 7.43 – 7.39 (m, 2H, $H_{2''}$), 7.35 (dd, *J* = 8.2, 1.3 Hz, 1H, $H_{8'}$), 7.33 – 7.29 (m, 1H, $H_{7'}$), 7.30 – 7.24 (m, 2H, $H_{3''}$), 7.24 – 7.19 (m, 1H, $H_{6'}$), 5.61 (d, *J* = 5.1 Hz, 1H, H_1), 5.12 (d, *J* = 5.7 Hz, 1H, H_{13} or H_{14}), 4.85 (d, *J* = 5.5 Hz, 1H, H_{14} or H_{13}), 4.52 (t, *J* = 6.0 Hz, 1H, H_{12}), 4.03 (s, 3H, $H_{10'}$), 3.90 – 3.80 (m, 2H, H_2, H_5), 3.66 – 3.51 (m, 2H, H_{6a}, H_{6b}), 3.48 – 3.39 (m, 1H, H_3 or H_4), 3.27 – 3.20 (m, 1H, H_4 or H_3), 2.44 (t, *J* = 7.5 Hz, 2H, H_9 or H_{11}), 2.25 – 2.11 (m, 2H, H_{11} or H_9), 1.75 – 1.59 (m, 2H, H_{10}).

^{13}C NMR (101 MHz, DMSO) δ 180.8 ($C_{1'}$ or $C_{4'}$), 179.0 ($C_{4'}$ or $C_{1'}$), 172.9 (C_8), 158.7, 138.2, 136.7, 135.5 (C), 131.8 (2C, $C_{2''}$), 130.2 (C), 129.4 (2C, $C_{3''}$), 127.4 ($C_{4''}$), 126.4 ($C_{7'}$), 124.3 ($C_{6'}$), 124.0 (C), 121.9 ($C_{5'}$), 114.4 ($C_{8'}$), 114.3 (C), 88.3 (C_1), 74.8 (C_2 or C_5), 71.2 (C_3 or C_4), 71.1 (C_4 or C_3), 61.9 ($C_{10'}$), 61.0 (C_6), 55.2 (C_5 or C_2), 35.7 (C_9 or C_{11}), 25.3 (C_{10}), 22.9 (C_{11} or C_9).

HRMS *m/z*: Calcd for $C_{29}H_{30}N_2O_8S$ 566.1723; Found 567.1820 [M+H], 589.1677 [M+Na].

Phenyl 2-deoxy-2-[5'-(3''-methoxy-9''H-carbazole-1'',4''-quinone-2''-yl)-pentanamido]-1-thio-α-D-glucopyranoside, 3.36

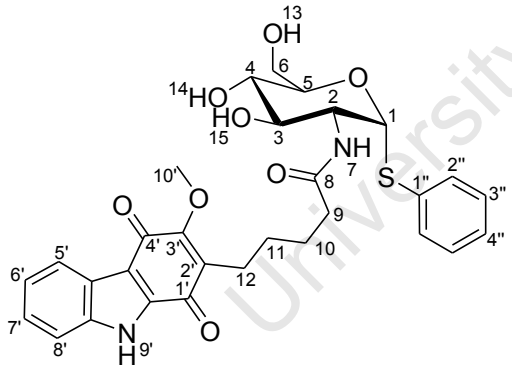

A red suspension of **3.32** (36 mg; 0.051 mmol) and NaOMe (0.8 mg; 0.015 mmol) in MeOH (20 ml) was stirred at room temperature for 24 h. After this, due to poor conversion to the product, additional NaOMe (1.4 mg; 0.026 mmol) was added. After 50 h, the temperature was raised to 50 °C, and stirring continued for a further 16 h. The resultant precipitate was isolated by filtration and purified by flash chromatography (silica gel, eluting in EtOAc:MeOH:THF, 8:2:10), followed by recrystallisation from MeOH, to afford the product as an orange solid (11 mg; 0.019 mmol; 37 %). M.p. 224-226 °C.

^{1}H NMR (400 MHz, DMSO) δ 12.74 (s, 1H, $H_{9'}$), 7.95 (d, *J* = 7.7 Hz, 1H, $H_{5'}$), 7.86 (d, *J* = 6.7 Hz, 1H, NH_7), 7.48 (d, *J* = 8.1 Hz, 1H, $H_{8'}$), 7.35 – 7.29 (m, 3H, $H_{2''}$, $H_{7'}$), 7.29 – 7.21 (m, 1H,

$H_{6'}$), 7.20 – 7.14 (m, 2H, $H_{3''}$), 7.13 – 7.07 (m, 1H, $H_{4''}$), 5.54 (d, *J* = 5.2 Hz, 1H, H_1), 5.06 (d, *J* = 5.7 Hz, 1H, H_{14} or H_{15}), 4.79 (d, *J* = 5.6 Hz, 1H, H_{15} or H_{14}), 4.46 (t, *J* = 5.9 Hz, 1H, H_{13}), 3.96 (s, 3H, $H_{10'}$), 3.82 – 3.74 (m, 2H, H_2, H_5), 3.60 – 3.44 (m, 2H, $H_{6a,b}$), 3.43 – 3.33 (m, 1H, H_3 or H_4), 3.21 – 3.15 (m, 1H, H_4 or H_3), 2.35 (t, *J* = 7.4 Hz, 2H, H_9 or H_{12}), 2.17 – 2.06 (m, 2H, H_{12} or H_9), 1.56 – 1.43 (m, 2H, H_{10} or H_{11}), 1.44 – 1.32 (m, 2H, H_{11} or H_{10}).

^{13}C NMR (101 MHz, DMSO) δ 180.9 ($C_{1'}$ or $C_{4'}$), 178.9 ($C_{4'}$ or $C_{1'}$), 173.1 (C_8), 158.5 (C), 138.1 (C), 136.6 (C), 135.5 (C), 131.7 (2C, $C_{2''}$), 130.7 (C), 129.4 (2C, $C_{3''}$), 127.3 ($C_{4''}$), 126.3 ($C_{6'}$ or $C_{7'}$), 124.3 ($C_{7'}$ or $C_{6'}$), 124.1 (C), 121.9 ($C_{5'}$ or $C_{8'}$), 114.5 ($C_{8'}$ or $C_{5'}$), 114.3 (C), 88.2 (C_1), 74.8 (C_2 or C_5), 71.2 (C_3 or C_4), 71.0 (C_4 or C_3), 61.8 ($C_{10'}$), 61.0 (C_6), 55.2 (C_5 or C_2), 35.6 (C_9 or C_{12}), 28.7 (C_{10} or C_{11}), 25.8 (C_{11} or C_{10}), 23.0 (C_{12} or C_9).

HRMS *m/z*: Calcd for $C_{30}H_{32}N_2O_8S$ 580.1879; 581.1972 [M+H], 603.1829 [M+Na].

Phenyl 2-deoxy-2-[6'-(2''-methyl-3''-methoxy-9''H-carbazole-1'',4''-quinone-9''-yl)-hexanamido]-1-thio-α-D-glucopyranoside, 3.37

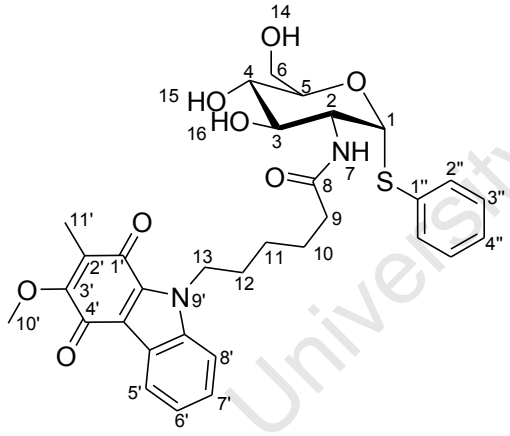

A solution of **3.34** (51 mg; 0.069 mmol) in MeOH (30 ml) was stirred at room temperature before NaOMe (0.8 mg; 0.014) was added, causing a red suspension to form. Stirring was continued for 10 days, after which time the precipitate was filtered off and purified by flash chromatography (silica gel, eluting in EtOAc:Acetone:THF, 14:3:3). Recrystallisation from MeOH afforded the product as an orange-red solid (20 mg; 0.033 mmol; 48 %). M.p. 191-192 °C.

^{1}H NMR (400 MHz, DMSO) δ 8.08 (d, *J* = 7.8 Hz, 1H, $H_{5'}$), 7.94 (d, *J* = 6.6 Hz, 1H, H_7), 7.69 (d, *J* = 8.3 Hz, 1H, $H_{8'}$), 7.44 – 7.38 (m, 3H, $H_{2''}$, $H_{7'}$), 7.35 (t, *J* = 7.1 Hz, 1H, $H_{6'}$), 7.32 – 7.25 (m, 2H, $H_{3''}$), 7.25 – 7.20 (m, 1H, $H_{4''}$), 5.63 (d, *J* = 5.1 Hz, 1H, H_1), 5.14 (d, *J* = 5.1 Hz, 1H, H_{15} or H_{16}), 4.90 (d, *J* = 4.9 Hz, 1H, H_{16} or H_{15}), 4.60 – 4.46 (m, 3H, H_{13}, H_{14}), 4.02 (s, 3H,

$H_{10'}$), 3.89 – 3.78 (m, 2H, H_2, H_5), 3.66 – 3.50 (m, 2H, $H_{6a,b}$), 3.49 – 3.35 (m, 1H, H_3), 3.34 – 3.23 (m, 1H, H_4), 2.22 – 2.04 (m, 2H, H_9), 1.91 (s, 3H, $H_{11'}$), 1.79 – 1.65 (m, 2H, H_{12}), 1.63 – 1.47 (m, 2H, H_{10}), 1.41 – 1.28 (m, 2H, H_{11}).

^{13}C NMR (101 MHz, DMSO) δ 181.5 ($C_{1'}$ or $C_{4'}$), 178.8 ($C_{4'}$ or $C_{1'}$), 173.1 (C_8), 157.4, 139.0, 135.5, 131.7 (2C, $C_{2''}$), 129.4 (2C, $C_{3''}$), 127.6, 127.4 ($C_{4''}$), 126.6 ($C_{7'}$), 124.9 ($C_{6'}$), 123.3, 122.2 ($C_{5'}$), 112.7 ($C_{8'}$), 88.2 (C_1), 74.8 (C_2 or C_5), 71.2 (C_3), 71.0 (C_4), 61.4 ($C_{10'}$), 61.0 (C_6), 55.2 (C_5 or C_2), 44.9 (C_{13}), 35.5 (C_9), 29.8 (C_{12}), 26.3 (C_{11}), 25.4 (C_{10}), 9.1 ($C_{11'}$). The quaternary $C_{1''}$ (~132 ppm) and another signal at ~115.3 ppm (based on the acetylated precursor) were not visible above the baseline noise and were not assigned.

HRMS *m/z*: Calcd for $C_{32}H_{36}N_2O_8S$ 608.2192; Found 609.2266 [M+H], 631.2113 [M+Na].

References

1. http://pubs.acs.org/paragonplus/submission/joceah/joceah_authguide.pdf, Pp.12
2. S.M. Rele, S.S. Iyler, S. Baskaran and E.L. Chaikof, *J. Org. Chem.*, **2004**, *69*, 9159-9170
3. S.S. Iyler, S.M. Rele, S. Baskaran and E.L. Chaikof, *Tetrahedron*, **2003**, *59*, 631-638
4. A. Titz, Z. Radic, O. Schwardt and B. Ernst, *Tetrahedron Lett.*, **2006**, *47*, 2383-2385
5. V. Pavliak and P. Kováč, *Carbohydrate Res.*, **1991**, *210*, 333-337
6. D.W. Gammon, D.J. Steenkamp, V. Mavumengwana, M.J. Marakalala, T.T. Mudzunga, R. Hunter, M. Munyololo, *Bioorg. Med. Chem.*, **2010**, *18*, 2501–2514
7. H. Ishida, Y. Imai, M. Kiso, A. Hasegawa, T. Sakurai, I. Azuma, *Carbohydr. Res*., **1989**, *195*, 59-66
8. J. Zhang and P. Kováč, *J. Carbohydr. Chem.*, **1999**, *18*, 461-469
9. M. Palme and A. Vasella, *Helv. Chim. Acta*, **1995**, *78*, 959-969
10. G.H. Posner and S.R. Haines, *Tetrahedron Lett.*, **1985**, *26*, 5-8
11. D. Vourloumis, G.C. Winters, M. Takahashi, K.B. Simonsen, B.K. Ayida, S. Shandrick, Q. Zhao and T. Hermann, *ChemBioChem*, **2003**, *4*, 879-885
12. S.K. Madhusudan, G. Agnihotri, D.S. Negi and A.K. Misra, *Carbohydrate Res*., **2005**, *340*, 1373–1377
13. W.A. Greenberg, E.S. Priestley, P.S. Sears, P.B. Alper, C. Rosenbohm, M. Hendrix, S.-C. Hung and C.-H. Wong, *J. Am. Chem. Soc.*, **1999,** *121,* 6527-6541

14. L. Salmon-Chemin, E. Buisine, V. Yardley, S. Kohler, M.-A. Debreu, V. Landry, C. Sergheraert, S.L. Croft, R.L. Krauth-Siegel, E. Davioud-Charvet, **2001**, *J. Med. Chem.*, *44*, 548-565

15. S. Adani, S. Raimondo, L. Forti, D. Monti and S. Riva, *Tetrahedron: Asymmetry*, **2005**, *16*, 2509-2513

Appendix

1. ^{1}H NMR Spectra of Synthesised Compounds Described in Chapter 2

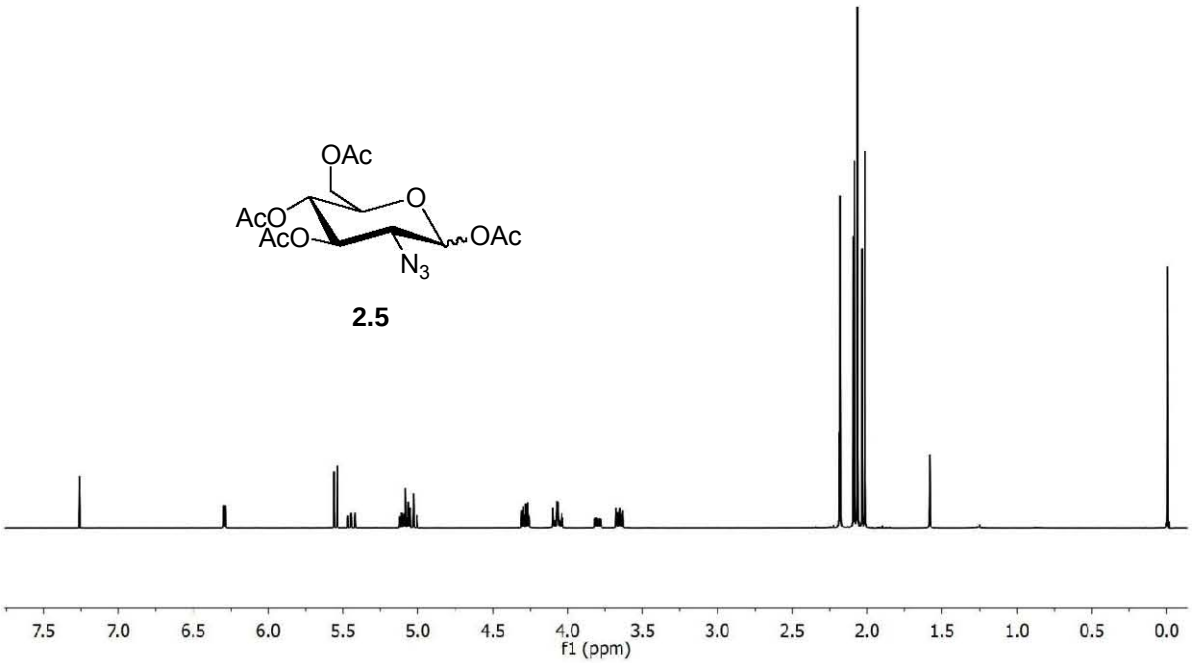

2.5

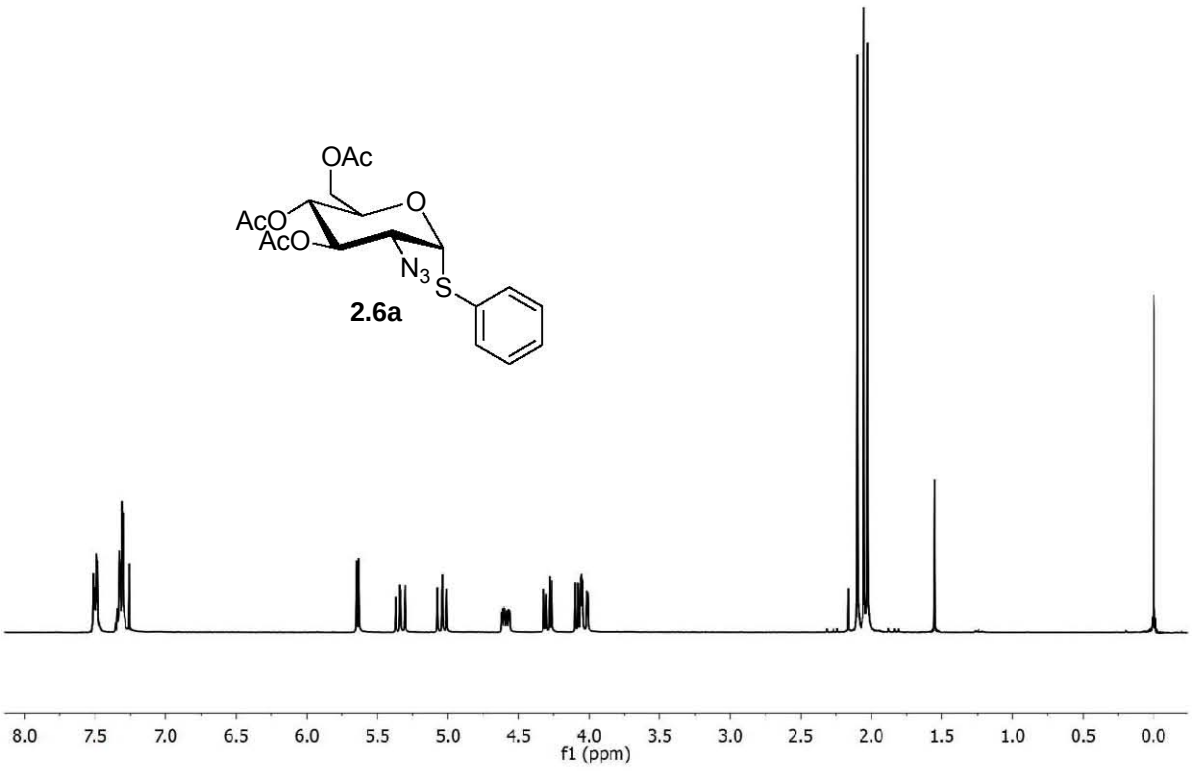

2.6a

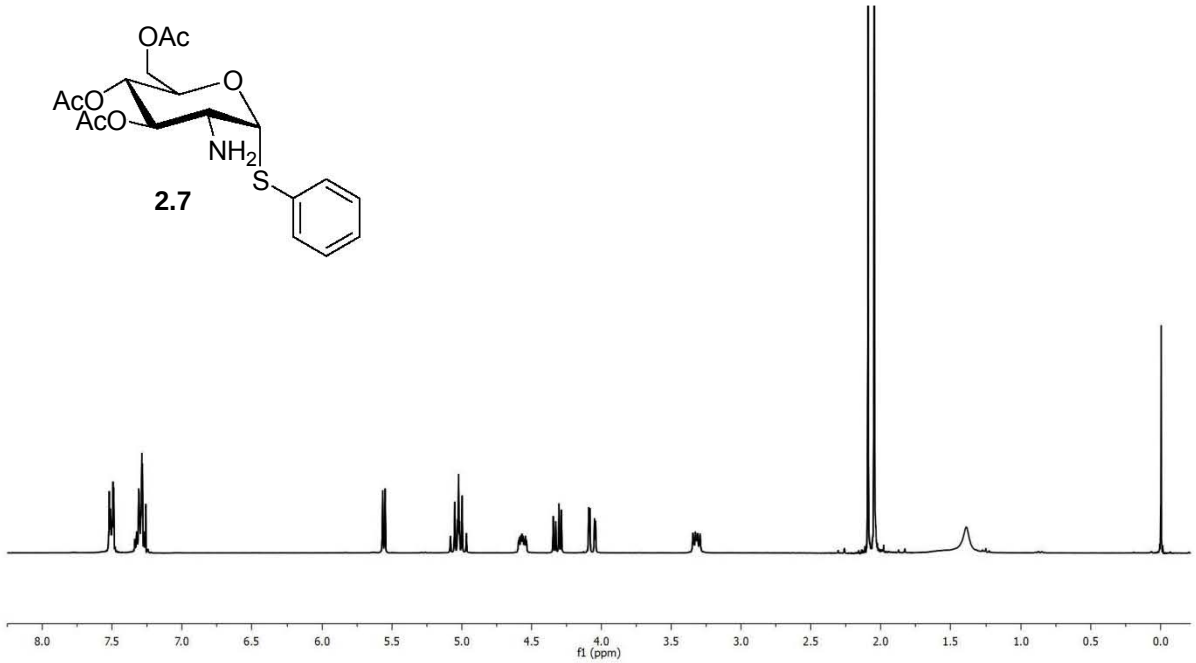
OAc
AcO
AcO
O
NH2
S
2.7
8.0
7.5
7.0
6.5
6.0
5.5
5.0
4.5
4.0
3.5
3.0
2.5
2.0
1.5
1.0
0.5
0.0
f1 (ppm)

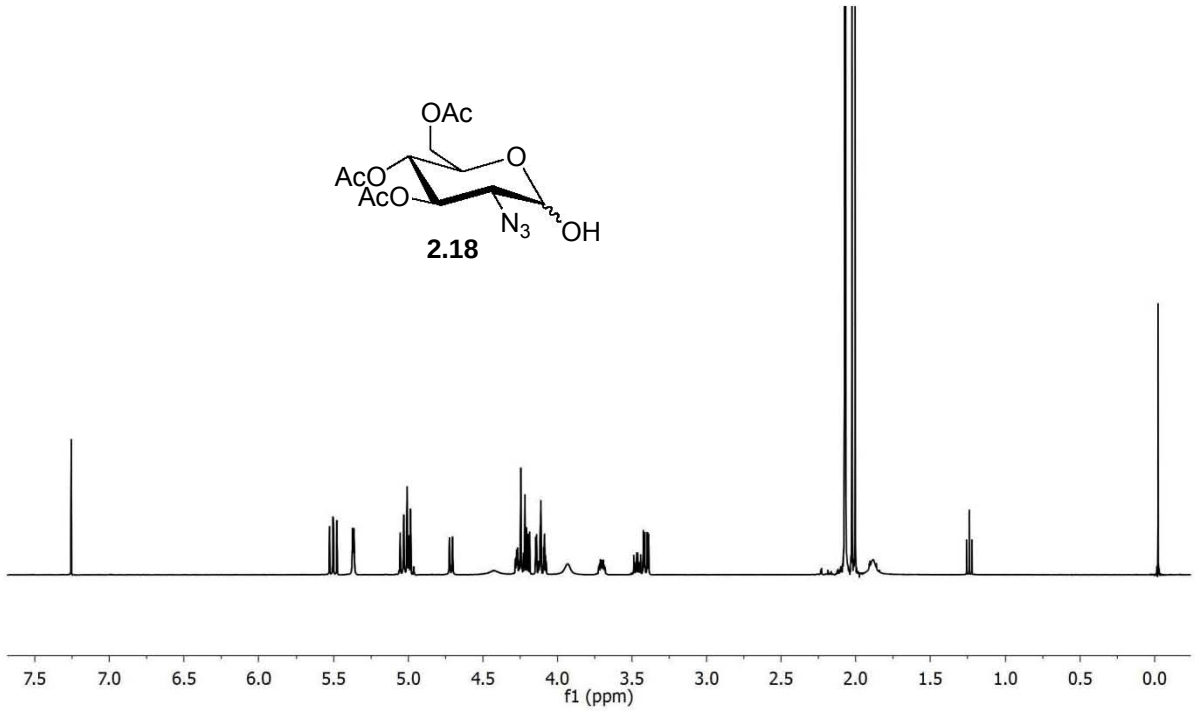
OAc
AcO
AcO
O
N3
OH
2.18
7.5
7.0
6.5
6.0
5.5
5.0
4.5
4.0
3.5
3.0
2.5
2.0
1.5
1.0
0.5
0.0
f1 (ppm)

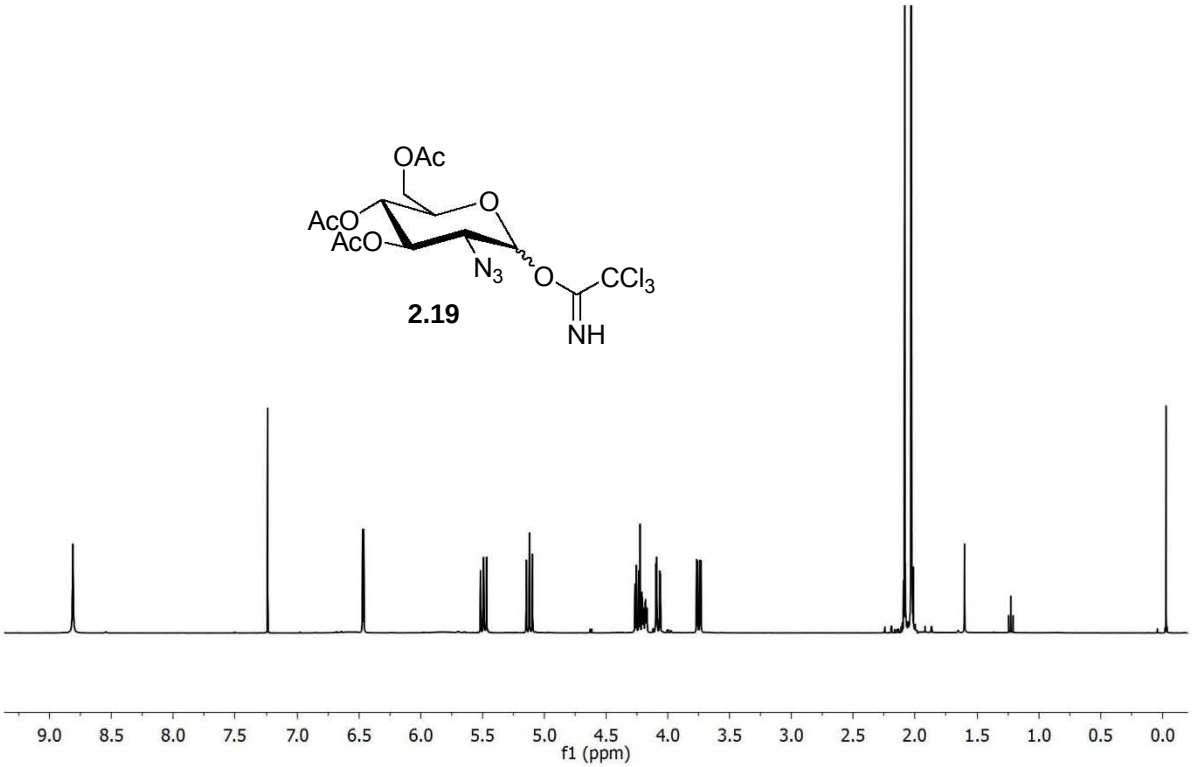
OAc
AcO
AcO
O
N3
O
CCl3
NH
9.0 8.5 8.0 7.5 7.0 6.5 6.0 5.5 5.0 4.5 4.0 3.5 3.0 2.5 2.0 1.5 1.0 0.5 0.0
f1 (ppm)

2.19

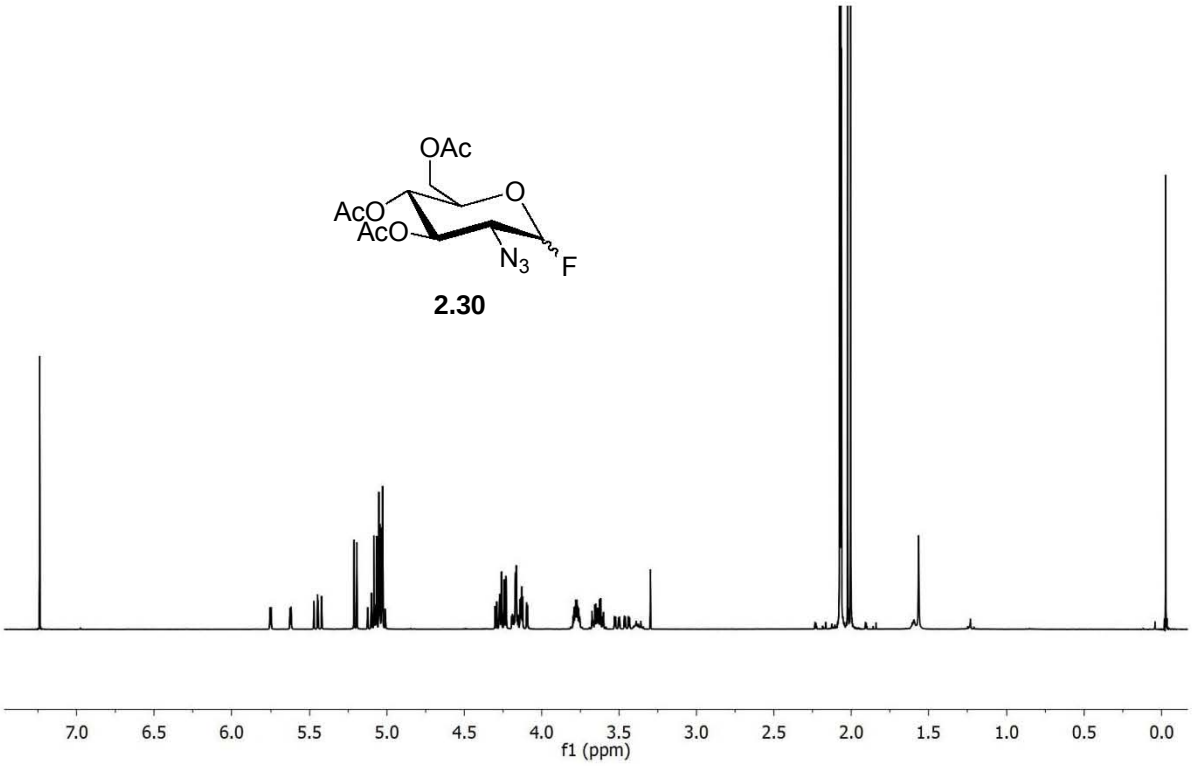
OAc
AcO
AcO
O
N3
F
7.0 6.5 6.0 5.5 5.0 4.5 4.0 3.5 3.0 2.5 2.0 1.5 1.0 0.5 0.0
f1 (ppm)

2.30

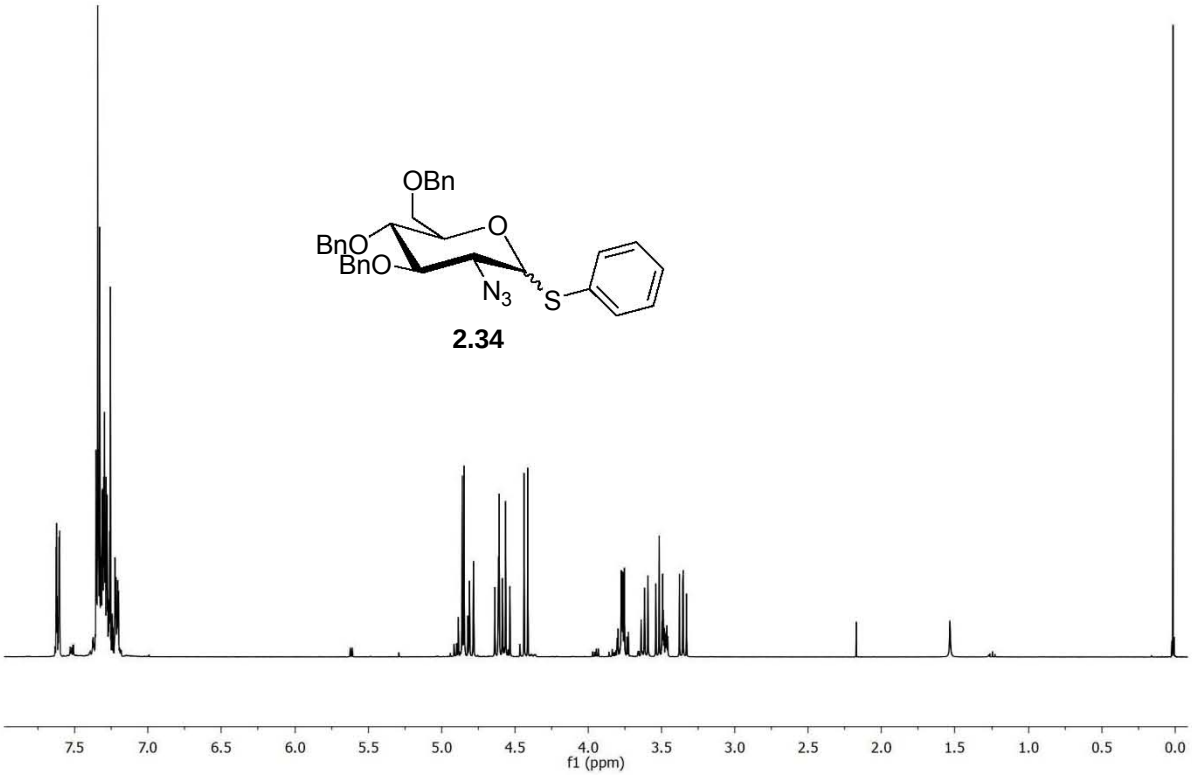
OBn
BnO
BnO
O
N3
S
7.5 7.0 6.5 6.0 5.5 5.0 4.5 4.0 3.5 3.0 2.5 2.0 1.5 1.0 0.5 0.0
f1 (ppm)

2.34

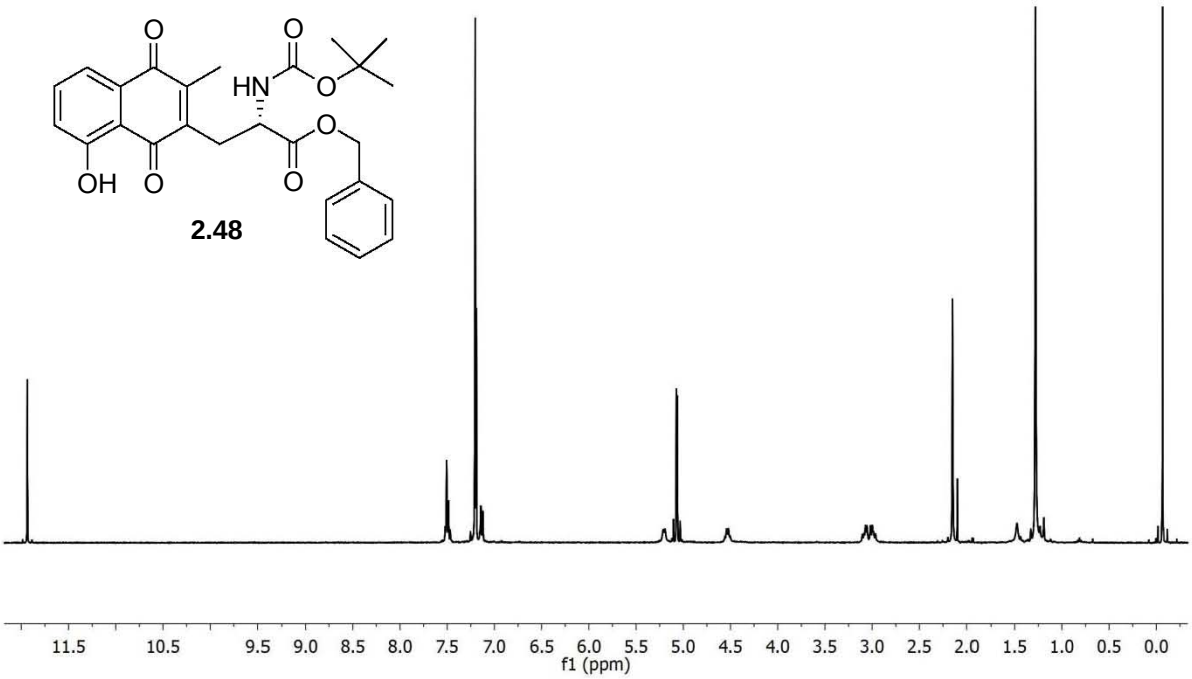
O
HN
O
O
O
OH
O
O
11.5 10.5 9.5 9.0 8.5 8.0 7.5 7.0 6.5 6.0 5.5 5.0 4.5 4.0 3.5 3.0 2.5 2.0 1.5 1.0 0.5 0.0
f1 (ppm)

2.48

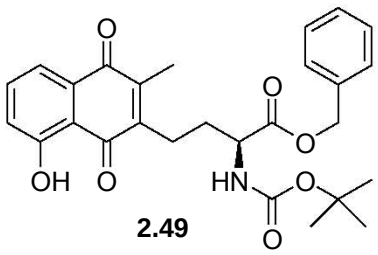
O
O
OH
O
HN
O
O
O

2.49

12.5 11.5 10.5 9.5 9.0 8.5 8.0 7.5 7.0 6.5 6.0 5.5 5.0 4.5 4.0 3.5 3.0 2.5 2.0 1.5 1.0 0.5 0.0
f1 (ppm)

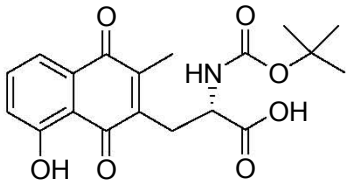
O
O
HN
O
OH
OH
O
O

2.54

12.5 11.5 10.5 9.5 9.0 8.5 8.0 7.5 7.0 6.5 6.0 5.5 5.0 4.5 4.0 3.5 3.0 2.5 2.0 1.5 1.0 0.5
f1 (ppm)

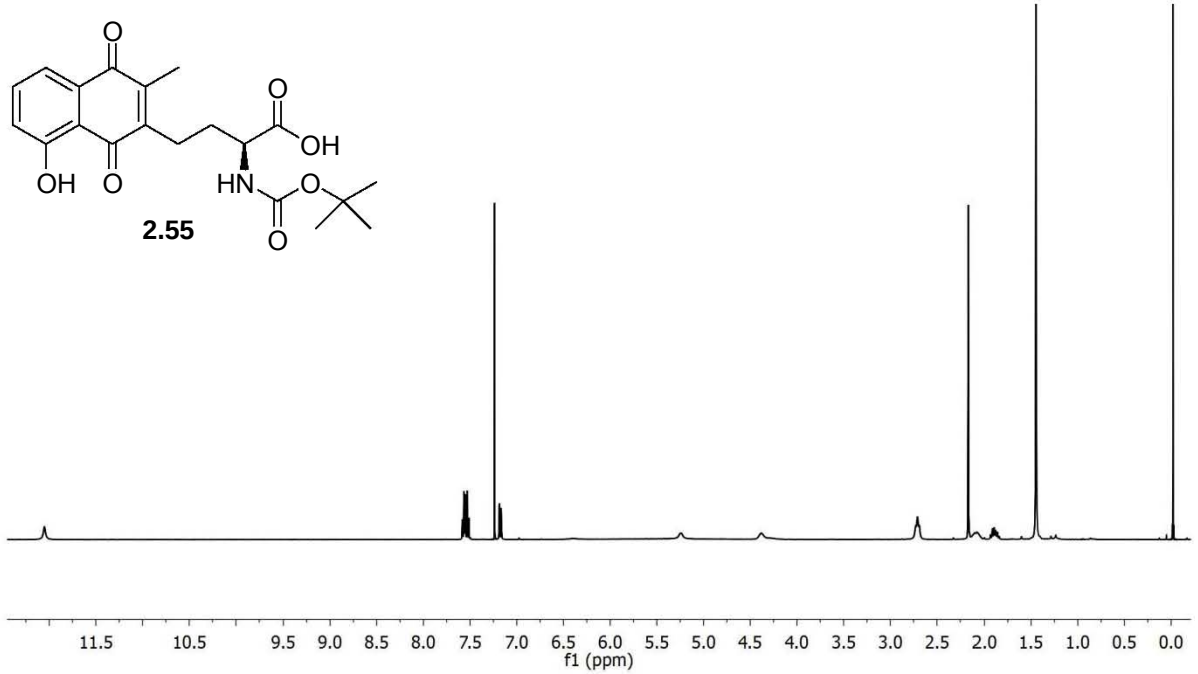
O
O
OH
OH
O
HN
O
O
11.5
10.5
9.5
9.0
8.5
8.0
7.5
7.0
6.5
6.0
5.5
5.0
4.5
4.0
3.5
3.0
2.5
2.0
1.5
1.0
0.5
0.0
f1 (ppm)

2.55

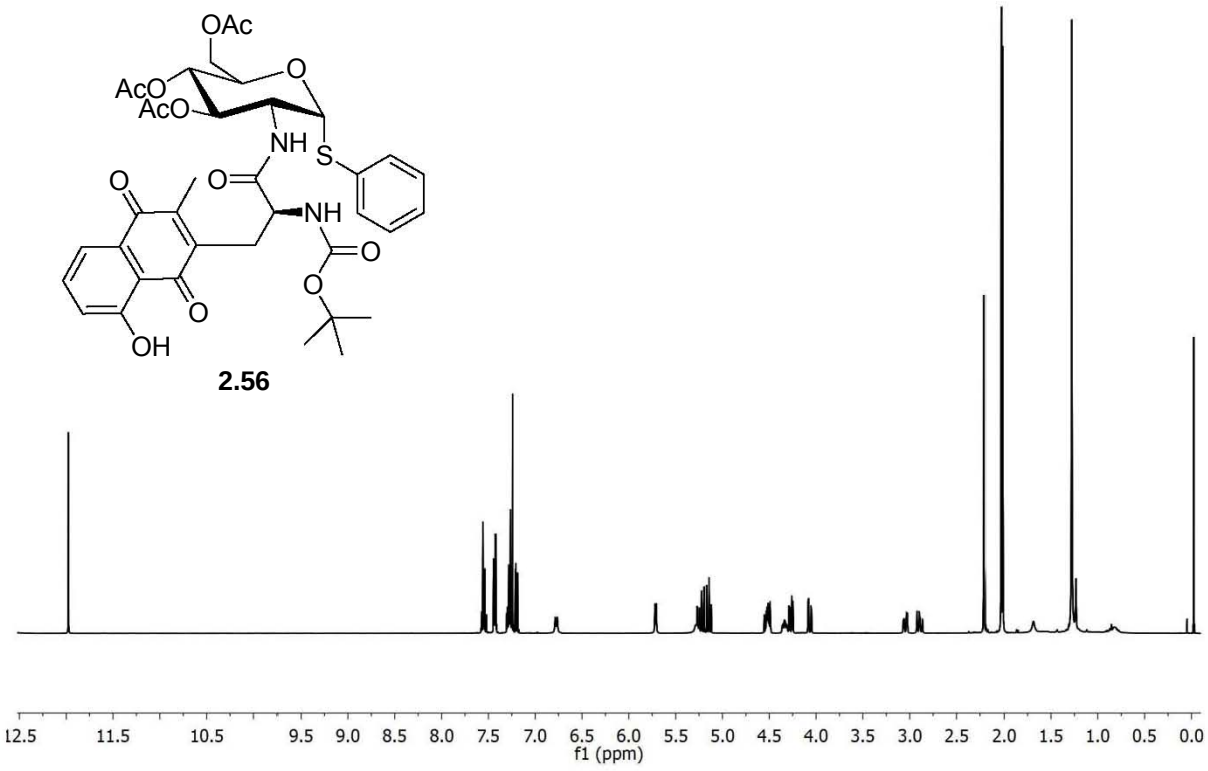
OAc
O
AcO
AcO
NH
S
O
O
NH
O
O
O
OH
12.5
11.5
10.5
9.5
9.0
8.5
8.0
7.5
7.0
6.5
6.0
5.5
5.0
4.5
4.0
3.5
3.0
2.5
2.0
1.5
1.0
0.5
0.0
f1 (ppm)

2.56

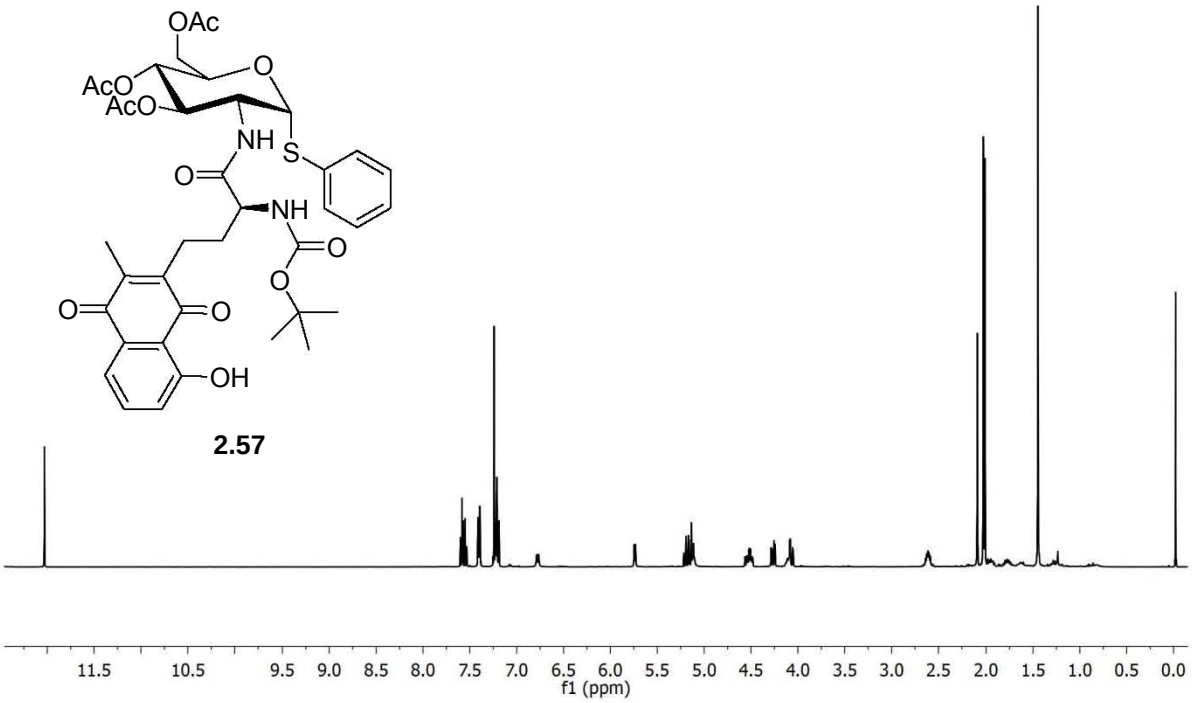
OAc
AcO
AcO
O
NH
S
O
NH
O
O
O
O
OH
11.5
10.5
9.5
9.0
8.5
8.0
7.5
7.0
6.5
6.0
5.5
5.0
4.5
4.0
3.5
3.0
2.5
2.0
1.5
1.0
0.5
0.0
f1 (ppm)

2.57

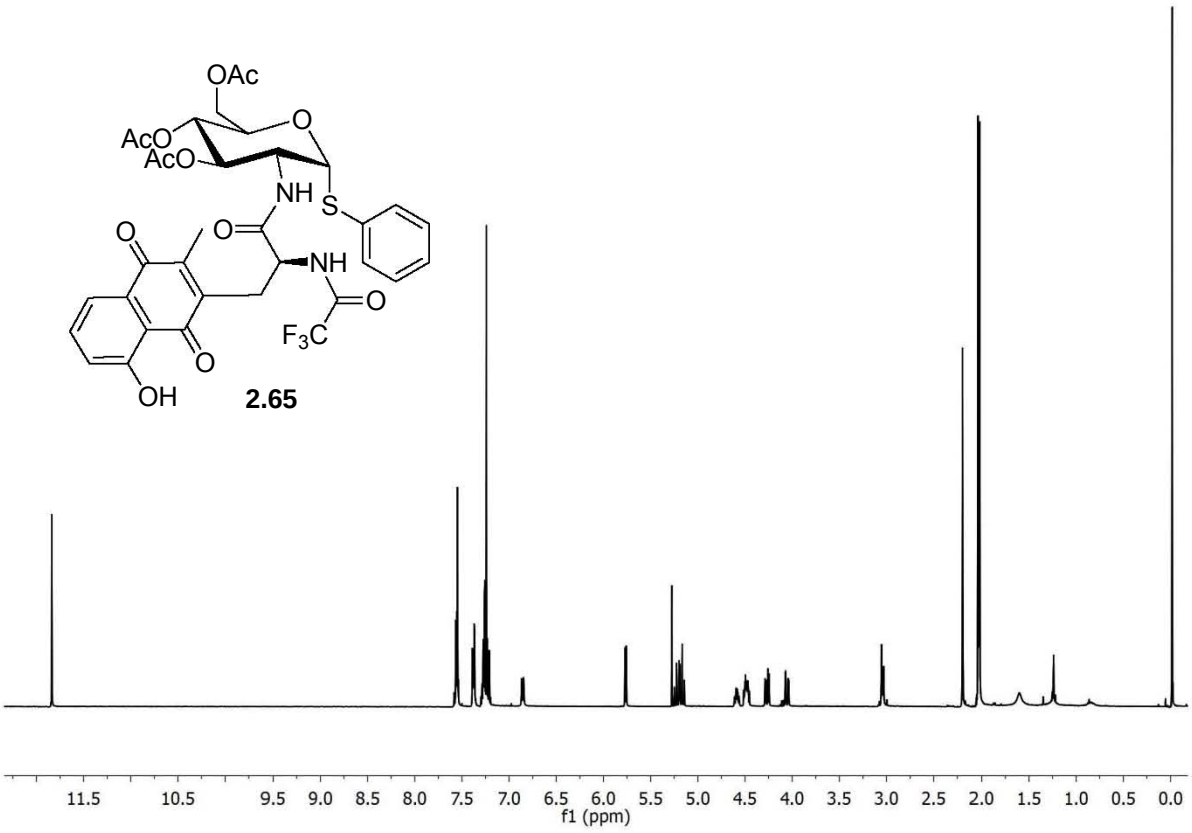
OAc
AcO
AcO
O
NH
S
O
O
NH
O
F3C
O
OH
11.5
10.5
9.5
9.0
8.5
8.0
7.5
7.0
6.5
6.0
5.5
5.0
4.5
4.0
3.5
3.0
2.5
2.0
1.5
1.0
0.5
0.0
f1 (ppm)

2.65

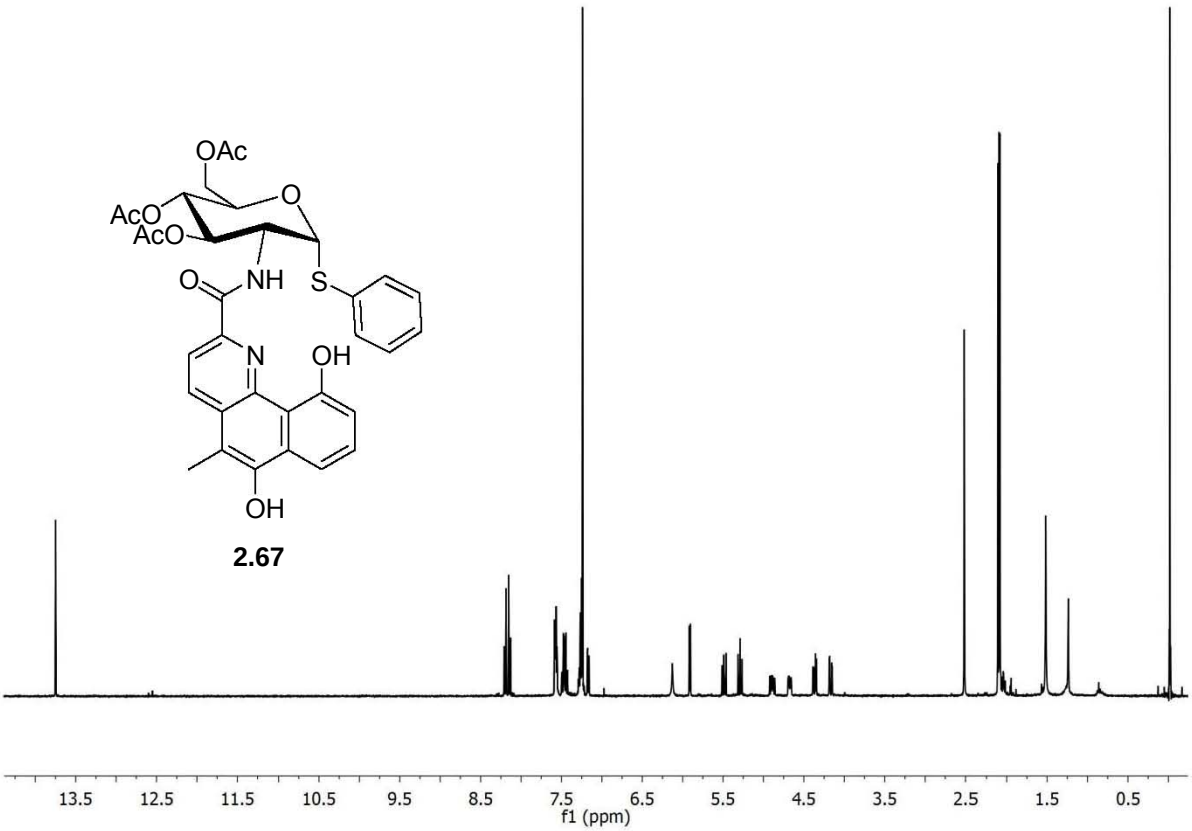
OAc
AcO
AcO
O
NH
S
N
OH
OH
13.5
12.5
11.5
10.5
9.5
8.5
7.5
6.5
5.5
4.5
3.5
2.5
1.5
0.5
f1 (ppm)

2.67

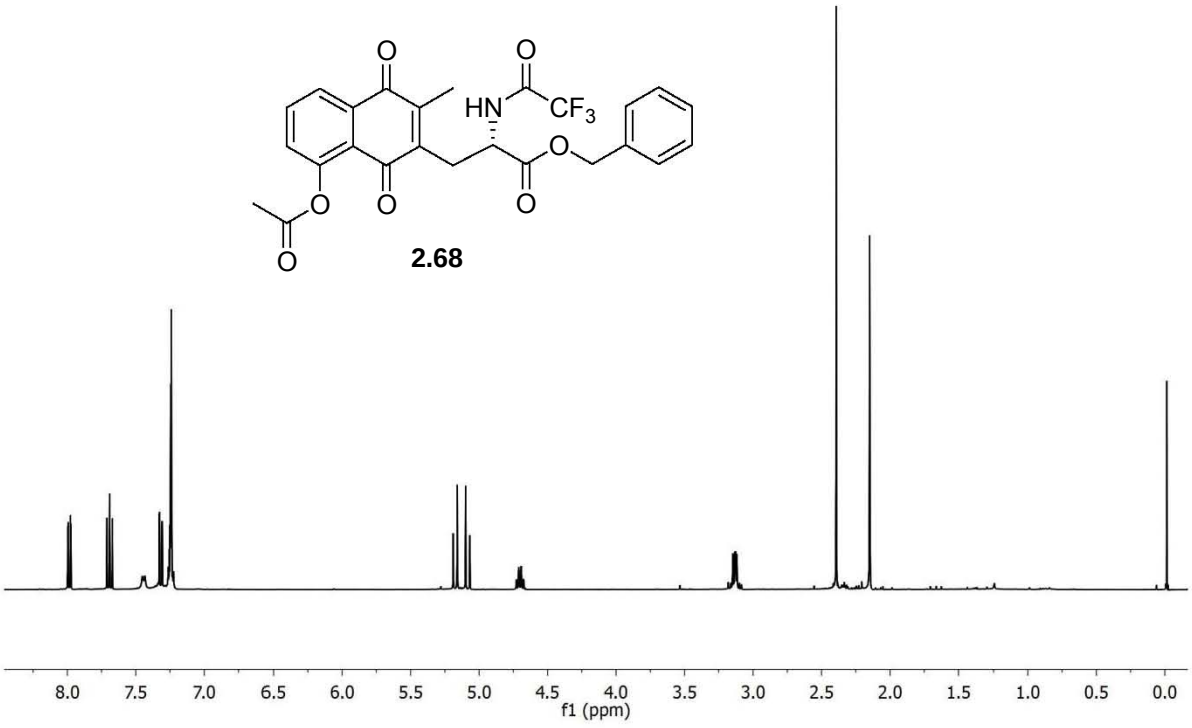
O
O
HN
CF3
O
O
O
O
O
8.0
7.5
7.0
6.5
6.0
5.5
5.0
4.5
4.0
3.5
3.0
2.5
2.0
1.5
1.0
0.5
0.0
f1 (ppm)

2.68

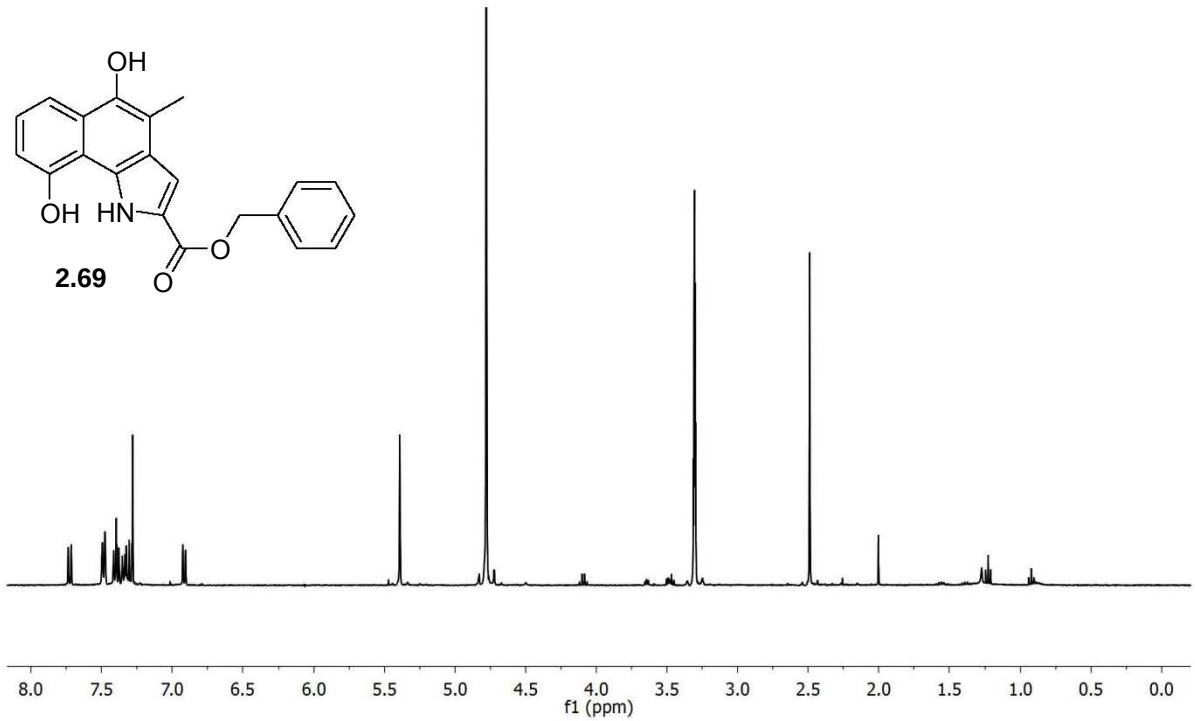
OH
OH
HN
O
O
8.0
7.5
7.0
6.5
6.0
5.5
5.0
4.5
4.0
3.5
3.0
2.5
2.0
1.5
1.0
0.5
0.0
f1 (ppm)

2.69

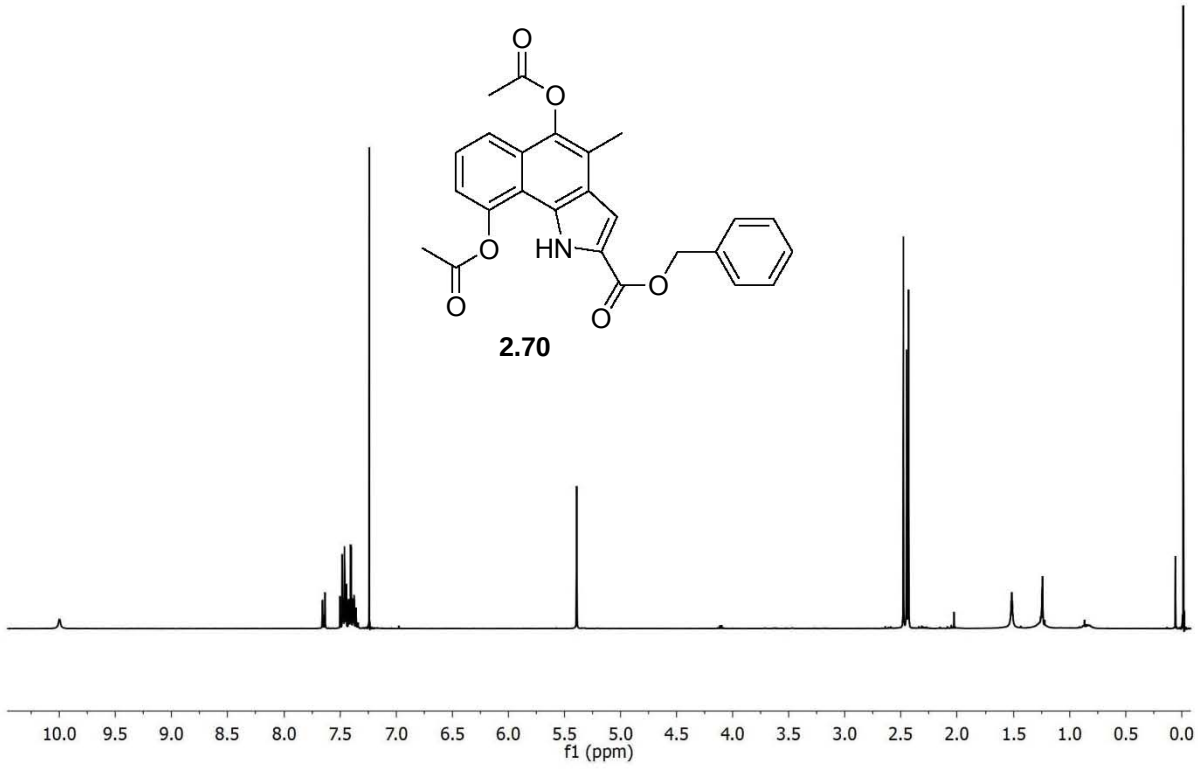
O
O
O
HN
O
O
10.0
9.5
9.0
8.5
8.0
7.5
7.0
6.5
6.0
5.5
5.0
4.5
4.0
3.5
3.0
2.5
2.0
1.5
1.0
0.5
0.0
f1 (ppm)

2.70

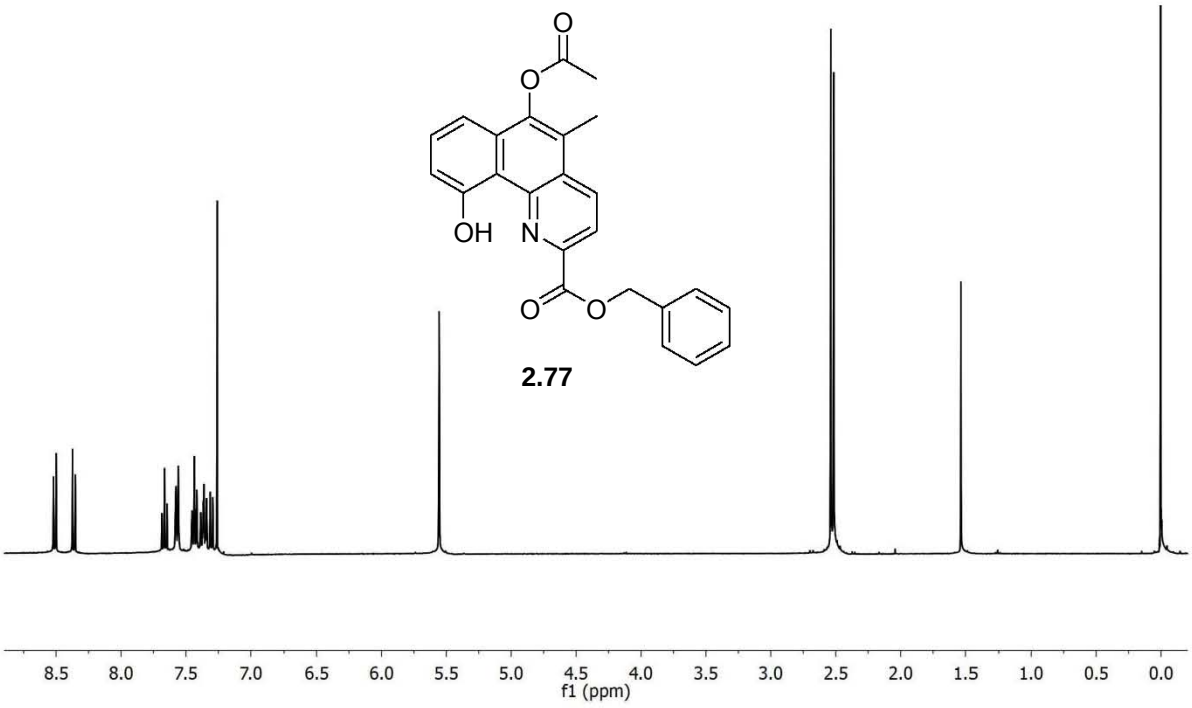
O
O
OH
N
O
O
8.5
8.0
7.5
7.0
6.5
6.0
5.5
5.0
4.5
4.0
3.5
3.0
2.5
2.0
1.5
1.0
0.5
0.0
f1 (ppm)

2.77

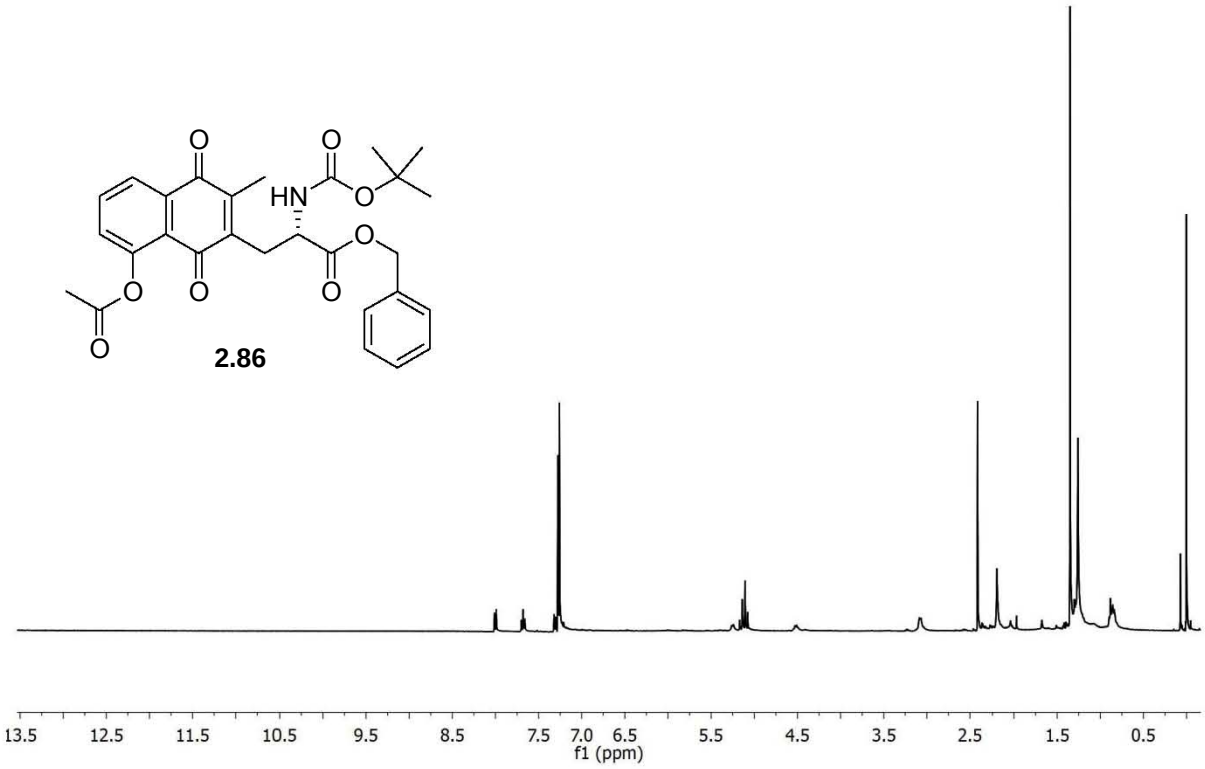
O
O
HN
O
O
O
O
O
O
13.5
12.5
11.5
10.5
9.5
8.5
7.5
7.0
6.5
5.5
4.5
3.5
2.5
1.5
0.5
f1 (ppm)

2.86

2. 1H NMR Spectra of Synthesised Compounds Described in Chapter 3

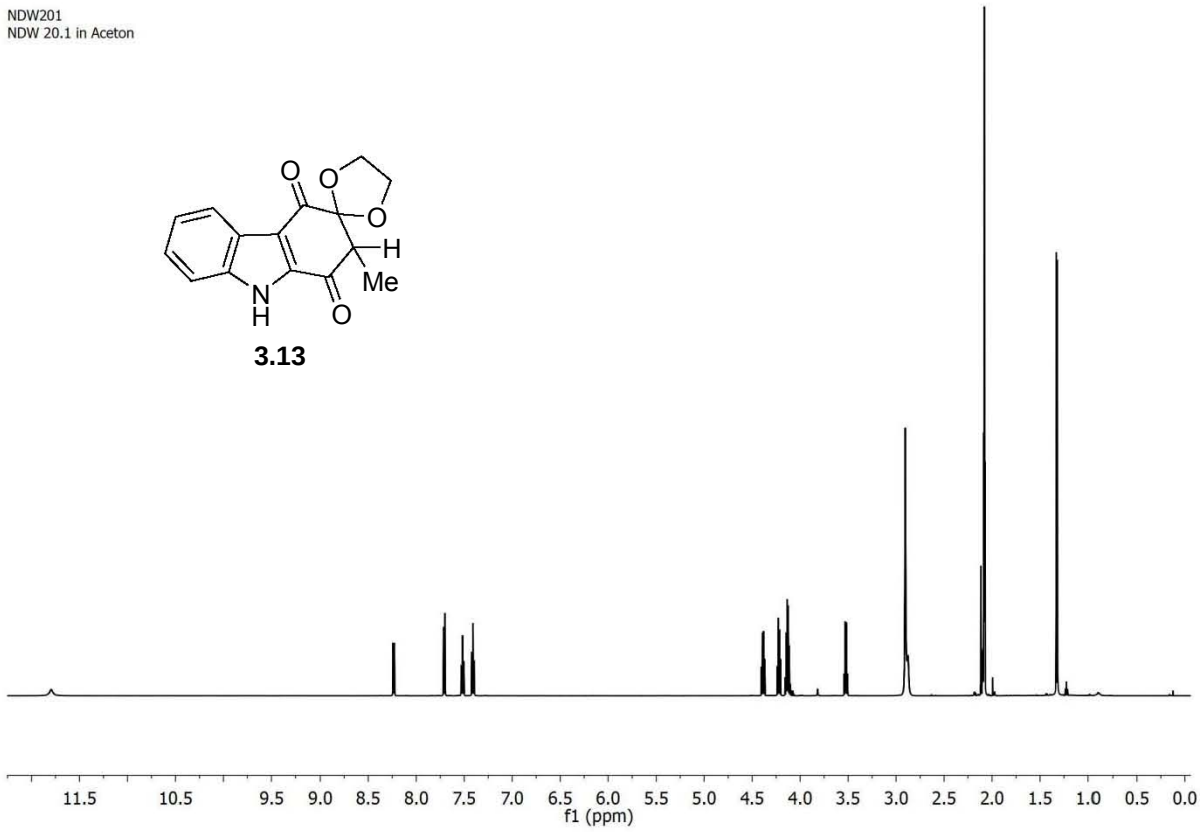

3.13

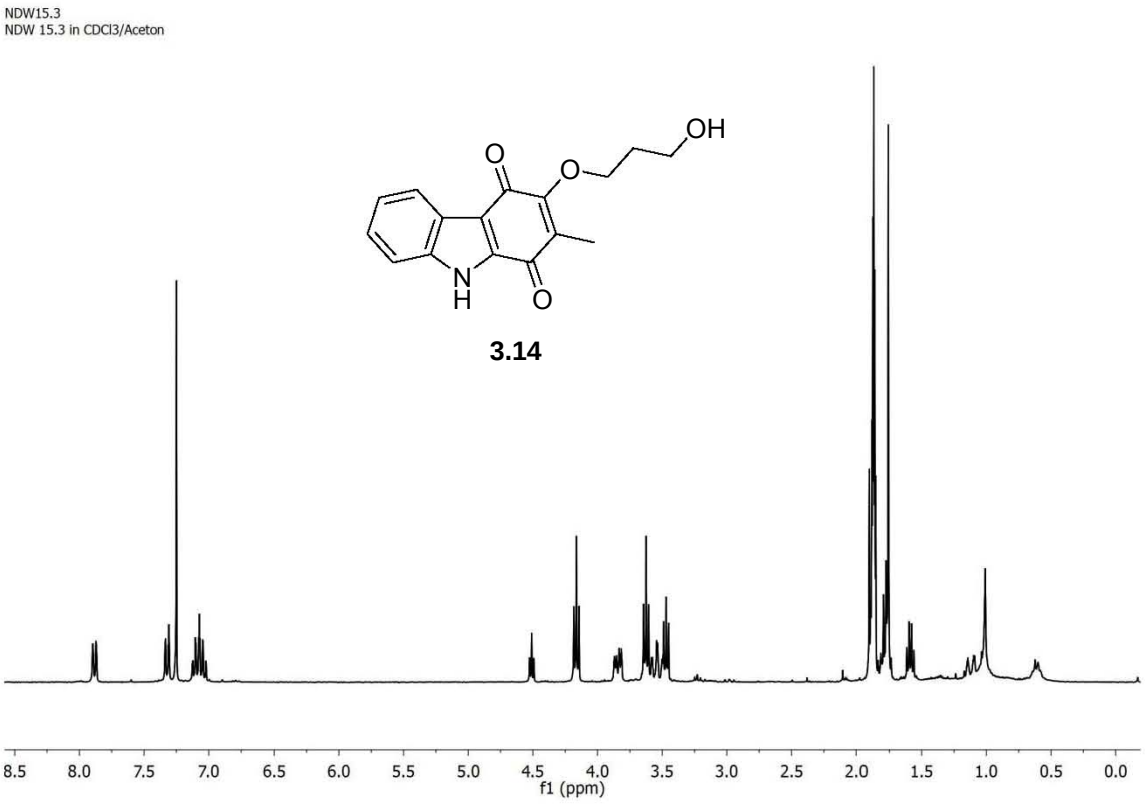

3.14

NDW19
NDW 19 in Aceton

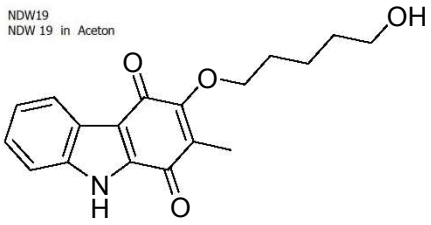

3.15

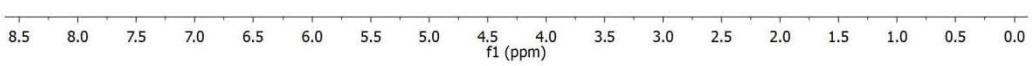

JSD2322
NDW-46/2 in DMSO/CDCl3

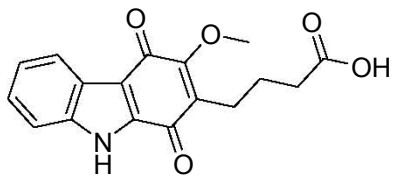

3.18

NDW35
NDW35 in DMSO

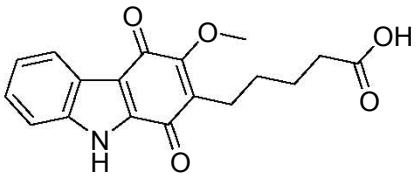

3.19

NDW21
NDW-2/1 in CDCl3

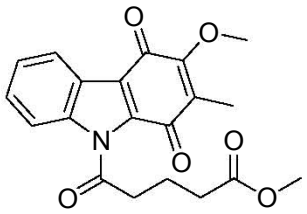

3.22

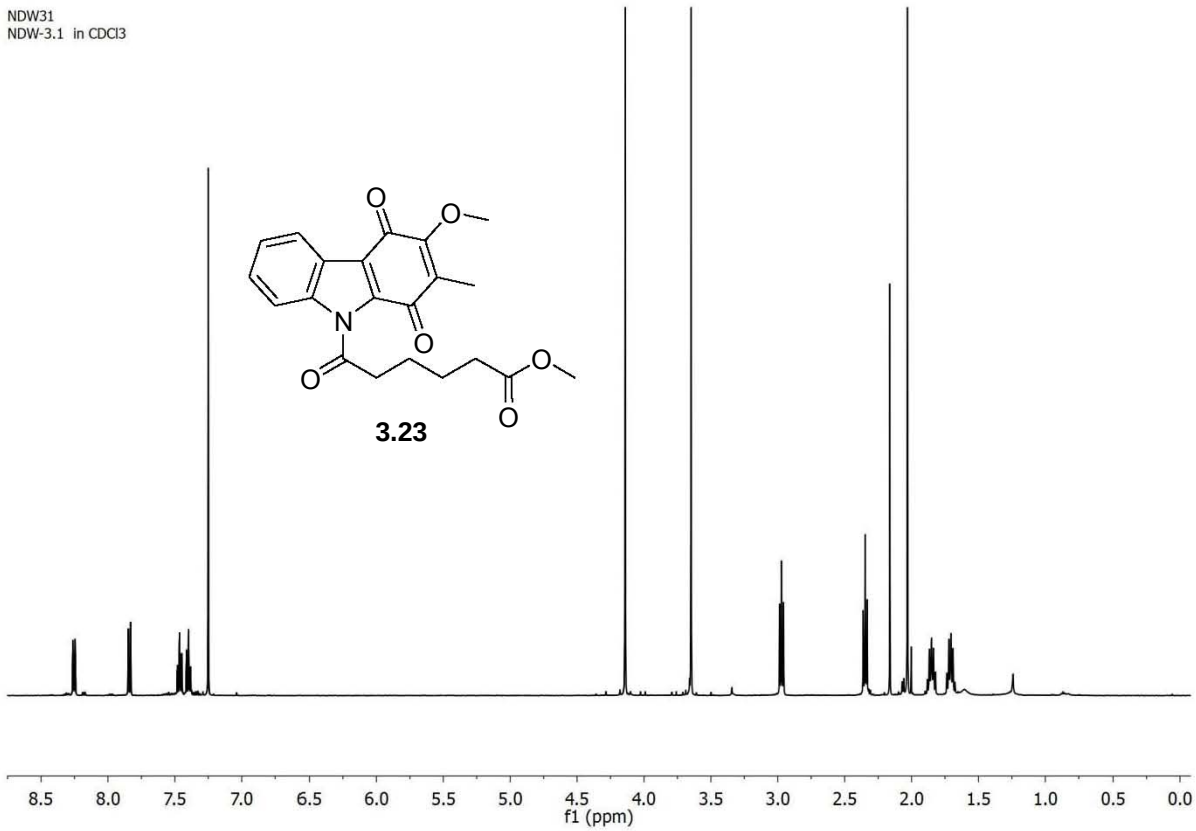
NDW31
NDW-3.1 in CDCl3
O
O
N
O
O
O
O
8.5 8.0 7.5 7.0 6.5 6.0 5.5 5.0 4.5 4.0 3.5 3.0 2.5 2.0 1.5 1.0 0.5 0.0
f1 (ppm)

3.23

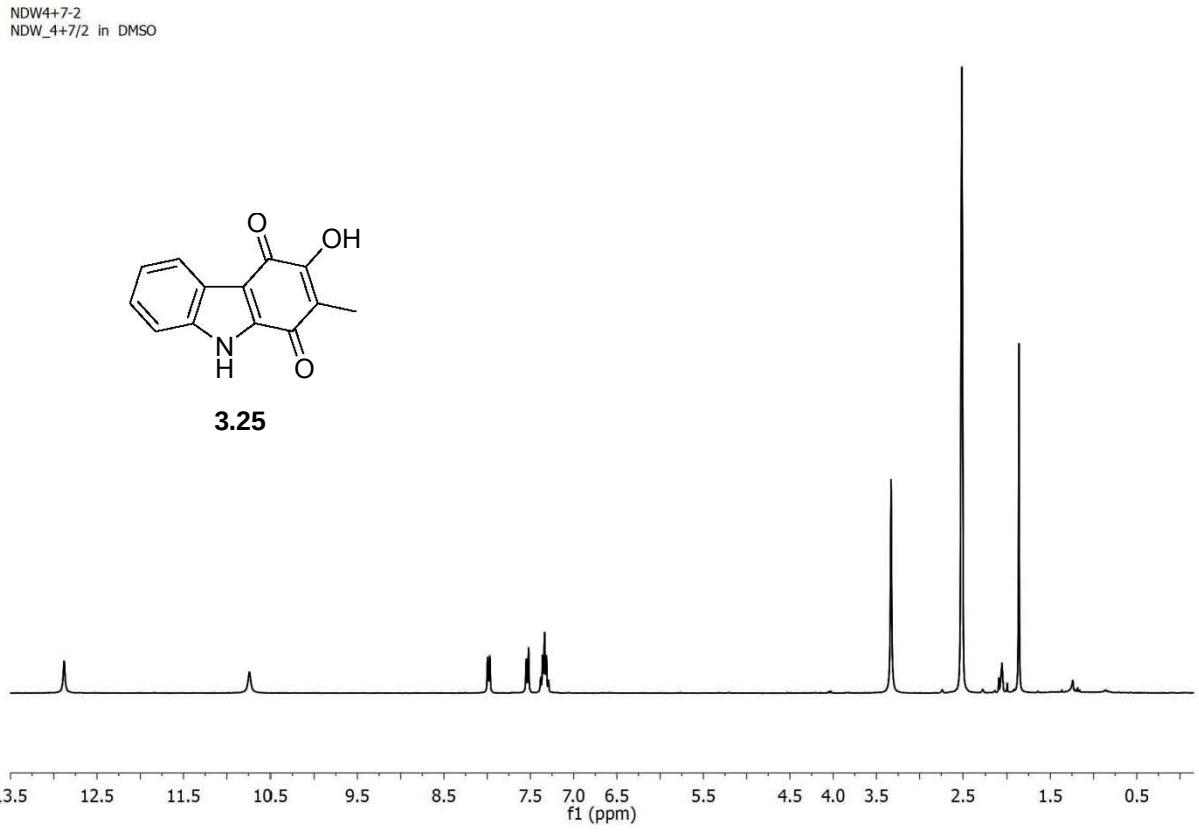
NDW4+7-2
NDW_4+7/2 in DMSO
O
OH
N
H
O
.3.5 12.5 11.5 10.5 9.5 8.5 7.5 7.0 6.5 5.5 4.5 4.0 3.5 2.5 1.5 0.5
f1 (ppm)

3.25

NDW22INT
NDW 22 INT in CDCl3

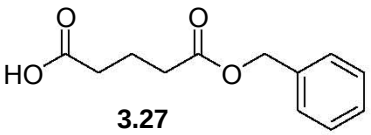

3.27

NDW44

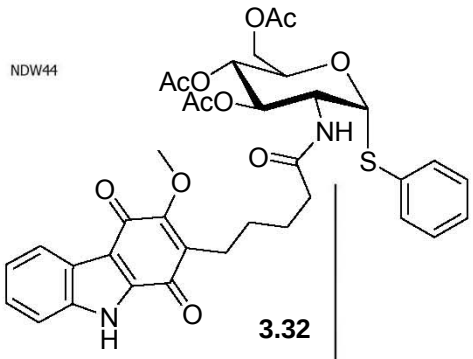

3.32

NDW48

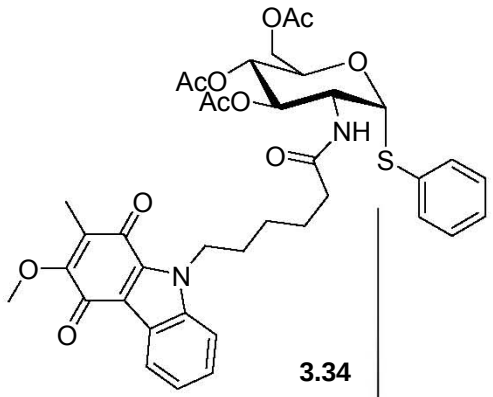

3.34

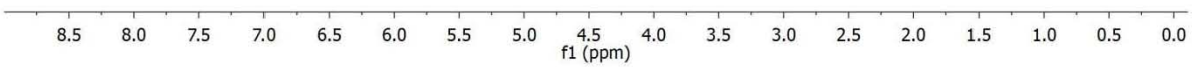

Final compound glutaric
RF 986/1 in D6-DMSO
1H Spectrum
Forke

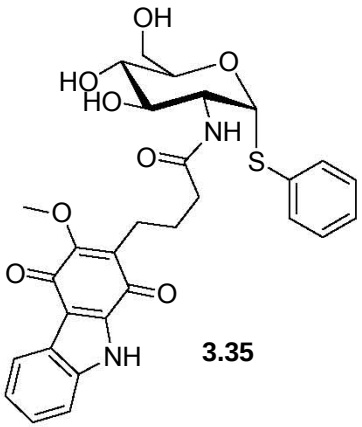

3.35

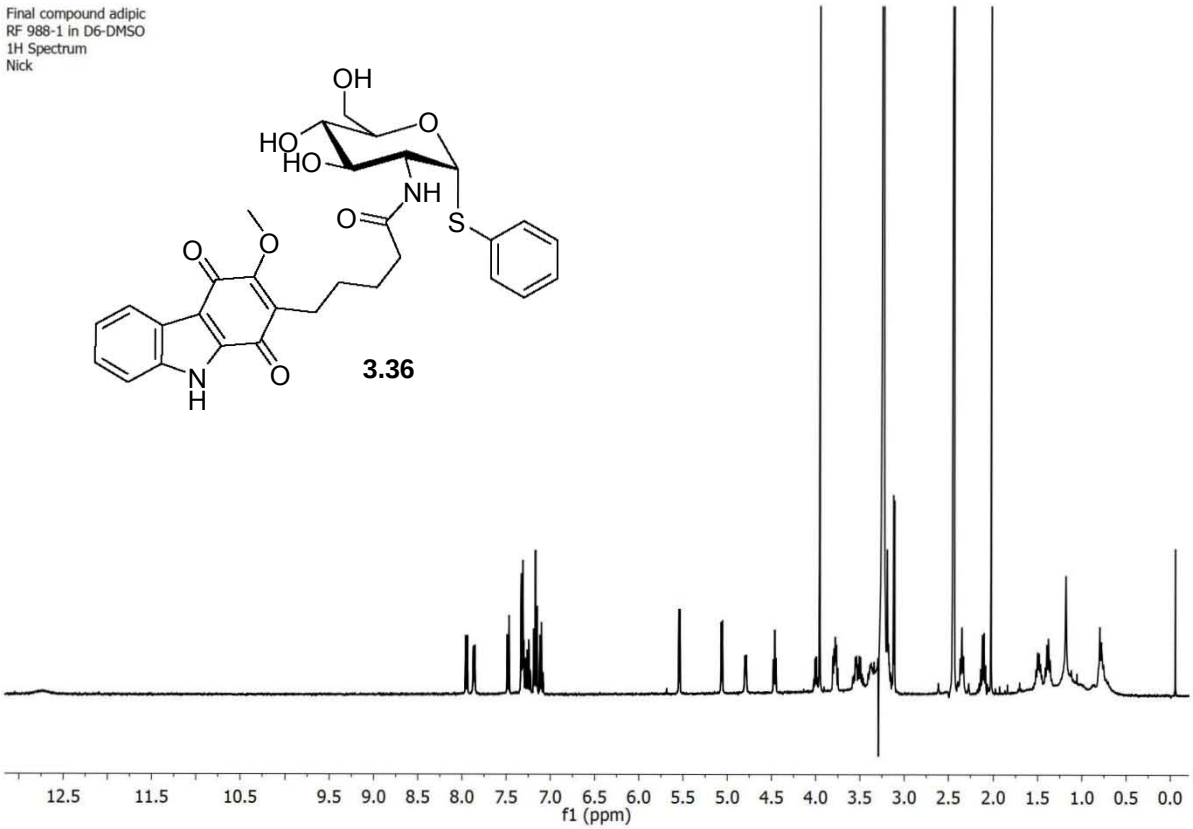
Final compound adipic
RF 988-1 in D6-DMSO
1H Spectrum
Nick
OH
HO
HO
O
NH
S
O
O
O
N
H
O
3.36
12.5 11.5 10.5 9.5 9.0 8.5 8.0 7.5 7.0 6.5 6.0 5.5 5.0 4.5 4.0 3.5 3.0 2.5 2.0 1.5 1.0 0.5 0.0
f1 (ppm)

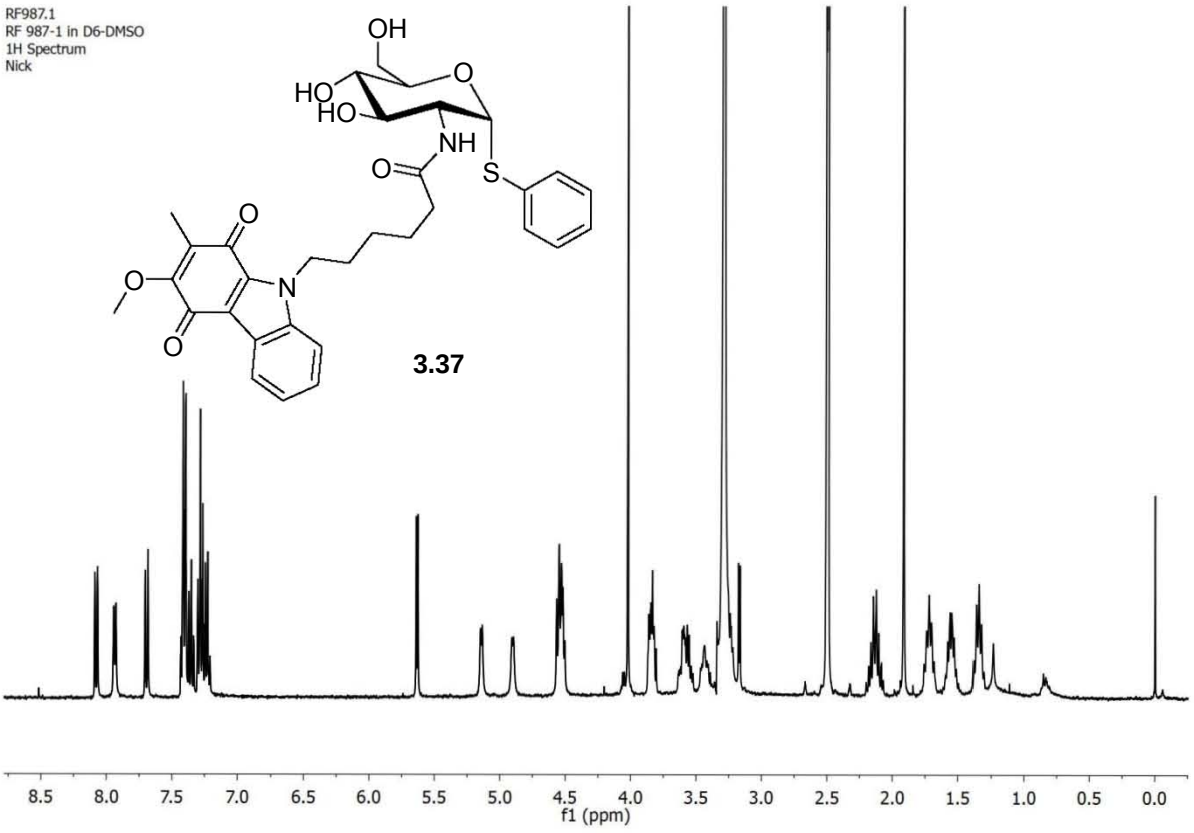
RF987.1
RF 987-1 in D6-DMSO
1H Spectrum
Nick
OH
HO
HO
O
NH
S
O
O
O
N
O
3.37
8.5 8.0 7.5 7.0 6.5 6.0 5.5 5.0 4.5 4.0 3.5 3.0 2.5 2.0 1.5 1.0 0.5 0.0
f1 (ppm)